Durham E-Theses

THE IDENTIFICATION OF NOVEL INORGANIC CARBON SENSITIVE ENZYMES

TOWNSEND, PHILIP,DAVID

How to cite:

TOWNSEND, PHILIP,DAVID (2010) *THE IDENTIFICATION OF NOVEL INORGANIC CARBON SENSITIVE ENZYMES*, Durham theses, Durham University. Available at Durham E-Theses Online: http://etheses.dur.ac.uk/415/

Use policy

The full-text may be used and/or reproduced, and given to third parties in any format or medium, without prior permission or charge, for personal research or study, educational, or not-for-profit purposes provided that:

- a full bibliographic reference is made to the original source
- a link is made to the metadata record in Durham E-Theses
- the full-text is not changed in any way

The full-text must not be sold in any format or medium without the formal permission of the copyright holders.

Please consult the full Durham E-Theses policy for further details.

Academic Support Office, Durham University, University Office, Old Elvet, Durham DH1 3HP
e-mail: e-theses.admin@dur.ac.uk Tel: +44 0191 334 6107
http://etheses.dur.ac.uk

PHILIP DAVID TOWNSEND

THE IDENTIFICATION OF NOVEL INORGANIC CARBON SENSITIVE ENZYMES

Ph.D. 2010

Abstract

Adenylyl cyclase catalyses the formation of the second messenger adenosine-3', 5'-monophosphate from adenosine triphosphate, and is involved in a number of diverse signalling pathways in eukaryotes and prokaryotes. Adenylyl cyclases are diverse in their structure and biochemistry, and have been grouped into six distinct Classes (I-VI). The Class III cyclase homology domain comprises the majority of prokaryotic and eukaryotic adenylyl cyclases, and has been further divided into 4 sub-Classes (a-d) based on active site polymorphisms. A number of Class IIIb adenylyl cyclases display elevated catalytic activity in the presence of inorganic carbon. Whether a response to inorganic carbon can be observed in enzymes which do not possess a Class IIIb cyclase homology domain remains to be established.

Experiments were performed to investigate the response to inorganic carbon of a Class IIIa cyclase homology domain; mammalian transmembrane adenylyl cyclase. *In vivo* experiments demonstrated that the activity of mammalian transmembrane adenylyl cyclase was potentially regulated by inorganic carbon, and that this had a downstream effect on the cAMP response element binding protein. *In vitro* experiments performed on a transmembrane adenylyl cyclase demonstrated that the increase in activity in the presence of inorganic carbon occurred through an increase in k_{cat} and increased metal affinity.

Experiments were performed to test the response to inorganic carbon of several enzymes that share a structurally similar active site with the adenylyl cyclases; the polymerase I family of prokaryotic DNA polymerases, the polymerase β family of DNA polymerases, and the guanylyl cyclases. Initial *in vitro* experiments performed on T7 RNA polymerase demonstrated a response to inorganic carbon, however, it was discovered that this was likely due to a non-specific effect of pH. It was shown that inorganic carbon increased assay pH over time, and this warranted a re-design of the *in vitro* assay used to test the response of an enzyme to inorganic carbon. This new *in vitro* assay methodology was used to re-test T7 RNA polymerase, as well as test DNA polymerase β and several guanylyl cyclase, and demonstrated that these enzymes were non-responsive to inorganic carbon.

Using this newly devised *in vitro* assay, experiments were performed to re-test the response of mammalian transmembrane adenylyl cyclase to

inorganic carbon, and demonstrated that this enzyme was unlikely to be regulated by inorganic carbon. Furthermore, this new *in vitro* assay was used to re-test the response of several Class IIIb cyclase homology domains to inorganic carbon. Results demonstrated that mammalian soluble adenylyl cyclase was responsive to inorganic carbon, however, results provided evidence to suggest that two prokaryotic Class IIIb cyclase homology domains (CyaB1 from *Anabaena* PCC 7120 and CyaC from *Spirulina platensis*) were possibly non-responsive to inorganic carbon.

Table of contents

List of tables

List of figures

Abbreviations

$7C_1$	C_1 domain of type VII AC
$2C_2$	C_2 domain of type II AC
AC	adenylyl cyclase
AM	acetoxymethyl ester
AMP	adenosine monophosphate
ATP	adenosine triphosphate
BCECF	2',7'-bis(carboxyethyl)-5(6)-carboxyfluorescein
BSA	bovine serum albumin
cAMP	adenosine 3', 5'-monophosphate or cyclic AMP
CA	carbonic anhydrase
CCM	carbon concentrating mechanism
CFTR	cystic fibrosis transmembrane conductance regulator protein
cGMP	guanosine 3', 5'-monophosphate or cyclic GMP
CHD	cyclase homology domain
Ci	inorganic carbon
CRE	cAMP response element
CREB	cAMP response element binding protein
dATP	deoxyadenosine triphosphate
DAF	abnormal dauer formation
DMEM	Dulbecco's modified eagles medium
DNA	deoxyribonucleic acid
dNTP	deoxy-nucleotide triphosphate
dSO	*Drosophila* stress odorant
FPLC	fast protein liquid chromatography
Fsk	forskolin
$G\alpha_s$	alpha subunit of the stimulatory G protein
$G\alpha_i$	alpha subunit of the inhibitory G protein
GC	guanylyl cyclase
GPI	glycosylphosphatidylinositol
GTP	guanosine triphosphate
HEK	human embryonal kidney
HIF	hypoxia inducible factor
IBMX	3-isobutyl-1-methylxanthine
IPTG	isopropyl β-D-1-thiogalactopyranoside
LB	lysogeny broth
Mes	2-(*N*-morpholino)ethanesulfonic acid
NFκB	nuclear factor kappa beta
NHE	sodium-hydrogen exchanger
NPR	natriuretic peptide receptor
NTA	nitrilotriacetic acid
NTP	nucleotide triphosphate
ORF	open reading frame
ORN	olfactory receptor neurons
PAGE	polyacrylamide gel electrophoresis
PBS	phosphate buffered saline
pCO_2	partial pressure of CO_2
PDE	phosphodiesterase
pH_i	intracellular pH
Pi	inorganic phosphate
PKA	cAMP dependent protein kinase
PKC	protein kinase C

RHD	Rel homology domain
PTH	parathyroid hormone
RNA	ribonucleic acid
RuBisCO	ribulose-1,5-bisphosphate carboxylase/oxygenase
sAC	soluble adenylyl cyclase
sAC_t	truncated sAC
sAC_{fl}	full-length sAC
SDS	sodium dodecylsulphate
SNAP	S-Nitroso-N-acetylpenicillamine
TCA	trichloroacetic acid
TGF	transforming growth factor
tmAC	transmembrane AC
Tris	tris(hydroxymethyl)aminomethane
V-ATPase	vacuolar ATPase

Acknowledgements

I would like to thank my supervisor Dr. Martin J. Cann (School of Biological and Biomedical Sciences, University of Durham) for help and guidance throughout this program. I would also like to thank my lab colleagues Dr. Arne Hammer, Dr. Phillip M. Holliday and Dr. Stepan Fenyk for advice, and discussion.

I would like to acknowledge the following people:

- Dr. Mike A. Gray (Institute for Cell and Molecular Biosciences, Newcastle University) for help with intracellular pH measurements.

- Dr. Stepan Fenyk for help with immunoblotting experiments.

- Dr. Lonny R. Levin (Professor of Pharmacology, Weill Cornell Medical College) and Dr. Jochen Buck (Professor of Pharmacology, Weill Cornell Medical College) for kind donation of sAC_t protein, and KH7. I would also like to thank them for helpful discussion.

- Dr. Roger K. Sunahara (Associate Professor of Pharmacology, University of Michigan) for kind donation of $7C_1$, $2C_2$ and $G\alpha_s$ expression plasmids.

- Dr. Catherine M. Joyce (Molecular Biophysics and Biochemistry Department, Yale University) for kind donation of Klenow expression plasmid and *E. coli* strain CJ376.

- Dr. Kent Hamra (Assistant Professor, University of Texas Southwestern medical centre) for kind donation of stable NIH 3T3 cells expressing receptor GCs.

- Dr. Clemens Steegborn (Junior Professor, Ruhr-Universität Bochum) for kind donation of CyaC protein, and $Sll0646_{434-635}$ expression plasmid.

The copyright of this thesis rests with the author. No quotation from it should be published without the prior written consent and information derived from it should be acknowledged.

This thesis is dedicated to my father,
Dr. Paul Richard Foxton Townsend

1

Introduction

1.1 The importance of Ci

All life on Earth is ultimately dependent upon inorganic carbon (Ci), as the substrate of the carbon fixing enzyme ribulose-1,5-bisphosphate carboxylase/oxygenase (RuBisCO). Ci is predominantly found as gaseous CO_2, however, in solution Ci is composed of CO_2, CO_3^{2-} and HCO_3^- (and to a lesser extent H_2CO_3), which exist in a pH dependent equilibrium (Figure 1.1). It is believed that ancient photosynthetic bacteria, first occurring somewhere between 2.7 and 1.9 billion years ago, were responsible for creating conditions suitable for sustaining modern O_2 dependent non-photosynthetic life through their evolution of O_2 and fixation of atmospheric CO_2 (Hetherington and Raven, 2005; Ohno, 1997). Due to many factors, all life on Earth has been subjected to large fluctuations in the levels of Ci in both the atmosphere and aquatic environments, yet life has continued to flourish (Beerling *et al.*, 2002). Photosynthetic organisms are known to be able to acclimate to relatively large changes in atmospheric CO_2 (Kaplan *et al.*, 2001). However, due to the currently accepted problem of anthropomorphic increases in atmospheric CO_2, understanding how Ci interacts with organisms has become more urgent. It would be prudent to assume that due to the continuous fluctuations in the level of Ci that organisms have been exposed to, that they have evolved mechanisms through which they can adapt their physiology, and indeed many examples of which are known.

In the long term, plants are thought to regulate the morphology and number of stomata expressed on their leaves in response to variable atmospheric CO_2 (Beerling *et al.*, 2002; Franks and Beerling, 2009). In the short term, plants are known to possess Ci sensitive signalling mechanisms through which they can regulate the opening and closing of their stomata in response to atmospheric CO_2 levels (Hashimoto *et al.*, 2006; Hu *et al.*, 2010). Furthermore, photosynthetic cyanobacteria have been shown to possess a mechanism through which they can regulate their carbon concentration mechanism (CCM) in response to available Ci (Giordano *et al.*, 2005). These CCMs are found in photosynthetic bacteria and represent a key mechanism though which an appropriate concentration of Ci can be exposed to the carboxysome; the main site of carbon fixation through the Calvin cycle.

Heterotrophic organisms can be exposed to large, short term fluctuations in the levels of Ci they are exposed to, since CO_2 is the predominant by-product

of metabolism. Due to the continuing need to excrete CO_2 as a metabolic by-product, mammals have evolved mechanisms through which they can vary their rate of ventilation in response to elevated blood CO_2 (Daristotle *et al.*, 1990). Certain species of nematode worms, organisms which feed off decaying plant matter, can be exposed to high levels of CO_2 (which can lead to hypoxia, anaesthetisation, and death) in the soil, and as such have evolved a mechanism through which they can sense elevated CO_2 and avoid it (Hallem and Sternberg, 2008). More ingeniously, certain species of blood feeding insects have evolved a mechanism which allows them to exploit plumes of exhaled CO_2 as a means to direct host location (Gillies, 1980).

Despite many organisms having evolved sensing mechanisms through which they can adapt their physiology in response to small fluctuations in Ci, large, uncontrolled changes can have severe effects. This is highlighted by a plethora of physiological problems associated with perturbations in the balance of Ci in the body of mammals. Increased or decreased whole body CO_2, which can be caused by respiratory acidosis or alkalosis, causes impaired function of almost all organs (Epstein and Singh, 2001; Foster *et al.*, 2001). Aside from direct effects as a result of a drop in blood pH during respiratory acidosis, the associated rise in whole body CO_2 concentration has been shown to cause a number of problems, such as impaired alveolar fluid re-absorption in the lungs and imbalanced ion re-absorption in the kidneys (Brazeau and Gilman 1953; Hoppe, Metler *et al.* 1982; Briva, Vadasz *et al.* 2007). Under conditions of respiratory alkalosis, the associated drop in plasma CO_2 concentrations have been shown to affect almost all organs in the body, notably the central nervous system, lungs and heart (Foster *et al.*, 2001).

Although organisms are heavily dependent upon Ci as a substrate or product for carboxylase and decarboxylase enzymes, they are also dependent upon the equilibrium between the two species of Ci in solution to provide a buffering mechanism through which they can resist small changes in pH (Adrogue and Adrogue, 2001; Boron, 2004). In solution at physiological pH, the two main species of Ci, CO_2 and HCO_3^-, exist in a pH dependent equilibrium, such that as pH is varied the 'contribution' of each Ci species to the total Ci pool varies (Figure 1.1). However, it is also true that as the concentration of either species of Ci is altered, the re-equilibration is able to effect pH. In fact, certain cell types in mammals are known to detect fluctuations in CO_2 concentration

through the effect that it has upon pH, and this is commonly referred to as CO_2/H^+ sensing (Lahiri and Forster 2003). Furthermore, although the CO_2/HCO_3^- equilibrium forms naturally, it is deemed so important that a family of enzymes have evolved in almost all organisms to speed the acquisition of equilibrium; the zinc dependent carbonic anhydrases (CAs) (see Figure 1.2 for mechanism) (Smith and Ferry, 2000; Tripp *et al.*, 2001).

Aside from CA, Ci is known to interact with a number of proteins, both as a substrate or product in catalysis, but also in an allosteric manner. There are a multitude of carboxylase enzymes, such as phosphoenolpyruvate carboxykinase and RuBisCO, which utilise either CO_2 or HCO_3^- directly within their catalytic mechanism (Cotelesage *et al.*, 2007). There are also several enzymes, such as RuBisCO and Class D β-lactamases, which require allosteric activation through CO_2 binding to specific amino acid side chains prior to gaining catalytic competence (Golemi *et al.*, 2001; Lorimer and Miziorko, 1980). Furthermore, certain prokaryotic and eukaryotic adenylyl cyclases (ACs), which are highly prevalent signalling enzymes, have been shown to increase their rate of catalysis in the presence of Ci (Cann *et al.*, 2003; Chen *et al.*, 2000; Hammer *et al.*, 2006; Klengel *et al.*, 2005; Mogensen *et al.*, 2006). However, despite a number of proteins being shown to interact with Ci, in many cases the way in which this interaction occurs is not completely understood, as is the case for ACs (Steegborn *et al.*, 2005b).

There is ongoing effort to understand the nature of how Ci interacts with proteins, however, much of the information gained to date has largely relied upon crystallisation and mutational studies and as such details have been slow to emerge. One way in which Ci has been shown to interact with a protein is through the formation of a carbamate with the ε-amino group (i.e. the side chain amine) of a lysine, as is typified in RuBisCO and Class D β-lactamases (Golemi *et al.*, 2001; Lorimer and Miziorko, 1980). However, it is also possible for carbamates to form at the α-amino group (i.e the N-terminal amine within the protein backbone) of lysine, as is the case in haemoglobin (Matthew *et al.*, 1977). Ci may also interact with proteins in a non-covalent manner, through the formation of hydrogen bonds with amino acid side chains, as is identified in phosphoenolpyruvate carboxykinase, where an arginine and lysine were shown to co-ordinate CO_2 in the active site in a position ideal for catalysis (Cotelesage *et al.*, 2007). In fact, a recent study has revealed that of the amino acids

reported to be involved in binding CO_2, arginine, histidine and lysine accounted for more than half, indicating that basic amino acid side chains represent a major CO_2 binding site (Cundari *et al.*, 2009). Although almost all amino acids were shown to be involved in binding CO_2, negatively charged amino acids were far less frequent, indicating that interaction with CO_2 predominantly occurs through the slightly negatively charged oxygens (Cundari *et al.*, 2009). Furthermore, work has identified that of the two predominant protein secondary structures, β-sheets were more commonly involved in CO_2 binding than α-helices (Cundari *et al.*, 2009). Although the knowledge of how Ci interacts with proteins is advancing fast, there is still no reliable way to predict Ci responsive proteins and as such their identity in many known Ci sensing pathways still remains a mystery.

The following sections will cover, as broadly as is feasible, the known mechanisms through which plants, invertebrates, mammals and prokaryotes sense Ci. Although fluctuations in Ci have a vast array of effects in various organisms, an emphasis will be placed upon systems where the Ci sensing pathway is at least partially characterised.

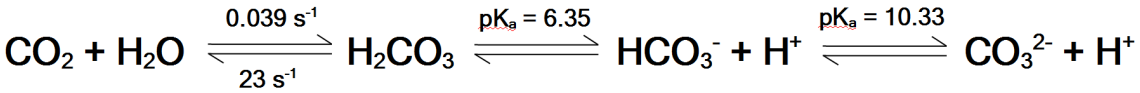

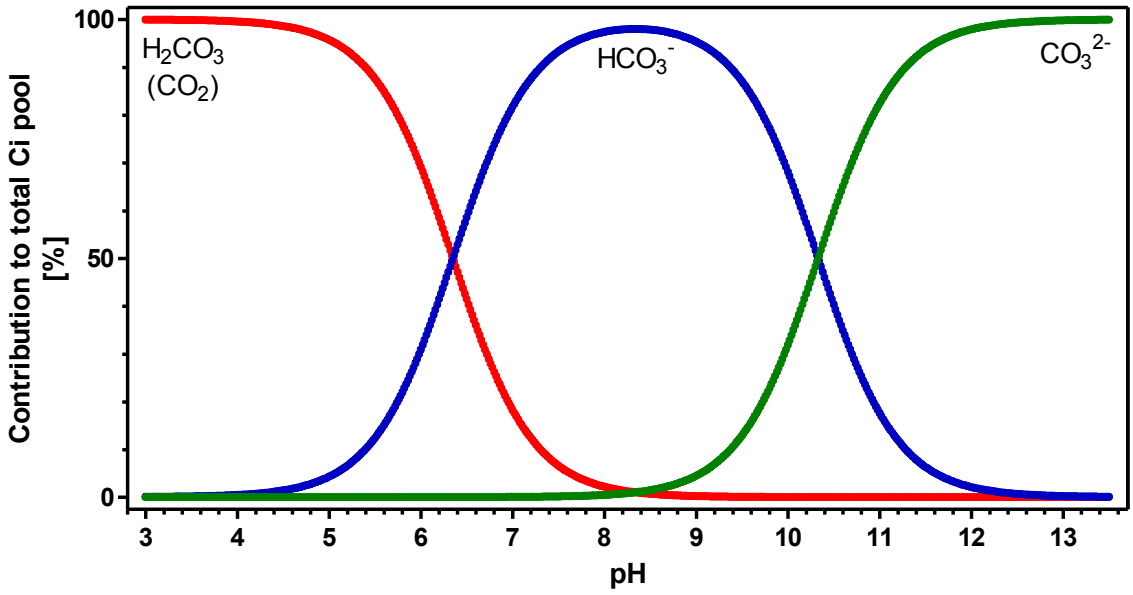

Figure 1.1: Inorganic carbon equilibria in solution, and the effect of pH on the relative contribution of each species to the total inorganic carbon pool.

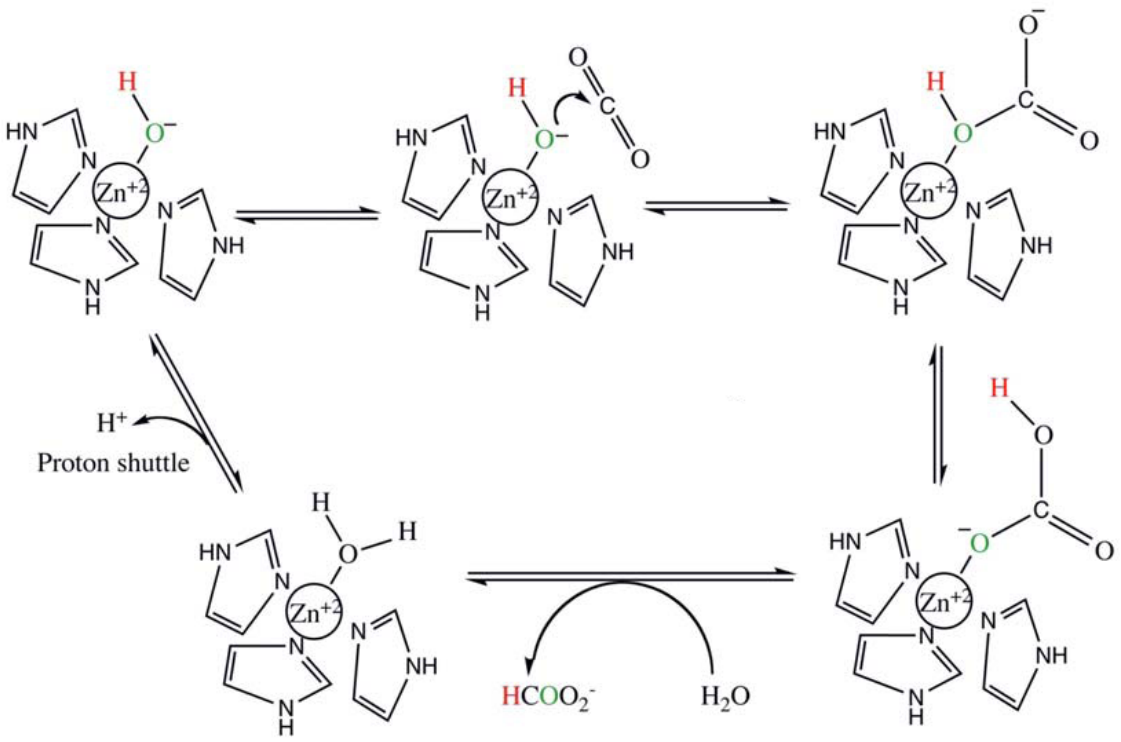

Figure 1.2: Proposed mechanism of carbonic anhydrase.

Taken from (Domsic *et al.*, 2008)

Originally proposed by (Liang and Lipscomb, 1987)

1.2 Ci sensing in prokaryotes

As a photosynthetic carbon fixing organism that is likely to be subjected to fluctuating levels of available Ci it would be advantageous to be able to sense available Ci and modify physiology accordingly. Cyanobacteria depend upon the accumulation of cytoplasmic HCO_3^- to supply the carboxysome with CO_2 for photosynthesis, carbon fixation and as such growth (Badger and Price, 1994). Indeed, a sufficient supply of HCO_3^- in the cytoplasm is of such importance to cyanobacteria that they have evolved a mechanism through which they can actively transport HCO_3^- into the cell when the extracellular supply is limited; the carbon concentrating mechanism (CCM, Figure 1.3) (Raven, 2003; Raven *et al.*, 2008).

Since the active transport of HCO_3^- into the cytoplasm is a process which consumes ATP it is likely that cyanobacteria have evolved a mechanism through which available HCO_3^- can be sensed and the transport mechanism turned on or off accordingly. In fact, it was observed that HCO_3^- uptake in *Anabaena flos-aquae* could be linked to intracellular cAMP, suggesting a cAMP signalling pathway could be involved (Franko and Wetzel, 1981).

1.2.1 *S. platensis*

Following the identification of mammalian sAC as an enzyme that has its activity increased by Ci, and the discovery that it shares significantly more sequence homology with prokaryotic ACs than mammalian tmACs, studies into the effect of Ci on prokaryotic ACs began (Buck *et al.*, 1999; Chen *et al.*, 2000). The AC activity of recombinant CyaC from *Spirulina platensis* was up-regulated by Ci *in vitro* at pH 7.5, showing an EC_{50} of 18.8 ± 1.6 mM for total Ci with a maximal stimulation seen at 30 mM total Ci (Chen *et al.*, 2000). More recent *in vitro* work has shown CyaC activity to increase almost four fold in the presence of 40 mM total Ci at pH 7.5, giving support to the earlier observation of regulation by Ci (Steegborn *et al.*, 2005b).

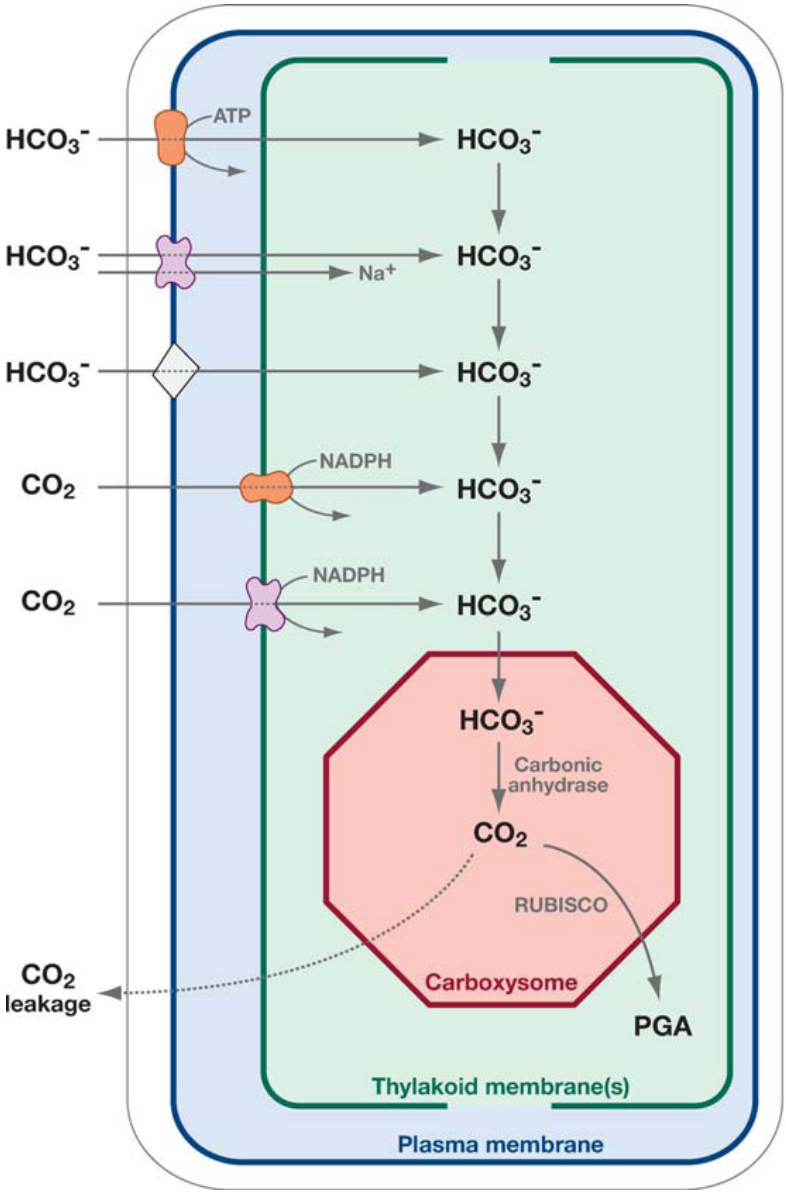

Figure 1.3: The mechanisms through which cyanobacteria obtain cytoplasmic HCO_3^-.

Taken from (Giordano *et al.*, 2005)

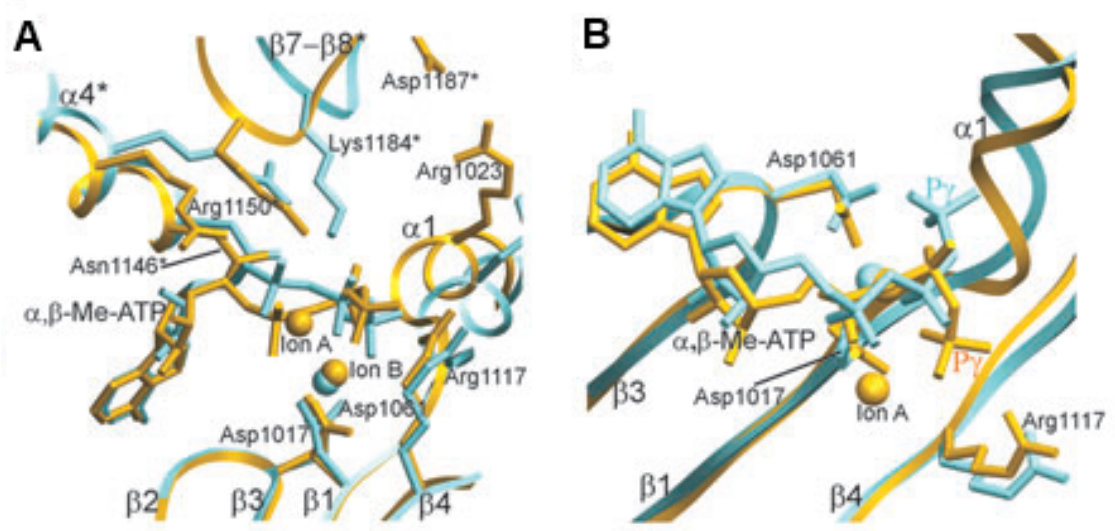

Figure 1.4: Crystal structures of *S. platensis* CyaC active site shown from different angles.

(A) Overlay of the active site before (blue) and after (yellow) the addition of HCO_3^-. **(B)** Overlay of a closer view of the active site, showing the substrate in more detail before (blue) and after (yellow) the addition of HCO_3^-.

Taken from (Steegborn *et al.*, 2005b)

Crystallisation studies have helped to provide some insight into the mechanism by which Ci stimulates these ACs. Crystals of CyaC soaked in 50 mM HCO_3^- dissolved, however, when soaked in ammonium nitrate or sodium phosphate or sodium acetate there was no effect (Steegborn *et al.*, 2005b). This suggested that Ci was specifically inducing some form of conformational change in the protein, although without further evidence this was purely speculative. Further evidence was obtained through flash soaking and freezing crystals to try and catch a glimpse of the conformational change. This method allowed the visualisation of an active site closure induced by HCO_3^-, mediated through a 4-5 Å movement of the β7-β8 loop and the α1 helix towards the centre of the CyaC dimer (Figure 1.4A) (Steegborn *et al.*, 2005b). This conformational change caused a re-orientation of the substrate ATP, causing a 180° turn of the terminal phosphate (Pγ) moiety to close proximity of an arginine group (Figure 1.4B) (Steegborn *et al.*, 2005b). It is possible that this arginine group aids the release of pyrophosphate following the synthesis of cAMP, and as such increases activity via acceleration of the rate of product release, and as such substrate uptake for a new round of catalysis (Steegborn *et al.*, 2005b).

1.2.2 *Anabaena* PCC 7120

Following the demonstration that Ci increases the activity of the Class IIIb AC CyaC from *S. platensis* investigation into the effects of Ci on other Class IIIb ACs began. The filamentous cyanobacterium *Anabaena* PCC 7120 encodes within its genome at least five adenylyl cyclases CyaA, CyaB1, CyaB2, CyaC and CyaD (Katayama and Ohmori, 1997). The ACs CyaB1 and CyaB2 were shown to possess significant sequence homology with the C_1 domain of sAC and CyaA was shown to possess significant homology with the C_2 domain of sAC (Buck *et al.*, 1999). Since the strongest homology was seen in CyaB1 this enzyme was chosen as a good candidate to begin testing whether the response to Ci was a conserved feature of Class IIIb ACs. Indeed, *in vitro* experimentation show the activity of CyaB1 to be up-regulated in the presence of Ci (Cann *et al.*, 2003). More recent research performed using *in vitro* experiments conducted under conditions of Ci disequilibrium, indicated that this enzyme may in fact respond to CO_2 directly and not HCO_3^- as was previously speculated (Hammer *et al.*, 2006).

1.2.3 *Synechocystis* PCC 6803

The genome of the freshwater photosynthetic cyanobacterium *Synechocystis* PCC 6803 encodes 3 putative nucleotide cyclases (Ochoa De Alda *et al.*, 2000; Terauchi and Ohmori, 1999). The gene *cya1* encodes an adenylyl cyclase (Slr1991) that is essential for regulation of motility in response to fluctuations in available light (Masuda and Ono, 2004; Terauchi and Ohmori, 1999). The gene *cya2* encodes a putative guanylyl cyclase (Sll0646), and although it has been subjected to some biochemical and crystallographic studies its physiological relevance has yet to be identified (Ochoa De Alda *et al.*, 2000; Rauch *et al.*, 2008). The final gene *cya3* (Sll1161) has not yet been studied, although it shares significant sequence homology with other nucleotide cyclases, and as such the question as to whether it is a nucleotide cyclase remains a mystery (Ochoa De Alda *et al.*, 2000)

Investigation has revealed Slr1991 to be the likely candidate for Ci sensing in this organism, however, there is slight ambiguity between studies as to how Slr1991 actually reacts to Ci. Early work carried out *in vitro* at pH 7.5 using a recombinant protein corresponding to the full length Slr1991 molecule showed a near 50 % inhibition of enzyme activity in the presence of 50 mM total Ci (Masuda and Ono, 2005). More recently, *in vitro* work at pH 7.5 has shown a truncated recombinant form of Slr1991 (amino acids 120-337) to increase in activity by nearly 100 % in the presence of only 20 mM total Ci (Hammer *et al.*, 2006). Furthermore, the recent study provided compelling evidence that this enzyme is in fact likely to be responsive to CO_2 and not HCO_3^- as was previously thought (Hammer *et al.*, 2006).

1.2.4 *M. tuberculosis*

Mycobacterium tuberculosis H37Rv is a pathogenic bacteria and is the main causative agent of tuberculosis. This pathogen, following entry to the lungs, is taken up by alveolar phagocytes that are unable to digest it, and subsequently the pathogen multiplies therein. *M. tuberculosis* encodes 15 putative ACs within its genome, and the production of cAMP is important for pathogenesis, and also the ability to resist degradation within the phagosome (Lowrie *et al.*, 1979). Furthermore, CO_2 has been shown to be an important molecular cue for *Mycobacterium microti* to resist degradation in the

phagosome (Lowrie *et al.*, 1975).

Two ACs from *M. tuberculosis*, Rv1625c and Rv1319c, have been shown to be stimulated by Ci (Cann *et al.*, 2003; Townsend *et al.*, 2009). It is possible that the stimulation of these ACs by Ci, resulting in the increase in cellular cAMP, provide the source of secreted cAMP needed to avoid degradation within the phagosome.

1.2.5 *C. aurantiacus*

Chloroflexus aurantiacus is a thermophilic, photosynthetic bacterium found in hot springs at temperatures up to 70°C (Pierson and Castenholz, 1974). *C. aurantiacus* produce energy through photosynthesis, harvesting light with a chlorosome containing bacteriochlorophyll *cs*, however, these anoxygenic phototrophs do not produce oxygen as a by-product of photosynthesis (Gloe and Risch, 1978). Instead of utilizing H_2O as an electron donor during photosynthesis *C. aurantiacus* (and all *Chloroflexi* species) utilise sulphur containing compounds (mainly H_2S and S_2O_3) as an electron source (Madigan and Brock, 1975).

C. aurantiacus possesses three ACs with strong sequence homology to mammalian sAC; Chlo1187, Chlo1066 and Chlo1431 (Kobayashi *et al.*, 2004). *In vitro* assays demonstrated Chlo1187 activity to be up-regulated in the presence of Ci, with an EC_{50} of 25 mM, and a nearly 10 fold increase in activity in the presence 50 mM total Ci (Kobayashi *et al.*, 2004). Although the regulation of this enzyme by Ci was demonstrated, no physiological relevance was cited and as such the full details of the Ci sensing pathway (if one exists) remain to be established.

1.2.6 *S. aurantiaca*

Stigmatella aurantiaca is a gram-negative bacteria found living in the soil and is a member of the Myxobacteria family. These Myxobacteria undergo a two phase life cycle, compromised of a vegetative growth cycle and a developmental phase in which cells aggregate into a multicellular fruiting body (myxospore) (Vasquez *et al.*, 1985). The developmental phase is initiated through nutrient depletion and is hypothesised to be similar to the formation of multicellular fruiting bodies in *Dictyostelium discoideum*, a process controlled by

cAMP signalling pathways (Coudart-Cavalli *et al.*, 1997).

S. aurantiaca possesses two ACs, CyaA and CyaB, and *in vitro* assay on CyaB have shown it to be activated by Ci, although the relevance of this is still unknown (Cann *et al.*, 2003).

1.3 Ci sensing in plants

1.3.1 RuBisCO

Although it does not represent a true sensing mechanism as such, the activation of RuBisCO by CO_2 does represent one of the earliest characterised regulatory interaction of Ci with a protein (Lorimer *et al.*, 1976). RuBisCO, which catalyses the first step in the Calvin cycle (addition of molecular CO_2 to ribulose-1,5-bisphosphate), requires CO_2 not only within its catalytic cycle but also as a covalent activator, enabling catalytic competence (Lorimer *et al.*, 1976). It was shown that formation of a carbamate, through covalent interaction of CO_2 with the ε-amino (i.e the side chain amine moiety) group of a lysine, was essential to facilitate the recruitment of a Mg^{2+} ion required for catalysis (Lorimer, 1981; Lorimer *et al.*, 1978; Lorimer and Miziorko, 1980). Furthermore, the ε-amino group of another lysine was shown to be involved in the co-ordination of substrate CO_2 to the active site, through non-covalent interaction (Lorimer *et al.*, 1993; Lorimer *et al.*, 1989).

1.3.2 Stomatal pore regulation

The stomata on plant leaves represent the main entry point for the atmospheric CO_2 required for the Calvin cycle. These small pores also represent a major site of water loss through transpiration, something that if not properly controlled can have deleterious effects for the plant (Casson and Hetherington, 2010). Due to the waxy cuticle present on plant leaves, these stomata are crucial for CO_2 entry and as such a balance must be established between CO_2 entry and H_2O loss. Due to this it is not surprising that plants possess mechanisms through which they can regulate stomatal opening and closing to maintain a balance (Vavasseur and Raghavendra, 2005). The control of stomatal opening is mediated through alterations in guard cell turgor, whereby a loss of turgor pressure results in stomata closure through an alteration in the shape of the guard cells (Taiz and Zeiger, 2006). Although the regulation of stomata in response to factors such as light and water stress are well characterised, the response to CO_2 is less well understood (Casson and Hetherington, 2010; Kinoshita *et al.*, 2001; Schroeder *et al.*, 2001). However, details are beginning to emerge, with a protein kinase and CA being shown to

be important in CO_2 induced stomatal closure in *Arabidopsis thaliana*, although the mechanism through which this occurs is not fully understood (Hashimoto *et al.*, 2006; Hu *et al.*, 2010).

It has also been known for many years that in the long term, fluctuations in atmospheric CO_2 can influence the number of stomata expressed on leaves (Woodward, 1987). Intriguingly, there is fossil evidence to suggest that long term variations in atmospheric CO_2 not only influences stomatal numbers, but also their morphology (Beerling *et al.*, 2002; Franks and Beerling, 2009). The mechanism through which plants couple atmospheric CO_2 to stomatal development is still poorly understood, however, the involvement of one gene has been demonstrated; the high carbon dioxide (*HIC*) gene (Gray *et al.*, 2000). *Arabidopsis thaliana* mutants lacking *HIC*, which encodes a protein involved in the synthesis of very long chain fatty acids, do not decrease the number of stomata in response to high CO_2, but in fact increase the number (Gray *et al.*, 2000). Although the actions of several environmental factors on stomatal development have been characterised, the mechanisms involving CO_2 still remain to be detailed (Casson and Hetherington, 2010).

1.4 Ci sensing in invertebrates

1.4.1 *D. melanogaster*

Drosophila melanogaster feed, mate and lay eggs on fallen fruit that are rapidly populated by microorganisms that cause fermentation; leading to the release of many volatile compounds including CO_2. Despite the release of CO_2 also being a marker for ripened fruit *D. melanogaster* actively avoid CO_2 (Suh *et al.*, 2004). This avoidance behaviour is possibly due to the toxicity and anaesthetising ability that CO_2 has on *D. melanogaster*, but may also be a mechanism to avoid predation through detection of CO_2 emitted from potential predators (Badre *et al.*, 2005). Furthermore, dSO (Drosophila stress odorant) released from stressed *D. melanogaster* is actively avoided by other flies and contains high levels of CO_2 among other volatile compounds (Suh *et al.*, 2004).

Research shows that hypercapnic conditions in *D. melanogaster* lead to problems such as a decreased rate of egg laying, defects in embryonic development and an increase in mortality related to bacterial infection (Helenius *et al.*, 2009). Hypercapnia specifically caused a decrease in the expression of genes related to fertility and immunity, and an increase in genes related to metabolism (Helenius *et al.*, 2009). The increased mortality due to bacterial infections was mediated through a decrease in the expression of antimicrobial peptide genes (Helenius *et al.*, 2009). Following detection of bacterial peptidoglycans, Relish (a homolog of mammalian nuclear factor κB; NF-κB) is endoproteolytically cleaved to release its N-terminal Rel homology domain (RHD) (Stoven *et al.*, 2000). The RHD activates transcription of antimicrobial peptides through binding to κB-sites on AMP promotors (Lemaitre and Hoffmann, 2007). CO_2 specifically inhibits the actions of Relish, however, the mechanism through which this occurs is not fully understood (Helenius *et al.*, 2009). This effect of CO_2 on Relish echoes the effects of CO_2 on NF-κB seen in human and mouse macrophages, and indicates that the effect of CO_2 on NF-κB (and its homologs) may be a conserved feature (Helenius *et al.*, 2009; Wang *et al.*, 2010).

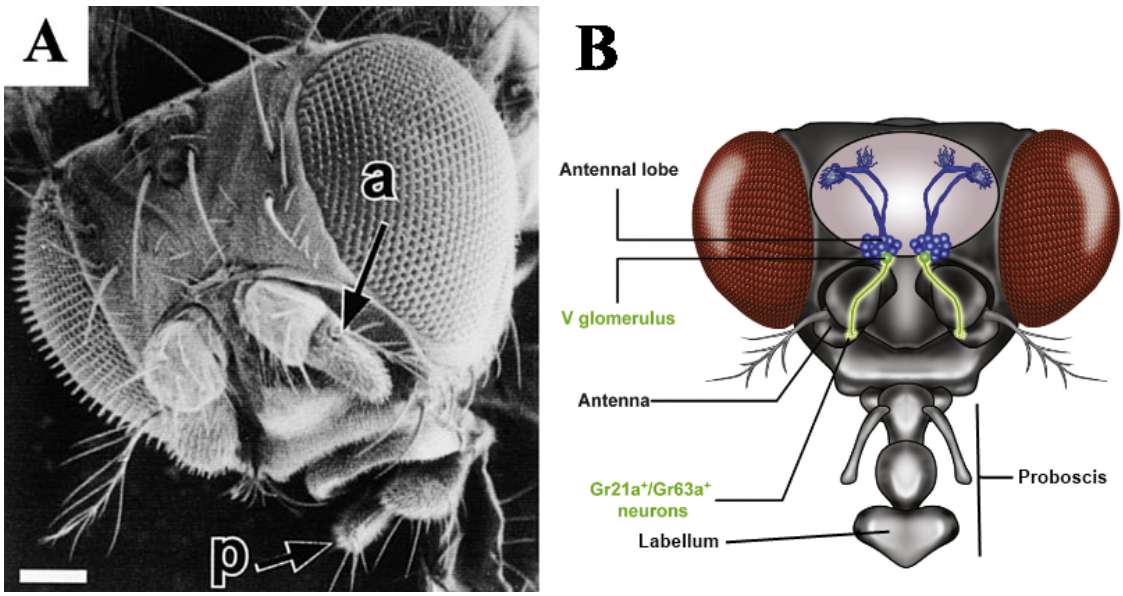

Figure 1.5: The basic anatomy of *D. melanogaster* olfactory organs.

(A) The third antennal segment (a) and maxillary palp (p). **(B)** Location of the CO_2 sensing Gr21a/Gr63a neurons, and other important features of fly olfactory and gustatory organs.

Taken from (de Bruyne *et al.*, 2001) and (Luo *et al.*, 2009)

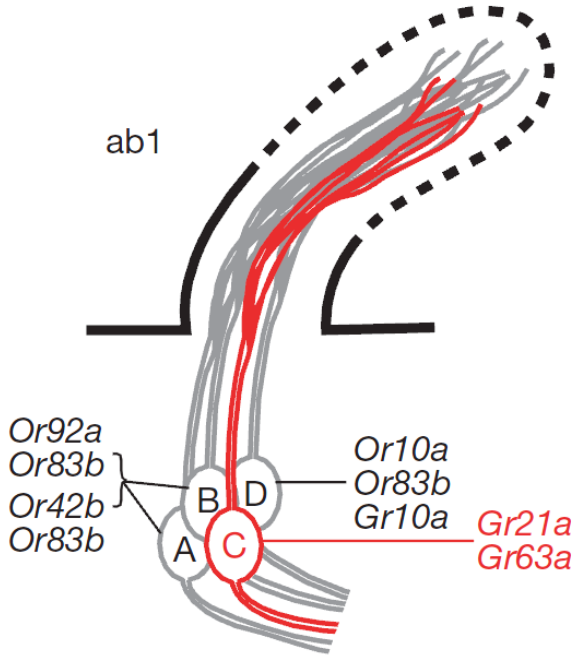

Figure 1.6: Composition of the ab1 sensillum in *D. melanogaster.*

Illustration of the ab1 sensillum, highlighting the CO_2 responsive ab1C neuron (red), and also indicating the olfactory receptors expressed in each type of neuron.

Taken from (Jones *et al.*, 2007)

D. melanogaster possess two olfactory organs; the antennae and maxillary palp (Figure 1.5) (de Bruyne *et al.*, 2001). On the antennae are found numerous small hair-like projections called sensilla (classed as basiconic, trichoid and coeloconic based on morphology) which contain the fly olfactory receptor neurons (ORNs) (Venkatesh, 1984). The basiconic sensilla are the main sites of olfactory detection (de Bruyne *et al.*, 2001; Venkatesh, 1984). Axons from ORNs located within these sensilla project directly to the antennal lobe (Figure 1.5) where different ORNs are clustered into structures called glomeruli (Gao *et al.*, 2000).

Drosophila melanogaster is known to be able to detect low levels of CO_2 and modulate its behaviour accordingly (de Bruyne *et al.*, 2001). When presented with a simple T-maze experiment, flies avoided CO_2 in a dose dependent manner, avoiding CO_2 from 0.1 % (v/v) above ambient levels (0.035 % (v/v)) (Suh *et al.*, 2004). Amputation of the third antennal segment (Figure 1.5A) removed this CO_2 avoidance behaviour (Suh *et al.*, 2004). Closer analysis using Ca^{2+} imaging identified the most ventral pair of glomeruli (the V-glomerulus; Figure 1.5B) as being involved in CO_2 detection (Suh *et al.*, 2004). The V-glomerulus is innervated by the ab1 class of ORNs (ab1A, ab1B, ab1C and ab1D) which are projected from the ab1 class of large basiconic sensilla (Figure 1.6), located on the third antennal segment. The ab1C neuron uniquely expresses the putative gustatory receptor Gr21a, a 7-transmembrane spanning receptor. These ab1C neurons are the primary site for CO_2 detection in *D. melanogaster* (Faucher *et al.*, 2006; Suh *et al.*, 2004).

Work has been carried out to establish whether Gr21a is simply a marker for CO_2 responsive neurons or is directly involved in CO_2 detection itself. Interference with *gr21a* in both adult and larval flies showed Gr21a to be a fundamental requirement of CO_2 detection (Faucher *et al.*, 2006; Jones *et al.*, 2007; Suh *et al.*, 2004). More recent work has identified a second putative gustatory receptor Gr63a in the ab1C neuron which co-expresses with Gr21a in these neurons (Jones *et al.*, 2007; Kwon *et al.*, 2007). Genetic knockout of *gr63a* produced a similar phenotype to that of *gr21a* null flies, with the ability to detect CO_2 lost (Jones *et al.*, 2007). Expression of either Gr63a or Gr21a individually in the CO_2 non-responsive ab3A neurons did not confer a CO_2 response. However, when Gr63a and Gr21a were expressed together in ab3A neurons a CO_2 response was established, suggesting that a Gr63a/Gr21a

heterodimer is required for CO_2 detection (Jones *et al.*, 2007; Kwon *et al.*, 2007). Interestingly, homologues of these two receptors have been identified in a number of other insect species (such as Gr22 and Gr24 in *Anopheles gambiae*) and may be involved in CO_2 detection in these species as well (Jones *et al.*, 2007; Robertson and Kent, 2009).

Recent investigation shows that this CO_2 avoidance behaviour can be inhibited by 2,3-butanedione and 1-hexanol (Turner and Ray, 2009). This effect was mediated through a direct inhibition of the CO_2 responsive ab1C neurons (Turner and Ray, 2009). These two compounds are found in *D. melanogaster* food sources, especially certain ripe fruits, and may serve as a means of overcoming innate CO_2 avoidance in favour of allowing feeding (Turner and Ray, 2009).

Whereas detection of gaseous CO_2 in the olfactory system provokes an avoidance behaviour in *D. melanogaster*, recent studies have shown that detection of aqueous CO_2 in the gustatory system has the opposite effect (Fischler *et al.*, 2007). It is possible that the acceptance behaviour initiated by CO_2 in solution could be a method through which *D. melanogaster* permit the feeding on microorganisms. Although the presence of microorganisms will eventually cause a rise in local CO_2 (a condition potentially harmful to *D. melanogaster*) there will be an initial period where atmospheric CO_2 is low and as such feeding could be beneficial. Research indicated that detection of aqueous CO_2 was mediated through E409 gustatory neurons, which innervate sensilla located on the labellum of the proboscis (Figure 1.5) (Fischler *et al.*, 2007). The exact molecular mechanism through which CO_2 sensing in these neurons occurred was not identified (Fischler *et al.*, 2007).

1.4.2 Mosquitos

Haematophagous (blood feeding) insects require acute sensory systems to enable them to identify and locate their hosts over potentially large distances. Female mosquitoes are able to detect various olfactory cues, such as plumes of CO_2 exhaled from the host, and utilise them to direct their flight to locate a host for oviposition (Bowen, 1991; Gillies, 1980). Since haematophagous insects such as mosquitoes are major disease vectors, research into the mechanisms of host-detection are vital. Such disease carrying CO_2 sensing mosquitoes include *Anopheles gambiae* (malaria), *Culex quinquefasciatus* (filariasis) and

Aedes aegypti (yellow and dengue fever) (Cooperband and Carde, 2006b; Dekker *et al.*, 2005; Healy and Copland, 1995). Research into the ability of mosquitoes to use CO_2 as a cue for host location has led to the development of CO_2 traps (traps that emit CO_2 to attract mosquitoes) as a means to controlling populations (Burkett *et al.*, 2001; Cooperband and Carde, 2006a, b; Reisen *et al.*, 2000).

Removal of the maxillary palp (Figure 1.7) of *Culex* mosquitoes removed the response to CO_2, identifying this organ as the likely site of CO_2 detection (Omer, 1971). More recent studies have confirmed that CO_2 detection is mediated through the maxillary palp, more specifically through capitate peg sensilla (Figure 1.7) containing cpA ORNs (Lu *et al.*, 2007). Receptors homologous to Gr63a/Gr21a from *D. melanogaster* were identified in *A. gambiae*; AgGr22 and AgGr24 (Jones *et al.*, 2007; Robertson and Kent, 2009). The response to CO_2 was confirmed to be dependent upon the co-expression of these two 7-transmembrane spanning receptors (Lu *et al.*, 2007). Furthermore, a third receptor AgGr23 was identified and although its co-expression was not a total requirement for CO_2 detection, its presence seemed to enhance the sensitivity of CO_2 detection (Lu *et al.*, 2007).

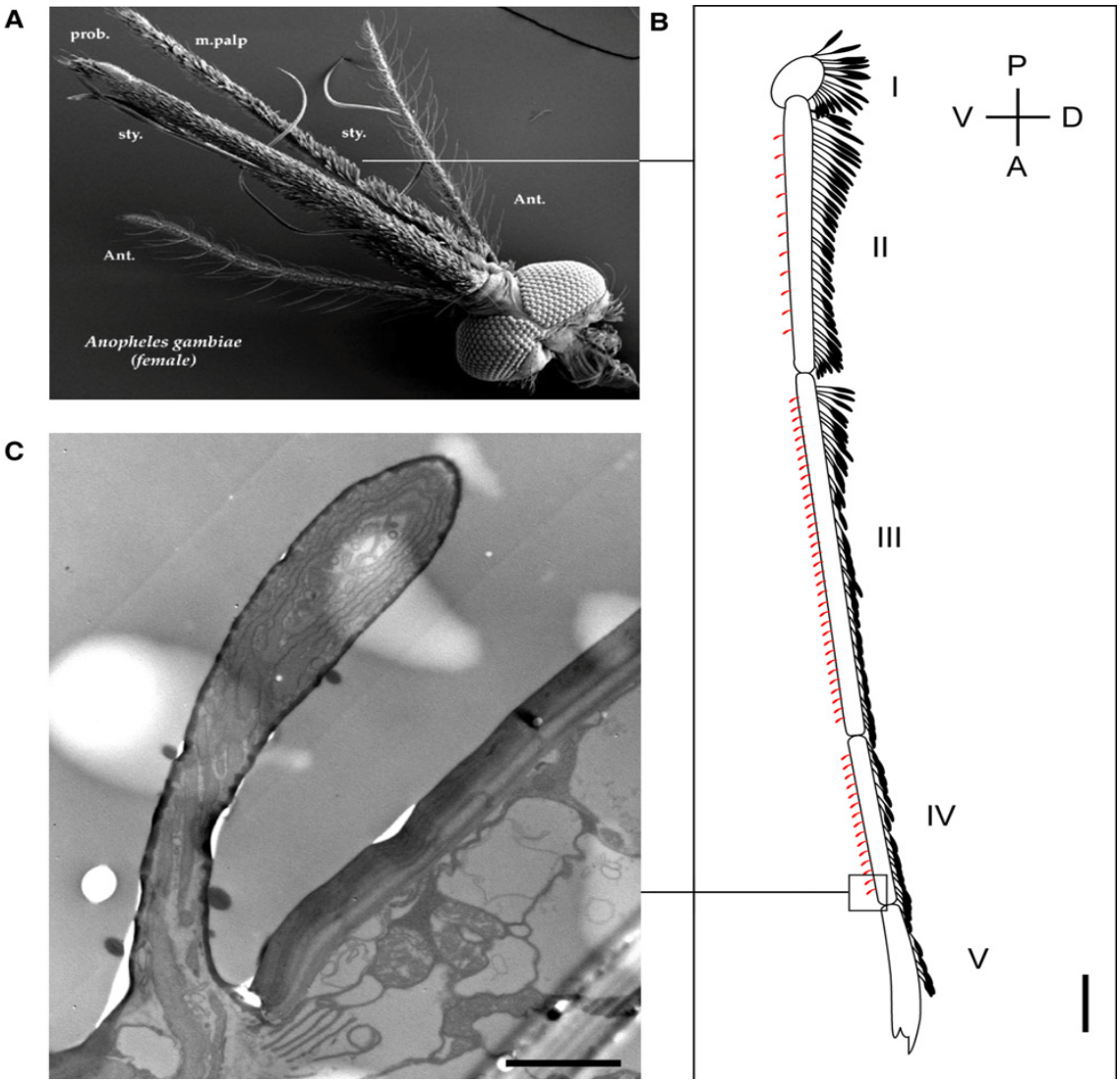

Figure 1.7: Basic anatomical features of female *A. gambiae* olfactory appendages.

(A) Scanning electron micrograph of the olfactory appendages **(B)** An illustration of the maxillary palp, highlighting the capitate pegs (red). **(C)** Transmission electron micrograph of an individual capitate peg sensillum.

Taken from (Lu *et al.*, 2007)

1.4.3 Other insects

The moth *Manduca sexta*, and other related moth species, are known to sense elevated CO_2 produced by flowering plants through receptor cells in the labial-palp pit organ (Guerenstein *et al.*, 2004a). It seems that certain night-blooming plants, such as *Datura wrightii* which is primarily pollinated by *M. sexta*, emit plumes of CO_2 during periods of high nectar availability (Guerenstein *et al.*, 2004b; Thom *et al.*, 2004).

Certain plant predatory insect larvae such as the larvae of *Diabrotica virgifera* and *Helicoverpa armigera* use elevated levels of CO_2 to locate food (Bernklau, 1998; Bernklau *et al.*, 2004; Rasch, 1994). Numerous subterranean termites of the *Reticulitermes* species are also known to use CO_2 gradients in the soil to guide themselves towards food (Bernklau *et al.*, 2005). Since these species feed on living and decaying (both sources of CO_2) plant matter, CO_2 would appear to be a useful environmental cue for food location.

Colonies of the honey-bee *Apis melifera* are also known to initiate fanning behaviour to ventilate the hive following detection of elevated CO_2 (Seeley, 1974). Elevated levels of CO_2 pose a risk to developing larvae and adults, and as such this fanning behaviour is vital to the survival of the colony.

Tsetse flies (*Glossina* species), the major disease vector for trypanosomes, are attracted to CO_2 exhaled from livestock and use it as a directional cue to find hosts (Willemse and Takken, 1994).

1.4.4 *C. elegans*

The nematode *Caenorhabditis elegans* feeds on bacteria found in compost and decomposing fruit, environments which are subjected to wide concentration ranges of O_2 and CO_2. High levels of CO_2 in the soil would likely cause an increase in CO_2 within the body of *C. elegans*, potentially causing an increase in cellular acidity. It would be expected that these two increases would have an adverse affect on the physiology of *C. elegans*, and in fact recent research has shown that hypercapnia (an increase in CO_2) within *C. elegans* causes impaired motility, decreased fertility and slowed development (Sharabi *et al.*, 2009a).

C. elegans was shown some time ago to alter its direction of motility in response to HCO_3^- gradients, but the effects of CO_2 were not studied

(Dusenbery, 1974). Recent investigation shows that *C. elegans* actively avoid areas with elevated CO_2 in a dose-dependent manner, displaying an avoidance of CO_2 at 0.5 % (v/v) and above (Bretscher *et al.*, 2008; Hallem and Sternberg, 2008). This avoidance was specific to CO_2 and was not due to acidification or increased HCO_3^- caused by CO_2 entering solution in the plate media (Bretscher *et al.*, 2008). Mutational studies have revealed that this CO_2 avoiding behaviour is dependent upon a cGMP gated ion channel encoded by *tax-2* and *tax-4*, with mutations in either gene disrupting the ability to sense CO_2 (Bretscher *et al.*, 2008). The involvement of Tax-2 and Tax-4 has been confirmed and also the receptor guanylyl cyclase Daf-11 has been shown to be a requirement for CO_2 sensing in this system (Hallem and Sternberg, 2008). 12 neurons in *C. elegans* co-express Tax-2 and Tax-4, and of those it was shown that the BAG neurons were mainly responsible for the CO_2 response with the ASH, ADL and AWB neurons playing a minor role in CO_2 avoidance (Figure 1.8) (Hallem and Sternberg, 2008).

Since the bacteria which *C. elegans* feeds off are responsible for elevating the local CO_2 concentration it was surprising that *C. elegans* avoided CO_2 since it would appear to be a good marker for the presence of food. It was discovered that if *C. elegans* was starved prior to the application of a CO_2 gradient then the CO_2 avoidance behaviour was abolished (Bretscher *et al.*, 2008; Hallem and Sternberg, 2008). It is possible that since the benefits of feeding for a starved animal outweigh potential deleterious effects of elevated CO_2 that a mechanism has evolved to overcome the innate avoidance behaviour. Once the worm has fed, and CO_2 levels begin rising (or were already high), the CO_2 avoidance behaviour would cause the worm to leave that environment in search of better feeding grounds.

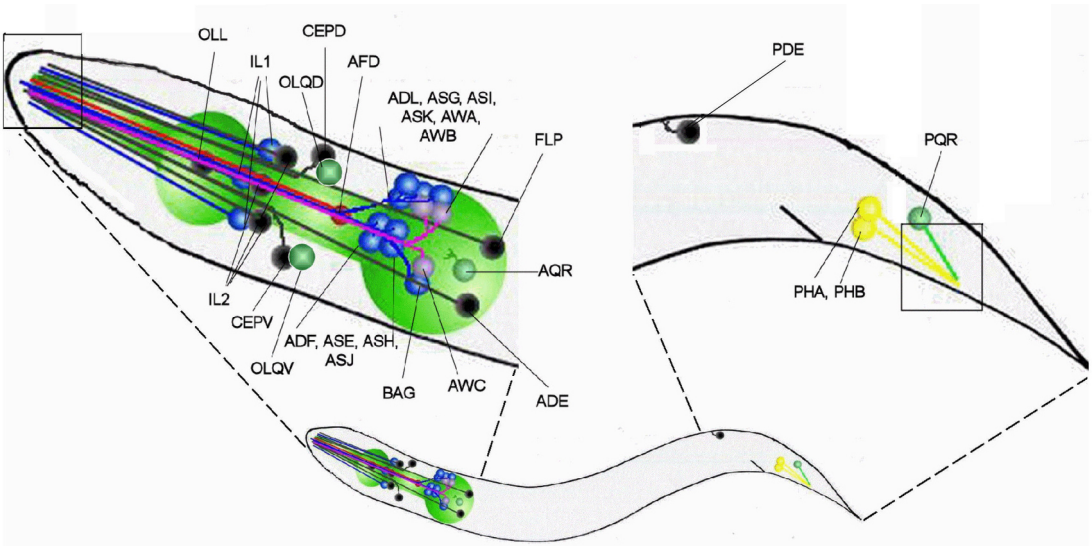

Figure 1.8: Relative location of all chemosensory cilia and ciliated neurons in *C. elegans*.

Taken from Inglis, P.N. *et al.* The sensory cilia of *Caenorhabditis elegans* (March 8, 2007), WormBook, ed. The *C. elegans* Research Community, WormBook, doi/10.1895/wormbook.1.126.2, http://www.wormbook.org.

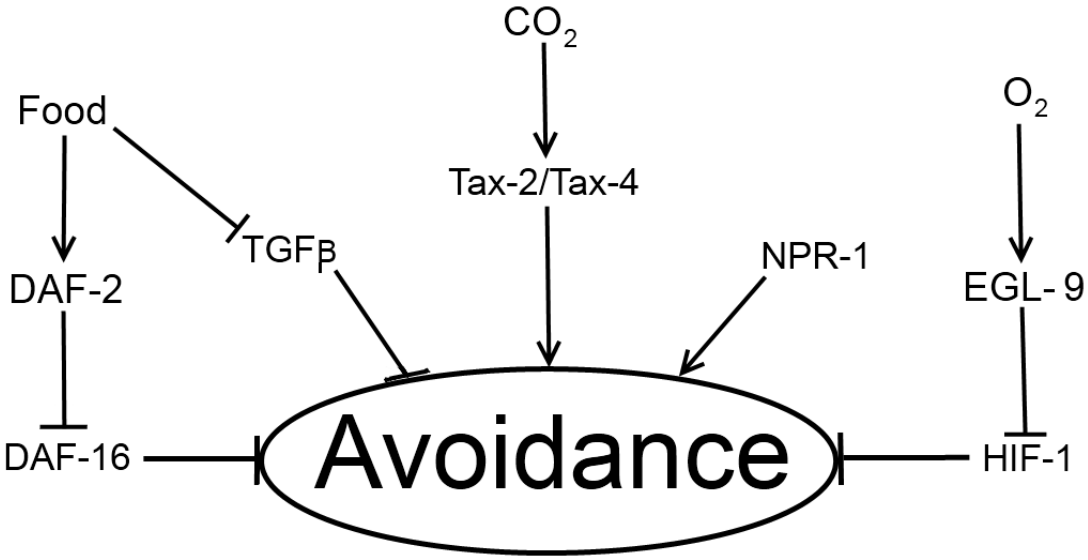

Figure 1.9: A model for the CO_2 avoidance pathway in *C. elegans*.

Further investigation has revealed the CO_2 sensing pathway in this organism to be surprisingly complex (Figure 1.9), with several other pathways modulating the ability of Tax-2/Tax-4 to elicit a CO_2 avoidance behaviour. Firstly, work shows that starved animals have a lowered activation of the abnormal dauer formation 2 (DAF-2) insulin-like receptor pathway, with a subsequently higher activation of the DAF-16 forkhead transcription factor leading to a depression of the CO_2 avoidance behaviour (Bretscher *et al.*, 2008; Hallem and Sternberg, 2008). Secondly, it has been shown that in starved animals the transforming growth factor β (TGFβ) pathway is able to depress the CO_2 avoidance behaviour in a similar fashion (Hallem and Sternberg, 2008). Thirdly, the CO_2 avoidance behaviour is also reduced through the activation of hypoxia inducible factor 1 (HIF-1) under hypoxic conditions (Bretscher *et al.*, 2008). Finally, the natriuretic peptide receptor A (NPR-1) has also been shown to be capable of modulating the CO_2 avoidance behaviour (Bretscher *et al.*, 2008; Hallem and Sternberg, 2008).

1.4.5 Fungi

The fungus *Cryptococcus neoformans*, which lives in pigeon guano among other locations, is an opportunistic pathogen that often infects patients with a depressed immune system (such as those suffering from acquired immunodeficiency syndrome (AIDS)). Outside of the host it is exposed to near atmospheric (about 0.035 % (v/v)) levels of CO_2, but following spore inhalation and subsequent entry into the vascular system is exposed to concentrations around 5 % (v/v). Aside from being able to tolerate this large fluctuation in CO_2 levels *C. neoformans* uses increased CO_2 as a molecular cue (as well as pH 7.4, 37°C and serum) to initiate synthesis of the polysaccharide capsule; an important virulence trait (Granger *et al.*, 1985). Although this response to CO_2 was documented long ago it was only relatively recently that the mechanism through which this CO_2 increase was signalled was identified.

Two CAs (Can1 and Can2) were identified in *C. neoformans*, and through mutational studies Can2 was shown to be involved in CO_2 sensing (Bahn *et al.*, 2005; Mogensen *et al.*, 2006). Not only was Can2 shown to be involved in the initiation of synthesis of the polysaccharide capsule but also was shown to prevent mating in response to high CO_2 (Bahn *et al.*, 2005). Although Can2 is involved in sensing CO_2 it was unlikely to be the actual molecular sensor since

can2 mutants were still able to respond to CO_2 albeit at much higher levels. This was proposed to be due to the fact that CO_2 naturally but slowly equilibrates into HCO_3^-, and that HCO_3^- is the species of Ci sensed (Bahn *et al.*, 2005). The observation that *in vitro* assays on a *C. neoformans* adenylyl cyclase (Cac1) showed activity to increase in the presence of Ci lead to the proposed mechanism (Figure 1.10) citing Cac1 as the molecular sensor (Klengel *et al.*, 2005; Mogensen *et al.*, 2006). However, the actual molecular species of Ci (HCO_3^- or CO_2) that Cac1 responds to has not yet been proven. Due to the apparent importance of CA in this system, and the ease with which inhibitors specific to it can be developed, Can2 appears a desirable pharmacological target. As such, Can2 has been subjected to crystallisation and inhibitor trials (Schlicker *et al.*, 2009).

Another pathogenic fungus which routinely infects patients with a depressed immune system is *Candida albicans*. This fungus, found naturally in the gastrointestinal and genito-urinary tracts, forms cylindrical cells in tubular arrays known as hyphae following invasion of mucosal linings. CO_2 has been shown to be induce this virulence trait through activation of a cAMP signalling pathway, however, until recently the mechanism through which this occurred was not fully understood (Rocha *et al.*, 2001). Mutational studies on *C. albicans* demonstrated the importance of a CA (Nce103) on pathogenesis under conditions of limited CO_2 (Klengel *et al.*, 2005). More importantly, research revealed that the activity of a *C. albicans* adenylyl cyclase (Cdc35) was increased in the presence of Ci, implicating it as the CO_2 sensor in *C. albicans*. *In vitro* experiments showed Cdc35 to be more sensitive to changes in Ci than Cac1, and it could be speculated that this difference in sensitivity is the reason for the differential requirement for CA between these two species (Bahn *et al.*, 2005; Klengel *et al.*, 2005).

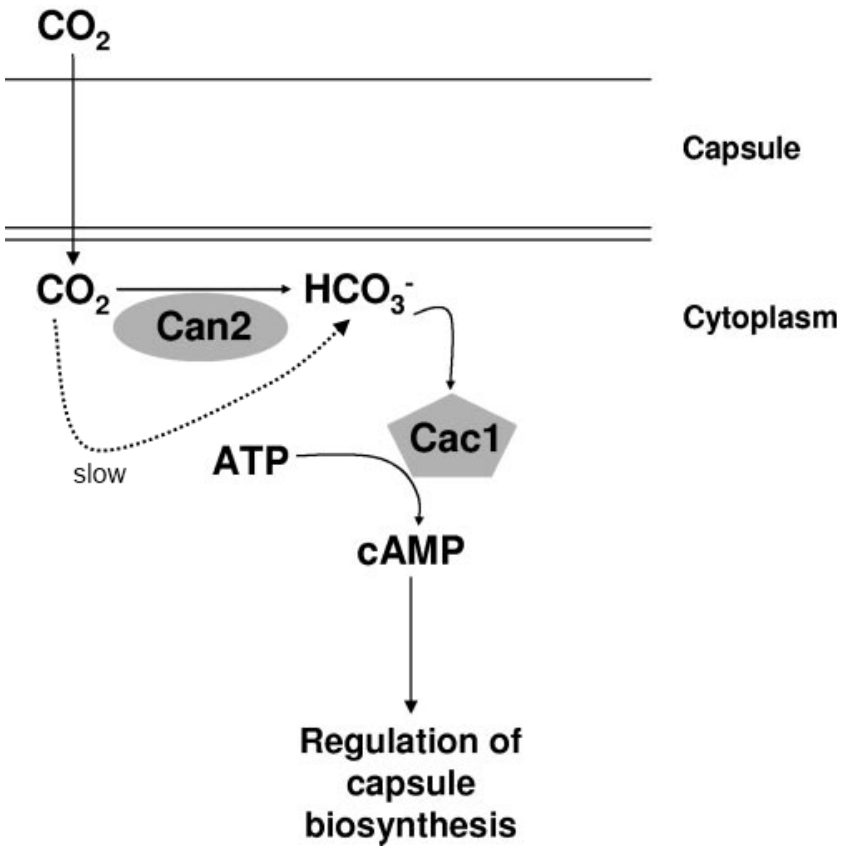

Figure 1.10: Proposed model for CO_2 sensing in *C. neoformans*.

Adapted from (Mogensen *et al.*, 2006)

1.5 Ci sensing in mammals

1.5.1 AC

1.5.1.1 General

The second messenger adenosine 3', 5'-monophosphate (cyclic AMP / cAMP) is produced from adenosine triphosphate (ATP) by a family of highly prevalent enzymes; adenylyl cyclases (ACs) (Sutherland *et al.*, 1962). ACs are found in both eukaryotes and prokaryotes, and are highly diverse in their structure and biochemistry, and as such have been grouped into 6 different Classes (Danchin, 1993). The Class I cyclase homology domain (CHD) includes ACs that are involved in the regulation of catabolic operons in enteric bacteria such as *Escherchia*, *Salmonella*, and *Haemophilus* species (Danchin, 1993). Class II CHDs are virulence factors produced by the pathogens *Bordetella pertussis* and *Bacillus anthracis* (Danchin, 1993; Drum *et al.*, 2002; Ladant and Ullmann, 1999). The Class III CHD is commonly referred to as the 'Universal' Class, since this Class comprises ACs and guanylyl cyclases (GCs) from both eukaryotes and prokaryotes (Danchin, 1993; Linder and Schultz, 2003). It is within Class III that the majority of ACs are placed, and as such has been further divided into 4 sub-Classes (a-d; see Table 1.1) (Linder and Schultz, 2003). Classes IV, V and VI CHDs include ACs from the species *Aeromonas hydrophila, Prevotella rumenicola* and *Rhizobium etli* respectively (Cotta *et al.*, 1998; Sismeiro *et al.*, 1998; Tellez-Sosa *et al.*, 2002).

Mammals express 10 ACs in total; 9 Class IIIa transmembrane ACs (tmACs) and one Class IIIb soluble AC (sAC) (Cooper, 2003b; Kamenetsky *et al.*, 2006).

1.5.1.2 tmAC

The tmACs are selectively expressed in various tissues, and are involved in the regulation of diverse physiological processes, ranging from memory formation to olfaction (Cooper, 2003b; Kamenetsky *et al.*, 2006; Sunahara and Taussig, 2002). Type I AC was shown to be specifically expressed in the brain, retina and adrenal medulla, indicating that is was likely to be neural specific (Pfeuffer *et al.*, 1985; Xia *et al.*, 1993). Type II AC is highly expressed in the brain, and to a lesser extent in the olfactory epithelium and lungs (Feinstein *et*

al., 1991). Type III AC was originally thought to be specifically expressed in sensory neuronal cilia in the nose, but was later shown to be more widely expressed, including tissues such as the brain, heart and lungs (Bakalyar and Reed, 1990; Xia *et al.*, 1992). Type IV AC is widely expressed in the body, with mRNA identified in tissues such as the lungs, liver, kidney and brain (Gao and Gilman, 1991). Type V AC is predominantly expressed in the heart, however, it was also identified in the brain (Ishikawa *et al.*, 1992; Katsushika *et al.*, 1992; Premont *et al.*, 1992). Type VI AC is highly expressed in the brain, but also to a lesser extent in the heart, kidneys and liver (Katsushika *et al.*, 1992; Premont *et al.*, 1992; Yoshimura and Cooper, 1992). Type VII AC is predominantly expressed in the lung, spleen and heart, but also to a lesser extent in the brain (Krupinski *et al.*, 1992; Watson *et al.*, 1994). Type VIII AC is localised to specific regions in the brain (Cali *et al.*, 1994). Type IX AC is widely distributed in the body, in tissues such as skeletal muscle, kidney and brain (Premont *et al.*, 1996).

Regulation by heterotrimeric G-proteins represents a major mechanism through which the production of cAMP by tmACs can be controlled (Cooper, 2003b; Defer *et al.*, 2000; Sunahara and Taussig, 2002). G proteins, which are membrane bound, are usually coupled to a membrane spanning receptor, which upon binding of its cognate ligand causes dissociation of the βγ and α subunits of the G-protein. Following dissociation, the βγ subunit of the G-protein can effect the catalytic activity of tmACs, stimulating type II, IV and VII, and inhibiting type I (Cooper, 2003b; Defer *et al.*, 2000). The α subunits, following dissociation, effects tmACs in different ways depending upon the type of G-protein and tmAC, for example the α subunit of the stimulatory G protein ($G\alpha_s$) stimulates all tmACs, however, the α subunit of the inhibitory G protein ($G\alpha_i$) only inhibits type I, V and VI (Cooper, 2003b; Defer *et al.*, 2000). Investigation into the biochemical and regulatory properties of tmACs has been aided by the construction of a 'soluble' tmAC. Work by Tang and Gilman demonstrated that the catalytic domains (C_1 and C_2) of tmACs could be expressed individually in *E. coli*, and when the two domains were combined, produced a catalytically active AC with properties very similar to the native enzyme (Tang and Gilman, 1995).

Class	Defining motifs	Class distribution
IIIa	(F/Y)XX(F/Y)D motif forming dimer interface. EKI**K** motif (**K** is substrate defining). Arm region required for catalytic domain dimerization 14 amino acids long.	Mammalian tmAC Higher eukaryotes e.g. mammals, *D. melanogaster*, *M. tuberculosis*, *S. platensis*
IIIb	Substrate defining D changed for T or S. Phosphate-binding R often changed for G or S. Arm region mostly 15 amino acids.	Mammalian soluble AC. Some gram negative bacteria (e.g. cyanobacteria and *P. aeruginosa*), *M. tuberculosis*, *Plasmodium*, *E. gracilis*
IIIc	Arm region reduced (7-11 amino acids) or absent. Considerable plasticity in canonical catalytic domains.	Some gram positive bacteria (e.g. *S. coelicolor* and *B. liquefaciens*)
IIId	YEV**K**T motif (**K** is substrate defining). Arm region 13 amino acids.	Protozoa and fungi

Table 1.1: Defining features of AC Class III sub-Classes.

Taken from (Cann, 2004)

Another mechanism through which regulation of the activity of tmACs can occur is mediated by phosphorylation by certain kinases, commonly through the cAMP dependent protein kinase (PKA) or protein kinase C (PKC) (Cooper, 2003b; Defer *et al.*, 2000). The effects of PKA and PKC vary depending upon the particular kinase isoform and type of tmAC, for example type V and VI ACs are inhibited by phosphorylation by PKA, however, the remaining 7 tmACs are unaffected (Cooper, 2003b; Defer *et al.*, 2000; Sunahara and Taussig, 2002). Receptor tyrosine kinase has also been shown to regulate tmAC activity, specifically increasing the activity of type VI AC through phosphorylation (Tan *et al.*, 2001). Furthermore, calmodulin kinase II and IV are known to phoshorylate and cause an inhibition of type III and I ACs, respectively (Wayman *et al.*, 1996; Wei *et al.*, 1996).

Ca^{2+} is another key regulator of tmAC activity, a process that is mediated through either the action of free Ca^{2+} on tmACs, the action of Ca^{2+}-bound calmodulin, or the activation of calmodulin kinases (Cooper, 2003a; Defer *et al.*, 2000; Kamenetsky *et al.*, 2006; Sunahara and Taussig, 2002). Ca^{2+}-bound calmodulin is able to stimulate the activity of certain tmAC isoforms, such as type I and VIII ACs (Cooper, 2003a; Kamenetsky *et al.*, 2006). Although high concentrations of free Ca^{2+} are able to inhibit all tmAC isoforms, sub-micromolar concentrations of free Ca^{2+}, independently of calmodulin, is able to inhibit type V and VI ACs (Cooper, 2003a; Kamenetsky *et al.*, 2006). This inhibition by Ca^{2+} has recently been shown to occur through binding to one of the metal ion binding sites, preventing binding of the second Mg^{2+} ion, and as such the conformational change required for catalysis does not occur (Mou *et al.*, 2009).

The effects of Ci on the activity of tmACs has been studied twice previously, however, the results obtained are contradictory (Chen *et al.*, 2000; Xie *et al.*, 2006). Early *in vitro* investigation, performed on a recombinant 'soluble' tmAC at pH 7.5 in the absence of any tmAC activators, did not detect a significant difference between basal tmAC activity and that in the presence of 40 mM total Ci (Chen *et al.*, 2000). More recently, *in vitro* experiments on type III tmAC, expressed and purified from mammalian cells, have shown a pH dependent stimulation of this AC by 25 mM total Ci, with a stimulation being seen between pH 7.2 and pH 8.2 (Xie *et al.*, 2006).

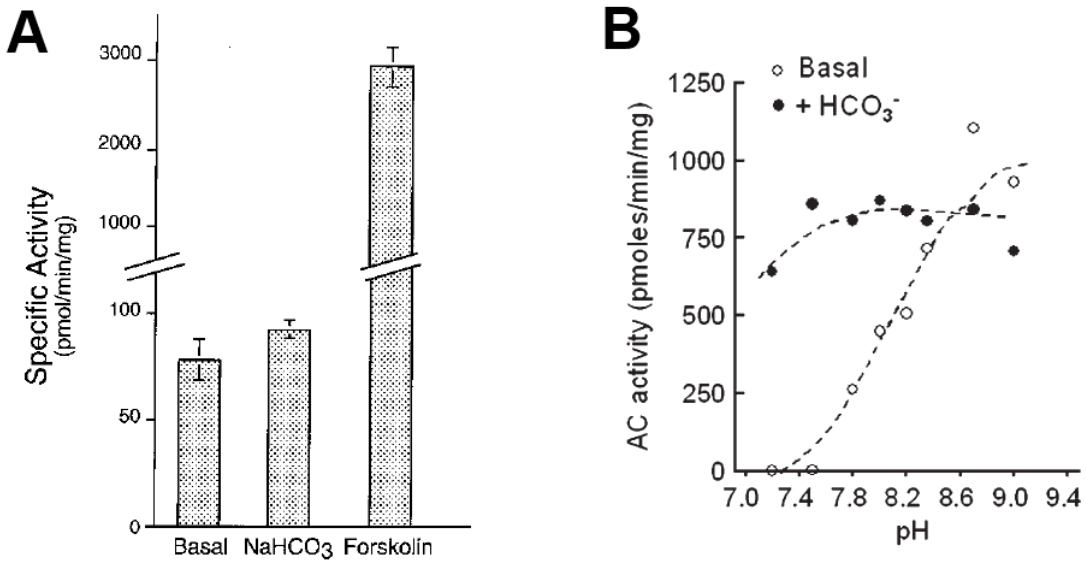

Figure 1.11: Previous *in vitro* Ci assays performed on mammalian tmAC.

(A - Chen *et al.*) *In vitro* assay was performed on an 'engineered' soluble tmAC ($5C_1 \bullet 5C_2$). Assay contained 50 mM Tris-HCl pH 7.5, 40 mM $MgCl_2$, 10 mM ATP. With or without 50 mM HCO_3^- or 100 µM forskolin. **(B - Xie *et al.*)** *In vitro* assay was performed at 37°C for 20 minutes, with native tmAC type III, purified from HEK 293 cells. Assay contained 40 mM Tris-HCl, 5 mM $MgCl_2$, 0.2 mM cAMP, 10 mM phosphoenolpyruvate, 3 units of pyruvate kinase, 10 µM GTP, 1 mM ATP. With or without 25 mM $NaHCO_3$.

Taken from (Chen *et al.*, 2000; Xie *et al.*, 2006)

1.5.1.3 sAC

While the tmACs are found in various tissues, sAC was originally found to be expressed highly in tissues and cells exposed to high fluxes of HCO_3^-, including sperm, testes, kidney and the choroid plexus (Braun and Dods, 1975; Braun *et al.*, 1977; Buck *et al.*, 1999; Chen *et al.*, 2000). However, the use of more sensitive methods has indicated that sAC is present in almost all tissues tested, albeit at lower levels than that of the tissues originally identified (Sinclair *et al.*, 2000; Xie and Conti, 2004). Two splice variants of sAC were originally identified, 48 kDa (referred to as truncated sAC: sAC_t) and 187 kDa (referred to as full-length sAC: sAC_{fl}) isoforms, of which sAC_t represents the predominantly active form in sperm (Buck *et al.*, 1999; Jaiswal and Conti, 2001). Although the role of sAC_{fl} has not yet been identified, it has been shown to possess an autoinhibitory domain on the C-terminus of the protein (Chaloupka *et al.*, 2006). Interestingly, a third isoform of sAC has been identified more recently in somatic tissues, however, its role remains unknown (Farrell *et al.*, 2008).

In vivo and *in vitro* studies on sAC_t have shown that its activity is up-regulated in the presence of Ci and Ca^{2+}, and is likely to be a sensor for these two species, although the species of Ci (CO_2 or HCO_3^-) that it responds to is still unproven (Chen *et al.*, 2000; Hammer *et al.*, 2006; Litvin *et al.*, 2003; Zippin *et al.*, 2001). Although sAC_t is not membrane bound, it is currently thought to be located in specific signalling microdomains within the cell, such as domains within the nucleus, mitochondria and microtubules (Bundey and Insel, 2004; Feng *et al.*, 2006; Feng *et al.*, 2005; Sayner *et al.*, 2006; Zippin *et al.*, 2010; Zippin *et al.*, 2003; Zippin *et al.*, 2004).

1.5.1.4 The role of sAC in sperm

Mammalian sperm, stored in the testis are immotile and incapable of successfully fertilizing an egg (Visconti *et al.*, 1999). In order for sperm to develop progressive forward motility and acquire fertilisational competence, they must complete a series of defined maturational events collectively termed as capacitation (Visconti *et al.*, 1995a; Visconti *et al.*, 1995b; Visconti *et al.*, 1999). Sperm capacitation is initiated by an increase in cytoplasmic Ci and Ca^{2+}, following ejaculation into the female reproductive tract (Visconti *et al.*, 1999). During capacitation a number of distinct changes in the sperm can be detected,

including changes in plasma membrane composition, altered protein tyrosine phosphorylation, acquisition of hyper-activated motility, and the ability to undergo acrosomal exocytosis (Visconti *et al.*, 2002). A defining hallmark of capacitated sperm is a distinct pattern of protein tyrosine phosphorylation, which is regulated by a cAMP dependent pathway involving the cAMP dependent protein kinase (PKA) (Breitbart and Naor, 1999; Visconti *et al.*, 1995b). These capacitation events are dependent upon signalling pathways involving the second messenger cAMP (Visconti *et al.*, 1999).

Following the identification of sAC, it was shown through *in vitro* experiments that sAC_t was activated by Ci (Chen *et al.*, 2000). The activation of sAC_t by Ci was also confirmed through *in vivo* experiments performed on rat sperm (Jaiswal and Conti, 2001). This activation by Ci, combined with the fact that sAC_t is highly expressed in sperm, indicated that sAC_t was involved in the initiation of capacitation events in sperm (Chen *et al.*, 2000). The importance of sAC in sperm activity was later highlighted through mutational studies performed on mice (Esposito *et al.*, 2004). Mice that carried a $sAC^{-/-}$ genotype were sterile, and although sAC was shown to be widely expressed in the body, displayed a normal phenotype with no other obvious abnormalities (Esposito *et al.*, 2004; Sinclair *et al.*, 2000). However, this apparently normal phenotype (with the exception of being sterile) has recently been proposed to be due to an isoform of sAC specifically expressed in somatic cells (Farrell *et al.*, 2008).

The $sAC^{-/-}$ sperm were shown to develop normally in the testes, but displayed impaired motility with a complete lack of forward progressive movement, a feature that could be restored through the addition of cAMP (Esposito *et al.*, 2004). Further evidence to support the role of sAC in capacitation was gained through studies on wild type sperm using the sAC specific inhibitor KH7 (Hess *et al.*, 2005). Under conditions conducive to *in vitro* fertilisation, application of KH7 prevented protein tyrosine phosphorylation and *in vitro* fertilisation in response to high concentrations of extracellular HCO_3^-, and again this was overcome with the addition of cAMP (Hess *et al.*, 2005).

1.5.1.5 sAC and membrane channels

Mature sperm are stored in the lumen of the epididymis in an inactive state, maintained by a low HCO_3^- concentration (about 2.5 mM) and acidic pH (about pH 6.7) (Levine and Marsh, 1971). The acidic pH in the lumen of the epididymis is maintained by the vacuolar H^+-ATPase (V-ATPase), which is located on the apical membrane of clear cells (Breton *et al.*, 1996). The function of V-ATPase is dependent upon HCO_3^- and its activity is controlled through the cycling of V-ATPase between the apical membrane and cytoplasmic vesicles (Breton *et al.*, 1998; Breton *et al.*, 2000; Brown and Breton, 2000). It was shown that sAC_t was present in clear cells, but not the surrounding epididymal cells, and that sAC_t was involved in regulating the cycling of V-ATPase from cytoplasmic vesicles and the apical membrane (Pastor-Soler *et al.*, 2003). How sAC_t regulates this system is still unknown, but it is proposed that it acts as a chemosensor for lumenal HCO_3^-. It is possible that in response to an increase in lumenal HCO_3^-, activation of sAC_t initiates a cAMP signalling cascade promoting V-ATPase cycling to the apical membrane, with the subsequent secretion of H^+ causing a drop in lumenal pH and subsequent conversion of HCO_3^- into CO_2 (Pastor-Soler *et al.*, 2003).

sAC_t has also been shown to be present in the kidneys, where it has been shown to be located in the epithelial cells of the distal tubule, thick ascending limb and collecting duct (Figure 1.12) (Hallows *et al.*, 2009; Pastor-Soler *et al.*, 2003; Paunescu *et al.*, 2008). It was shown that sAC_t co-localised with the V-ATPase in intercalated epithelial cells (cells responsible for acid-base homeostasis) (Paunescu *et al.*, 2008). Although no direct evidence for the involvement of sAC_t in the regulation of this V-ATPase was obtained, the parallel with that seen in the epididymis raises the possibility of a role. More recently, sAC_t has also been shown to regulate a Na^+,K^+-ATPase located on the apical membrane in these intercalated cells (Hallows *et al.*, 2009).

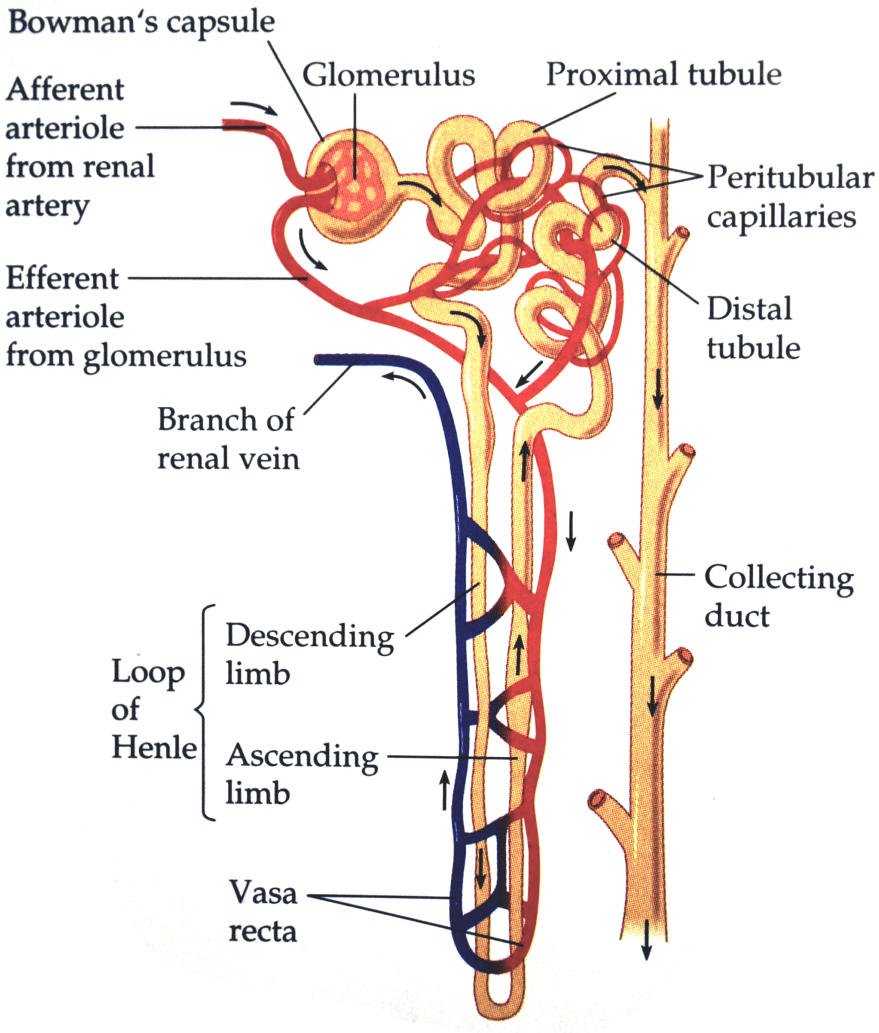

Figure 1.12: Schematic representation of a kidney nephron.

Taken from (Campbell, 1996)

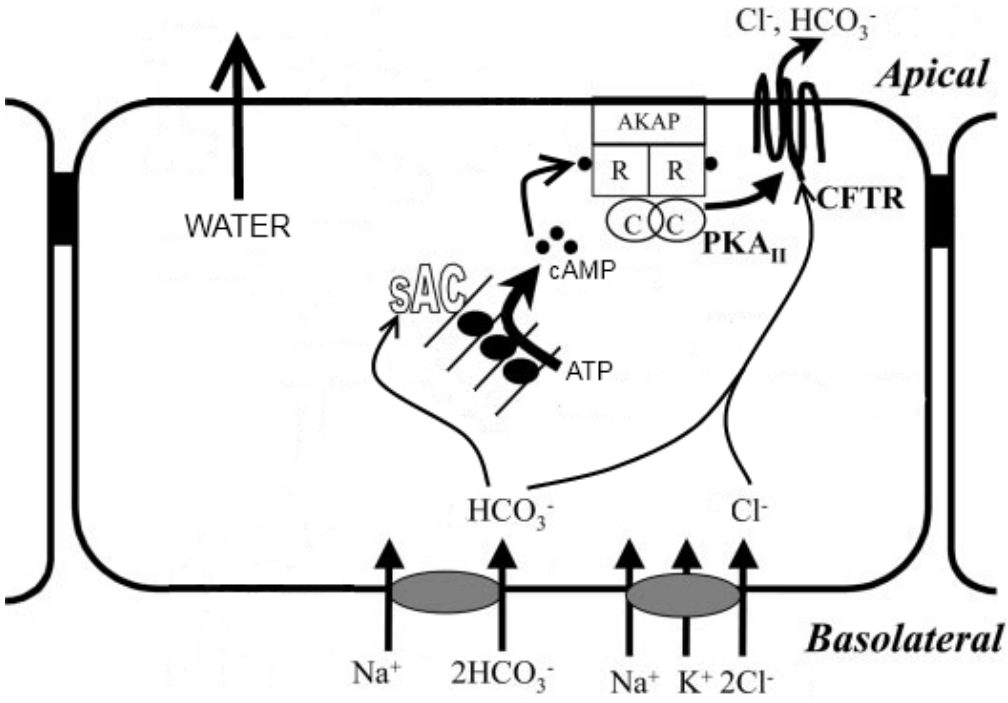

Figure 1.13: Proposed model for the role of sAC in the regulation of the CFTR protein in corneal epithelial cells.

Adapted from (Sun *et al.*, 2003)

sAC_t has also been implicated in the regulation of the cystic fibrosis transmembrane conductance regulator (CFTR) protein in corneal endothelium and airway epithelial cells (Sun *et al.*, 2003; Wang *et al.*, 2005). The CFTR protein is subject to complex regulation by a number of enzymes involved in phosphorylation/dephosphorylation reactions, of which PKA appears to be the most important (Rommens *et al.*, 1991; Tabcharani *et al.*, 1991). The corneal endothelium is responsible for maintaining hydration of the cornea through secretion of anions (Cl^- and HCO_3^-) by CFTR, leading to the formation of an osmotic gradient and subsequent diffusion of H_2O (Riley *et al.*, 1997). HCO_3^- and Cl^- are required in the corneal epithelial cells for CFTR to function on the apical membrane, and as such channels exist on the basolateral membrane to allow their entry (Figure 1.13) (Jelamskii *et al.*, 2000; Sun *et al.*, 2000). It is proposed that sAC_t in this cell acts as a sensor of HCO_3^-, activating the function of CFTR when intracellular concentrations are high enough (Sun *et al.*, 2003). It is possible that sAC_t activation by HCO_3^- produces cAMP which in turn activates PKA, which phosphorylates CFTR to promote its activity (Sun *et al.*, 2003). In airway epithelial cells CFTR performs a similar function, maintaining the correct fluid balance of mucus lining the airway (Wang *et al.*, 2005).

Whether sAC_t regulates different membrane channels in other tissues still remains to be addressed.

1.5.2 The kidney proximal tubule

The kidneys play a major role in whole body acid-base homeostasis, through a controlled re-absorption of filtered HCO_3^-, a process mediated through the secretion of H^+ into the urine (Gilman and Brazeau, 1953). This filtered HCO_3^-, which would otherwise end up in urine, is re-absorbed by the proximal tubule, and also to a lesser extend by the thick ascending limb and distal tubule (Figure 1.12). The proximal tubule actively secretes H^+ into the urine through a sodium-hydrogen exchanger (NHE3) and a V-ATPase located on the apical membrane (Gluck *et al.*, 1998; Weinman *et al.*, 2005). The increase in lumenal H^+ consequently alters the position of the HCO_3^-/CO_2 equilibrium, leading to a CA converting HCO_3^- into CO_2 (Sly and Hu, 1995). This CO_2 subsequently diffuses into the proximal tubule cell, where it is converted back to HCO_3^-, and is subsequently pumped across the basolateral membrane by a Na^+/HCO_3^- co-transporter (Seki *et al.*, 1996; Sly and Hu, 1995). This re-absorbed HCO_3^- then

passes into the blood stream where it is vital for neutralising various acids produced through metabolism, and as such maintaining a stable blood pH (Gilman and Brazeau, 1953).

Due to the importance of the proximal tubule in maintaining a stable blood pH, a regulatory mechanism exists through which it can moderate HCO_3^- re-absorption. It has long been known that in response to increased blood pCO_2 (hypercapnia), the proximal tubule increases its rate of HCO_3^- re-absorption (Brazeau and Gilman, 1953). Until recently, it was unknown whether the proximal tubule responded to CO_2 directly, or through a decrease in intracellular pH associated with CO_2. Investigation using 'out-of-equilibrium' CO_2/HCO_3^- solutions, demonstrated that the basolateral membrane of proximal tubule cells responded to CO_2 (and HCO_3^-), and not pH (Zhou *et al.*, 2005). Further investigation revealed, through the use of inhibitors specific to the ErbB family of receptor tyrosine kinases, that a receptor tyrosine kinase was involved in signalling changes in basolateral CO_2 (Zhou *et al.*, 2006).

The proximal tubule is also an important contributor to whole body phosphate homeostasis, through the regulation of phosphate uptake from the urine (Murer *et al.*, 2003). The control of phosphate re-absorption is mediated through the controlled endocytosis of type IIa Na-Pi co-transporters from the apical membrane to intracellular lysosomes for degradation (Murer *et al.*, 2000, 2003). Binding of parathyroid hormone (PTH) to its cognate receptor on the basolateral membrane is an important initiator of type IIa Na-Pi co-transporter endocytosis, and represents the main phosphaturic (reduced phosphate re-absorption) agent in this system (Malmstrom and Murer, 1986). Binding of PTH to its receptor (a G-protein coupled receptor) activates a complex signalling pathway, involving PKA and PKC, and consequently mediates the internalisation of the type IIa Na-Pi co-transporter (Traebert *et al.*, 2000).

It has been known for many years that respiratory alkalosis, with its associated decrease in plasma pCO_2, causes an inhibition of the phosphaturic effects of PTH, and a subsequent increase in phosphate reabsorption (Berndt and Knox, 1985; Hoppe *et al.*, 1982). The blunting of PTH's phosphaturic effect is mediated through a decrease in pCO_2 at the basolateral membrane of proximal tubules, and not through an accompanied pH effect (Berndt and Knox, 1985; Hoppe *et al.*, 1982). The effects of respiratory alkalosis on PTH signalling were shown to be mediated through a β-adrenergic signalling pathway, although

the exact details of this still remain to be elucidated (Hoppe *et al.*, 1988; Tucker *et al.*, 1996).

1.5.3 The carotid body

The carotid body, located near the fork of the carotid artery (Figure 1.14), contributes to the regulation of CO_2 (and O_2) homeostasis in the blood stream (Gonzalez *et al.*, 1994). The carotid body is composed of type I glomus cells that are the chemoreceptors and glial-like type II cells that are principally supporting cells (Gonzalez *et al.*, 1994). It is known that when arterial blood is hypercapnic (elevated CO_2) these cells respond by releasing neurotransmitters at their basolateral boundary, causing firing of the carotid sinus nerve. The excitation of these neurons causes several physiological changes, principle of which is an increased rate of ventilation (Gonzalez *et al.*, 1994).

Although the exact mechanism through which CO_2 is sensed by these cells is not fully understood, it is known that hypercapnic conditions cause an increase in cAMP levels within type I cells (Perez-Garcia *et al.*, 1990; Summers *et al.*, 2002). Activation of PKA, with subsequent phosphorylation of downstream targets, has long been known to modulate the activity of Ca^{2+} channels (Hartzell, 1988). More recently CO_2 has been shown to cause the activation of L-type Ca^{2+} channels in type I cells, with an associated increase in cellular cAMP and subsequent activation of PKA (Summers *et al.*, 2002).

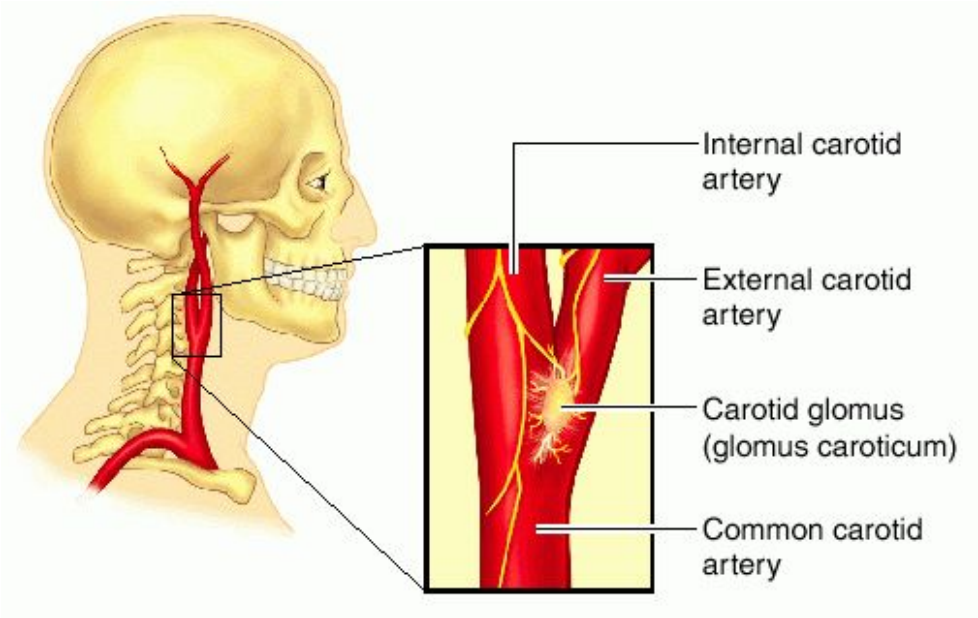

Figure 1.14: Location of the carotid body in humans.

Taken from (Dorland, 2003)

1.5.4 The brain

Whilst the peripheral chemoreceptors in the carotid body are thought to contribute about 30 % of the ventilatory response to hypercapnia, the central chemoreceptive neurons in the brain account for the remaining contribution (Lahiri and DeLaney, 1975; Lahiri and Forster, 2003). The carotid body, since it senses CO_2 levels directly in the arterial blood, is fast to react to conditions of hypercapnia, whereas the central chemoreceptors are much slower since they detect CO_2 levels in the cerebro-spinal fluid (Smith *et al.*, 2006). The central chemoreceptive neurons are currently acknowledged to predominantly sense alterations in pH as a response to CO_2, i.e. CO_2/H^+ sensing (Jiang *et al.*, 2005; Lahiri and Forster, 2003; Putnam *et al.*, 2004; Sharabi *et al.*, 2009b). However, the existence of direct CO_2 sensors is supported by the observation that the ventilatory response is much stronger under conditions of hypercapnic acidosis than normocapnic acidosis (Wang *et al.*, 1998). There is some evidence to suggest that direct sensing of CO_2 in cerebral neurons occurs through cGMP signalling pathways, although this is poorly understood (Wang *et al.*, 1999).

Hypercapnia is a potent signal in mammals, which also causes cerebral vasodilation through the relaxation of vascular smooth muscle in the brain. Crosstalk between cAMP and cGMP, is known to be a major contributor to the control of cerebral vasodilation (Wang *et al.*, 1999). Although the mechanism through which CO_2 sensing occurs is still not fully understood, there is certain evidence to suggest the involvement of cyclic nucleotides (Leblanc and Peterson, 1989; Parfenova and Leffler, 1996; Wang *et al.*, 1999). One study has shown the levels of cAMP produced by cerebral microvascular and smooth muscle cells to increase in the presence of elevated CO_2, although it is still not known whether this is simply a downstream effect of CO_2 sensing (Parfenova and Leffler, 1996).

1.5.5 The lungs

In alveolar epithelial cells in the lungs, the main site of CO_2 excretion, the rate of fluid re-absorption is known to be impaired under conditions of hypocapnia and hypercapnia (Briva *et al.*, 2007; Myrianthefs *et al.*, 2005). Alveolar fluid re-absorption is mediated through apical Na^+ channels and basolateral Na^+,K^+-ATPases, and a controlled rate of re-absorption is critical for

effective gas exchange (Matthay *et al.*, 2002). It has been demonstrated that under hypercapnic conditions, the reduced rate of fluid re-absorption is caused by endocytosis of the Na^+,K^+-ATPase (Briva *et al.*, 2007; Vadasz *et al.*, 2008). Endocytosis of the Na^+,K^+-ATPase in response to hypercapnia was shown to proceed through phosphorylation of the Na^+,K^+-ATPase by PKC-ζ, a process dependent upon AMP-activated protein kinase (Vadasz *et al.*, 2008). Interestingly, it was noticed that application of β-adrenergic receptor agonists ameliorated the impaired fluid re-absorption seen in response to hypercapnia (Vadasz *et al.*, 2008). Although the possibility exists that sAC is acting as the initial sensor of CO_2 in this system, the effects of β-adrenergic receptor agonists indicate the involvement of tmACs.

Studies in the lung have also provided strong evidence that CO_2 can effect the activation of nuclear factor κB (NF-κB), an important protein complex that is involved in the control of DNA transcription (Takeshita *et al.*, 1999; Takeshita *et al.*, 2003). In response to hypercapnia, a decreased activation of NF-κB was identified in pulmonary artery endothelial cells, but also in alveolar macrophages (Takeshita *et al.*, 1999; Takeshita *et al.*, 2003). In alveolar macrophages, hypercapnia was shown to attenuate the activation of NF-κB in response to endotoxins released from the cell wall of gram-negative bacteria (Takeshita *et al.*, 2003). Lipopolysaccharides released from the walls of gram-negative bacteria stimulate specific signalling pathways in alveolar macrophages, which trigger the release of certain inflammatory proteins, such as tumour necrosis factor α and interleukin 1β (Takeshita *et al.*, 2003; Wang *et al.*, 2010).

1.5.6 The taste and smell of CO_2

Mammals are known to detect CO_2 through taste receptors on the tongue, however, until recently the mechanism through which this occurred was unknown (Chandrashekar *et al.*, 2009; Dessirier *et al.*, 2001; Simons *et al.*, 1999). Rodents have also been shown to be able to detect CO_2 through olfactory receptors in the nose (Hu *et al.*, 2007; Youngentob *et al.*, 1991). Why certain mammals are able to taste and smell CO_2 is still unknown but it is hypothesised to be a mechanism through which they can detect CO_2 as a marker of fermenting fruit, and as such avoid the potentially lethal effects of alcohol.

Investigation into the detection of CO_2 in carbonated beverages through taste receptors on the tongue demonstrated that the oral sensation of CO_2 was not due to the mechanical actions of CO_2 bubbles. Firstly, experiments performed in a hyperbaric chamber (at 3.4 atmospheres), where bubbles of CO_2 could not form, still identified a strong taste sensation (McEvoy, 1998). Secondly, experiments performed with the CA inhibitors dorzolamide and acetozolamide, where bubbles of CO_2 were still present, were unable to detect a taste response of CO_2 (Graber and Kelleher, 1988; Simons *et al.*, 1999). Recent work demonstrated that the detection of CO_2 was specific to a set of sour sensing cells on the tongue (Chandrashekar *et al.*, 2009). Furthermore, microarray analysis and subsequent knock-out studies identified one gene, *car4*, as being responsible for conferring a response to CO_2 (Chandrashekar *et al.*, 2009). This gene encodes an extracellular, glycosylphosphatidylinositol (GPI) anchored CA and is the key CO_2 sensor in this system. The molecular mechanism through which Car4 transmits the CO_2 signal into the cell is still unknown.

Studies into the detection of CO_2 through olfactory receptors in rodents revealed a remarkable sensitivity to CO_2, detecting CO_2 at near atmospheric concentrations (Hu *et al.*, 2007; Youngentob *et al.*, 1991). Studies revealed that the detection of CO_2 was specific to olfactory neurons that express phosphodiesterase 2A (PDE2A), guanylyl cyclase D (GC-D), CA II (Car2) and cGMP-sensitive cyclic nucleotide gated (CNG) channels (Hu *et al.*, 2007; Leinders-Zufall *et al.*, 2007). More recent work has shown that GC-D is directly acted upon by Ci to increase its activity, and as such it is possibly the CO_2 sensor in these cells, leading to the proposed mechanism of CO_2 detection in these cells (Figure 1.15) (Guo *et al.*, 2009; Sun *et al.*, 2009).

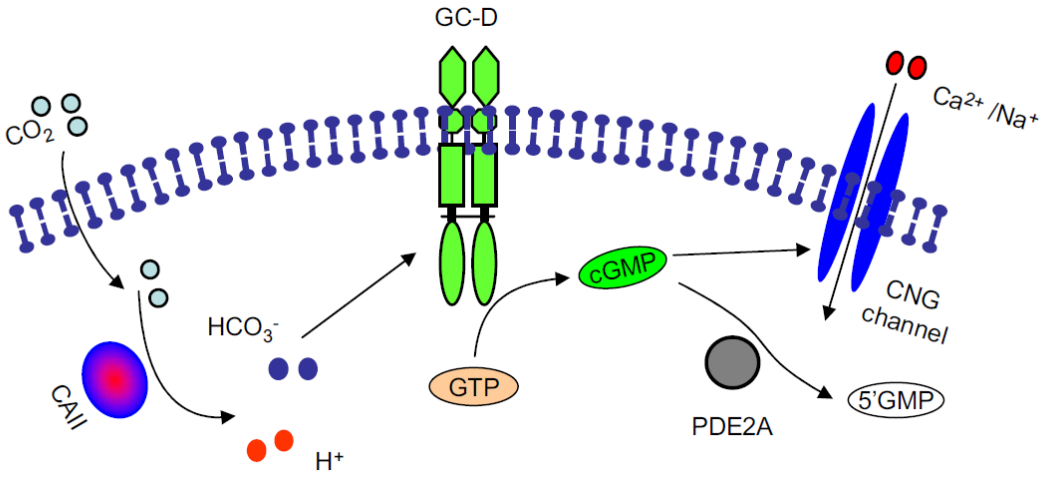

Figure 1.15: Proposed model for CO_2 sensing in mouse olfactory neurons.

Taken from (Guo *et al.*, 2009)

1.6 Aims of the thesis

There is a wealth of information in the literature pertaining to the physiological effects of Ci in many diverse organisms, both prokaryotic and eukaryotic. However, despite the importance of understanding the mechanisms through which these physiological changes occur, the details of many Ci sensing pathways remain largely unknown. This is particularly apparent in mammals, where despite many of the physiological effects of Ci being well documented, the molecular mechanisms through which these effects occur are poorly understood. Much of the current focus has been upon Ci sensing pathways involving sAC, a proven Ci sensitive signalling enzyme, however, there is amounting evidence to suggest that sAC is not the only Ci sensitive cyclase. Despite sAC being shown to act as a Ci sensor in many pathways in mammals, there are still several Ci sensing pathways which are unlikely to involve sAC. As such, this thesis will attempt to answer the following questions:

1. The tmACs and sAC share a structurally homologous active site, and the experimental evidence in the literature is contradictory as to whether tmACs are also regulated by Ci. Does sAC represent the sole Ci sensitive AC in mammals or are the tmACs also Ci sensitive?

2. Given the structural similarities between the AC and GC active site, and the evidence suggesting the involvement of a GC in the olfactory detection of Ci in rodents, are cyclases universally regulated by Ci? Can a Ci responsive GC be identified?

3. Analysis of the crystal structures of ACs and certain DNA polymerases revealed that their tertiary structures are similar, in that they both possess a 'palm' domain (see Chapter 4.1 for discussion). Given this structural similarity, and the fact that their catalytic mechanisms are related, are DNA or RNA polymerases also regulated by Ci?

4. How does Ci interact with ACs? Given the fact that the mechanism through which Ci acts upon ACs is largely unknown, a biochemical analysis will be performed to attempt to gain information regarding the mode of action of Ci.

2

Materials and methods

2.1 Materials

Chemicals and reagents	Company	Product code
Agarose	Bioline	BIO-41026
Tris(hydroxymethyl)aminomethane	Sigma	93362
Glacial acetic acid	Sigma	A6283
Ethylenediaminetetraacetate	Sigma	E5134
DNA marker ladder	Fermentas	SM0311
Ethidium bromide	Sigma	E7637
Sodium perchlorate	Sigma	S1513
Sodium chloride	Sigma	S3014
Ethanol	Sigma	E7023
Tryptone	Sigma (Fluka)	T7293
Glucose	Sigma	G7528
Yeast extract	Sigma	Y1625
Magnesium chloride	Sigma	M8266
Lysogeny broth (LB) agar	Sigma	L2897
Dulbecco's Modified Eagle Medium (DMEM)	Gibco (Invitrogen)	31966-021
DMEM/F12 (1:1)	Gibco (Invitrogen)	31331-028
Non-essential amino acids	Gibco (Invitrogen)	11140-050
Penecillin/streptomycin	Gibco (Invitrogen)	15070-063
Heat inactivated newborn calf serum	Gibco (Invitrogen)	26010-074
Trypsin-EDTA	Gibco (Invitrogen)	15400-054
Isopropyl β-D-thiogalactoside	Sigma	I5502
LB medium	Merck	10285.5000
Imidazole	Sigma	I5513
Phenylmethylsulfonyl fluoride	Sigma	P7626
Glycerol	Sigma	G5516
Sodium dodecyl sulphate	Sigma	L4390
Bromophenol blue	Sigma	B0126
Dithiothreitol	Sigma	43816
Glycine	Sigma	G7126
Coomassie G-250	Sigma	201391
Tween-20	Sigma	63158
Anti-mouse IgG, HRP-linked Antibody	Cell Signalling Technology	7076
Phospho-CREB (Ser133) Mouse mAb	Cell Signalling Technology	9196

α-Tubulin Mouse mAb	Cell Signalling Technology	3873
Potassium chloride	Sigma	P9333
Sucrose	Sigma	S7903
Calcium chloride	Sigma	C2661
Isobutylmethylxanthine (IBMX)	Sigma	I5879
Sodium bicarbonate	Sigma	S6297
Forskolin	Sigma	F6886
Isoproterenol	Sigma	I6504
Trichloroacetic acid	Sigma	T6399
Adenosine triphosphate (ATP)	Sigma	A6559
Adenosine 3,5 cyclic monophosphate (cAMP)	Sigma	A9501
Guanosine triphosphate (GTP)	Sigma	G8877
Guanosine 3,5 cyclic monophosphate (cGMP)	Sigma	G7504
Optiphase HiSafe 3	Perkin Elmer	1200-437
[α-^{32}P]-ATP	Perkin Elmer	BLU003H
[α-^{32}P]-GTP	Perkin Elmer	BLU006H
[α-^{32}P]-deoxyATP	Perkin Elmer	BLU012H
[2,8-^{3}H]-cAMP	Perkin Elmer	NET275
[8-^{3}H]-cGMP	Perkin Elmer	NET337
[2,8-^{3}H]-adenine	Perkin Elmer	NET063
Ampicillin	Sigma	A9518
Kanamycin	Sigma	K1377
G418	Sigma	G5013
Tetracycline	Sigma	T7660
Chloramphenicol	Sigma	C0378
Dowex AG 50W-X4 resin	Biorad	142-1341
Aluminium oxide (Activity grade 1, Type WN-3: neutral)	Sigma	A9003
Activated calf thymus DNA	Sigma	D4522

Kits	Company	Product code
Zero Blunt® TOPO® PCR cloning kit	Invitrogen	K2830-20
Wizard® *Plus* Miniprep kit	Promega	A7100
Ni^{2+}-NTA superflow resin	Qiagen	30410
Vivaspin 20 centrifugal concentrator	Sartorius Biolab	VS2011
Vivaspin 6 centrifugal concentrator	Sartorius Biolab	VS0611
PageRuler™ Prestained Protein Ladder	Fermentas	SM0671
PageRuler™ Plus Prestained Protein Ladder	Fermentas	SM1811
ECL™ Western Blotting Detection Reagent	Amersham	RPN2109
dNTP set	Bioline	BIO-39025
Polyprep chromatography column	Biorad	731-1550
Mini-PROTEAN Tetra Electrophoresis System	Biorad	165-8038

Enzymes	Company	Product code
Pfu DNA polymerase	Promega	M774A
BIOTAQ™ Red DNA polymerase	Bioline	BIO-21061
Xho I	Fermentas	ER0691
Eco RV	Fermentas	ER0301
Pst I	Fermentas	ER0611
Sph I	Fermentas	ER0601
T4 DNA ligase	Fermentas	EL0015
Calf intestinal alkaline phosphatase	Fermentas	EF0431

Cell lines	Company	Product code
HEK 293T	ATCC	CRL-11268
NIH 3T3	ATCC	CRL-1658
E. coli Tuner (DE3)	Novagen	70623
E. coli M15 (DE3) pREP4	Qiagen	34210
E. coli BL21 (DE3)	Novagen	69387
E. coli CJ376	See section 4.3	
E. coli Mach1 T1	Invitrogen	K2830-20

2.2 Cloning procedures

2.2.1 Polymerase chain reaction

Reactions using *Pfu* DNA polymerase were set up on ice following the manufacturers protocol. Reactions typically contained 20 mM Tris-HCl pH 8.8, 10 mM KCl, 10 mM $(NH_4)_2SO_4$, 2 mM $MgSO_4$, 1 % (v/v) Triton® X-100, 0.1 mg mL^{-1} BSA, 25 pmoles of each primer, 200 µM dNTPs, 250 ng DNA template and 1 unit *Pfu* DNA polymerase. Polymerase chain reaction (PCR) was typically cycled as listed below (Table 2.1).

Reactions using BIOTAQ™ Red DNA polymerase were set up on ice. Reactions typically contained 16 mM $(NH_4)_2SO_4$, 67 mM Tris-HCl pH 8.8, 25 pmoles of each primer, 200 µM dNTPs and 1.5 units DNA polymerase. DNA was added as 0.5 µL of a DNA miniprep (see 2.2.6) or by directly picking a single colony from an lysogeny broth (LB) agar plate containing *Escherichia coli* transformants, and scraping into the PCR reaction. PCR reactions were typically cycled as listed below (Table 2.2).

Reactions were analysed by agarose gel electrophoresis (see 2.2.2).

2.2.2 Agarose gel electrophoresis

1 % or 1.5 % (w/v) agarose gels in TAE buffer (40 mM Tris-acetate, 1 mM EDTA pH 8.0) were run at 12 V cm^{-1}. DNA sample was mixed 4:1 (sample:buffer) with loading buffer (2 % (w/v) orange G and 20 % (w/v) sucrose in TAE buffer) prior to loading, DNA sizes were estimated relative to a 1 kilobase DNA marker ladder. Visualisation of DNA was attained through the in gel presence of ethidium bromide (0.5 µg mL^{-1}) and a UV transilluminator.

2.2.3 Extraction of DNA from agarose gels

The DNA band was excised from an agarose gel (see 2.2.2) and was allowed to dissolve in 600 µL binding buffer (6 M Sodium Perchlorate, 50 mM Tris-HCl pH 8.0, 10 mM EDTA). 10 µL 166 mg mL^{-1} silica in water was added and the suspension was incubated at room temperature for 30 minutes. The suspension was centrifuged (12,000 g, 30 sec), the supernatant was discarded, and the pellet was re-suspended in 200 µL binding buffer. This new suspension was centrifuged (12,000 g, 30 sec) and the pellet was re-suspended in 750 µL

wash buffer (400 mM NaCl, 20 mM Tris-HCl pH 7.5, 2 mM EDTA and 50 % (v/v) ethanol). The previous wash step was repeated, the suspension was centrifuged (12,000 g, 30 sec), the supernatant was discarded, and the pellet left to air dry for 30 minutes at room temperature. The dry pellet was re-suspended in 15 µL H_2O and incubated at 37°C for 15 minutes. The sample was then centrifuged (12,000g, 2 min) and the supernatant containing DNA was removed and stored at -20°C until further use.

2.2.4 Zero Blunt® TOPO® PCR cloning reaction

A 6 µL Zero Blunt® TOPO® PCR cloning reaction was assembled on ice and contained 200 mM NaCl, 10 mM $MgCl_2$, 5 ng pCR®-Blunt II-TOPO® vector and 3 µL of blunt ended purified PCR product (see 2.2.3). Reaction was incubated at 22°C for 30 minutes before a 2 µL aliquot was transformed into competent *E. coli* (see 2.2.5).

2.2.5 Transformation of chemically competent *E. coli*

Frozen 50 µL aliquots of chemically competent *E. coli* were thawed quickly in the hand and transferred immediately onto ice. 25 ng of plasmid DNA or 2 µL of a DNA ligation mixture (see 2.2.4 and 2.2.8) was added, gently mixed, and left on ice for 30 minutes. Cells were heat shocked for 45 seconds in a 42°C water bath and immediately placed back on ice for 2 minutes. 950 µL of 37°C SOC medium (2 % (w/v) tryptone, 0.5 % (w/v) yeast extract, 8.5 mM NaCl, 10 mM $MgCl_2$ and 20 mM glucose) was added to the cells and then cultured at 37°C for 2 hours before plating onto LB agar plates containing required selection agents. Plates were grown at 37°C overnight.

2.2.6 Purification of plasmid DNA

A 5 mL overnight culture of *E. coli* was centrifuged (5,000 g, 10 min) and the pellet was processed using a commercial plasmid miniprep kit according to the manufacturers protocol.

	Time / minutes	Temperature / ºC
Initial denaturation	2	95
Denaturation	0.5	95
Annealling	0.5	55
Elongation	1 per 0.5 kb *	72
Final Elongation	5	72

Table 2.1: Cycling conditions for *Pfu* DNA polymerase.

** Manufacturer recommends allowing Pfu DNA polymerase 1 minute to extend 500 base pairs*

	Time / minutes	Temperature / ºC
Initial denaturation	5	95
Denaturation	0.5	95
Annealling	0.5	55
Elongation	1 per 1 kb *	72
Final Elongation	5	72

Table 2.2: Cycling conditions for BIOTAQ™ Red DNA polymerase.

** Manufacturer recommends allowing BIOTAQ™ Red DNA polymerase 1 minute to extend 1000 base pairs*

	Fermentas Buffer	Enzyme 1 / µL	Enzyme 2 / µL
(1) *Bam* HI (2) *Hind* III	R	2	1
(1) *Pst* I (2) *Sph* I	B	2	1
(1) *Eco* RV (2) *Xho* I	R	1	1

Table 2.3: Buffer and relative enzyme amounts used for double digests.

2.2.7 Restriction digestions

40 µL restriction digests were set up on ice, contained 200 ng plasmid DNA (see 2.2.6), and were incubated for 2 hours at 37°C. Digests contained 2 different restriction endonucleases; the reaction buffer used and relative amounts of enzyme used were determined following guidelines on the manufacturers website for double digests (Table 2.3). DNA vectors were also digested in the presence of 2 Units of Calf alkaline intestinal phosphatase. Digests were analysed by agarose gel electrophoresis (see 2.2.2) and correct DNA fragments were purified (see 2.2.3) for further use.

2.2.8 DNA ligations

10 µL DNA ligation reactions were set up on ice and contained 40 mM Tris-HCl pH 7.8, 10 mM $MgCl_2$, 10 mM DTT, 5 mM ATP, 3 Units T4 DNA Ligase, and a 3:1 molar ratio of purified DNA insert:vector (see 2.2.7). Ligations were incubated at 22°C for 1 hour before a 2 µL aliquot was transformed into competent *E. coli* (see 2.2.5).

2.2.9 Preparation of chemically competent *E. coli*

25 mL LB medium was inoculated with 250 µL of an overnight LB starter culture and grown with shaking (180 rpm) at 30°C to an OD_{600} of 0.5. Cells were transferred to ice for 15 minutes, centrifuged (2700 g, 10 min, 4°C) and re-suspended in 30 mL ice cold wash solution (80 mM $MgCl_2$ and 20 mM $CaCl_2$). Cells were centrifuged again (2700 g, 10 min, 4°C), re-suspended in 1 mL ice cold 100 mM $CaCl_2$, split into 50 µL aliquots in chilled micro-centrifuge tubes, and stored at -80°C.

2.2.10 Preparation of genomic DNA from *Synechocystis* PCC 6803

2 mL of a confluent culture of *Synechocystis* PCC 6803 was pelleted (12,000 g, 2 min) and re-suspended in 500 µL H_2O. Suspension was boiled for 10 min and then pelleted (16,700 g, 10 min) to yield a crude preparation of genomic DNA in the supernatant.

2.2.11 Estimation of DNA concentration

Concentrations of DNA in solution were estimated using a quartz crystal cuvette and a Biowave S2100 Diode Array Spectrophotometer using the inbuilt software to automatically estimate concentration of double stranded DNA. A preparation of DNA free from contaminating proteins was deemed present if the A_{260} / A_{280} reported was between 1.8 and 2.0.

2.2.12 Preparation of bacterial -140ºC freezer stocks

E. coli cells were grown in 10 mL LB containing appropriate antibiotics at 37°C overnight. The cells were harvested by centrifugation (5,500 g, 5 min and 4°C). The bacterial pellet was re-suspended in 1 mL LB containing 40 % (v/v) glycerol. The suspension was placed in a labelled cryovial and stored at -140°C.

2.2.13 Sll0646 and Sll1161 expression constructs

Coding sequences for Sll0646 (amino acids 424-756), Sll0646 (amino acids 1-756) and Sll1161 (amino acids 73-285) were amplified (Table 2.4) from *Synechocystis* PCC 6803 genomic DNA (see 2.2.10) by PCR with *Pfu* DNA polymerase (see 2.2.1). DNA was analysed by agarose gel electrophoresis (see 2.2.2), purified (see 2.2.3), ligated into the pCR®-Blunt II-TOPO® vector (see 2.2.4), and transformed into chemically competent *E. coli* Mach1 T1 (see 2.2.5). Positive colonies were identified through PCR (see 2.2.1) and were isolated, and grown in 5 mL LB medium at 37ºC overnight. Plasmid DNA from overnight *E. coli* Mach1 T1 cultures was isolated (see 2.2.6), digested with restriction endonucleases (see 2.2.7), analysed by agarose gel electrophoresis (see 2.2.2), and purified (see 2.2.3). Purified DNA was ligated into the required plasmid vector (see 2.2.8) and transformed into chemically competent *E. coli* DH5α for maintenance (see 2.2.5).

	Direction	Sequence (5'-3')	Restriction site	Vector
Sll0646$_{424-756}$	Sense	GGCGCATGCGCCACCCTACTGGAAAACCCC	*Pst* I	pQE30
Sll0646$_{424-756}$	Antisense	GGCCTGCAGCTAGCCCCCCTGAGCGGAAG	*Sph* I	pQE30
Sll0646$_{1-756}$	Sense	GGCGCATGCATGGGTTGGACCATACCGTCA	*Pst* I	pQE30
Sll0646$_{1-756}$	Antisense	GGCCTGCAGCTAGCCCCCCTGAGCGGAAG	*Sph* I	pQE30
Sll0646$_{1-756}$	Sense	GGCGATATCCTAGCCCCCCTGAGCGGAAG	*Eco* RV	pCDNA3.1
Sll0646$_{1-756}$	Antisense	GGCCTCGAGATGGGTTGGACCATACCGTCA	*Xho* I	pCDNA3.1
Sll1161$_{73-285}$	Sense	GGCGGATCCCTATTAATGGCTAATATTCGTGGG	*Bam* HI	pQE30
Sll1161$_{73-285}$	Antisense	GGCAAGCTTTTAAGAAGATTTTAGCCAAGAACC	*Hind* III	pQE30

Table 2.4: Primers used for cloning *Synechocystis* PCC 6803 CHDs.

2.3 Mammalian cell culture

2.3.1 General cell culture

Mammalian cell lines were routinely cultured at 37°C in a humidified CO_2 incubator set to 5 % (v/v) CO_2 in air. HEK 293T cells were cultured in DMEM supplemented with 10 % (v/v) heat inactivated newborn calf serum, 100 µM non-essential amino acids, 50 Units penicillin, and 50 µg streptomycin. NIH 3T3 cells were cultured in DMEM/F12 (1:1 (v/v) DMEM:F12) medium supplemented with 10 % (v/v) heat inactivated newborn calf serum, 100 µM non-essential amino acids, 50 Units penicillin, and 50 µg streptomycin. Cells were sub-cultured at about 90 % confluency by aspirating the medium, washing cell monolayer twice with phosphate buffered saline (PBS), and incubating with 1 mL 0.05 % (w/v) trypsin for 3 minutes at 37°C. Trypsinisation was halted with the addition of fresh medium; cell clumps were broken by pipetting up and down in a 10 mL serological pipette.

2.3.2 Coating tissue culture plates with poly-D-lysine

100 µg mL^{-1} poly-D-lysine solution was added to completely cover the surface to be coated and was incubated at room temperature for 1 hour. The poly-D-lysine solution was aspirated, plates were washed 3 times with water and left to dry.

2.3.3 Intracellular pH measurement

HEK 293T cells attached to a 24 mm^2 glass coverslip were loaded with the pH sensitive fluorescent dye 2',7'-bis(carboxyethyl)-5(6)-carboxyfluorescein (BCECF) through exposure to 1 µM BCECF-AM (an acetoxymethyl ester derivative) for 30 minutes. The cell monolayer was constantly perfused with each incubation solution and intracellular pH (pH_i) was measured by exciting a small patch of cells at 490 and 440 nm using a microspectrofluorometric system, and measuring emission at 535 nm. pH_i was calibrated using the high potassium nigericin method (Hegyi *et al.*, 2004).

2.3.4 Preparation of cell lysates

Unless indicated all steps were performed on ice or at 4°C. Cell

monolayer was washed with PBS, suspended in 10 mL hypotonic lysis buffer (10 mM Tris-HCl pH 7.5, 10 mM $MgCl_2$ and 5 mM $CaCl_2$), and incubated for 20 minutes. The cell suspension was pelleted (200 g, 2 min), re-suspended in 10 mL hypotonic lysis buffer and incubated for a further 20 minutes. The cell suspension was pelleted (200 g, 2 min), re-suspended in 1 mL lysis buffer (20 mM Tris-HCl pH 7.5, 5 mM NaCl, 1 mM DTT, 1 mM IBMX and 20 % (v/v) glycerol), and homogenised with vigorous passage through a G21 needle. Samples were aliquoted and stored at -20°C until further use. Samples were only allowed to freeze-thaw once.

2.4 Protein manipulations

2.4.1 Expression of recombinant proteins in *E. coli*

For conditions related to individual proteins refer to Table 2.5. 1 L LB medium was inoculated with 10 mL of an overnight *E. coli* starter culture and was grown in a 37°C temperature controlled shaking incubator at 180 rpm. Protein expression was induced once cells reached the specified absorbance value with the addition of isopropyl β-D-thiogalactoside (IPTG) to the required final concentration (Table 2.5). Bacteria were grown with shaking at the required temperature and for the required time (Table 2.5).

A different induction procedure was used for the Klenow D424A *exo-* fragment of *E. coli* DNA polymerase I. Four flasks of 750 mL LB medium (100 μg μL^{-1} ampicillin) were inoculated with 10 mL of an overnight LB (100 μg μL-1 ampicillin) starter culture of *E. coli* CJ376 pXS106 (Klenow D424A *exo-* KF) and cultured at 30°C with shaking (180 rpm) till an OD_{600} of 0.6 was reached. Protein expression was induced with the addition of 250 mL LB preheated to 90°C and cultures were grown at 42°C for 2 hours (Joyce and Derbyshire, 1995).

All bacteria were harvested through centrifugation (12,000g, 4°C, 10 min). The pellet (one pellet corresponds to cells from 2 L LB) was washed with 40 mL bacterial wash buffer (50 mM Tris-HCl pH 8.5, 1 mM EDTA), centrifuged (5,500g, 4°C, 15 min), and frozen at -80°C.

2.4.2 Lysis of bacteria

Frozen bacterial pellets (see 2.4.1) were thawed quickly in a 37°C water bath. All subsequent steps were performed on ice or at 4°C. The pellet (one pellet corresponds to cells from 2 L LB; see 3.4.1) was re-suspended in 30 mL lysis buffer (50 mM Tris-HCl pH 8.0, 150 mM NaCl, 5 mM imidazole, 2 mM DTT, 5 mM $MgCl_2$, and 1 mM PMSF), sonicated (2.5 min, 74 W, 2 pulses per second), and centrifuged (50,000g, 30 min). Crude supernatant containing soluble proteins was saved for purification.

	E. coli strain	OD_{600} at induction	[IPTG] / µM	Temperature / °C	Time / hours
$7C_1$	Tuner (DE3)	0.5	30	22	19
$2C_2$	M15 (DE3)	0.5	30	22	16
$G\alpha_s$	M15 (DE3)	0.5	30	22	16
$Sll0646_{424-756}$	M15 (DE3)	0.5	500	30	4
$Sll0646_{434-635}$	BL21 (DE3)	0.5	500	30	4
CyaB1	M15 (DE3)	0.5	300	30	3
T7 RNAP	BL21 (DE3)	0.5	400	37	4
Klenow	CJ376	0.5	1000	30	4
Pol β	BL21 (DE3)	0.5	50	22	15

Table 2.5: Expression conditions for each recombinant protein.

(see 2.4.1)

	1° / 2°	Species	Dilution Ab : block *	Temperature / °C	Time / hour
$pSer^{133}CREB$	1°	mouse	1 : 250	4	15
α-tubulin	1°	mouse	1 : 1000	22	4
Anti-mouse IgG	2°	mouse	1 : 1000	22	1

Table 2.6: Conditions used for individual antibodies.

** Ab denotes antibody and block denotes blocking buffer (see 2.4.6)*

2.4.3 Ni^{2+}-NTA affinity chromatography

All steps were performed on ice or at 4°C. 1 mL Ni^{2+}-NTA resin was added to 30 mL crude supernatant (see 2.4.2) and incubated with gentle rocking for 2 hours. Ni^{2+}-NTA resin was pelleted (200g, 2 min), loaded into a 10 mL polyprep chromatography column, and allowed to settle. Resin was washed with 15 mL (per 1 mL of Ni^{2+}-NTA resin) wash buffer (50 mM Tris-HCl pH 8.0, 150 mM NaCl, 20 mM imidazole, 2 mM DTT, and 5 mM $MgCl_2$) and eluted with 5 mL (per 1 mL of Ni^{2+}-NTA resin) elution buffer (50 mM Tris-HCl pH 8.0, 150 mM NaCl, 150 mM imidazole, 2 mM DTT, and 5 mM $MgCl_2$). An aliquot of eluate was saved for analysis by SDS-PAGE (see 2.4.5). Eluate was concentrated to 2 mL with a vivaspin 20 centrifugal concentrator as per the manufacturers guidelines. Concentrated eluate was dialysed (3 x 1 hour) into storage buffer (50 mM Tris-HCl pH8.0, 2 mM DTT, 10 mM NaCl, 20 % (v/v) glycerol) and stored at -20°C until needed.

2.4.4 Ammonium sulphate fractionation

All steps were performed on ice or at 4°C. 9.03 g solid ammonium sulphate was slowly added to the crude supernatant with stirring (see 2.4.2) to 50 % (w/v) saturation, the suspension was centrifuged (5,500 g, 10 min), and the pellet was discarded. A further 8.26 g ammonium sulphate was added to the supernatant with stirring to 85 % (w/v) saturation, the suspension was centrifuged (5,500 g, 10 min), and the pellet was re-suspended in 5 mL fast protein liquid chromatography (FPLC) buffer (20 mM Tris-HCl pH 8.0, 1 mM DTT, 0.5 mM EDTA, and 2 mM $MgCl_2$).

2.4.5 SDS-PAGE

0.75 mm polyacrylamide gels (12 % or 15% (v/v) bis-acrylamide resolving and 5% (v/v) bis-acrylamide stacking) were poured using the Mini-PROTEAN Tetra Electrophoresis System. Samples were mixed 1:1 (v:v) with loading buffer (50 mM Tris-HCl pH 6.8, 2 % (w/v) SDS, 0.1 % (w/v) bromophenol blue, 10 % (v/v) glycerol, and 100 mM DTT), incubated at 95°C for 5 minutes and run at 20 V cm^{-1} in running buffer (25 mM Tris-HCl pH 6.8, 200 mM glycine, 0.1 % (w/v) SDS). Protein sizes were estimated relative to a protein marker ladder. Gels were stained with Coomassie Brilliant Blue dye (0.1 % (w/v) Coomassie G-250

dye, 10 % (v/v) acetic acid, and 50 % (v/v) methanol) and de-stained in de-staining solution (10 % (v/v) acetic acid and 50 % (v/v) methanol).

2.4.6 Immunoblotting

Freshly run agarose gels were assembled along with Hybond ECL Nitrocellulose membrane in the Mini-PROTEAN Tetra Electrophoresis System. Proteins were transferred at 2 V cm^{-1} at 4°C overnight in transfer buffer (25 mM Tris-HCl pH 8.5, 190 mM glycine, and 15 % (v/v) methanol). Membranes were washed for 5 minutes in TBS-T (25 mM Tris-HCl pH 7.5, 150 mM NaCl, 0.05% (v/v) Tween-20) and incubated in blocking buffer (5 % (w/v) non-fat milk in TBS-T) for 2 hours at room temperature. Membranes were washed 3 times in TBS-T for 10 minutes each and then probed with primary antibody diluted in blocking buffer (Table 2.6). Membranes were washed again with TBS-T and then probed with secondary antibody diluted in blocking buffer (Table 2.6). Membranes were again washed with TBS-T before a 5 minute incubation with ECL™ Western Blotting Detection Reagent at room temperature. Western blots were scanned using a Fuji Las-1000 chemiluminescent scanner.

2.4.7 Fast protein liquid chromatography

All steps are performed on ice or at 4°C. Protein (see 2.4.3 and 2.4.4) was thawed, dialysed (3 x 1 hour) into FPLC buffer (20 mM Tris-HCl pH 8.0, 1 mM DTT, 0.5 mM EDTA, and 2 mM $MgCl_2$) and was applied to a 25 mL Q-sepharose liquid chromatography column (Biorad) pre-equilibrated with FPLC buffer. Columns were always run at 1 mL min^{-1}. Columns were washed with 100 mL FPLC buffer and protein was eluted in 5 mL fractions with a 100 mL linear gradient of 0 – 400 mM NaCl and a 50 mL steep gradient of 400 mM – 1 M NaCl. Fractions were analysed for protein content and peak fractions were analysed via SDS-PAGE (see 2.4.5). Clean fractions were pooled and concentrated to 2 mL with a vivaspin 20 centrifugal concentrator (Sartorius Biolab) as per the manufacturers guidelines. Concentrated eluate was dialysed (3 x 1 hour) into storage buffer (50 mM Tris-HCl pH 7.5, 5 mM NaCl, 2 mM $MgCl_2$, 20 % (v/v) glycerol) and stored at –20°C until needed.

2.4.8 Estimating protein concentration

The concentration of purified recombinant proteins in solution were estimated using a quartz crystal cuvette and a Biowave S2100 Diode Array Spectrophotometer scanning at 280 nm. Concentrations were estimated from the A_{280} value using the Beer-Lambert law and the Lasergene software package by DNASTAR to estimate the molar extinction coefficient of the protein based on the predicted sequence.

2.5 Biochemistry

2.5.1 Preparation of CO_2 solutions for *in vivo* assays

10 mL of incubation medium stock (200 mM Hepes-NaOH pH 7.0, 1.17 M NaCl, 45 mM KCl, 10 mM $MgCl_2$, 110 mM glucose, 100 mM sucrose, and 25 mM $CaCl_2$) was added to 80 mL H_2O and left in a 37°C water bath for 30 minutes while 0, 5 or 10 % (v/v CO_2 in air) was constantly bubbled through. Small aliquots of 1 M $NaHCO_3$ (Table 2.7) were then added to adjust the media to the desired pH and once established the solutions were adjusted to a 100 mL final volume. 100 µL 100 µM isobutylmethylxanthine (IBMX) was added to each solution and they were then quickly transferred to their respective humidified tissue culture incubator ready for use.

2.5.2 *In vivo* AC assay

HEK 293T cells were sub-cultured (see 2.3.1) into 12 well poly-lysine coated plates (see 2.3.2) and labelled overnight with 1.5 µCi [2,8-^{3}H]-adenine once 80-90 % confluence was achieved. The following day, cells were washed three times with PBS and incubated at 37°C at the required CO_2 concentration in 980 µL incubation media (20 mM Hepes-NaOH pH 7.0, 117 mM NaCl, 4.5 mM KCl, 1 mM $MgCl_2$, 11 mM glucose, 10 mM sucrose, 2.5 mM $CaCl_2$, and 1 mM IBMX; see 2.5.1) for 30 minutes. After 30 minutes the assay was initiated by the addition of 20 µL agonist, incubated at the required CO_2 concentration and at 37°C. Assays were stopped after 30 minutes by aspirating the media and adding 1 mL ice cold 5 % (w/v) trichloroacetic acid (TCA) containing 1 mM ATP and 1 mM cAMP. Cells were lysed at 4°C with mixing for 30 minutes before the TCA solution was removed and stored for quantification of total adenine nucleotides.

Condition	pH	CO_2 / % *	HCO_3^- / mM	CO_2 / mM
Acidotic hypocapnic	7.0	0.04	0	0
Acidotic normocapnic	7.0	5	7	2
Acidotic hypercapnic	7.0	10	15	4

Table 2.7: Final concentration of HCO_3^- in each incubation mix.

** [% = percentage (v/v) CO_2 / Air]*

Products were quantified via modification of the twin column chromatography approach used to purify nucleotides. 1 mL samples were applied to 1 mL Dowex columns and the flow-through was collected. The Dowex column was washed with 2 mL H_2O, this was pooled with the previous flow-through, mixed with 3 mL scintillation fluid, and counted on a liquid scintillation counter. Nucleotides bound to the Dowex column were washed onto 1 mL aluminium oxide columns with 5 mL H_2O. cAMP was then eluted twice from the aluminium oxide columns with 3 mL 100 mM Tris-HCl pH 7.5, mixed with 3 mL scintillation fluid and counted. Total counts were defined as the combined counts from the Dowex elutions and the two aluminium oxide elutions. Product counts were defined as the combined counts from the two aluminium oxide elutions. Percentage nucleotide converted was defined as (product counts / total counts)*100.

2.5.3 *In vitro* AC assays (old method – Sections 3.4 and 4.2)

Adenylyl cyclase assays were performed at 37°C unless otherwise stated and were carried out in a final volume of 100 µL in a 1.5 mL microcentrifuge tube. Assays were buffered with 50 mM Mes-NaOH (pH 6.5) or Tris-HCl (pH 7.0 and above). Assays were spiked with [α-^{32}P]-ATP (25 kBq) as a substrate. An ATP regenerating system (5 units creatine phosphokinase and 5 µM creatine phosphate) and 1 mM IBMX was included when assaying crude cell preparations (see 2.3.4).

Assays were always initiated by the addition of substrate and reactions were stopped with the addition of 150 µL stop solution (50 mM Tris-HCl pH 7.5 and 5 % (w/v) SDS). 100 µL tritium control solution (1 mM ATP, 1 mM cAMP and [2,8-^{3}H]-cAMP (150 Bq)) was added to each sample followed by 650 µL H_2O.

cAMP was resolved using the twin column chromatography approach. 1 mL samples were applied to 1 mL Dowex columns, allowed to flow through, and washed with 2 mL H_2O. Nucleotides bound to the Dowex column were washed onto 1 mL aluminium oxide with 5 mL H_2O. Cyclic nucleotides were then eluted from the aluminium oxide columns with 3 mL 100 mM Tris-HCl pH 7.5, mixed with 3 mL scintillation fluid, and counted. Protein concentration was adjusted to limit substrate utilisation to below 10%.

2.5.4 *In vitro* AC assays (new method – Section 4.3 onwards)

100 µL assays were carried out in closed 1.5 mL microcentrifuge tubes at 37°C. Assays were buffered with 100 mM Mes-NaOH (pH 6.5) or Tris-HCl (pH 7.0 and above). An ATP regenerating system (5 units creatine phosphokinase and 5 µM creatine phoshate) and 1 mM IBMX was included when assaying crude cell preparations.

For each $NaHCO_3$ assay pH a series of NaCl assay pHs were used to ensure that the pH of the $NaHCO_3$ point fell between that of the NaCl points (see section 4.3).

While the main assays were spiked with [α-^{32}P]ATP (25 kBq) as a substrate, an identical series of assays was set up without radioactive substrate. This set of assays was used to accurately measure pH at the end of the assay using a computer driven pH microelectrode (see 2.5.9).

Assays were stopped and analysed as previously (see 2.5.2).

2.5.5 Preparation of DNA template for RNA polymerase assays

Using M13 forward and M13 reverse primers, the 3.8 kb DNA fragment of pQ3N1 was amplified through PCR with BIOTAQ™ Red DNA polymerase (see 2.2.1), analysed by agarose gel electrophoresis (see 2.2.2), and purified (see 2.2.3) (Katayama and Ohmori, 1997).

2.5.6 *In vitro* RNA polymerase assays

RNA polymerase assays were performed at 37°C in a final volume of 100 µL in a 1.5 mL microcentrifuge tube, following essentially the same protocol as that used used for ACs (see 2.5.3 for experiments in Section 4.2 and 2.5.4 for experiments in Section 4.3). Assays were buffered with 50 mM Mes-NaOH (pH 6.5) or Tris-HCl (pH 7.0 and above). Assays were all spiked with [α-^{32}P]-ATP (25 kBq) as a substrate and contained 10 µg DNA template (see 2.5.5). Following completion of the reaction 40 µL was spotted onto Whatmann 3MM paper (which had been pre-soaked in 10 % (w/v) TCA and dried), allowed to dry fully and then washed in 10 % (w/v) TCA for 1 hour. Filters were then washed three times in 2.5 % (w/v) TCA for 30 minutes each, placed in scintillation vials containing 4 mL scintillation fluid, and then counted on a liquid scintillation counter. Protein concentration was adjusted to limit substrate utilisation to below

10%.

2.5.7 *In vitro* DNA polymerase assays

DNA polymerase assays were performed essentially the same as the RNA polymerase assays in Section 4.3, with the exceptions that assays were spiked with [α-^{32}P]-dATP (25 kBq) and 10 µg activated calf thymus DNA as a template.

2.5.8 *In vitro* GC assay

Guanylyl cyclase assays were performed essentially the same as the new method adenylyl cyclase assays (see 2.5.4), but with a few modifications. Assays were spiked with [α-^{32}P]-GTP (25 kBq) as substrate and 100 µL tritium control solution (1 mM GTP, 1 mM cGMP and [8-^{3}H]-cGMP (150 Bq)) was added following the termination of the assay.

62 mg of total protein from GC-A transfected NIH 3T3 cell lysates, and 45 mg of total protein from GC-E transfected NIH 3T3 cell lysates were used.

1 mL samples were applied to 1 mL Dowex columns, allowed to flow through and washed with 1 mL with H_2O. Nucleotides bound to the Dowex column were washed onto 1 mL aluminium oxide columns with 5 mL H_2O. Aluminium oxide columns were washed with 2 mL 100 mM Tris-HCl pH 7.5, and cGMP was eluted from the aluminium oxide columns with 3 mL 100 mM Tris-HCl pH 7.5, mixed with 3 mL scintillation fluid and counted.

2.5.9 pH measurements

pH measurements were made using a computer driven micro-pH electrode (Hamilton Biotrode connected to the Orion pH SensorLink program) to measure 100 µL solution in a 1.5 mL microcentrifuge tube. The pH meter was calibrated using standard pH buffer solutions (pH 4, 7 and 10).

2.6 Statistics

All error bars represent the standard error of mean. All statistics and graphical analysis was performed using GraphPad Prism 4 (GraphPad Software, inc.). All data shown is representative of at least 2 independent experiments.

3

Ci and mammalian tmAC

3.1 Introduction

Following the identification of mammalian soluble adenylyl cyclase (sAC) as a Ci responsive enzyme, several other adenylyl cyclases (ACs) were shown to respond to Ci, including ACs from *Spirulina platensis* (CyaC), *Anabaena* PCC 7120 (CyaB1), *Synechocystis* PCC 6803 (Slr1991), *Chloroflexus aurantiacus* (Chlo1187) and *Stigmatella aurantiaca* (CyaB) (Cann *et al.*, 2003; Chen *et al.*, 2000; Hammer *et al.*, 2006; Masuda and Ono, 2005; Steegborn *et al.*, 2005b). These ACs all possess a Class IIIb cyclase homology domain (CHD), and the defining feature of this group (the replacement of a substrate defining aspartate with a serine or threonine residue) was hypothesised to be a marker for Ci responsiveness (Cann *et al.*, 2003; Linder and Schultz, 2003). Despite the response to Ci being thought to be a feature unique to ACs in possession of a Class IIIb CHD, several ACs possessing other CHDs were shown to be Ci responsive, including ACs from *Mycobacterium tuberculosis* (Rv1625), *Cryptococcus neoformans* (Cac1), and *Candida albicans* (Cdc35) (Klengel *et al.*, 2005; Mogensen *et al.*, 2006; Townsend *et al.*, 2009).

These Ci responsive enzymes were originally proposed to be activated by HCO_3^-, as opposed to the other physiologically relevant species of Ci; CO_2 (Cann *et al.*, 2003; Chen *et al.*, 2000). However, recent work has provided strong evidence that these Ci responsive enzymes are actually activated by CO_2 and not HCO_3^-, as was previously assumed (Hammer *et al.*, 2006). Due to the effect that pH has upon the equilibrium formed between CO_2 and HCO_3^-, the relative molar amounts of each species varies significantly as the pH is changed (Figure 1.1). At pH 8.5 the total Ci pool is almost totally comprised of HCO_3^-, but as the pH is lowered the concentration of HCO_3^- decreases as CO_2 increases, such that at pH 6.5 the Ci pool is about 40 % (mol/mol) CO_2 and 60 % (mol/mol) HCO_3^- (Figure 1.1).

Previous investigation into the effect of Ci on a mammalian transmembrane AC (tmAC), which possesses a Class IIIa CHD, has provided contrasting data (Chen *et al.*, 2000; Xie *et al.*, 2006). Although more recent investigation suggested that mammalian type III AC was activated by Ci *in vitro* (Figure 1.11B), earlier research showed no response of a recombinant 'soluble' tmAC to Ci *in vitro* (Figure 1.11A) (Chen *et al.*, 2000; Xie *et al.*, 2006). When new evidence suggesting that CO_2 (as opposed to HCO_3^-) was the activating

species of Ci was taken into account, it became apparent that a response of the 'soluble' tmAC to Ci *in vitro* had possibly been missed, since the concentration of CO_2 was potentially too low at the pH tested to elicit a response (Chen *et al.*, 2000; Hammer *et al.*, 2006). The assays performed *in vitro* on the 'soluble' tmAC were conducted at pH 7.5, a pH where the levels of CO_2 were relatively low (Chen *et al.*, 2000). Working on the assumption that CO_2 activates these Ci responsive ACs, the response of a tmAC to Ci was re-tested at a more suitable pH where the concentration of CO_2 was higher. Since it is possible that not all 9 tmACs are Ci responsive, this was initially carried out using an *in vivo* approach to study the endogenous tmACs in a mammalian cell line. To build upon previous experimentation, the response of a tmAC would also be tested biochemically *in vitro*, to aid the identification of the mechanism through which Ci mediates its effects.

3.2 The effect of Ci on intracellular pH

The effects of Ci on the production of cAMP by tmACs *in vivo* was examined through a cAMP accumulation assay using Human Embryonal Kidney (HEK) 293T cells. Cultured HEK 293T cell monolayers were exposed to hypocapnic (below normal levels of CO_2; 0.03 % (v/v) CO_2 in air), normocapnic (normal levels of CO_2; 5 % (v/v) CO_2 in air) or hypercapnic (above normal levels of CO_2; 10 % (v/v) CO_2 in air) conditions. However, before cAMP accumulation assays were performed, a series of control experiments were performed to identify any effects that variable CO_2 concentrations could have upon intracellular pH (pH_i).

HEK 293T cells were grown under normocapnic conditions until the start of the experiment whereby they were exposed to hypocapnic, normocapnic or hypercapnic conditions. Due to the fact that the equilibrium formed between CO_2 and HCO_3^- (Figure 1.1) can affect pH, it was possible that exposing cells to elevated CO_2 would cause an intracellular acidification through an influx of CO_2 into the cell (and vice versa). Following diffusion of CO_2 into the cell, carbonic anhydrases (CAs) would accelerate the equilibration of CO_2 into HCO_3^-, causing a release of protons (Figure 1.1 and Figure 1.2). Although there is some evidence to suggest that certain tmACs are protected from changes in pH_i through co-localisation with a Na^+/H^+ exchanger on lipid rafts, it was still necessary to quantify any pH changes since they could effect a plethora of intracellular processes (Willoughby *et al.*, 2005).

This pH control experiment was performed in collaboration with Dr. Mike Gray at Newcastle University and involved exposing cells to a pH sensitive dye which was used to quantify pH_i using a microspectrofluorometric system. Cells were grown on a glass coverslip to confluence and then loaded with the pH sensitive dye 2',7'-bis(carboxyethyl)-5(6)-carboxyfluorescein (BCECF) in the form of its acetoxymethyl ester (BCECF-AM). Following entry into the cell BCECF-AM was cleaved by the endogenous esterases in the cell, liberating the active molecule BCECF. The coverslip carrying BCECF loaded cells was placed onto a specially adapted microspectrofluorometric system and the incubation solutions (see 2.5.1; hypocapnic, normocapnic or hypercapnic) allowed to perfuse across the cell monolayer, and pH_i was recorded (Figure 3.1).

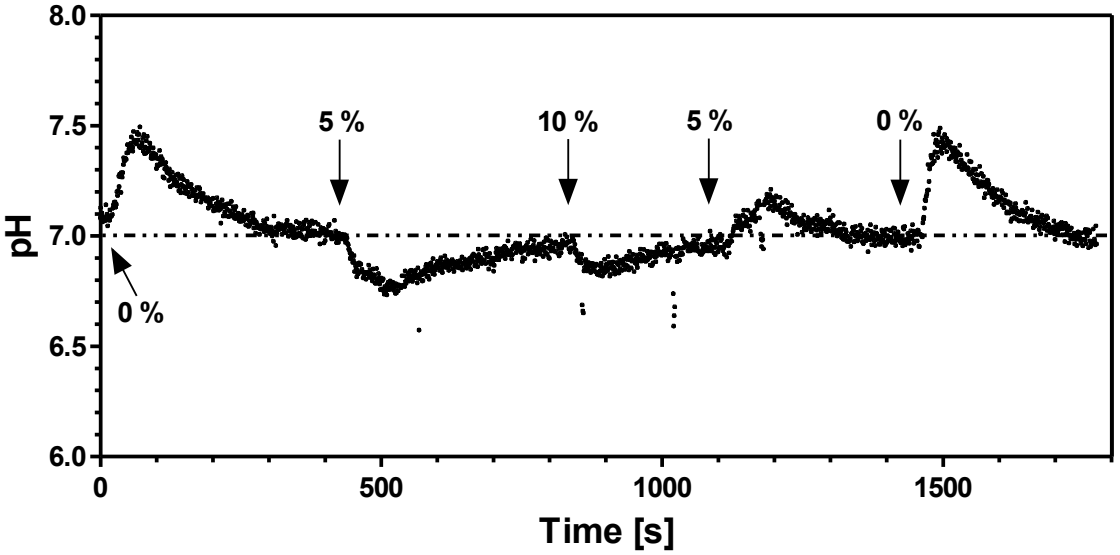

Figure 3.1: Intracellular pH measurements on HEK 293T cells.

Cells were adhered to a 24 mm^2 coverslip and loaded with 1 µM 2',7'-bis(carboxyethyl)-5(6)-carboxyfluorescein acetoxymethyl ester. Calibration of intracellular pH was carried out using the high potassium nigericin method. % = percentage (v/v) CO_2 in Air.

As can be seen (Figure 3.1), changing between different CO_2 solutions had a moderate effect on pH_i, however, this change in pH_i was always followed by a gradual recovery back to the starting pH_i. It was observed that when the CO_2 concentration in the perfused solution was raised, an initial rapid acidification of the cell would occur, followed by a gradual recovery of pH_i back to the original pH 7.0 over a period of about 8 - 10 minutes (Figure 3.1). The converse was seen when reducing the CO_2 concentration in the perfused solution; a rapid increase in pH_i, followed by a gradual recovery back to the original pH_i (Figure 3.1). This data demonstrated that if the cells were given at least 10 minutes to recover following a change in the CO_2 concentration of the incubation medium that the pH_i would return to the initial value.

3.3 The effect of Ci on the production of cAMP *in vivo*

Since the level of cAMP within cells is controlled by two opposing forces, ACs producing cAMP and phosphodiesterases (PDEs) degrading cAMP, an incubation with the generic PDE inhibitor isobutylmethylxanthine (IBMX) was required prior to the stimulation of cAMP production, to allow all cAMP produced to be quantified. This incubation with IBMX was carried out for 30 minutes, following the addition of the required CO_2 medium to the cells. The incubation allowed the pH_i of the HEK 293T cells to recover following exposure to hypercapnic or hypocapnic conditions, and also allowed IBMX to act upon its target. As such, *in vivo* cAMP accumulation assays on HEK 293T cells were always performed in a two step manner. Step one was the pre-incubation phase, where cells were pre-incubated for 30 minutes at 37°C in the required CO_2 media containing 1 mM IBMX. Step two was the stimulation of the cells with an agonist for 30 minutes, to stimulate the production and thus accumulation of cAMP within the cell.

Before studies into the effects of Ci on the production of cAMP by tmACs *in vivo* could commence it was necessary to ensure that cells were exposed to the correct concentration of agonist. If too high a concentration of agonist were used it was possible that tmAC activity would be high enough to convert all ATP available to the tmACs into cAMP, preventing any effects of Ci being seen. A suitable concentration of isoproterenol was determined by exposing HEK 293T cells to a range of isoproterenol concentrations and quantifying the amount of cAMP produced (Figure 3.2A). It was observed that there was a significant difference in cAMP accumulated between 1 and 100 nM isoproterenol, but no further increase in cAMP between 100 and 1000 nM suggesting the endogenous tmACs were at maximal activity at 100 nM. From this experiment it was concluded that the most suitable concentration of isoproterenol would be 10 nM. An identical control experiment was performed to identify the appropriate concentration of forskolin (a plant diterpene and non-specific activator of tmACs) to suitably stimulate tmACs within HEK 293T cells (Seamon *et al.*, 1981). A dose response of forskolin was performed on HEK 293T cells (Figure 3.2B) and indicated that 5 µM forskolin would be a suitable concentration.

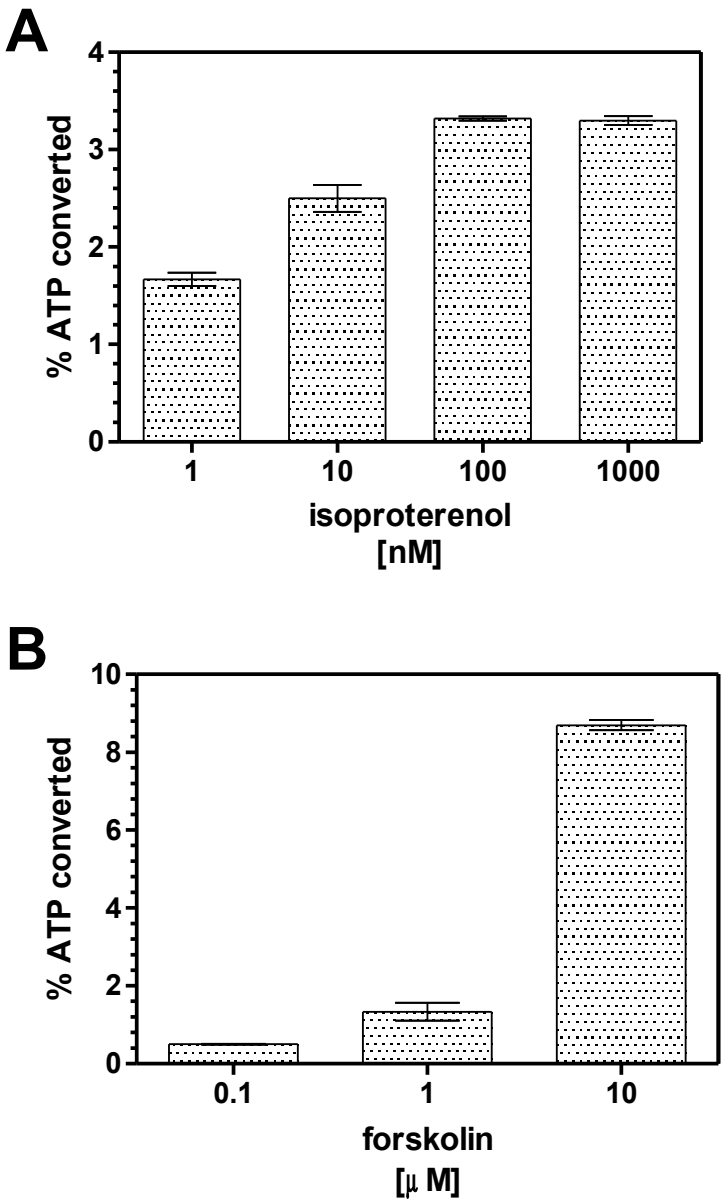

Figure 3.2: Preliminary cAMP accumulation assays on HEK 293T cells.

Cells were incubated under normocapnic conditions at pH 7.0 for 30 minutes at 37°C in incubation medium (see Section 2.5.1) containing 1 mM IBMX. Cells were then incubated for 30 minutes at 37°C in the presence of variable isoproterenol **(A)** or forskolin **(B)**. (n = 3)

With suitable concentrations of agonists identified it was possible to investigate the effects of Ci on the production of cAMP in HEK 293T cells. HEK 293T cells were exposed to hypocapnic, normocapnic and hypercapnic conditions and the production of cAMP through tmACs was quantified (Figure 3.3). When cells were stimulated with 10 nM isoproterenol (Figure 3.3A) a clear decrease in the production of cAMP could be seen when the CO_2 concentration was dropped from normocapnic (5 %) to hypocapnic (0.03 %) levels. A similar effect was also seen when the endogenous tmACs in HEK 293T were stimulated with forskolin (Figure 3.3B), where a clear decrease in cAMP production was seen from normocapnic to hypocapnic levels. Interestingly, an increase in cAMP production was not seen when moving from normocapnic to hypercapnic (10 %) levels of CO_2, in either the presence of isoproterenol or forskolin (Figure 3.3A/B).

These experiments provided strong evidence that a decrease in intracellular Ci in HEK 293T cells resulted in a decrease in cAMP production, when the tmACs were stimulated with an agonist (Figure 3.3A/B). However, the possibility that sAC was in fact responsible for these increases in cAMP could not be ruled out and was investigated further. This was done by repeating the forskolin experiment (Figure 3.3B) in the presence or absence of the sAC specific inhibitor KH7 (kind gift from Professors Lonny Levin and Jochen Buck) (Figure 3.4) (Hess *et al.*, 2005). The addition of KH7 had no effect on the decrease in cAMP seen between normocapnic and hypocapnic conditions (Figure 3.4).

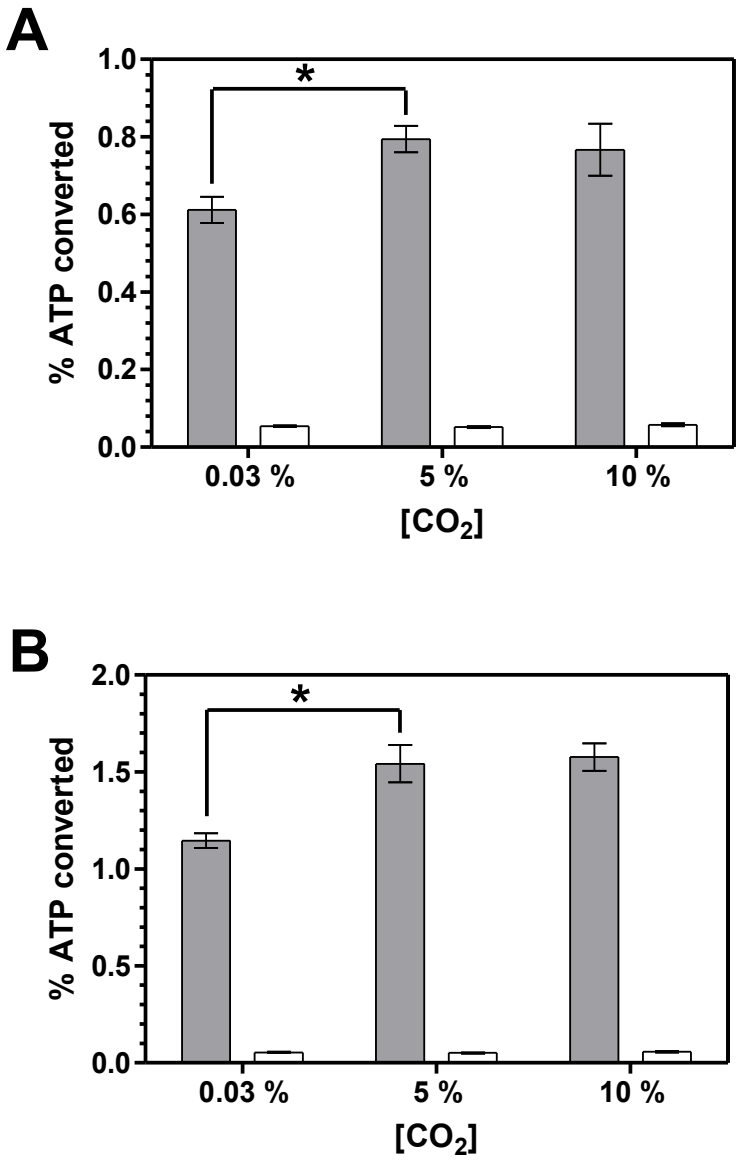

Figure 3.3: The effect of Ci on the accumulation of cAMP in HEK 293T cells.

HEK 293T cells were exposed to varied CO_2 concentrations (% = percentage (v/v) CO_2/Air), and cAMP accumulation was quantified over a 30 minute time period in the presence of 1 mM IBMX. **(A)** Cells were stimulated with (dark) or without (clear) 10 nM isoproterenol. **(B)** Cells were stimulated with (dark) or without (clear) 5 µM forskolin. * $p < 0.05$ ($n = 12$)

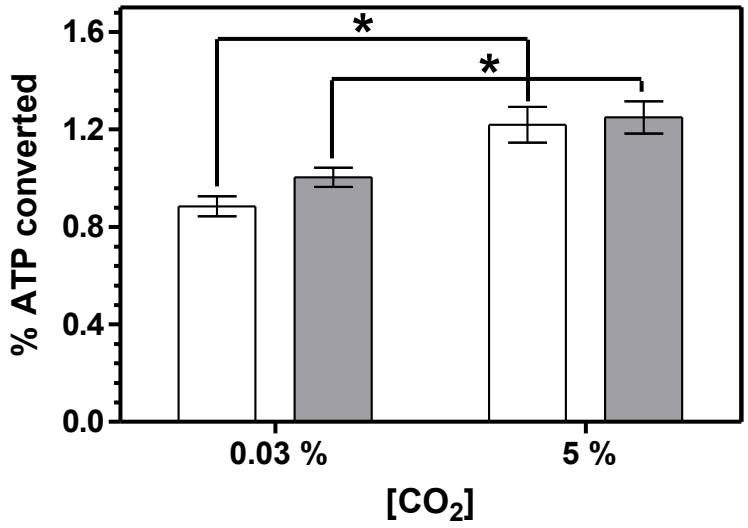

Figure 3.4: Ci dependent cAMP accumulation was due to tmACs and not sAC.

HEK 293T cells were exposed to varied CO_2 concentrations (% = percentage (v/v) CO_2/Air) and cAMP accumulation was stimulated with 5 µM forskolin over a 30 minute time period in the presence of 1 mM IBMX, with (dark) or without (clear) 1 µM KH7. * $p < 0.05$ ($n = 12$)

These *in vivo* experiments (Figure 3.3 and Figure 3.4) provided evidence that Ci was either directly or indirectly acting upon tmACs, with the resulting effect of increasing their production of cAMP. However, at this stage the question still remained as to whether the effect of Ci on intracellular cAMP production could have any downstream physiological effects. In order to address this it was decided to investigate the effect of Ci on the phosphorylation of the cAMP response element binding protein (CREB). It was expected that if the levels of cAMP produced from tmACs were increased (or decreased) then a subsequently stronger (or weaker) activation of protein kinase A (PKA) would occur, leading to more (or less) phosphorylation of CREB at serine 133 (Figure 3.5) (Gonzalez and Montminy, 1989).

The phosphorylation state of CREB in HEK 293T cell lysates was quantified through immunoblotting with an antibody specific for CREB phosphorylated at serine 133 (phospho-CREB). Cell lysates were prepared by repeating the the isoproterenol experiment (Figure 3.4A) with the exception that cells were not loaded with [^{3}H]-adenine, and the assay was stopped by the addition of 1 mL SDS-PAGE loading buffer instead of trichloroacetic acid. The protein content of cell lysates was resolved through SDS-PAGE, transferred to nitrocellulose membrane, and the membrane was probed with antibodies specific to phospho-CREB and α-tubulin. The antibody specific to α-tubulin was used as a loading control to allow any small differences in total protein loaded to be compensated for. Western blots were scanned using a Fuji Las-1000 chemiluminescent scanner and bands were quantified using the in built software package.

It was clear when comparing cells exposed to hypocapnia and normocapnia that a marked increase in the ratio of phospho-CREB : α-tubulin was present in the normocapnic sample (Figure 3.6), demonstrating an increase in phospho-CREB in this sample. The amount of CREB phosphorylation was derived as the ratio of phospho-CREB : α-tubulin, such that the larger the ratio the more phospho-CREB was present. Interestingly, the levels of phospho-CREB in the samples exposed to hypercapnia were not significantly different to those samples exposed to hypocapnia, however, the reasons for this remains unclear.

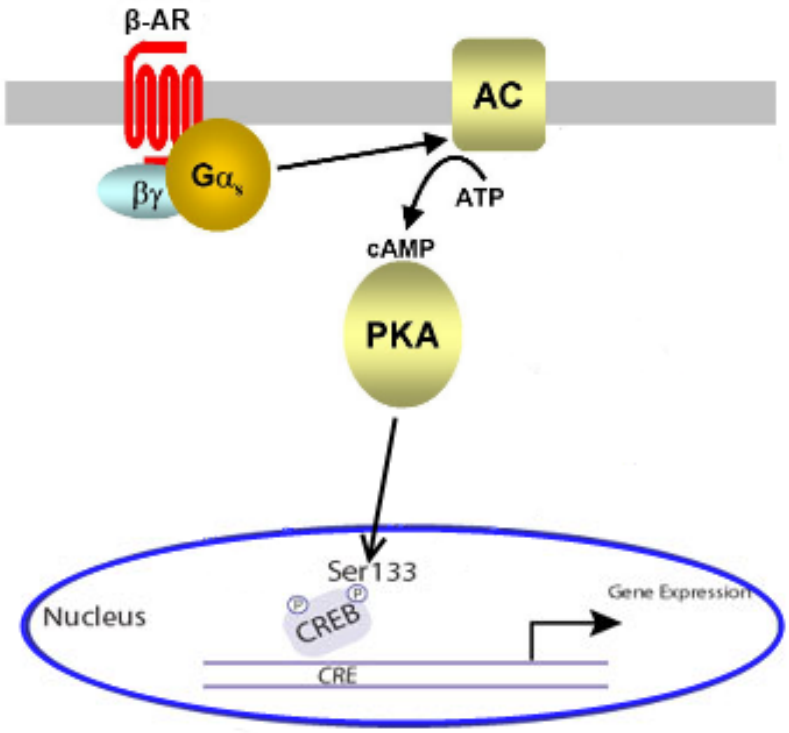

Figure 3.5: Activation of CREB through a β-adrenergic receptor linked cAMP signalling pathway.

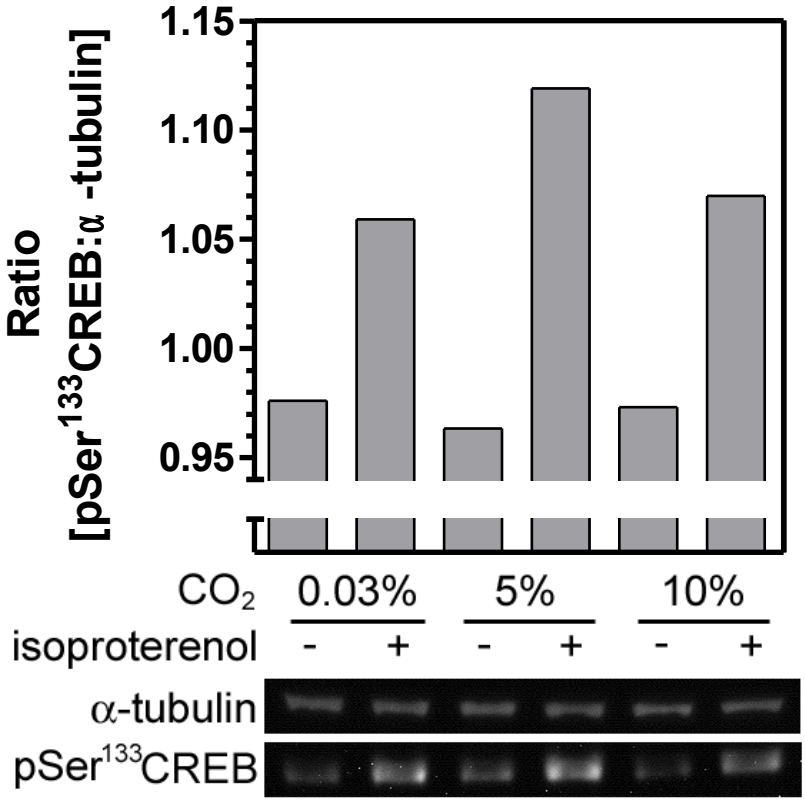

Figure 3.6: The effect of varied CO_2 concentration on the phosphorylation of CREB.

(Lower) Immunoblot of HEK 293T cell lysates after a 10 minute incubation with or without 10 nM isoproterenol at varying CO_2. **(Upper)** The ratio of phospho-CREB:α-tubulin bands from the quantified bands.

3.4 The effect of Ci on a mammalian tmAC *in vitro*.

With *in vivo* experiments providing evidence to suggest that Ci can act in HEK 293T cells to increase the production of cAMP by tmACs, attention was turned to the effect of Ci on tmACs *in vitro*, in order to establish whether Ci was acting in a direct or indirect manner on tmACs. It was decided to perform *in vitro* biochemical assays on recombinant proteins expressed in *E. coli.* Work done previously had shown that an active AC with biochemical properties similar to the native protein could be obtained through independently expressing the two tmAC catalytic domains (C1a and C2a, C_1 and C_2 herein; Figure 3.7) and mixing the two domain together (Sunahara *et al.*, 1997; Tang and Gilman, 1995; Whisnant *et al.*, 1996).

The AC chosen was a soluble chimera consisting of the C_1 domain (amino acids 263-476) of human type VII AC ($7C_1$) and the C_2 domain (amino acids 821-1090) of rat type II AC ($2C_2$) (Tesmer *et al.*, 2002; Yan and Tang, 2002). These two hexa-histidine tagged recombinant proteins were independently expressed in *E. coli* (plasmids kind gift of Roger Sunahara, University of Michigan), and purified to homogeneity through Ni^{2+}-NTA affinity chromatography and anion exchange chromatography (Figure 3.8). Mixing of these two domains resulted in an active AC ($7C_1 \bullet 2C_2$) that was activated by forskolin (Figure 3.12B). Although forskolin was to be used during the biochemical analysis it was also important to perform assays in the presence of a physiological activator of tmACs; the alpha stimulatory subunit of the heterotrimeric G protein ($G\alpha_s$). Hexa-histidine tagged recombinant $G\alpha_s$ was expressed in *E. coli* (plasmid kind gift from Roger Sunahara, University of Michigan), and purified through Ni^{2+}-NTA affinity chromatography and anion exchange chromatography (Figure 3.8). Following purification, $G\alpha_s$ was permanently activated through incubation with GTPγS, which is a non-hydrolysable GTP analog. $G\alpha_s \bullet$GTPγS ($G\alpha_s$ herein) also activated $7C_1 \bullet 2C_2$ (Figure 3.12B).

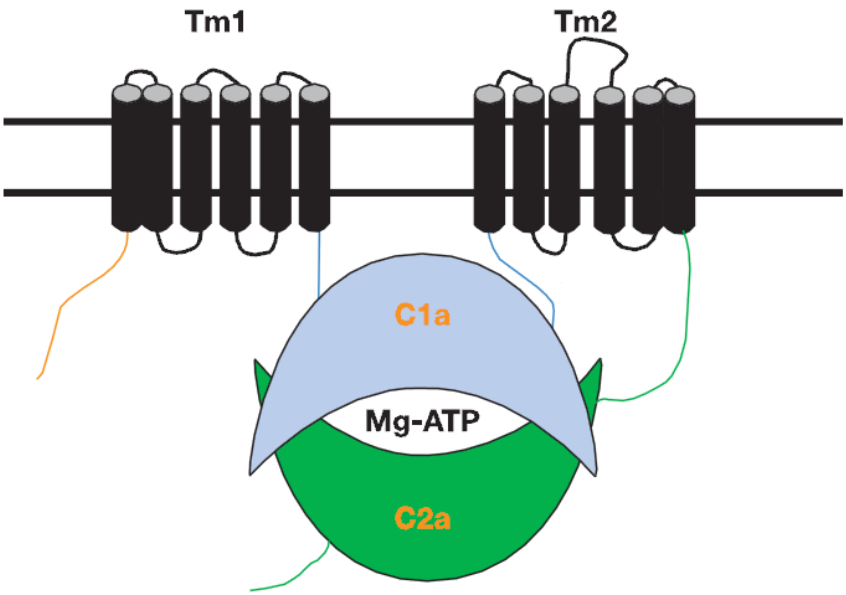

Figure 3.7: Structure of a tmAC.

Taken from (Cooper, 2003b)

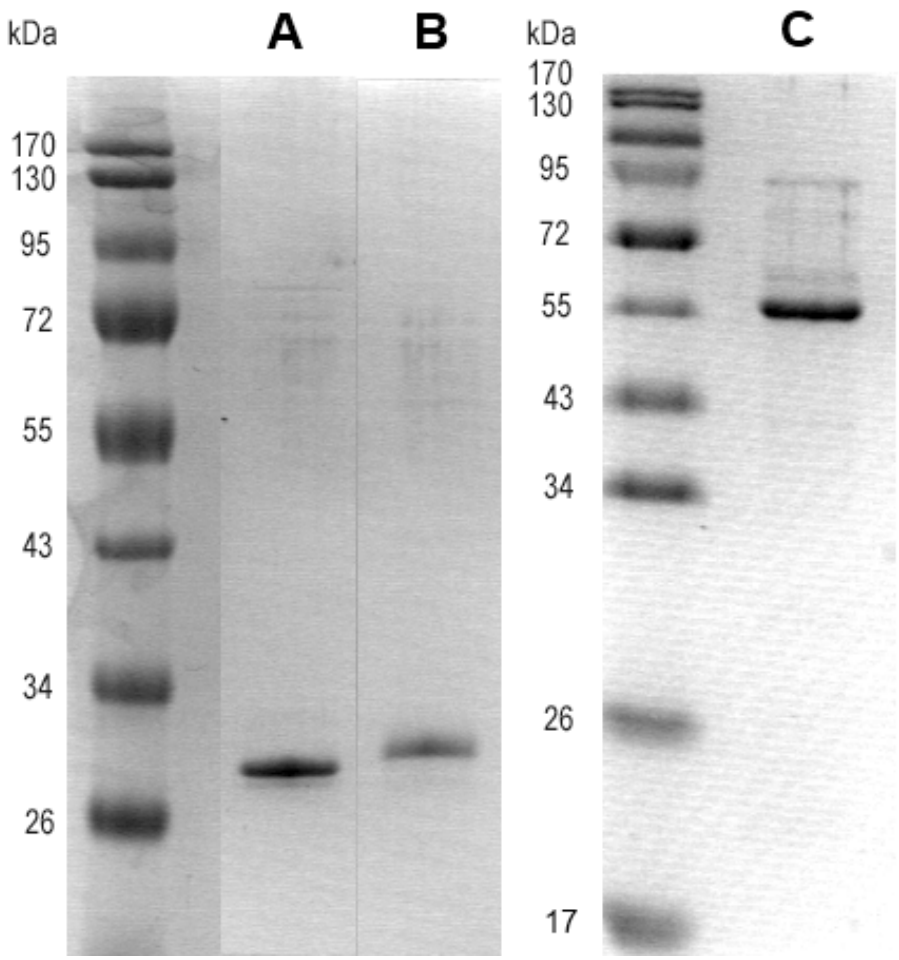

Figure 3.8: SDS-PAGE showing purified $7C_1$, $2C_2$ and $G\alpha_s$.

2 µg of purified protein resolved on 12 % SDS-PAGE gel. **(A)** $7C_1$ **(B)** $2C_2$ **(C)** $G\alpha_s$. Proteins were stained with Coomassie Brilliant blue dye and protein size was estimated relative to Fermentas PagerRuler™ Prestained Protein ladder.

Before the effects of Ci on the G protein stimulated activity of $7C_1 \bullet 2C_2$ could be studied, one important factor required consideration. It was paramount for the pH within each assay to be tightly controlled since this variable has a pronounced effect on AC activity. Suitable buffers were chosen to generate the desired pH prior to the initiation of catalysis, but also to maintain a stable pH throughout the reaction. Since HCO_3^- and CO_2 exist in a pH dependent equilibrium, and addition of one or the other to a solution can effect pH, it was necessary to use a relatively high buffer concentration of 50 mM, to attempt to minimise any possible effects of Ci on pH. Both the reaction mixture without substrate and substrate (used for initiation of catalysis) were buffered appropriately to ensure a minimal pH change following the addition of the substrate to the assay. Furthermore, the 100 mM salt stock mixture (NaCl or $NaHCO_3$) was buffered with 50 mM buffer to the appropriate pH to minimise any change in pH following addition to the reaction mixture.

The pH control assays were performed in a microcentrifuge tube, using a computer driven micro pH electrode to measure the pH of the 100 µL mock AC assay. Before the desired salt solution was added, the pH of the 80 µL reaction mixture lacking salt was recorded. After 20 seconds, 20 µL of the buffered 100 mM salt mixture was added to give a final concentration of 20 mM salt. The solution was mixed and the pH was recorded over a 20 minute period. These pH control assays demonstrated that the desired pH could be achieved in the presence and absence of Ci, and that pH was stable throughout the time course of reaction (Figure 3.9A).

The first important *in vitro* experiment performed was an assessment of the effect of Ci on $7C_1 \bullet 2C_2$ activity across a range of different pHs. Assays were carried out between pH 6.5 and 8.5 in the presence of 20 mM total Ci (supplied as 20 mM $NaHCO_3$) or NaCl. The pH activity profile of $7C_1 \bullet 2C_2$ in the presence of NaCl (Figure 3.9B) was consistent with data acquired for a similar recombinant tmAC, showing a pH optimum at about pH 8.0 (Hatley *et al.*, 2002). Comparing the activities in the presence or absence of Ci across pH showed that a strong 2 fold activation of $7C_1 \bullet 2C_2$ by Ci occurred at pH 6.5, with a slight stimulation being consistently seen at pH 7.0 (Figure 3.9C). This was consistent with what was seen previously with prokaryotic class IIIb ACs, and was possibly due to the fact that the levels of CO_2 are high at pH 6.5 and that these ACs are activated by CO_2 and not HCO_3^- as was previously assumed(Hammer *et al.*,

2006). Since a strong activation of $7C_1 \bullet 2C_2$ by Ci was only seen at pH 6.5 and not at pH 7.0 and above, all further biochemical assays were carried out at pH 6.5 only.

An ATP dose response in the presence or absence of Ci was performed to investigate any effects of Ci on substrate affinity (Figure 3.10A). This dose response was performed across a range of 0.1 – 5 mM ATP at pH 6.5, and in the presence or absence of 20 mM total Ci. The data generated was analysed for Michaelis-Menten kinetics using the non-linear regression package in Graphpad Prism, and V_{max} and K_m(ATP) values were generated. Analysis showed that whilst V_{max} was increased in the presence of Ci (76.4 ± 4.1 nmoles cAMP mg^{-1} min^{-1} with Ci and 44.9 ± 2.8 nmoles cAMP mg^{-1} min^{-1} with Cl^-), K_m(ATP) remained unchanged (2.0 ± 0.23 mM with Ci and 1.9 ± 0.2 mM with Cl^-). Analysis of the data also revealed that substrate turnover, k_{cat}, increased in the presence of Ci (10.7 s^{-1} with Ci and 6.4 s^{-1} with Cl^-).

Mammalian tmACs are magnesium dependent enzymes, with two Mg^{2+} cations critical for catalysis being coordinated to the active site by two aspartate residues located on the C_1 domain (D284 and D328 on recombinant $7C_1$) (Tesmer *et al.*, 1999; Zimmermann *et al.*, 1998). Previous investigation into the effect of Ci on CyaC (*Spirulina platensis*) had revealed that the effects of Ci were possibly mediated through altered metal binding (Steegborn *et al.*, 2005b). Thus, it was of interest to look at whether the metal binding dynamics of $7C_1 \bullet 2C_2$ were similarly altered by the presence of Ci. A dose response to Mg^{2+} was generated across the range of 1 – 20 mM Mg^{2+} (Figure 3.10B). Interestingly, the presence of Ci appeared to increase the affinity of $7C_1 \bullet 2C_2$ for Mg^{2+} (1.6 ± 0.2 mM with Ci and 2.6 ± 0.4 mM with Cl^-), indicating that Ci may mediate its effects through altered metal binding. Following binding of Mg^{2+}-ATP to the active site the second Mg^{2+} ion binds and subsequent closure of the active site promotes catalysis (Steegborn *et al.*, 2005a). One could speculate that the effects of Ci are mediated through a more rapid recruitment of the second Mg^{2+} ion, and subsequent active site closure.

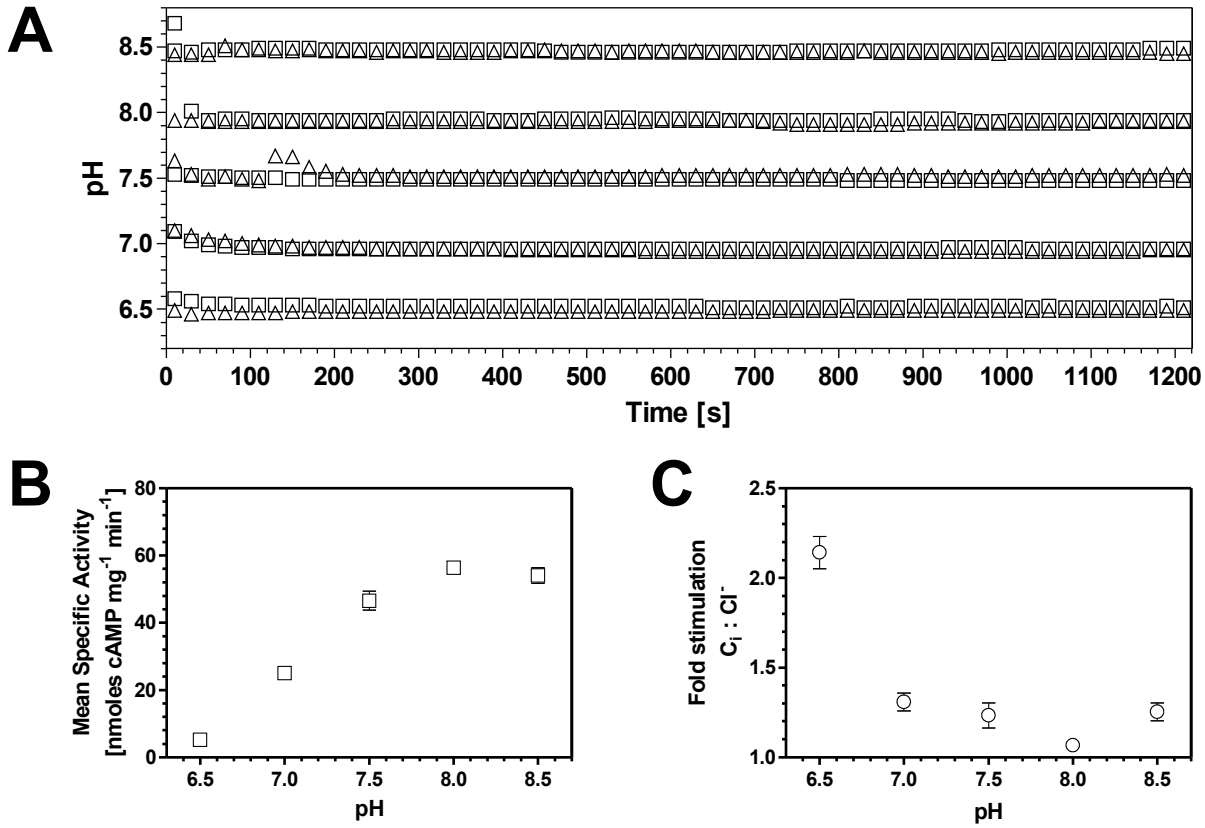

Figure 3.9: $7C_1 \bullet 2C_2$ is activated by Ci independently of pH.

1.1 µM $7C_1$, 5.8 µM $2C_2$ and 7 µM $G\alpha_s$ was assayed at varying pH in the presence of 500 µM Mg^{2+}-ATP. **(A)** Mock AC assay carried out in the absence of [α-^{32}P]-ATP with a micro pH electrode to monitor assay pH. 20 mM NaCl (squares) or $NaHCO_3$ (triangles), buffered to the appropriate pH, was added after 20 seconds. **(B)** Mean specific activity of $7C_1 \bullet 2C_2$ at varying pH in the presence of 20 mM NaCl **(C)** Fold stimulation (Inorganic carbon [C_i] : chloride) of $7C_1 \bullet 2C_2$ at varying pH.

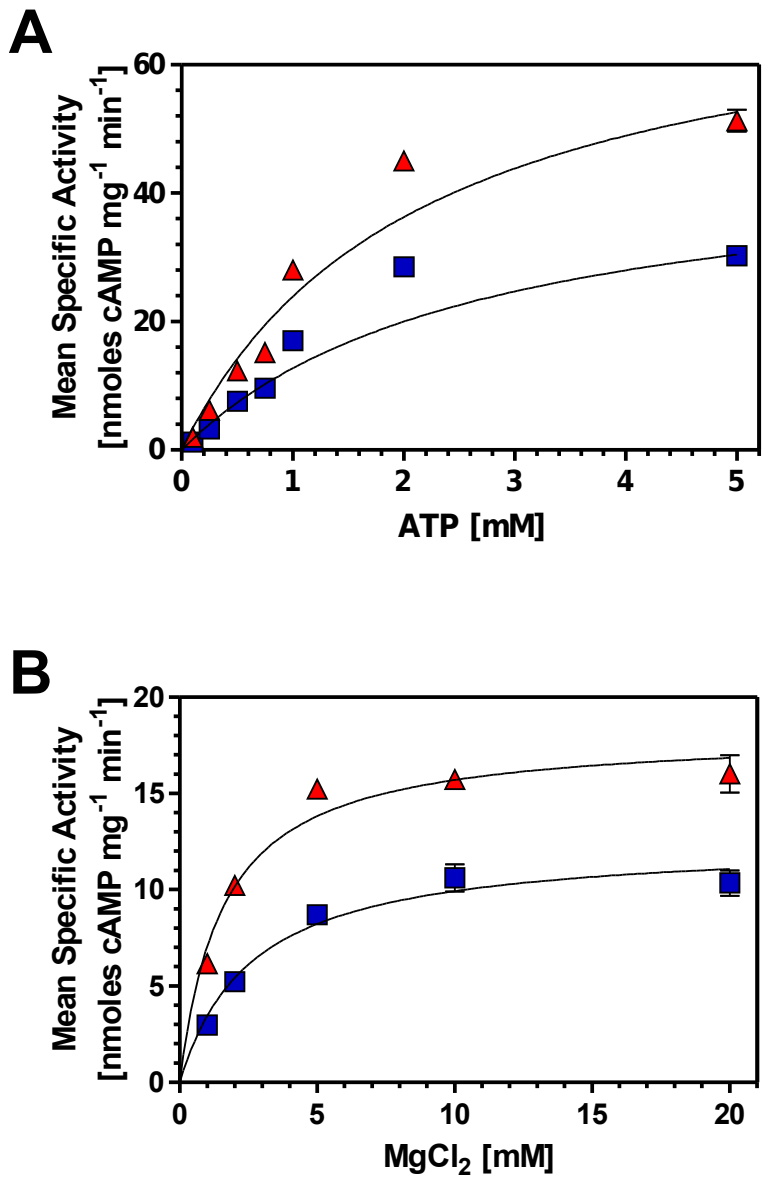

Figure 3.10: The effects of Ci on $7C_1 \bullet 2C_2$ activity *in vitro*.

1.1 µM $7C_1$, 5.8 µM $2C_2$ and 7 µM $G\alpha_s$ was assayed at 37°C for 20 minutes in the presence of 100 mM Mes-NaOH pH 6.5. **(A)** ATP dose response in the presence of 20 mM NaCl (blue squares) or $NaHCO_3$ (red triangles), and 20 mM $MgCl_2$. **(B)** Magnesium dose response in the presence of 20 mM NaCl (blue squares) or $NaHCO_3$ (red triangles), and 500 µM Mg^{2+}-ATP. (n = 9)

The response of $7C_1 \bullet 2C_2$ to $G\alpha_s$ under increasing concentrations of Ci was investigated to establish whether a stimulation by Ci could be observed in the presence of a physiologically relevant Ci concentration (Figure 3.11A). It was again demonstrated that Ci elicits a significant stimulatory effect upon $7C_1 \bullet 2C_2$, noting that the total salt concentration in the assay was controlled through the addition of $NaHCO_3$ or NaCl as appropriate. Significant stimulation of $7C_1 \bullet 2C_2$ by Ci began at a physiologically relevant concentration of 4 mM total Ci, as assessed with 95 % confidence intervals. Analysis of the data with the non-linear regression package in Graphpad Prism revealed an EC_{50} (app) of 10.6 ± 0.8 mM for Ci. Due to the observation that CO_2 rapidly degassed from solution at pH 6.5 when the total Ci concentration was higher than 20 mM, it was not possible to extend this assay to include a these higher concentrations. Another possible way that Ci could act to increase activity was through reducing the overall activation energy required for bond cleavage or formation during the catalytic cycle. In order to investigate this an Arrhenius plot was derived in the presence and absence of Ci at 5ºC, 10ºC, 15ºC, 19.5ºC, 24.5ºC, 30ºC and 35ºC (Figure 3.11B). No effect of Ci on the energy of activation was seen (100.4 ± 4.0 kJ mol^{-1} with Ci and 99.6 ± 6.7 kJ mol^{-1} with Cl^-), when the linear portion of the Arrhenius plot was analysed (Figure 3.11B).

It was demonstrated that $7C_1 \bullet 2C_2$ was activated by Ci, and although results indicate that Ci may act through an increased affinity for Mg^{2+}, other variables still required testing. Previous work indicated that Ci may also act through promoting active site closure, producing a catalytically active enzyme (Steegborn *et al.*, 2005b). Promotion of active site closure may also occur by increasing each domains relative affinity for the other or by mediating a stronger association of $G\alpha_s$, which stabilises the closed active site conformation (Tesmer and Sprang, 1998; Tesmer *et al.*, 1997). By producing a dose response curve to $G\alpha_s$ in the presence and absence of Ci, the relative effects of Ci on the association of $G\alpha_s$ with $7C_1 \bullet 2C_2$ were be studied. The effects of Ci on the activity of $7C_1 \bullet 2C_2$ under different concentrations of $G\alpha_s$ was tested at pH 6.5 and it was observed that the effects of Ci were additive to that of $G\alpha_s$. The stimulation of $7C_1 \bullet 2C_2$ by Ci was apparent, with data showing a roughly 5 fold lower concentration of $G\alpha_s$ being required to elicit a similar specific activity to that in the absence of Ci (Figure 3.12A). Analysis of the data with the non-linear regression package in Graphpad Prism demonstrated that a high enough

concentration of $G\alpha_s$ had not been used to reach a maximal stimulation of $7C_1 \bullet 2C_2$ by $G\alpha_s$. Unfortunately, due to the low final yield of $G\alpha_s$ following the expression and purification procedure, it was not possible to extend the assay to use higher concentrations and extend the experiment across the entire sigmoid. The EC_{50}(app) values for $G\alpha_s$ were calculated (1.56 ± 0.82 μM with Ci and 4.49 ± 0.69 μM with Cl^-), and indicated that Ci increased the apparent effects of $G\alpha_s$, however, these values may be inaccurate since a complete sigmoid was not obtained.

Both $G\alpha_s$ and the plant diterpene forskolin are known to activate $7C_1 \bullet 2C_2$ through promotion and stabilisation of the closed, catalytically active enzyme conformation (Tesmer and Sprang, 1998; Tesmer *et al.*, 1999). Experiments done in the presence of one or both of these activators demonstrated a synergism between them, whereby the binding of one activator would increase the affinity for the other and thus result in a significantly higher rate of catalysis (Hatley *et al.*, 2002). Assays in the presence of $G\alpha_s$ and/or forskolin validated this original observation, however, a further synergism of Ci with either $G\alpha_s$ or forskolin or both was not seen (Figure 3.12B). The effects of Ci were purely additive to the effects of $G\alpha_s$ and forskolin, and had no effect on the synergism between $G\alpha_s$ and forskolin. In each instance, about a two fold stimulation (Ci : Cl^-) was observed.

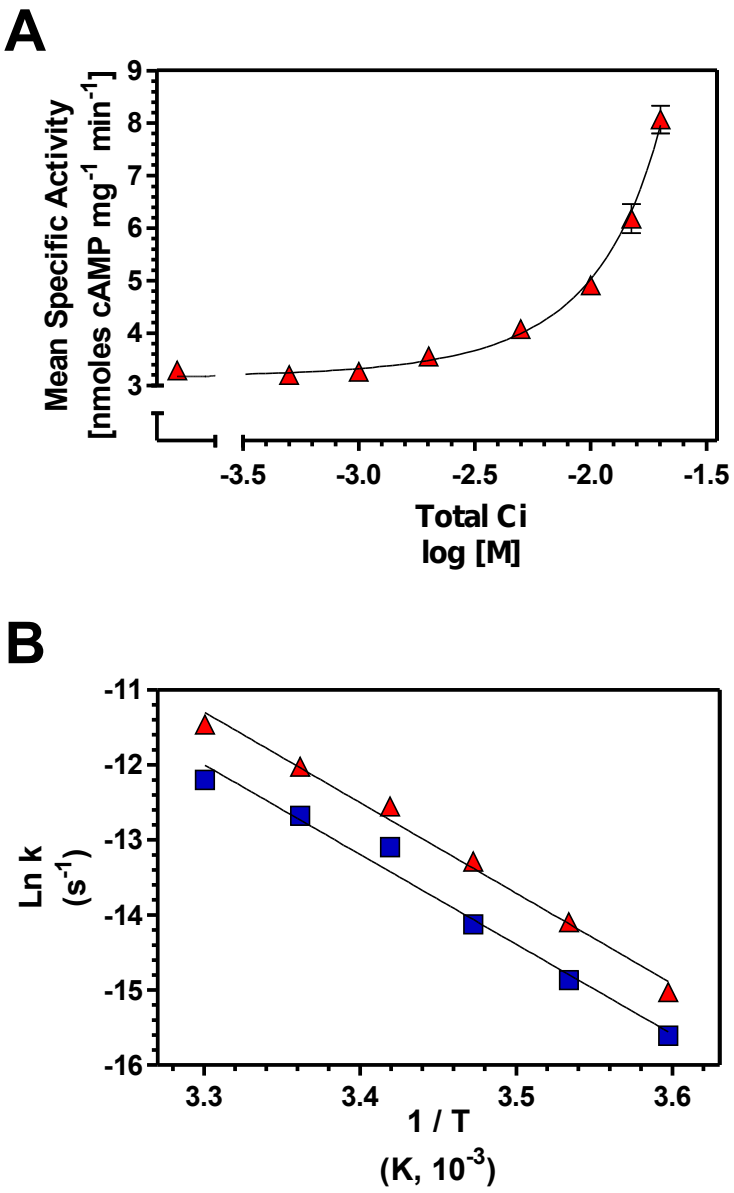

Figure 3.11: The effects of Ci on $7C_1 \bullet 2C_2$ activity *in vitro*.

1.1 µM $7C_1$, 5.8 µM $2C_2$ and 7 µM $G\alpha_s$ was assayed for 20 minutes in the presence of 100 mM Mes-NaOH pH 6.5, 5 mM $MgCl_2$ and 500 µM Mg^{2+}-ATP. **(A)** Ci dose response at 37°C in the presence of 20 mM total salt (NaCl or $NaHCO_3$). **(B)** The activation energy in the presence of 20 mM NaCl (blue squares) or $NaHCO_3$ (red triangles). (n = 9)

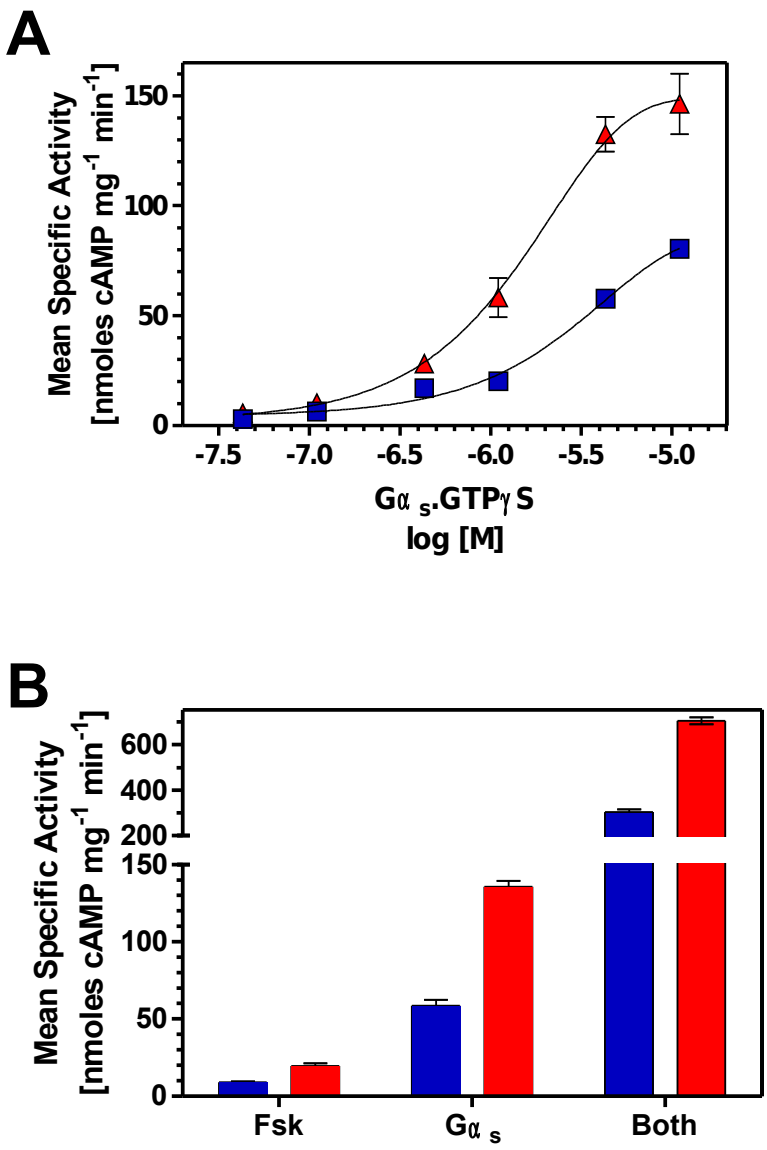

Figure 3.12: The effects of Ci on $7C_1 \bullet 2C_2$ activity *in vitro*.

1.1 µM $7C_1$ and 5.8 µM $2C_2$ was assayed for 20 minutes at 37°C under various conditions in the presence of 100 mM Mes-NaOH pH 6.5, 500 µM Mg^{2+}-ATP and 5 mM $MgCl_2$. **(A)** $G\alpha_s$ dose response in the presence of 20 mM NaCl (blue squares) or $NaHCO_3$ (red triangles). **(B)** $7C_1 \bullet 2C_2$ activity was stimulated in the presence of 20 mM NaCl (blue) or $NaHCO_3$ (red), and either 100 µM forskolin (Fsk) or 7 µM $G\alpha_s$ or both. (n = 9)

3.5 Discussion

Control experiments were performed on HEK 293T cells prior to studying the effects of Ci on the production of cAMP by tmACs *in vivo*. HEK 293T cells were routinely cultured under normocapnic conditions, and the effect of hypercapnic and hypocapnic conditions on pH_i was not known. Since studying the effects of Ci on tmACs relied upon altering the concentration of CO_2 that cells were exposed to, and since tmAC activity varies with pH, it was necessary to quantify any possible effects that varied CO_2 could have upon pH_i. As such, HEK 293T cells were exposed to normocapnic, hypocapnic and hypercapnic conditions, and through a fluorescent pH sensitive dye and a microspectrofluorometric system, pH_i was quantified.

It was observed that when the CO_2 concentration was increased, the cells would undergo a rapid intracellular acidification. This acidification was caused by CO_2 influx into the cells, with CO_2 subsequently being quickly converted into HCO_3^- by the action of CAs, liberating protons (Figure 1.1 and Figure 1.2). The converse was seen when the concentration of CO_2 was decreased, whereby an outflux of CO_2 from the cell caused a reversal of the CO_2/HCO_3^- equilibrium and as such a removal of intracellular protons. Following this initial increase or decrease in pH, the HEK 293T cells were always seen to recover, with their pH_i returning the the starting pH_i over a period of no more that 10 minutes. This recovery in pH_i was most likely brought about by the actions of various cell surface ion transporters, such as Na^+-H^+ exchangers (Figure 3.13) (Boron, 2004).

With the knowledge that pH_i was not likely to cause inaccurate results when studying tmAC activity *in vivo*, investigation into the effects of Ci upon tmACs was able to begin. Through cAMP accumulation assays on HEK 293T cells, it was shown that when the incubation conditions were altered from normocapnic to hypocapnic, a clear decrease in the production of cAMP by tmACs was seen. This Ci dependent cAMP production was proven, through experiments with a sAC specific inhibitor (KH7), not to be due to sAC. Whether or not this response holds any physiological relevance remains to be determined, however, it may provide an explanation for an observed effect of hypocapnia in kidney proximal tubules. In response to respiratory alkalosis (which causes a systemic hypocapnia), proximal tubules in the kidney increase

their phosphate re-absorption in response to a decrease in intracellular CO_2 (Hoppe *et al.*, 1988). Control of phosphate re-absorption is mediated through G-protein regulated cAMP signalling pathways, and the decrease in tmAC activity associated with reduced pCO_2 may be responsible for the increased phosphate re-absorption (Hoppe *et al.*, 1988).

The decrease in cAMP production by tmACs *in vivo*, observed when CO_2 load was adjusted from normocapnic to hypocapnic conditions was routinely no more than a 25 % drop in the levels of cAMP produced. Although this was a relatively large change in total cAMP produced, it was not clear whether an effect downstream of tmACs would occur. If a signalling pathway involving tmAC was involved in sensing Ci then it was reasoned that there would be a noticeable effect on a downstream target in a cAMP signalling pathway. In order to address this question, it was chosen to quantify the phosphorylation status (at serine 133) of CREB. In this β-adrenergic signalling pathway, binding of isoproterenol to the β-adrenergic receptor causes an activation of a heterotrimeric G protein, which in turn stimulates production of cAMP by tmACs (Figure 3.5). This cAMP then diffuses away from the membrane and activates PKA, which in turn phosphorylates CREB, allowing the binding of CREB to cAMP response elements (CREs) on DNA and subsequent production of mRNA (Figure 3.5). It was expected that the decrease in cAMP levels seen between normocapnic and hypocapnic conditions would cause a reduced level of activated PKA and as such a decrease in the levels of phosho-CREB. Indeed, Western blot analysis confirmed this expectation, with a marked decrease in phosho-CREB being seen in the hypocapnia treated cells when compared to normocapnia. Although the degree of hypocapnia (0.03 % CO_2) that these cells were exposed to does not occur in most tissues, it can be found in various alkaline tissues within the body, such as those involved in base secretion (e.g. the pancreas). Intriguingly, there was a decrease in phospho-CREB seen between normocapnia and hypercapnia treated samples. This was not expected since changing the culture conditions from normocapnic to hypercapnic resulted in no change in the production of cAMP by tmACs, however, the reasons for this remain unclear.

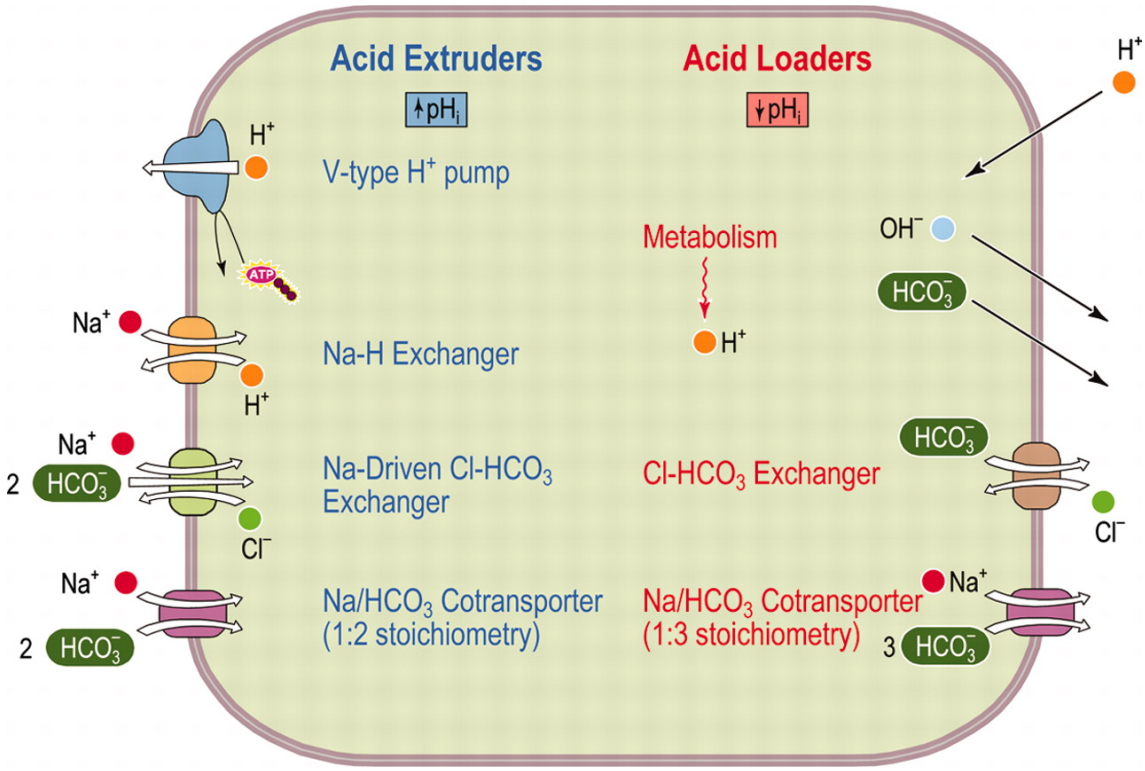

Figure 3.13: The main mechanisms through which cells respond to intracellular acidification and alkalinisation.

Taken from (Boron, 2004)

These *in vivo* experiments provided strong evidence to suggest that in mammalian cells, tmACs are involved in sensing Ci, however, the *in vivo* experiments do not identify whether this is through a direct or indirect effect of Ci on tmAC. However, it is clear that although the effect of Ci on sAC has been known for years, until now, the involvement of tmAC in Ci sensing had been missed (Chen *et al.*, 2000; Townsend *et al.*, 2009). Although inhibitor studies have ruled out the possibility that sAC was acting as the Ci sensor in this system, the possibility existed that Ci was somehow having an indirect effect on tmACs. As such, in order to determine whether the increase in cAMP seen *in vivo* was due to the specific action of Ci on tmACs, *in vitro* experiments were performed. These *in vitro* experiments were performed on a recombinant protein equating to a tmAC lacking transmembrane domains, and consisted of the C_1 domain of human type VII AC ($7C_1$) and the C_2 domain (amino acids 821-1090) of rat type II AC ($2C_2$). Upon mixing these two domains *in vitro*, an active AC ($7C_1$●$2C_2$) was produced, which was stimulated by both forskolin and $G\alpha_s$, mimicking the native protein.

It is important to point out at this stage that *in vitro* experiments performed in Sections 4.3 and 6.2 indicate that the observed effects of Ci *in vitro*, in Section 3.4 (i.e. those discussed below), are likely to be due to a non-specific effect of pH, caused by the effects of Ci on assay pH.

When the response of $7C_1$●$2C_2$ to Ci was tested *in vitro*, it was seen that a significant stimulation by Ci (routinely about 2 fold) occurred at pH 6.5, with a slight stimulation routinely being seen at pH 7.0. The observation that Ci stimulated $7C_1$●$2C_2$ at lower pH matched other research that showed the stimulation of type III AC by Ci to increase as the pH was lowered (Xie *et al.*, 2006). Furthermore, this observation provided a possible explanation as to why a previous study into the effects of Ci on a 'soluble' tmAC *in vitro* had failed to detect an effect (Chen *et al.*, 2000). This prior study had relied upon the assumption that HCO_3^- was the activating species of Ci, and as such, experiments had been performed at pH 7.5 and above (where HCO_3^- concentrations were high) (Chen *et al.*, 2000). Recent investigation had proven that certain prokaryotic Class IIIb ACs are activated by CO_2 and not HCO_3^-, and it was possible in this case that $7C_1$●$2C_2$ was also activated by CO_2 (Hammer *et al.*, 2006). Due to this, a stimulation was only seen at low pH, since at higher pH the levels of CO_2 were not high enough to elicit a response (Figure 1.1).

In order to try and establish a mechanism through which Ci causes its effect on these ACs, a series of *in vitro* biochemical assays were performed on $7C_1 \bullet 2C_2$. The results of these experiments indicated that although the affinity for ATP was not affected by Ci, the overall substrate turnover of the enzyme was increased in the presence of Ci, through an apparent increase in V_{max} and k_{cat}. The Arrhenius plot derived from a temperature response assay indicated that the observed increase in substrate turnover was not likely to be due to an alteration in the catalytic mechanism since the energy of activation for conversion of ATP into cAMP remained unchanged by Ci. The possibility that Ci did not alter the energy of activation matched a previous biochemical study on CyaB1 (*Anabaena* PCC 7120), which possesses a Class IIIb CHD (Cann *et al.*, 2003).

Results indicated two possible mechanisms through which CO_2 acts on $7C_1 \bullet 2C_2$ to increase its substrate turnover. Firstly, a Mg^{2+} dose response assay indicated that Ci increased the affinity of $7C_1 \bullet 2C_2$ for Mg^{2+}. The case for Ci acting through increased metal affinity was strong, since recruitment of the second Mg^{2+} ion was known to be a rate limiting step and had already been implicated as a mechanism through which Ci acts (Steegborn *et al.*, 2005b; Tesmer *et al.*, 1999). Following binding of Mg^{2+}-ATP to the catalytic site, a second Mg^{2+} is required to bind before active site closure and subsequent catalysis can occur (Tesmer and Sprang, 1998; Tesmer *et al.*, 1999). It could be reasoned that a more rapid recruitment of the second metal ion, following substrate binding, would accelerate the adoption of a catalytically competent active site conformation. Secondly, the lower EC_{50}(app) for $G\alpha_s$ determined in the presence of Ci indicated that Ci could possibly enhance the effect of certain activators. In the case of tmACs, the active site closure (following second metal ion recruitment) is mediated through binding of $G\alpha_s$ (or forskolin), however, recent evidence has suggested that in CyaC from *Spirulina platensis,* active site closure is initiated by Ci (Steegborn *et al.*, 2005b; Tesmer *et al.*, 1997). It is possible that Ci is mediating a similar effect in $7C_1 \bullet 2C_2$, whereby Ci and $G\alpha_s$ act in cohort through different sites to promote active site closure.

4

Ci and nucleotidyltransferases

4.1 Introduction

Investigation into the effect of Ci on Class IIIa ACs provides strong evidence to suggest that a response to Ci was not solely limited to Class IIIb ACs, but could also be found in Class IIIa ACs (Townsend *et al.*, 2009). Work performed *in vivo* demonstrated that Ci was able to either directly or indirectly influence the production of cAMP by the endogenous tmACs in HEK 293T cells (Townsend *et al.*, 2009). *In vitro* biochemical assays performed on the recombinant catalytic domains of two tmACs ($7C_1$●$2C_2$), seemed to suggest that Ci was directly influencing the activity of tmAC. Furthermore, *in vitro* biochemical assays on an AC (Rv1625) from *Mycobacterium tuberculosis*, demonstrated that this Class IIIa AC was also activated by Ci (Townsend *et al.*, 2009).

It is important to point out at this stage that experiments performed in Sections 4.3 and 6.2 introduce the strong possibility that the above mentioned Class IIIa ACs are not activated by Ci.

Further evidence supporting the idea that a Ci response is not restricted to Class IIIb ACs can be found in several organisms. Notably, two gustatory receptors in *Drosophila melanogaster* (Gr63a and Gr21a) have been shown to be directly involved in Ci sensing, although the mechanism by which these receptors mediate this is not known (Jones *et al.*, 2007; Kwon *et al.*, 2007). It has also been known for many years that the plant enzyme RuBisCO requires activation by CO_2 prior to it gaining catalytic competence (Lorimer *et al.*, 1976). Furthermore, a CA has been implicated in Ci sensing in mammalian taste receptor cells (Chandrashekar *et al.*, 2009). In light of this, the question was asked as to whether a response to Ci could be found in other enzyme families.

Ci has been shown to interact with proteins through several different amino acids, of which the most common was through the interaction (both covalent and non-covalent) with the ε-amino group of a basic amino acid (predominantly arginine, histidine or lysine) (Cundari *et al.*, 2009). Due to the fact that Ci can interact with many different amino acids, and since binding of Ci must influence the tertiary structure of a protein in order to produce a biologically relevant outcome, it is currently not possible to predict biologically significant Ci binding sites (Cundari *et al.*, 2009; Drummond *et al.*, 2010). Due to this it was decided to begin investigation into potential novel Ci responsive

enzymes by studying a family of enzymes that are structurally and catalytically related to ACs. It was decided to begin investigation into a family of enzymes that share a similar active site structure with ACs; the polymerase I (Pol I) family of prokaryotic DNA polymerases (Ito and Braithwaite, 1991). Pol I polymerases are similar to ACs in that they are dependent upon two Mg^{2+} ions for catalysis, and comparison of crystal structures reveals a remarkable structural similarity (Artymiuk *et al.*, 1997; Zhang *et al.*, 1997b). Following the crystallisation of an AC catalytic site it was noted that the structural topology of the AC active site was similar to the 'palm' domain found in the Pol I family of prokaryotic DNA polymerases (Figure 4.1) (Artymiuk *et al.*, 1997; Beese *et al.*, 1993; Zhang *et al.*, 1997a). The structure of Pol I polymerases has been compared to a right hand grasping a rod (with the rod being a strand of DNA), with 'fingers', 'thumb' and 'palm' domains (Beese *et al.*, 1993; Moras, 1993). The active site of these polymerases is located within the 'palm' domain, which consists of 4 β-strands and 3 helices, and it is this structure that is also found in ACs (Artymiuk *et al.*, 1997). Although this similarity was unexpected, it is unsurprising in retrospect as these enzymes all share a similar catalytic mechanism; an attack of the 3' ribose hydroxyl on the α phosphate of a nucleotide triphosphate (with DNA and RNA polymerases performing this in an intermolecular fashion and ACs in an intramolecular fashion).

Given the structural similarity and the fact that these enzymes are also dependent upon two Mg^{2+} ions for catalysis it was appropriate to investigate Pol I enzymes for a response to Ci. The effects of Ci on two members of the Pol I family of prokaryotic DNA polymerases was studied. These were chosen as T7 RNA polymerase (T7 bacteriophage) and DNA polymerase I (*E. coli*), as they represent two of the Pol I subfamilies (bacterial and bacteriophage), and are also readily expressed as recombinant proteins (Dunn and Studier, 1983; Ito and Braithwaite, 1991; Joyce *et al.*, 1982). The effects of Ci on a member of the Pol β family of DNA polymerases was also investigated; DNA polymerase β (Polβ) from *Rattus norvegicus* (Sawaya *et al.*, 1994). Although Polβ possesses a structural topology similar to the 'palm' domain found in Pol I polymerases, it was shown to be more structurally related to a family of enzymes not involved in the synthesis of DNA; the kanamycin nucleotidyltransferases (Holm and Sander, 1995).

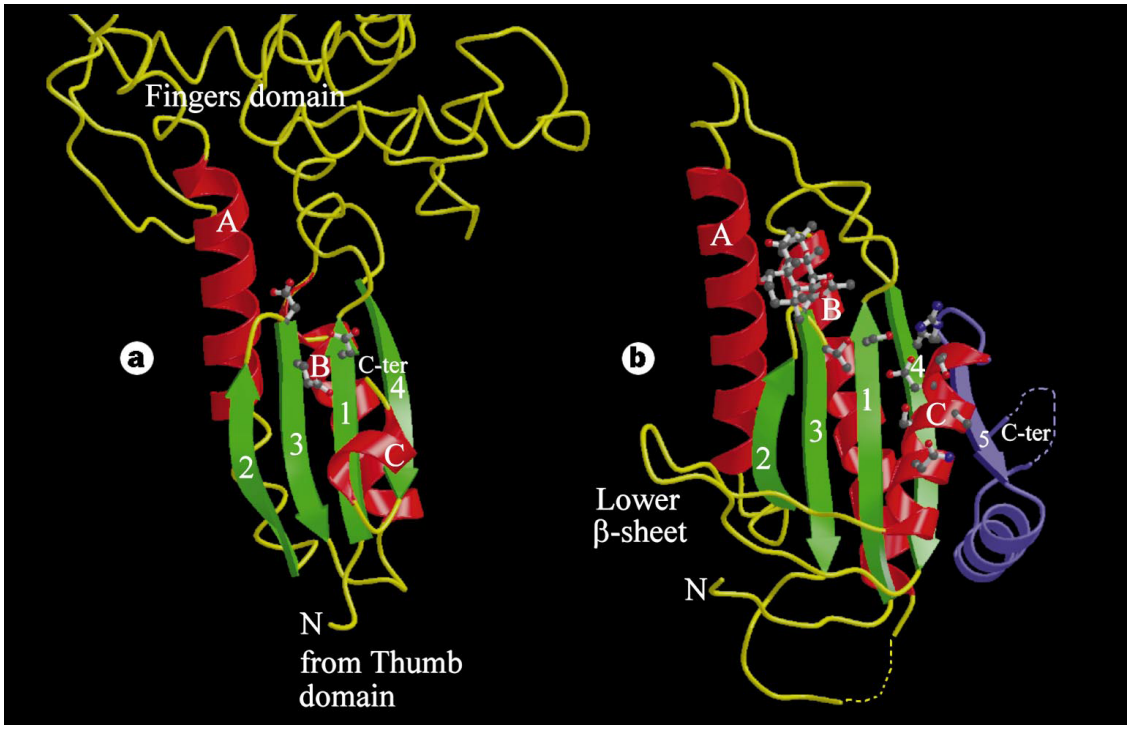

Figure 4.1: Crystal structure of the palm domain.

Chain traces derived from crystal structure data of **(a)** *Thermus aquaticus* DNA polymerase (Taq) and **(b)** the C_2 domain of *Rattus norvegicus* type II AC ($2C_2$).

Taken from (Artymiuk *et al.*, 1997)

4.2 T7 RNA polymerase

T7 RNA polymerase (T7 RNAP), an enzyme that is involved in the transcription of DNA, binds the T7 promoter on DNA and catalyses the incorporation of nucleotides into a nascent mRNA chain in a 5' to 3' direction (Summers and Siegel, 1970). T7 RNAP is a member of the bacteriophage subfamily of Pol I DNA polymerases, and since it can be expressed to high yields as a recombinant protein was chosen to begin investigation (He *et al.*, 1997; Ito and Braithwaite, 1991). The expression construct pBH161A, containing T7 RNAP with a N-terminal hexa-histidine tag, was transformed into *E. coli* BL21 (DE3), and was expressed and purified essentially as described (He *et al.*, 1997). Typical yields were reported as 0.5 – 1.5 mg per 20 mL of bacterial culture, however, since purity was deemed more important than yield in this particular case a slight modification to the purification procedure was made to sacrifice yield for purity (see 2.4.3). Ultimately, a homogeneous preparation of recombinant T7 RNAP was obtained and was more that 95 % pure as shown by SDS-PAGE (Figure 4.2).

The activity of T7 RNAP was tested *in vitro* using a suitable expression template for RNA synthesis, and [α-^{32}P]-ATP was used to spike the NTP mix to allow quantification of ATP incorporation. The DNA template used for RNA synthesis was derived from pQ3N1, which was originally constructed to allow the expression of an AC from *Anabaena* PCC 7120 (Katayama and Ohmori, 1997). The multiple cloning site of pQ3N1, including the T7 promoter and the AC coding sequence, was amplified by BIOTAQ™ PCR (see 2.2.1), and the 3.8 kb product was analysed by agarose gel electrophoresis (see 2.2.2), and purified (see 2.2.3). The purified 3.8 kb DNA fragment was used directly within the assay as a template for RNA synthesis.

Assays were set up and performed in a similar fashion to those used to test the *in vitro* response of $7C_1 \bullet 2C_2$ to Ci, however, since the composition of the assay was slightly different it was necessary to perform new pH control assays. The pH control assays were carried out at a range of different pHs, in the presence of 20 mM $NaHCO_3$ or NaCl (Figure 4.3A). These pH controls demonstrated that the desired assay pH could be obtained and that the pH during the course of the assay was stable.

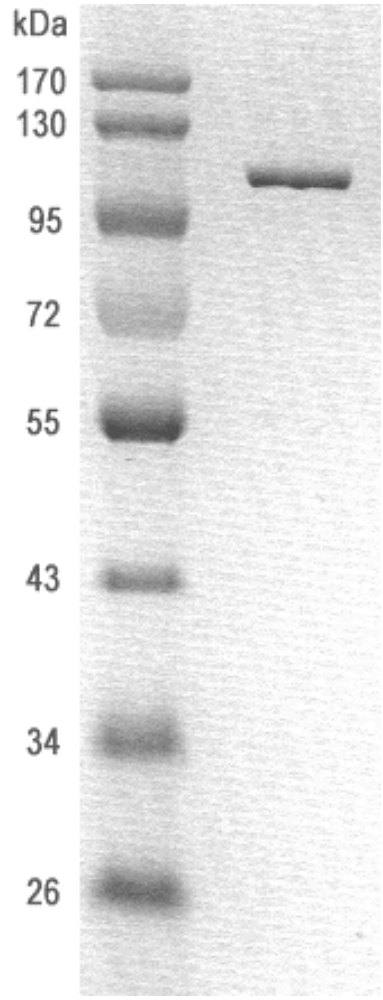

Figure 4.2: Purified recombinant T7 RNAP.

2 µg of purified T7 RNAP was resolved on a 12 % SDS-PAGE gel. Protein was stained with Coomassie Brilliant blue dye and protein size was estimated relative to Fermentas PagerRuler™ Plus Prestained Protein ladder.

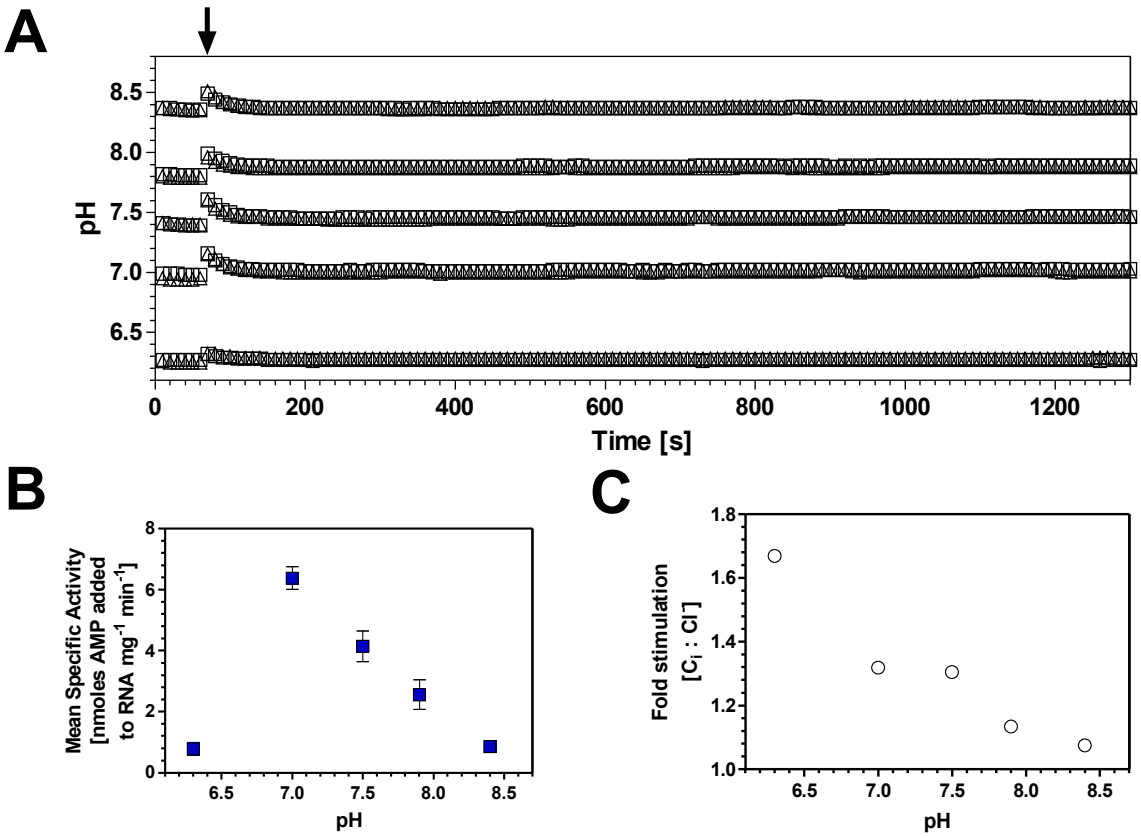

Figure 4.3: The effect of Ci on assay pH and the activity of T7 RNAP.

Reactions were run at 37°C for 30 minutes in 100 µL containing 4.7 µM T7 RNAP, 30 mM $MgCl_2$, 3 units Rnasin, 200 µM rNTP, 7 µg DNA template **(A)** Mock assay carried out in the absence of [α-^{32}P]-ATP with a micro pH electrode to monitor assay pH. 20 mM NaCl (squares) or $NaHCO_3$ (triangles) was added after 60 seconds (arrow). **(B)** pH profile of T7 RNAP in the presence of 20 mM NaCl. **(C)** Fold stimulation (Ci : Cl^-) of T7 RNAP at varying pH. (n = 6)

The first assay performed was a response of T7 RNAP to pH and was carried out in the absence of any Ci (Figure 4.3B). This assay showed a pH optimum of about pH 7.0, and rather surprisingly a profound difference in the activity seen at pH 7.0 compared to pH 6.5 (Figure 4.3B). The activity of T7 RNAP at pH 7.0 was about 5 fold greater than the activity at pH 6.5, highlighting the importance of performing pH controls. When assays were performed in the presence of Ci a clear effect on T7 RNAP activity could be seen, with T7 RNAP showing about a 1.7 fold increase in activity at pH 6.5 in the presence of 20 mM total Ci, when compared to 20 mM NaCl (Figure 4.3C). This effect by Ci decreased as the pH was increased, showing a statistically significant (albeit small) 1.3 fold stimulation at pH 7.0 and pH 7.5, but no significant effect by Ci was seen at pH 8.0 and above (Figure 4.3C). This effect was consistent with what was seen for $7C_1 \bullet 2C_2$, although in that case a greater than 2 fold stimulation was seen at pH 6.5. This result suggested that T7 RNAP was possibly activated by CO_2, and as such further assays would be conducted at pH 6.5 to ensure a high concentration of CO_2.

At this stage the possibility remained that the effect ascribed to Ci could be due to an inhibitory effect by Cl^-, however, this was tested and shown not to be likely (Figure 4.4A). Although a very slight decrease in activity was seen in the presence of Cl^- (when compared to basal), this could in no way account for the large increase in activity seen in the presence of Ci (when compared to Cl^-). When the relative effects of Ci on T7 RNAP were tested over time an unexpected result was obtained (Figure 4.4B). Whereas in the presence of 20 mM NaCl the specific activity of T7 RNAP appeared to gradually decrease over time (although this was not statistically significant when assessed to 95 % confidence intervals), in the presence of 20 mM $NaHCO_3$ the specific activity almost doubled over 30 minutes (14.4 ± 1 nmoles ATP mg^{-1} min^{-1} after 5 minutes and 25.9 ± 0.7 nmoles ATP mg^{-1} min^{-1} after 30 minutes; an effect that was statistically significant when assessed to 95 % confidence intervals). The gradual decrease in specific activity in the presence of NaCl was to be expected, since over time the concentration of substrate would fall, and also that T7 RNAP itself would suffer heat degradation over time, both contributing to a decreasing rate of catalysis. The gradual increase in specific activity seen in the presence of 20 mM $NaHCO_3$ could only be explained by one of two reasons. First, it was possible that the effects of Ci were slow at first and that it took time

for Ci to bind its cognate site. It could take a while for all Ci binding sites on T7 RNAP to become occupied and thus for a maximum stimulation by Ci to be seen. Second, it was possible that this was indicative of a pH effect, whereby a slow increase in pH over time was responsible for the steady increase in specific activity.

An increase in assay pH over time was possible in the presence of Ci at pH 6.5, as the relatively high concentration of dissolved CO_2 would tend to diffuse from solution into the surrounding atmosphere; as predicted by Henry's law. This loss of CO_2 from solution would cause the equilibrium formed between CO_2 and HCO_3^- to become unbalanced, and as a result the equilibrium would shift to liberate more CO_2, taking up a proton from solution (Figure 1.1). If the solution was not suitably buffered then removal of a proton would result in an increase in pH, however, in this case the solution was buffered with 50 mM Mes-NaOH, and an increase in pH was unlikely. Although the possibility of pH explaining the response to Ci was not supported by pH control experiments (Figure 4.3A) the importance of the possibility of non-specific pH effects meant that it was wise to re-investigate the pH control experiments to absolutely rule out an effect of pH.

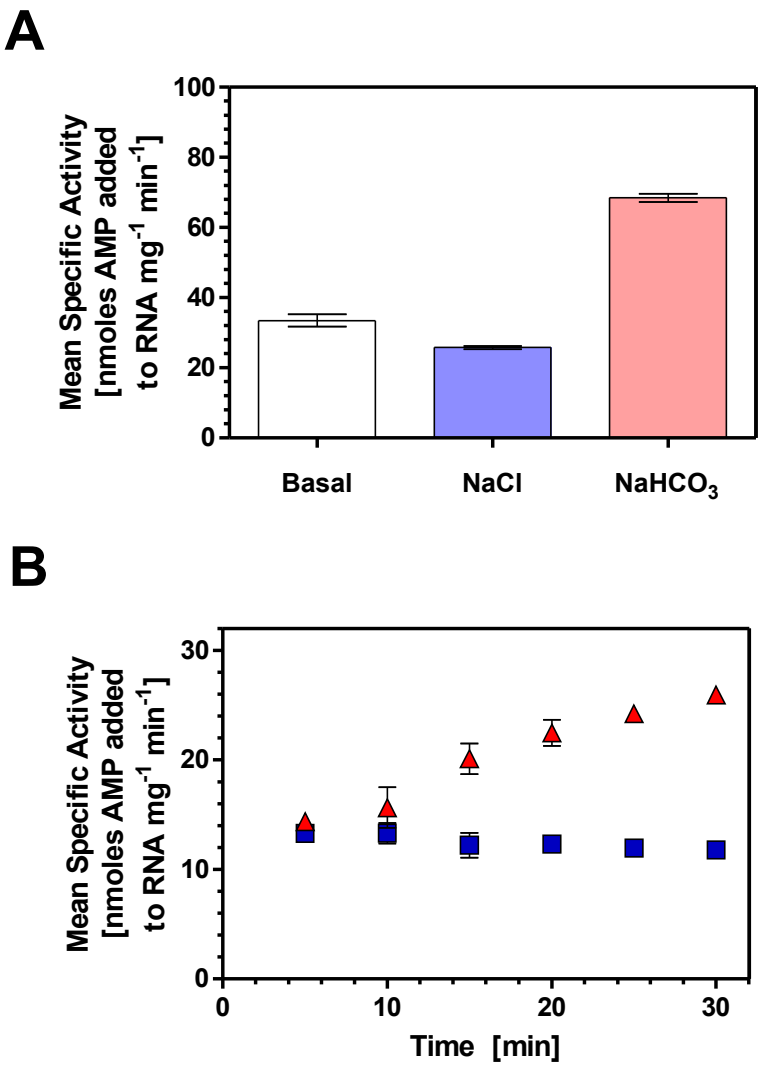

Figure 4.4: Other Ci assays performed on T7 RNAP *in vitro.*

Reactions were run at 37°C for 30 minutes in 100 µL containing 100 mM Mes-NaOH pH 6.5, 4.7 µM T7 RNAP, 30 mM $MgCl_2$, 3 units Rnasin, 200 µM rNTP, 7 µg DNA template. **(A)** T7 RNAP assay at pH 6.5 containing 20 mM NaCl or $NaHCO_3$ or neither (basal). **(B)** T7 RNAP assay carried out over time in the presence of 20 mM $NaHCO_3$ (red triangles) or NaCl (blue squares). 6 sets of experiments were set up in parallel, and after 5, 10, 15, 20, 25 and 30 minutes, one set of experiments was stopped and the specific activity determined. (n = 3)

4.3 The effect of Ci on assay pH

Due to the large effect that pH had upon the activity of T7 RNAP between pH 6.5 and pH 7.0 (Figure 4.3B), and the fact that the increase in T7 RNAP activity observed over time (Figure 4.4B) in the presence of Ci could be explained by increasing assay pH, it was deemed extremely prudent to revisit the pH controls. The pH controls were repeated at pH 6.5, but this time using several slightly different methods, all of which were performed using a computer driven micro pH electrode to quantify pH. In all cases the new pH control assays were carried out in a volume of 100 µL, containing the same components as the actual biochemical assay.

When the same method used for previous pH controls (Figure 4.3A) was repeated at pH 6.5 it was seen that the pH of the solution gradually rose from about pH 6.48 to pH 6.52 over the period of 40 minutes (Figure 4.5 blue line), although it is unclear why this pH increase was not seen previously. Although this pH change was very small it was still evidence to support the idea that even 50 mM buffer was not capable of completely clamping assay pH. It was noticed during these experiments that movement of the pH micro-electrode within the solution being tested resulted in small rapid increases in pH being recorded. When an identical pH control assay (i.e. identical to Figure 4.5 blue line) was run, except after 20, 30 and 40 minutes the solution was mixed (Figure 4.5 arrows), rapid pH increases were immediately seen following mixing (Figure 4.5 black line). It was noted that if mixing was carried out in this way, the pH of the assay would rise nearly 0.2 pH units over the course of 40 minutes.

This observed increase in pH was alarming, and cast heavy doubt over many of the experiments carried out at pH 6.5 involving Ci. However, it was necessary to validate this observation by another method. For this, a more reliable method was devised, whereby the conditions used for the actual biochemical assays were more rigorously mimicked. Essentially, a large master-mix was created and 100 µL was aliquoted into several 1.5 mL microcentrifuge tubes, which were then closed and incubated at 37°C. After every 5 minutes, one of these identical tubes was opened, the pH was measured and the tube was discarded (Figure 4.5 red circles). This method demonstrated that there was potentially a very significant increase in pH occurring, when assay pH was around pH 6.5. This pH change was consistently about a 0.15 – 0.2 pH unit increase over 40 minutes.

Due to the fact that it was not possible to avoid this newly identified assay pH increase, it was necessary to modify the method by which the biochemical Ci assays were performed. The composition of the assay solution was kept the same, except 100 mM buffer was used instead of 50 mM to minimise these increases in assay pH, and the protocol was modified in two ways. Firstly, each experiment now comprised a biochemical and a pH control assay run parallel to each other to allow exact pH values to be obtained every time an assay was performed. Secondly, instead of just one pH 6.5 Cl^- and one pH 6.5 Ci experiment being used, 4 Cl^- (roughly at pH 6.4, 6.5, 6.6 and 6.7) and one pH 6.5 Ci experiments would be used to ensure the starting and final pH of the Ci experiment fell between that of the Cl^- experiments (see Figure 4.6). It is worth noting that in the presence of Ci, pH measurements were recorded at the start and the end of the assay, so that the pH increase due to Ci could be monitored.

When T7 RNAP was re-tested using this new *in vitro* Ci assay methodology the result demonstrated that T7 RNAP was not activated by Ci and that the response to Ci seen previously was actually a non-specific effect of pH (Figure 4.6).

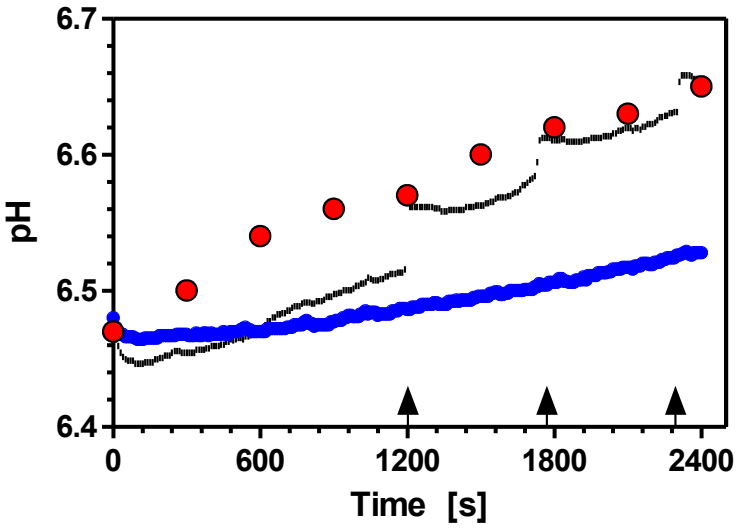

Figure 4.5: New *in vitro* pH control assays.

Mock assays were set up using several different methods. Assays were performed at 37°C in 100 µL containing 50 mM Mes-NaOH, 10 mM $MgCl_2$ and 20 mM $NaHCO_3$. (blue line) - Original method for pH controls (see Figure 4.3A). (red circles) - Several identical mock assays were set up in closed micro-centrifuge tubes and after each 5 minutes the pH of a new tube was sampled. (black line) – This was identical to the original method (blue line), however, after about 20/30/40 minutes (arrows) the probe was used to mix the solution.

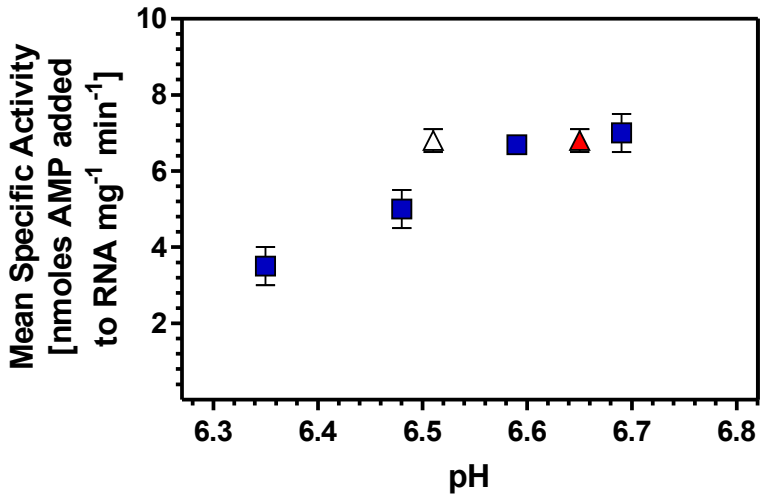

Figure 4.6: T7 RNAP was not activated by Ci using the new *in vitro* Ci assay methodology.

The new *in vitro* Ci assay methodology carried out at 37°C for 30 minutes, in 100 µL containing 100 mM Mes-NaOH, 4.7 µM T7 RNAP, 10 mM $MgCl_2$, 3 units Rnasin, 200 µM rNTP, 7 µg DNA template and 20 mM $NaHCO_3$ (triangles; starting pH – clear, final pH - red) or NaCl (blue squares). (n = 6)

4.4 *E. coli* DNA polymerase I

Although T7 RNAP was shown not to be regulated by Ci, it was still deemed wise to test another member of the Pol I family of prokaryotic DNA polymerases. A response to Ci may not be a universal feature of Pol I polymerases, but may only be a feature restricted to individual proteins in this enzyme family. The second protein chosen was the Klenow *exo*$^-$ fragment of DNA polymerase I (Klenow herein) from *E. coli*, which is a member of the bacterial subfamily of Pol I DNA polymerases (Ito and Braithwaite, 1991).

The Klenow fragment was expressed from the plasmid pXS106 in *E. coli* strain CJ376 (plasmid and strain both kind gifts from Professor Catherine Joyce) as previously described (Joyce and Derbyshire, 1995). The crude preparation of Klenow obtained following ammonium sulphate precipitation was resolved to greater than 95 % homogeneity by subsequent anion exchange FPLC (Figure 4.7).

Klenow was tested under similar conditions to those used at pH 6.5 to test the response of T7 RNAP to Ci (Figure 4.6). Since this enzyme was a DNA polymerase, the components of the assay mix were altered slightly to contain [α-^{32}P]-dATP, dNTPs, and activated calf thymus DNA as a template. The assay was a nick filling assay, with Klenow repairing damage in the calf thymus DNA by incorporating dNTPs into sites on calf thymus DNA which needed repair. It was clearly seen that there was no effect of Ci on this enzyme (Figure 4.8).

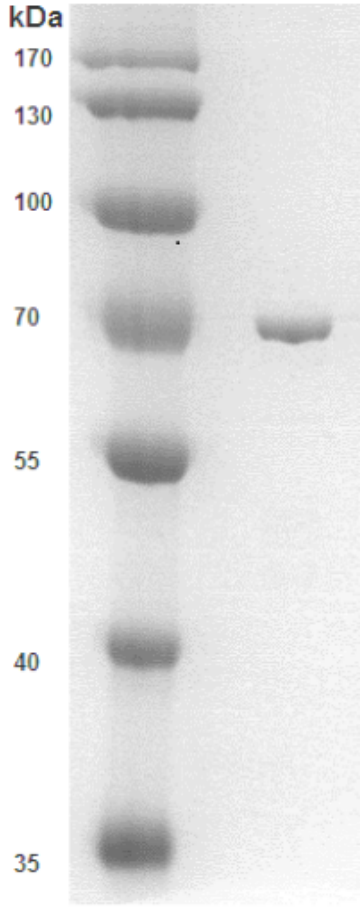

Figure 4.7: Purified recombinant Klenow.

2 µg of purified Klenow was resolved on a 12 % SDS-PAGE gel. Protein was stained with Coomassie Brilliant blue dye and protein size was estimated relative to Fermentas PagerRuler™ Prestained Protein ladder.

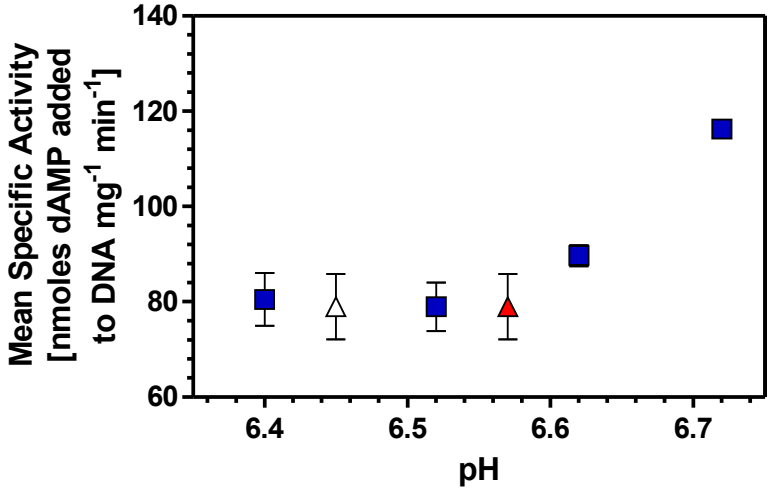

Figure 4.8: Klenow was not activated by Ci using the new *in vitro* Ci assay methodology.

Assays were performed for 30 minutes at 37°C, in 100 µL containing 100 mM Mes-NaOH, 10 mM $MgCl_2$, 6.4 µM dATP, 32 µM dNTP, 1.3 nM Klenow and 10 µg DNA template. Reactions were carried out in the presence of 20 mM NaCl (blue squares) or 20 mM $NaHCO_3$ (triangles; starting pH – clear, final pH – red). (n = 6)

4.5 DNA polymerase beta

Neither of the two members of the Pol I family of prokaryotic DNA polymerases were shown to be regulated by Ci, however, the 'palm' structure is not a unique feature restricted to this family. The 'palm' domain structure is also found in the polymerase β family of DNA polymerases, so it was decided to test a member of this family. The enzyme chosen was DNA polymerase β (Polβ herein) from *Rattus norvegicus* as it had already been cloned, expressed as a recombinant protein, and had been biochemically characterised.

Polβ was over-expressed in *E. coli* BL21 (DE3) from a pET28a expression plasmid as a 43 kDa hexa-histidine tagged fusion protein. Recombinant protein was purified with a Ni^{2+}-NTA FPLC column and was greater than 95 % pure when visualised on SDS-PAGE (Figure 4.9).

Following the same nick filling experiment as that used for Klenow (see Figure 4.8), the effect of Ci on Polβ was tested at pH 6.5. This assay clearly demonstrated that there was no effect of Ci on this enzyme (Figure 4.10).

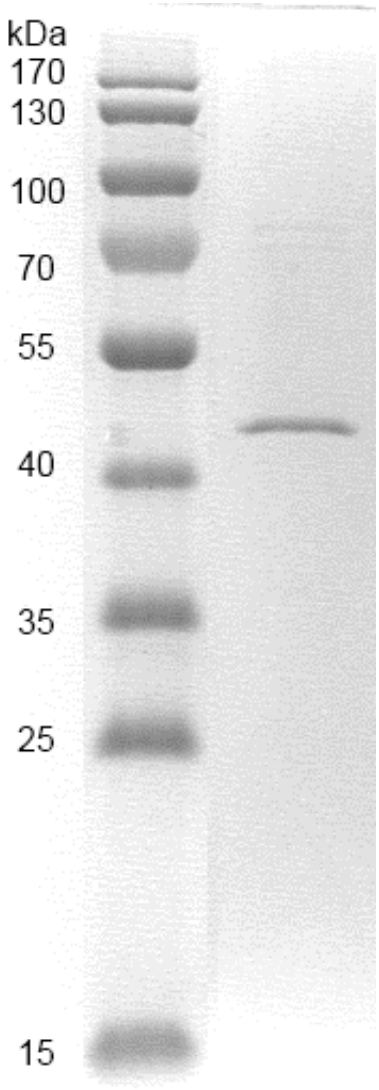

Figure 4.9: Purified recombinant Polβ.

1.5 µg of purified Polβ was resolved on a 15 % SDS-PAGE gel. Protein was stained with Coomassie Brilliant blue dye and protein size was estimated relative to Fermentas PagerRuler™ Prestained Protein ladder.

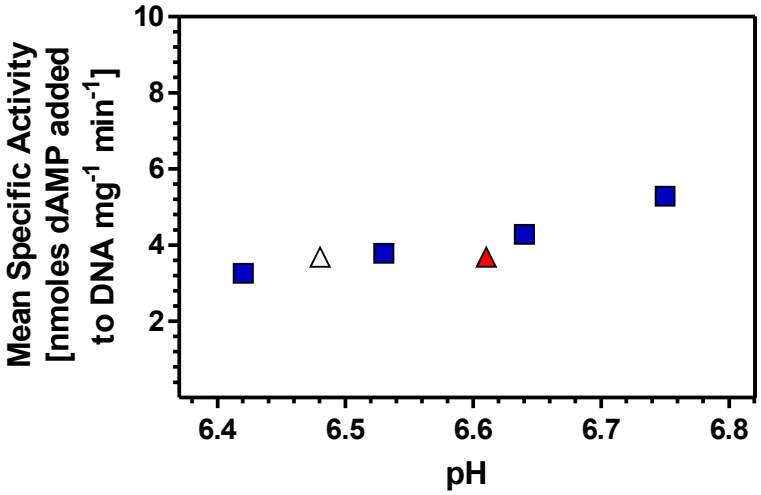

Figure 4.10: Polβ was not activated by Ci using the new *in vitro* Ci assay methodology.

Assays were performed at for 30 minutes at 37°C in 100 µL containing 100 mM Mes-NaOH, 10 mM $MgCl_2$, 6.4 µM dATP, 32 µM dNTP, 200 nM Polβ and 10 µg DNA template. Reactions were carried out in the presence of 20 mM NaCl (blue squares) or 20 mM $NaHCO_3$ (triangles; starting pH – clear, final pH – red). (n = 10)

4.6 Discussion

Initial investigation into the effects of Ci on T7 RNAP suggested that its activity was increased in the presence of Ci. This initial experimentation demonstrated a strong stimulation by Ci at pH 6.5, indicating that CO_2 may be the activating species of Ci on this enzyme. Despite the early evidence suggesting that Ci increased the activity of T7 RNAP, one biochemical experiment cast doubt upon this observation. When the specific activity of T7 RNAP at pH 6.5 in the presence of Cl^- or Ci was tested over time, it appeared that whilst the specific activity in the presence of Cl^- decreased slightly over time, the specific activity in the presence of Ci increased considerably over time. Of course, one possible explanation for this result was that the effects of Ci on T7 RNAP were slow to reach a maximal effect, a possible consequence if Ci has a low k_{on} rate, and as such does not rapidly occupy its cognate site on all T7 RNAP molecules. However, it was also possible that this increase in specific activity was caused through a gradual increase in assay pH as the experiment progressed. An increase in assay pH between pH 6.5 and 7.0 would undoubtedly increase the specific activity of T7 RNAP, and as such would cause a misleading increase in specific activity. At pH 6.5 this increase in assay pH in the presence of Ci could occur since the relatively high concentration of CO_2 in the assay would diffuse out of solution into the atmosphere. This loss of CO_2 from solution would cause a shift in the equilibria formed between CO_2 and HCO_3^-, ultimately generating more CO_2 and removing H^+ from the assay. However, the reason why a small stimulation by Ci was seen at pH 7.0, where an increase in assay pH would appear not to cause an increase in enzyme activity, is unclear.

Due to the possibility that the apparent stimulation of T7 RNAP by Ci could be an artefact of pH, caused by Ci increasing the assay pH, it was deemed necessary to perform an even more thorough pH control experiment. Previous pH control assays had provided evidence to suggest that only 50 mM buffer was required to ensure that the desired starting pH of the assay could be achieved and that pH was stable throughout the assay. When the pH control assay (at pH 6.5) was repeated, the results were very much different to those done previously, in that although the start pH could be obtained, there was a very small increase in pH over time (about a 0.04 pH unit increase over 40 minutes). Furthermore, it was noticed that periodic mixing of the pH control

assay mix resulted in rapid increases in recorded pH. When the pH control was repeated to include these mixes, the results were remarkably different, demonstrating that the assay pH actually increased in pH at a much more rapid rate than had previously been detected (nearly 0.2 pH units over 40 minutes). Although this mixing could be argued as causing potentially misleading results, an independent pH control experiment following a different method validated this pH control. This second method provided strong evidence to suggest that previous pH control experiments had failed to detect a considerable increase in assay pH, and there was in fact a considerable increase in assay pH occurring.

Although the reason for the failure of previous pH control experiments to detect this pH increase was not known, a few suggestions can be made. Although care was taken to maintain the cleanliness of the micro pH electrode, the possibility exists that over time the old micro pH electrode had become contaminated. If this contamination had occurred on the ceramic filter that separates the electrode from the solution to be measured then it was possible that the electrode could have become inaccurate at detecting pH changes. However, this was not likely since mixing the pH control experiments caused a rapid increase in pH to be detected, suggesting that the micro pH electrode was functioning correctly. Another explanation was that somehow a small micro-environment was occurring around the ceramic filter on the micro pH electrode. It was possible that since the electrode was stationary in solution that somehow the solution that the electrode was monitoring was in part separated from the rest of the assay solution. As such, when the pH of the assay solution increased due to the efflux of CO_2, the small micro-environment around the electrode remained at the same pH, although this would not be expected due to the effects of Brownian motion. A final explanation is that a pH gradient was being established within the pH control assay. Since loss of CO_2 from the solution was occurring predominantly at the air-liquid interface, a localised decrease in CO_2, and a subsequent localised pH increase, would be occurring here. Since the solution was not stirred, the localised increase in pH at the air-liquid interface would cause a pH gradient to be established within the pH control assay, since the effects of Brownian motion would not be sufficient to rapidly normalise the pH within the pH control assay. As such, the micro pH electrode (which monitors the pH at the bottom of the pH control assay) would be monitoring a region of the pH control assay that most closely reflected the starting pH of the solution,

and would be unable to take account of the increasing pH gradient formed between the micro pH electrode and the air-liquid interface.

With this newly identified increase in assay pH taken into consideration, it became clear that the method originally employed to test a response of an enzyme to Ci *in vitro* was no longer suitable. As such, a new *in vitro* Ci assay methodology was devised, and although this new method was not capable of preventing this increase in assay pH, even with an increased buffer concentration of 100 mM, it allowed it to be taken into account. Thus, even with an increase in assay pH, the new *in vitro* Ci assay methodology allowed Ci responsive proteins to be identified without the risk of the result being mislead by pH. When this new *in vitro* Ci assay methodology was employed to re-test the effect of Ci on the activity of T7 RNAP the results were remarkably different. With pH fully accounted for, the assay demonstrated that T7 RNAP was not stimulated by Ci.

Although this work has shown T7 RNAP to be non-responsive to Ci, it was still necessary to test another member of the Pol I family of prokaryotic DNA polymerases. This was the Klenow *exo*$^-$ fragment of *E. coli* DNA polymerase I, and using the new *in vitro* Ci assay methodology was shown to be non-responsive to Ci. The findings that two members of Pol I family of prokaryotic DNA polymerases were not regulated by Ci indicates that a response to Ci is not likely to be a conserved feature of this family of enzymes. Furthermore, Polβ from *Rattus norvegicus*, a member of the Pol β family of DNA polymerases, was also tested and also shown to be non-responsive to Ci. Overall, this work provided evidence suggesting that a Ci response is unlikely to be a conserved feature of nucleotidyltransferases possessing a 'palm' domain, although it is possible that one could exist.

Due to these newly identified increases in assay pH, this work has indicated the need for a reinvestigation of Ci responsive ACs.

5

Ci and GCs

5.1 Introduction

Although GCs are involved in a number of diverse physiological processes in eukaryotes, their presence in prokaryotes is still debatable (Garbers *et al.*, 2006; Linder, 2010; Poulos, 2006). All known GCs possess Class IIIa CHDs (with the exception of soluble GC (sGC) from *Dictyostelium discoideum,* which possesses a Class IIIb CHD), and are diverse in their structure and biochemical properties (Garbers *et al.*, 2006; Linder and Schultz, 2003; Poulos, 2006; Roelofs *et al.*, 2001). In mammals, the difference between AC and GC substrate specificity has been shown to depend upon two active site amino acids, with a lysine and aspartate defining substrate ATP, and a glutamate and cysteine defining substrate GTP (Sunahara *et al.*, 1998). With an increasing number of ACs being shown to be responsive to Ci, and the fact that ACs and GCs share a structurally related active site, it has become more plausible that Ci could have an effect on some GCs (Cann *et al.*, 2003; Chen *et al.*, 2000; Hammer *et al.*, 2006; Klengel *et al.*, 2005; Mogensen *et al.*, 2006; Steegborn *et al.*, 2005b). Indeed, the case for Ci acting on GCs is strong, given that several known Ci sensing pathways are known to involve cGMP (see Sections 1.4.4 and 1.5.6). Although the initial Ci sensing protein in these pathways had not been proven it was reasonable to speculate that GC could perform this role.

In mammals there are two distinct sources of cGMP; membrane bound receptor GCs and sGC (Garbers *et al.*, 2006; Poulos, 2006). sGC is expressed in most tissues, is the sensor for NO, and is involved in the regulation of diverse physiological processes (Poulos, 2006). In rodents, receptor GCs (GC-A, GC-B, GC-C, GC-D, GC-E, GC-F and GC-G) are expressed in various tissues where they respond to various extracellular ligands (Garbers *et al.*, 2006). Although there is little evidence to suggest that sGC is involved in the detection of Ci in mammals, studies into the olfactory detection of Ci in rats has provided good evidence for the involvement of a receptor GC. Rodents are able to detect Ci through olfactory receptors in the nose, and work has shown that neurons which uniquely express GC-D (it is worth noting that in Humans, GC-D is a pseudogene) are responsible for this (Fulle *et al.*, 1995; Hu *et al.*, 2007). Although another protein could potentially be responding to Ci (e.g. PDE2A) in this system, the fact that ACs are known to respond to Ci provides support to

the notion of GC-D acting as the initial Ci sensor (Hu *et al.*, 2007; Leinders-Zufall *et al.*, 2007)

Further evidence supporting the notion of GCs being involved in the detection of Ci was found in *Caenorhabditis elegans.* Studies showed that the detection of Ci in this organism was dependent upon a cGMP gated ion channel (Tax-2/Tax-4) and a receptor GC (Daf-11) (Bretscher *et al.*, 2008; Hallem and Sternberg, 2008). Again, given the number of known Ci responsive ACs it was possible that the Ci responsive protein in this system was the receptor GC Daf-11.

Using the new *in vitro* Ci assay methodology, the response of several GCs to Ci was tested. The response of mammalian GCs, both sGC and receptor GCs, was tested. Furthermore, following the recent identification of a prokaryotic GC (see Section 5.4 for discussion), the response of this enzyme to Ci was also tested.

5.2 Receptor GCs

NIH 3T3 cells stably expressing various mouse receptor GCs (GC-A, GC-B, GC-D, GC-E, GC-F and GC-G) were obtained (kind gift from Dr. Kent Hamra, Department of Pharmacology, University of Texas). Cells were grown under standard conditions (see 2.3.1) in the presence of G418, and the membrane fractions from lysates of these cells were extracted (see 2.3.4). Significantly elevated GC activity was detected in GC-A and GC-E transfected cells when compared to non-transfected cells, but not in GC-B, GC-D, GC-F, or GC-G transfected cells. The reason for this remains unclear, but it was possible that since the cell lines were old (Dr. Kent Hamra, personal communication), loss of the transfected GC gene had occurred. Unfortunately, subsequent attempts to resolve the issue failed and it was not possible to obtain a source of the prime candidate for a Ci response, GC-D, within the time frame available.

The GC activity of membrane fractions derived from non-transfected NIH 3T3 cells was always tested along side transfected NIH 3T3 cells to ensure the GC activity was specific to the over-expressed receptor GC. The effect of Ci on GC-A and GC-E was tested *in vitro* at pH 6.5 with Ci supplied in the form of 20 mM $NaHCO_3$, however, no response was observed (Figure 5.1).

GC-A and GC-E were also similarly tested *in vitro* at pH 7.5 and 8.5, but again no response to Ci was seen (Figure 5.2). It is worth noting that in the cases of both GC-A and GC-E it was seen that their GC activity was significantly higher at pH 6.5 than it was at pH 7.5 or 8.5, which was surprising since the pH optimum for these enzymes is reported at around pH 7.5 (Hardman and Sutherland, 1969). It is probable that due to the fact that the experiments conducted at pH 6.5 were performed on fresh membrane fractions, with those done at pH 7.5 and 8.5 a few days later, that storage at -20°C and subsequent freeze-thaw lead to inactivation of membrane bound proteins and a subsequently artificial decrease in specific activity.

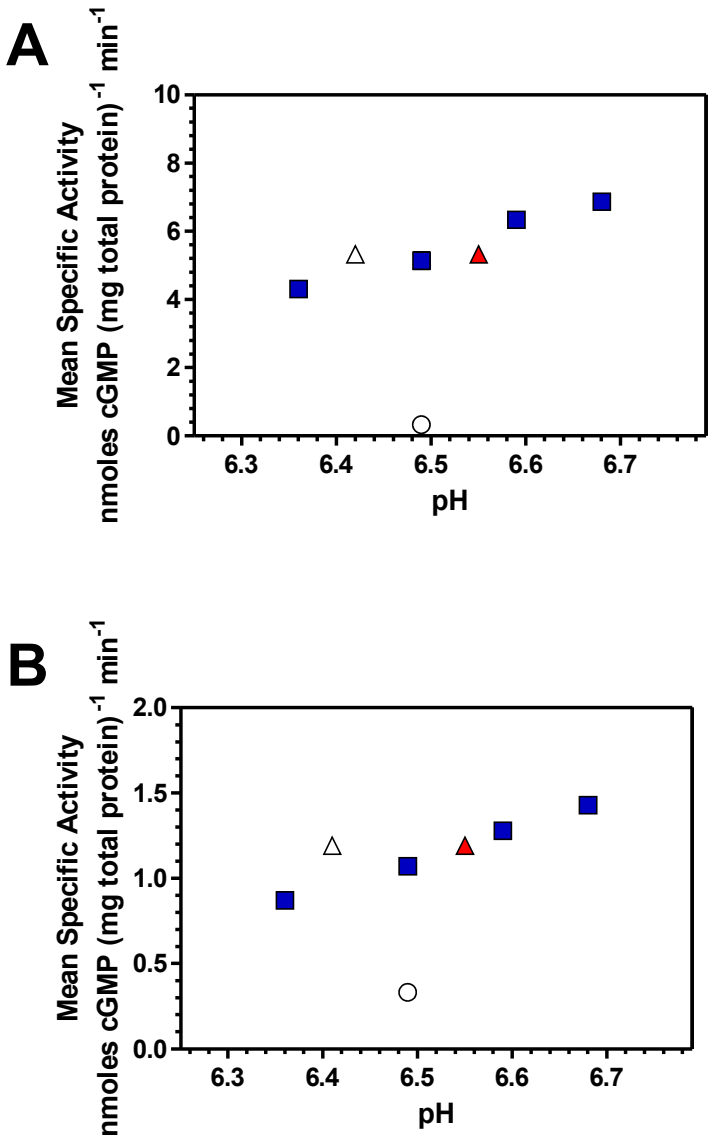

Figure 5.1: The effect of Ci on GC-A and GC-E activity *in vitro* at pH 6.5.

Assays were carried out in 100 µL for 30 minutes at 37°C in the presence of 100 mM Mes-NaOH, 10 mM $MgCl_2$, 1 mM IBMX, 5 mM creatine phosphate, 5 units creatine phosphokinase, 1 mM DTT, 1 mM GTP, 1 % (w/v) triton X-100 and either 20 mM NaCl (blue squares) or $NaHCO_3$ (triangles; starting pH – clear, final pH red). Non-transfected NIH 3T3 cell lysate (circles). **(A)** NIH 3T3 cell lysates over-expressing GC-A. **(B)** NIH 3T3 cell lysates over-expressing GC-E. (n = 3)

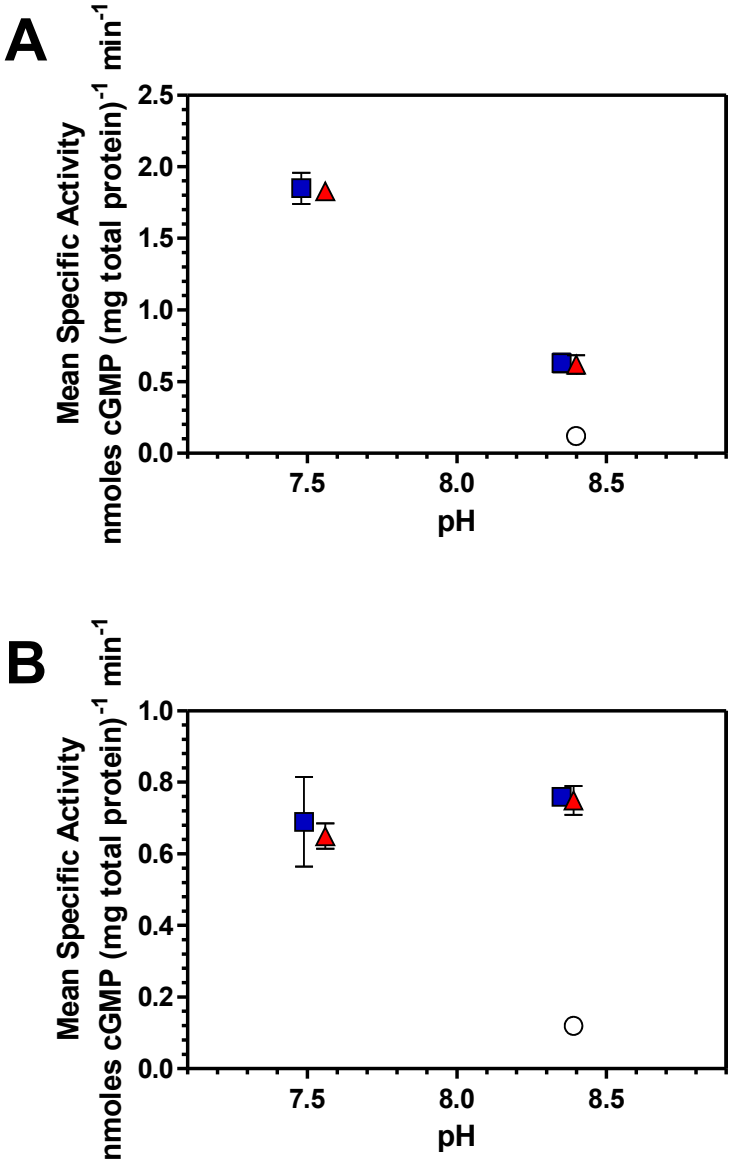

Figure 5.2: The effect of Ci on GC-A and GC-E activity *in vitro* at pH 7.5 and 8.5.

Assays were carried out in 100 µL for 30 minutes at 37°C in the presence of 100 mM Tris-HCl, 10 mM $MgCl_2$, 1 mM IBMX, 5 mM creatine phosphate, 5 units creatine phosphokinase, 1 mM DTT, 1 mM GTP, 1 % (w/v) triton X-100 and either 20 mM NaCl (blue squares) or $NaHCO_3$ (red triangles). Non-transfected NIH 3T3 cell lysate (circles). **(A)** NIH 3T3 cell lysates over-expressing GC-A. **(B)** NIH 3T3 cell lysates over-expressing GC-E. (n = 4)

5.3 Soluble GC

Due to GCs being implicated in Ci sensing in several diverse pathways, it was wise to assess the response of sGC to Ci. Since sGC is expressed in most mammalian tissues, and a previous biochemical study performed on sGC used lysates obtained from HEK 293 cells, it was decided to study the effects of Ci on sGC using a similar method (Parkinson *et al.*, 1999). HEK 293T cells were grown under standard conditions, and the soluble fraction derived from HEK 293T cell lysates was initially probed to determine whether NO dependent GC activity could be detected. GC activity of the soluble fraction derived from HEK 293T cell lysates was significantly up-regulated in the presence of the NO donor S-Nitroso-N-acetylpenicillamine (SNAP) at a concentration of 1 mM, demonstrating that sGC specific activity could be detected (Figure 5.3). In subsequent biochemical assays performed a control sample without SNAP was included to demonstrate that the majority of GC activity reported was specific to sGC and not the endogenous receptor GCs.

The effect of Ci on sGC was studied at 3 different pHs (pH 6.5, 7.5 and 8.5) *in vitro*, with Ci supplied in the form of 20 mM $NaHCO_3$, and using 20 mM NaCl as a control for non-specific anion or cation effects. At all pHs tested there was no stimulatory effect of Ci seen (Figure 5.3), demonstrating that sGC is unlikely to be regulated by Ci.

Although a very slight decrease in specific activity was seen at pH 6.5 in the presence of Ci (when compared to NaCl), this was not likely to be a specific effect due to Ci. Given the relatively high concentration of CO_2 in the assay, and the fact that NO mediates its effects on sGC through binding to haem, it is likely that the drop in specific activity is due to CO_2 competing with NO for haem binding (Poulos, 2006). However, it is worth noting that due to this competition for haem binding the converse could occur, where NO binding to haem prevents CO_2 binding and thus masking any possible effects of Ci.

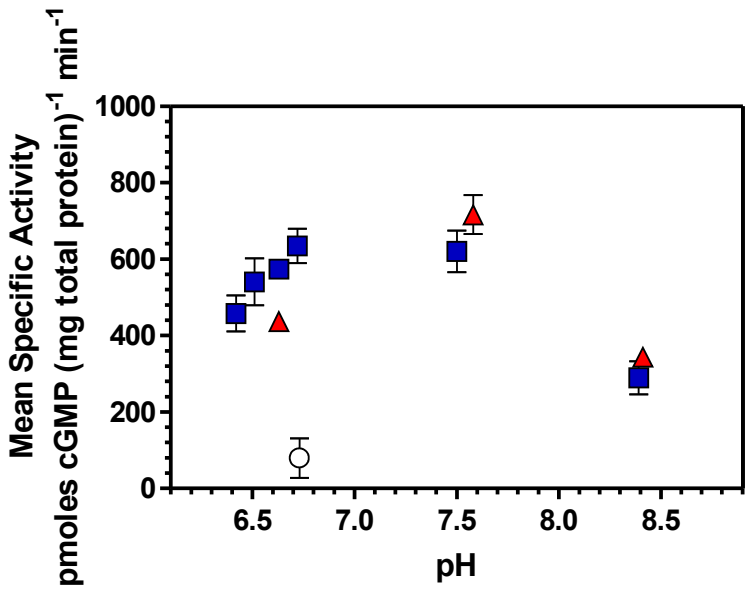

Figure 5.3: The effect of Ci on sGC activity *in vitro*.

Assays were carried out in 100 µL for 40 minutes at 37°C. Assay contained 100 mM Mes-NaOH, 10 mM $MgCl_2$, 1 mM IBMX, 5 mM creatine phosphate, 5 units creatine phosphokinase, 1 mM DTT, 1 mM GTP and 45 mg total soluble protein. Assays also contained 20 mM NaCl (circle), 20 mM NaCl + 1 mM SNAP (blue squares) and 20 mM $NaHCO_3$ + 1 mM SNAP (red triangles). (n = 3)

5.4 Sll0646 from *Synechocystis* PCC 6803

The genome of *Synechocystis* PCC 6803 contains 3 putative CHD encoding open reading frames (ORFs) (*cya1*, *cya2* and *cya3*), of which two have been shown to express a functional cyclase (Ochoa De Alda *et al.*, 2000; Rauch *et al.*, 2008; Terauchi and Ohmori, 1999). Slr1991 (*cya1*) has already been confirmed as a functional AC, and has also been shown to be regulated by Ci (Hammer *et al.*, 2006; Masuda and Ono, 2005). Sequence analysis of Sll0646 (*cya2*) indicated that is was likely to be a GC, and mutation resulted in a drop of cGMP levels in *Synechocystis* PCC 6803 (Ochoa De Alda *et al.*, 2000). Recently, crystallographic and biochemical evidence has been obtained to support the idea of Sll0646 being a functional GC (Rauch *et al.*, 2008). Although Sll1161 (*cya3*) shares some sequence similarity with other CHDs, it appears to lack several amino acid residues essential for catalysis and as such is unlikely to be functional, although this has not been confirmed (Masuda and Ono, 2005; Ochoa De Alda *et al.*, 2000). Given the recent evidence demonstrating Sll0646 as a functional GC, and the fact that Slr1991 from this organism is known to be Ci sensitive, the response of this prokaryotic GC to Ci would be tested using an *in vitro* Ci assay (Hammer *et al.*, 2006; Masuda and Ono, 2005; Rauch *et al.*, 2008). Furthermore, it was decided to clone, express and biochemically study Sll1161 to identify whether it is a functional AC or GC, and if AC or GC activity was detected, determine if it shared a Ci response with Slr1991.

Before *in vitro* biochemical investigation on Sll0646 and Sll1161 could start it was necessary to obtain sufficient pure recombinant enzyme. Since previous work carried out on Slr1991 had successfully relied upon purifying a recombinant hexa-histidine tagged protein over-expressed in *E. coli*, a similar method was adopted (Masuda and Ono, 2004). Previous biochemical analysis of Slr1991 had studied a recombinant protein consisting of the CHD, but lacking the amino acids to the N-terminus of the CHD. Sll0646 and Sll1161 CHDs were identified using the SMART database (http://smart.embl-heidelberg.de) and oligonucleotide primers were subsequently designed (Table 2.4) to clone the CHDs of Sll0646 and Sll1161 (Figure 5.4). The nucleotides corresponding to amino acids 424-756 of Sll0646 and amino acids 73-285 of Sll1161 were cloned into the pQE30 vector at the *Pst* I/*Sph* I and *Bam* HI/*Hind* III sites, respectively (see 2.2.13). Expression constructs were validated by DNA sequencing. 38 kDa,

hexa-histidine tagged, Sll0646$_{424-756}$ was over-expressed in *E. coli* M15 (DE3) [pREP4], and pure recombinant Sll0646$_{424-756}$ was obtained following Ni^{2+}-NTA affinity FPLC, and was sufficiently homogeneous for in vitro biochemical studies (Figure 5.5A). Unfortunately, attempts to over-express Sll1161$_{73-285}$ failed and it was not possible to obtain any recombinant protein within the limited timeframe available.

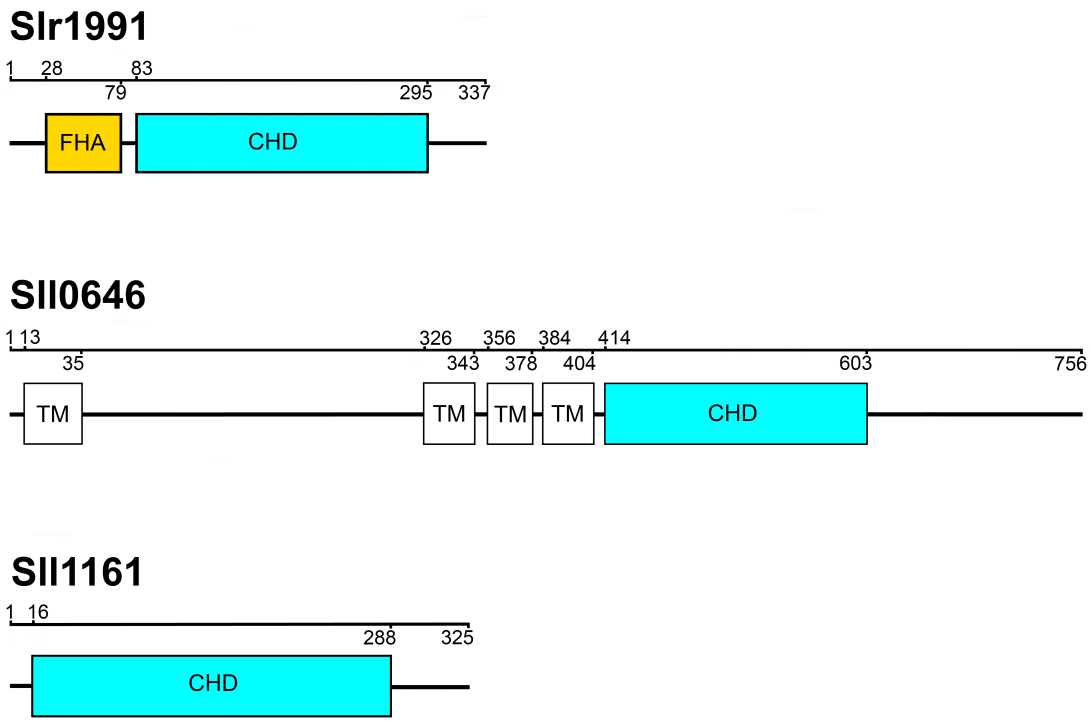

Figure 5.4: Domain architecture of *Synechocystis* PCC 6803 CHD encoding proteins.

Domain architecture was constructed using SMART (http://smart.embl-heidelberg.de). Domain abbreviations are; FHA – forkhead-associated domain; CHD – cyclase homology domain; TM – predicted transmembrane domain. Numbers correspond to amino acid numbers (ascending N-terminal to C-terminal).

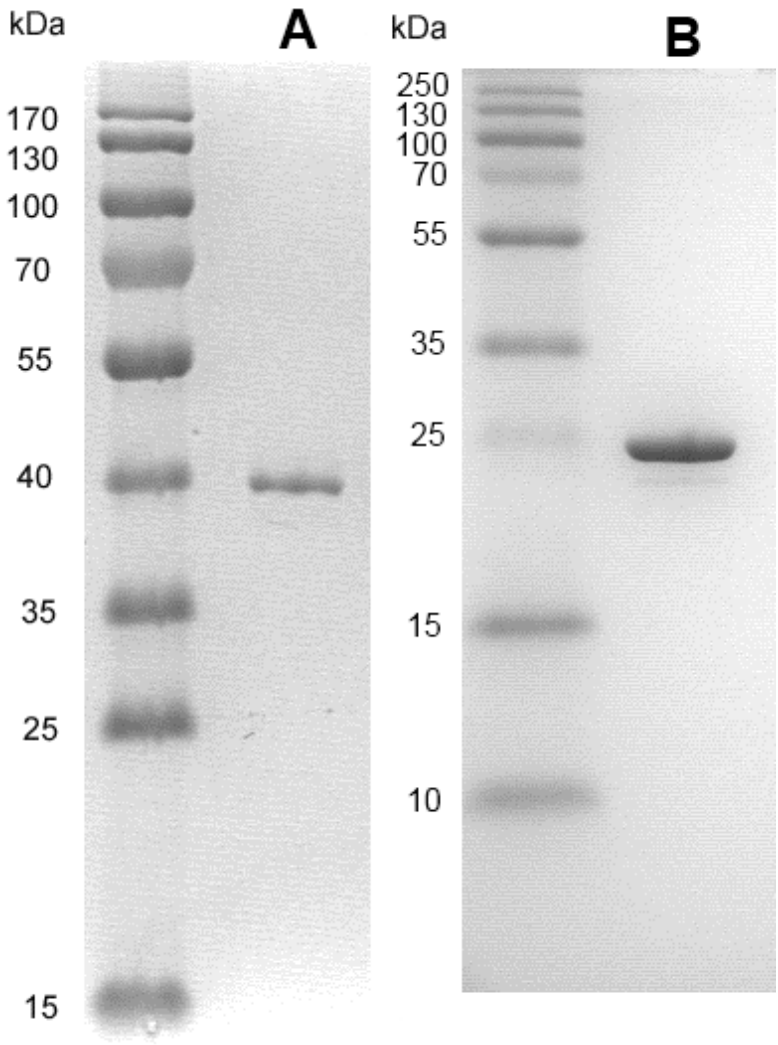

Figure 5.5: Purified recombinant Sll0646.

(A) 12 % (v/v) bis-acrylamide SDS-PAGE gel loaded with 1 µg $Sll0646_{424-756}$ **(B)** 15 % (v/v) bis-acrylamide SDS-PAGE gel loaded with 2 µg $Sll0646_{434-635}$. Proteins were stained with Coomassie Brilliant blue dye and protein size was estimated relative to Fermentas PagerRuler™ Prestained Protein ladder (A) and Fermentas PagerRuler™ Plus Prestained Protein ladder (B).

An *in vitro* biochemical assay on Sll0646$_{424-756}$ was performed at pH 7.5 to confirm the activity of the expressed protein, however, it indicated that Sll0646 was likely to be an AC and not a GC. The enzyme showed an AC activity greater than 20 fold that of the GC activity (3288 ± 67 pmoles cAMP mg^{-1} min^{-1} Vs. 137 ± 5 pmoles cGMP mg^{-1} min^{-1}), an observation that was in contrast to the published work (Rauch *et al.*, 2008). The biochemical assays performed by Rauch *et al.* also used a recombinant hexa-histidine tagged form of Sll0646, except corresponding to amino acids 434-635. In order to address this conflict the expression vector pET151TOPO.cya2cat (kind gift of Dr. Clemens Steegborn) was transformed into *E. coli.* The 26 kDa Sll0646$_{434-635}$ was over-expressed, purified to homogeneity through Ni^{2+}-NTA affinity FPLC (Figure 5.5B) and was compared biochemically to Sll0646$_{424-756}$ (Rauch *et al.*, 2008).

The AC and GC activity of Sll0646$_{434-635}$ was tested at a range of pHs and it was observed that the GC activity was more that 10 fold greater than the AC activity (Figure 5.6B), matching the findings of the published work (Rauch *et al.*, 2008). It was apparent that the GC activity of Sll0646$_{434-635}$ displayed no significant dependence on pH, whereas the AC activity increased progressively from pH 6.5 to 8.5 (Figure 5.6B). When Sll0646$_{424-756}$ was subjected to the same pH response assay the results were remarkably different, showing the enzyme to possess a far greater AC than GC activity (Figure 5.6A). Similarly, the GC activity of Sll0646$_{424-756}$ showed no dependence on pH, whereas the AC activity showed a response to pH comparable with other ACs (Figure 5.6A).

Although the GC activity of both Sll0646$_{424-756}$ and Sll0646$_{434-635}$ were similar (at pH 8.35: 1.12 ± 0.06 pmoles cGMP mg^{-1} min^{-1} for Sll0646$_{424-756}$ and 2.33 ± 0.17 pmoles cGMP mg^{-1} min^{-1} for Sll0646$_{434-635}$), the AC activities were vastly different (at pH 8.35: 31.4 ± 0.41 pmoles cAMP mg^{-1} min^{-1} for Sll0646$_{424-756}$ and 0.35 ± 0.1 pmoles cAMP mg^{-1} min^{-1} for Sll0646$_{434-635}$).

Although these results indicate that Sll0646 is likely to be an AC, definitive proof was dependent upon testing the full length native protein. As such, the full length gene was cloned into pQE30 and pCDNA3.1 at the *Pst* I/*Sph* I and *Eco* RV/*Xho* I, respectively. However, with limited time available it was not possible to successfully express recombinant protein in *E. coli* and HEK 293T cells, respectively.

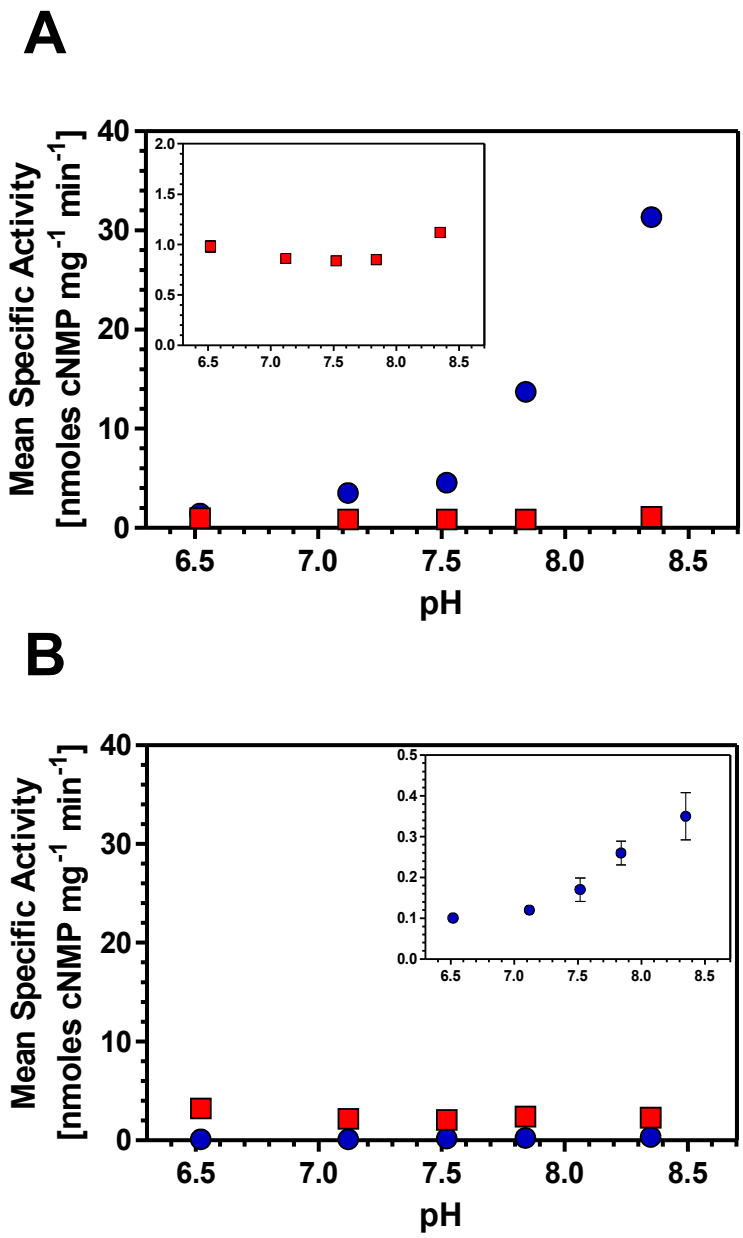

Figure 5.6: Sll0646 is an AC with GC side activity.

Assays were carried out in 100 µL for 30 minutes at 37ºC in the presence of 500 µM ATP **(blue circles)** or GTP **(red squares)**. Assays also contained 2 mM $MnCl_2$, and 100 mM Mes-NaOH (pH 6.5) or Tris-HCl (pHs 7.0, 7.5, 8.0 and 8.5). **(A)** 650 nM Sll0646 (amino acids 424-756), inset shows a closer view of the GC activity. **(B)** 650 nM Sll0646 (amino acids 434-635), inset shows a closer view of the AC activity. (n = 3)

In order to provide some insight into the conflict in cyclase activities of these two recombinant forms of Sll0646, substrate dose responses were carried out. Each recombinant form of Sll0646 was subjected to an ATP does response at pH 7.5 (and also pH 8.5 for $Sll0646_{424-756}$) in order to determine V_{max} and K_m parameters (Figure 5.7). Using the Michaelis-Menten graphs and the non-linear regression package in Graphpad Prism, V_{max} values were determined for $Sll0646_{434-635}$ at pH 7.5 (0.49 ± 0.03 nmoles cAMP mg^{-1} min^{-1}), $Sll0646_{424-759}$ at pH 7.5 (2.9 ± 0.1 nmoles cAMP mg^{-1} min^{-1}) and $Sll0646_{424-759}$ at pH 8.5 (25.7 ± 1.2 nmoles cAMP mg^{-1} min^{-1}). K_m parameters were estimated following the same procedure as V_{max} and were determined for $Sll0646_{434-635}$ at pH 7.5 (0.46 ± 0.1 mM), $Sll0646_{424-759}$ at pH 7.5 (0.19 ± 0.02 mM) and $Sll0646_{424-759}$ at pH 8.5 (0.30 ± 0.04 mM).

Both recombinant forms of Sll0646 were also subjected to a GTP dose response assay and they displayed substrate inhibition by GTP (Figure 5.8). This substrate inhibition was most apparent in $Sll0646_{424-756}$, with a 50 % decrease in enzyme activity being seen from 50 µM to 125 µM substrate (3.85 ± 0.07 nmoles cGMP mg^{-1} min^{-1} to 1.89 ± 0.13 nmoles cGMP mg^{-1} min^{-1}). Due to this substrate inhibition it was not possible to accurately determine K_m or V_{max}, however, it appeared that $Sll0646_{424-756}$ possessed a much stronger substrate affinity since its highest activity was seen at 50 µM substrate whereas $Sll0646_{434-635}$ at 1 mM.

Substrate inhibition usually occurs when an enzyme possesses more than one substrate binding site, and substrate binding to the second non-catalytic site causes a conformational change, decreasing catalytic activity through the first binding site. As such it was necessary to perform further analysis on the data acquired in order to determine whether it is likely that this enzyme possesses more than one substrate binding sites. This was done through producing a sigmoidal dose curve through plotting enzyme activity against the Log_{10} of substrate concentration (Figure 5.9A/B). Non-linear regression analysis using the Prizm graphical analysis software determined the Hill slope of the linear portion of the sigmoid. At pH 7.5 the Hill slope of $Sll0646_{424-756}$ was 1.96 ± 0.26 and at pH 8.5 the Hill slope was 2.24 ± 0.25. The Hill slopes close to 2 indicate that this enzyme, like most ACs, possesses two substrate binding sites (or multiples of two).

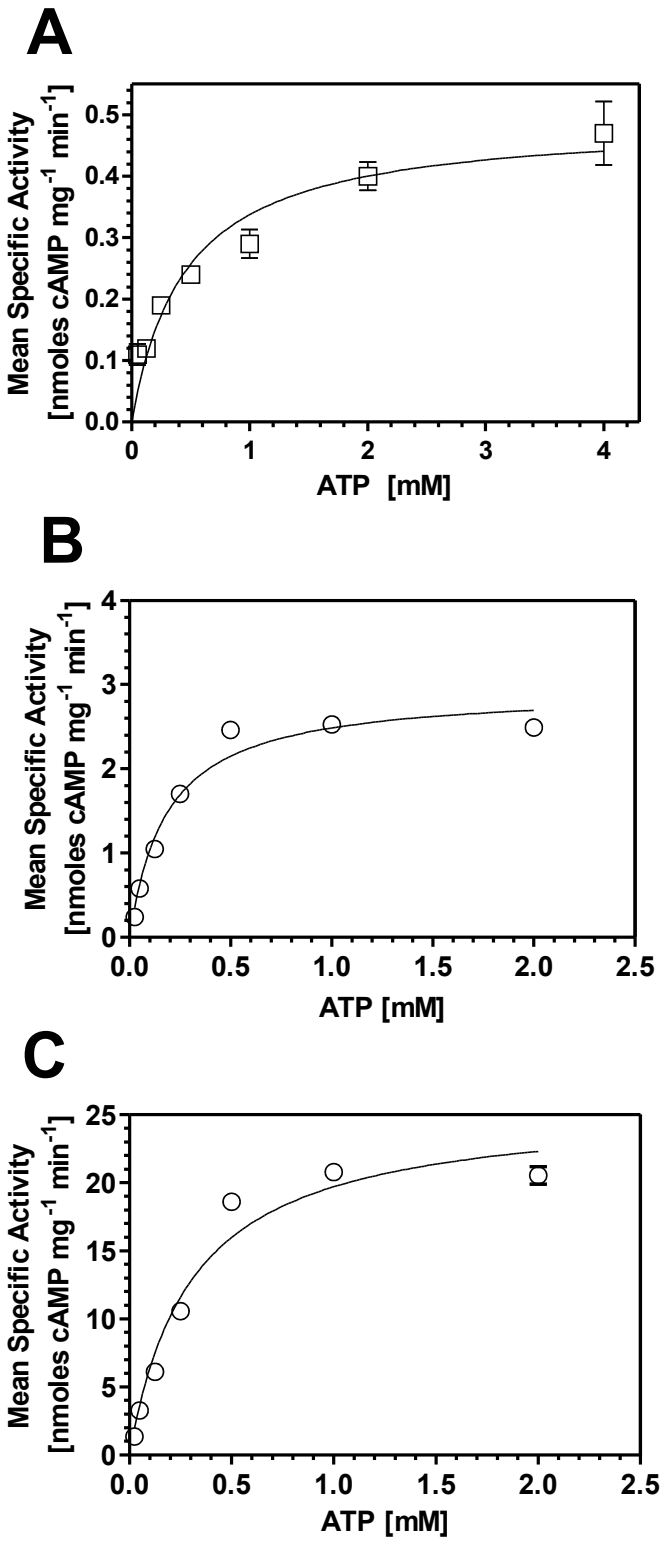

Figure 5.7: ATP dose responses on Sll0646.

Assays were carried out in 100 µL for 30 minutes at 37°C in the presence of 10 mM $MnCl_2$, and Tris-HCl (pHs 7.5 and 8.5). **(A)** 650 nM Sll0646 (amino acids 434-635) at pH 7.5. **(B)** 650 nM Sll0646 (amino acids 424-756) at pH 7.5. **(C)** 650 nM Sll0646 (amino acids 424-756) at pH 8.5. (n = 3)

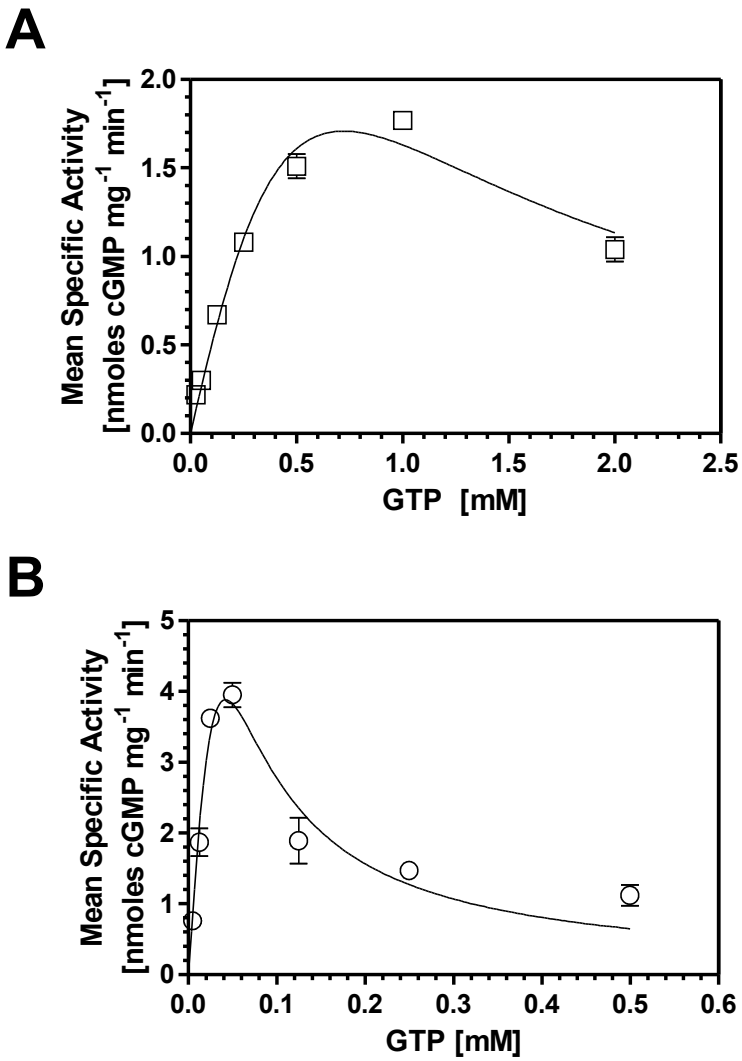

Figure 5.8: GTP dose responses of Sll0646.

Assays were carried out in 100 µL for 30 minutes at 37°C in the presence of 10 mM $MnCl_2$, and Tris-HCl pH 7.5. **(A)** 650 nM Sll0646 (amino acids 434-635). **(B)** 650 nM Sll0646 (amino acids 424-756). (n = 3)

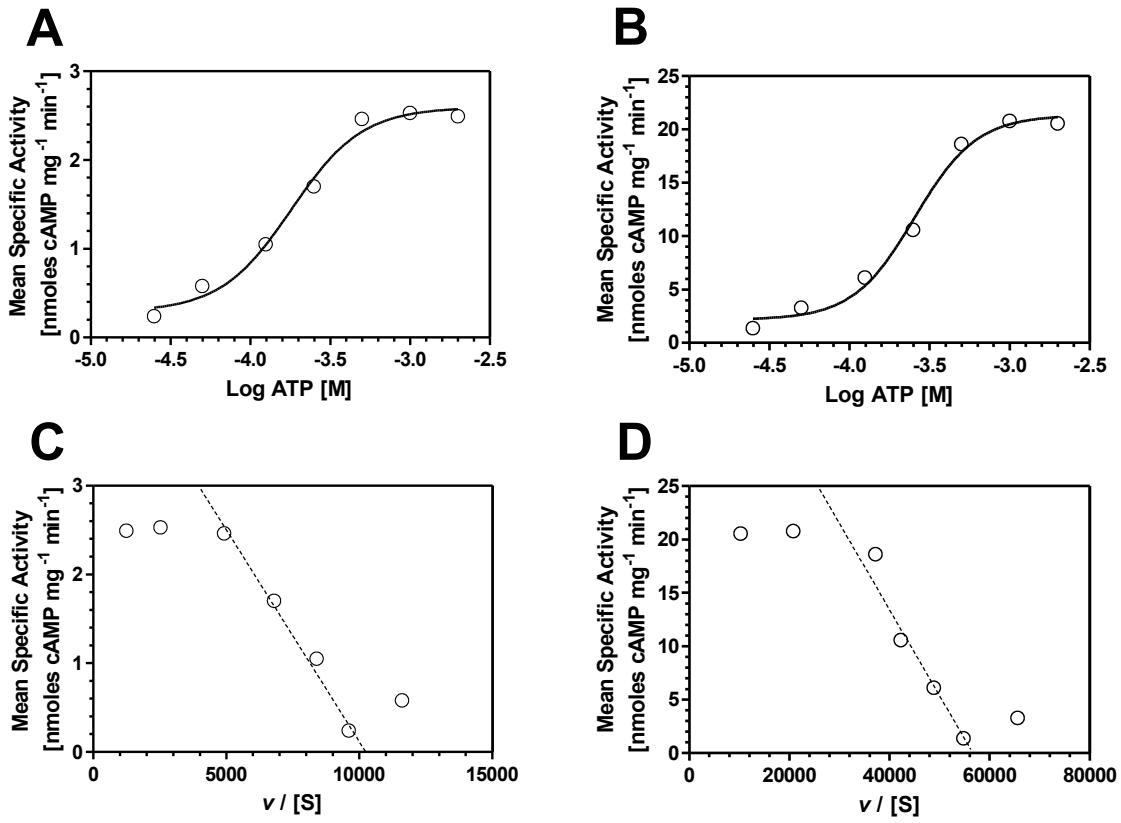

Figure 5.9: Graphical analysis of Sll0646$_{424-756}$ ATP dose responses shows substrate inhibition.

Further analysis of data from Figure 5.7A/B. (A) Sigmoidal dose response at pH 7.5. (B) Sigmoidal dose response at pH 8.5. (C) Eadie-Hoftsee plot at pH 7.5 (D) Eadie-Hoftsee plot at pH 8.5.

v - velocity; Mean Specific Activity, S - Substrate

Although substrate inhibition by GTP was easily identified from the raw plots of Sll0646 (Figure 5.8) it was necessary to more closely analyse the responses in the presence of ATP. This analysis was done via an Eadie-Hofstee plot whereby enzyme velocity (*v,* i.e. mean specific activity) was plotted against enzyme velocity over substrate concentration (*v* / [S]). True Michaelis-Menten enzymes, when plotted in this manner, demonstrate a complete straight line bisecting all data points. It was clear that $Sll0646_{424-756}$ at pH 7.5 and 8.5 did not fit a straight line, with the points at low *v* / [S] deviating below the straight line (Figure 5.9C/D). This drop below the straight line indicated that at higher substrate concentrations there was negative co-operativity between the two substrate binding site, indicating substrate inhibition.

Using the newly devised *in vitro* Ci assay methodology the response of $Sll0646_{424-756}$ (both the GC and AC activity) was tested at pH 6.5 and revealed no response to Ci (Figure 5.10).

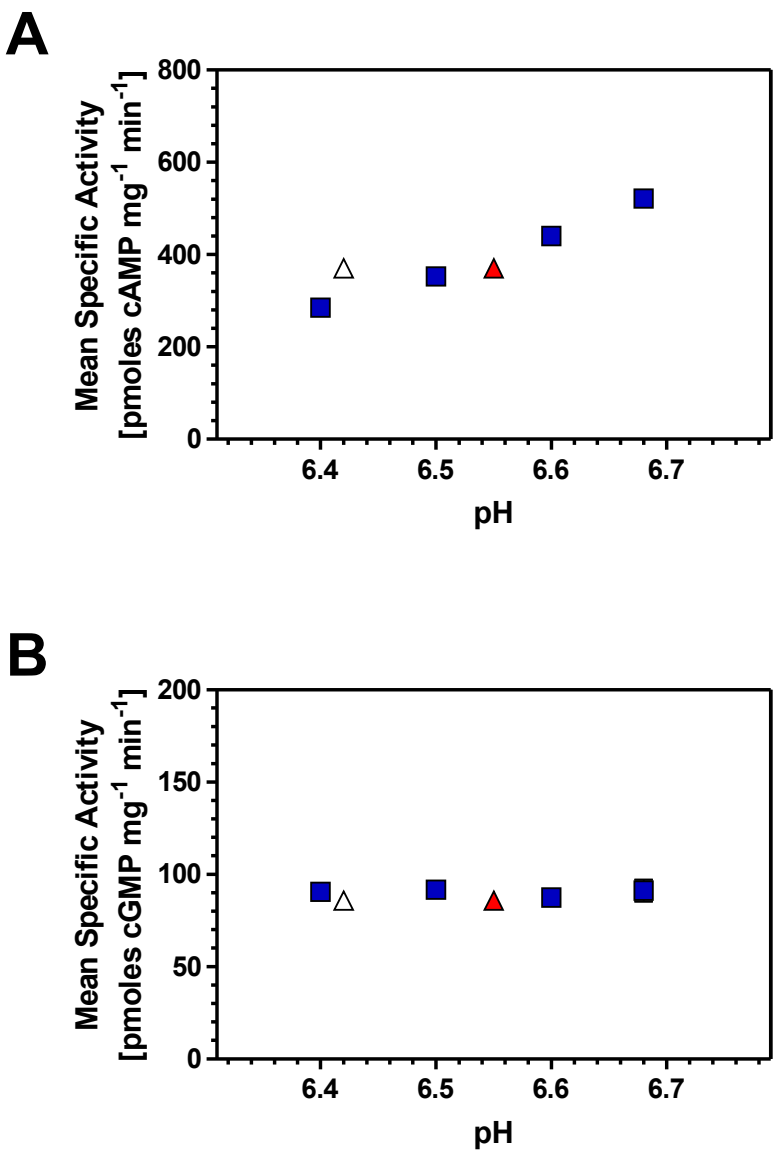

Figure 5.10: Neither the AC or GC activity of Sll0646 were activated by Ci.

Assays were performed for 30 minutes at 37°C in a volume of 100 µL containing 100 mM Mes-NaOH, 10 mM $MnCl_2$, 9 µM Sll0646 (amino acids 424-756) and 20 mM NaCl (squares) or $NaHCO_3$ (triangle). **(A)** 1 mM ATP **(B)** 1 mM GTP. (n = 4)

5.5 Discussion

In vitro biochemical analysis of three mammalian GCs (GC-A, GC-E and sGC) and Sll0646 from *Synechocystis* PCC 6803, has revealed that these enzymes are not regulated by Ci. Although *in vitro* Ci experiments performed on sGC showed a slight inhibition of GC activity in the presence of Ci, this is possibly due to CO_2 competing with NO for haem binding. Since sGC activity is dependent upon NO binding to haem, it is likely that a reduction in NO-bound haem would result in a decrease in GC specific activity. With hindsight, it would be wise to re-investigate the response of sGC to Ci, using a slightly different method to avoid potential competition between CO_2 and NO for haem. This could be achieved through studying the response of sGC to Ci in the absence of NO, although whether detectable sGC activity could be detected under these conditions is unclear. Unfortunately, due to the failure to obtain GC activity from stable cell lines expressing several other receptor GCs, including the prime candidate for a Ci response (GC-D), a more complete investigation into possible responses of mammalian GCs as a whole was not possible within the time available.

Work published shortly after investigation in this area was ceased indicated that, as hypothesized in whole organism and *in vivo* studies, GC-D was regulated by Ci (Sun *et al.*, 2009). When our current knowledge of the problems associated with studying Ci responses *in vitro* (see Section 4.2) was taken into account it was apparent that several experiments contained in that paper could potentially be misleading due to pH effects. However, this initial work was soon validated by a more complete biochemical study into all receptor GCs, which proved that whilst six of the receptor GCs and sGC were non-responsive, GC-D was responsive to Ci (Guo *et al.*, 2009). Furthermore, this later work also identified the pH issues that arise when working with Ci in solution and due to this observation the biochemical assays were suitably controlled (Guo *et al.*, 2009).

Biochemical work carried out on two different truncated recombinant proteins derived from Sll0646 has provided contrasting evidence as to whether the native enzyme is an AC or GC. Work performed on $Sll0646_{424-756}$ indicates that this enzyme is an AC, whereas work performed on $Sll0646_{434-635}$ indicates that it is a GC. However, the fact that the GC activity for both isoforms is very

similar, but the AC activity is much higher in Sll0646$_{424-756}$ than in Sll0646$_{434-635}$, indicates that the enzyme may be an AC. It is possible that removal 121 amino acids from the C-terminus of the protein resulted in an abnormal tertiary structure, causing a loss of AC activity, however, this is purely speculative.

The possibility that Sll0646 is an AC is further supported by the fact that the AC activity of both isoforms displays a standard pH dependence, whereas the GC activity is constant across the pH range tested. Most enzymes, especially ACs and GCs, display a fairly standard bell shaped activity response to pH, most commonly displaying a pH optimum around pH 7.5 to pH 8 (Hardman and Sutherland, 1969; Hatley *et al.*, 2002). The fact that the GC activity showed no significant pH dependence was strange, since it was in contrast to other cyclases. However, when the apparent strong substrate inhibition by GTP is taken into account a possible explanation becomes apparent. Since the GTP concentration in the pH dependence assay was maintained at 500 µM and that in the case of Sll0646$_{434-635}$ the effects of substrate inhibition become apparent at concentrations of 500 µM at pH 7.5 it is possible that the effects of substrate inhibition are causing misleading results. It is possible that the GC activity of the enzyme does follow a standard bell shaped response to pH, but due to the effects of substrate inhibition possibly varying with pH, the activity is being artificially lowered dependent upon pH.

It would be more appropriate to have conducted the pH dependence assays with a much lower substrate concentration to remove strong effects of substrate inhibition. However, when the fact that substrate inhibition at pH 7.5 begins at around 50 µM in the case of Sll0646$_{424-756}$, choosing a suitable concentration of GTP to use becomes difficult. A series of GTP and ATP dose response curves would first need to be generated across a range of pHs in order the choose the most suitable concentration to conduct a pH response at. Within the time available it was not possible to conduct a deeper and more lengthy investigation, and this remains an important consideration for future work.

Finally, this work has highlighted a largely overlooked issue concerning working with recombinant proteins, and especially truncated recombinant proteins; that the behaviour of recombinant proteins does not always accurately reflect that of the native protein. Much biochemical work reported in the literature relies upon *in vitro* data derived from truncated recombinant proteins,

which are largely assumed to be accurate tools through which native proteins can be studied. This work emphasizes the need to be cautious when working with such proteins and ensure through comparison to native protein that their behaviours are comparable.

6

Ci and ACs re-visited

6.1 Introduction

With experimental evidence demonstrating that during *in vitro* Ci assays on T7 RNAP (see Section 4.3) there was a significant increase in pH over time it became necessary to perform a re-investigation of the response of many ACs to Ci. This pH increase of about 0.15 pH units (see Section 4.3) over the course of a 30 minute assay (at pH 6.5 with 20 mM total Ci) would result in a substantial increase in enzyme specific activity for most ACs. Since the activity of these enzymes commonly increases almost 2 fold from pH 6.5 to pH 7.0 and that the stimulatory effects so far seen on ACs by Ci are relatively small (commonly no more than a 2 fold increase seen by myself) it was necessary to re-investigate.

It was important to carry out experiments using the new *in vitro* Ci assay methodology derived through work on T7 RNAP to allow pH to be ruled out from any possible response to Ci. It was immediately important to perform these new experiments on the mammalian tmAC ($7C_1 \bullet 2C_2$) studied in a previous chapter (see Section 3.4). However, due to the magnitude of these newly identified pH issues it was also deemed prudent to use this new *in vitro* Ci assay methodology to re-test some already published Ci responsive Class IIIb ACs. These ACs were chosen as CyaB1 from *Anabaena* PCC 7120 and CyaC from *Spirulina platensis* (Cann *et al.*, 2003; Chen *et al.*, 2000; Hammer *et al.*, 2006; Steegborn *et al.*, 2005b).

6.2 Mammalian tmAC

Since previous work only demonstrated a significant stimulation by Ci on $7C_1 \bullet 2C_2$ at pH 6.5 and that the $7C_1 \bullet 2C_2$ pH profile derived previously showed a roughly 2 fold increase in specific activity between pH 6.5 and pH 7.0 it was necessary to re-evaluate the apparent response to Ci. The new *in vitro* Ci assay methodology (see Section 2.5.4) used to address the pH issues identified when working on T7 RNAP was employed to test $7C_1 \bullet 2C_2$. Since a Ci effect was seen when $7C_1 \bullet 2C_2$ was activated by both $G\alpha_s$ and forskolin, it was decided to perform this re-investigation using only forskolin to avoid the lengthy purification and activation of $G\alpha_s$.

Using the new *in vitro* Ci assay methodology $7C_1 \bullet 2C_2$ was assayed in the presence or absence of Ci under conditions replicating those used in the *in vitro* assays done previously (see Section 3.4). When the new *in vitro* Ci assay methodology was used to test the Ci response of $7C_1 \bullet 2C_2$ at pH 6.5, no response to Ci was observed (Figure 6.1). This indicated that it was probable that the stimulation of $7C_1 \bullet 2C_2$ ascribed to Ci earlier (see Section 3.4) was in fact a non-specific effect of pH. When the effects of pH were ignored (i.e. the starting pH was used; Figure 6.1 clear triangle), the activity of $7C_1 \bullet 2C_2$ appeared to be stimulated by Ci by an amount comparable to previous experiments (see Section 3.4), however, when the effects of pH were considered (Figure 6.1 red triangle), $7C_1 \bullet 2C_2$ did not appear to be stimulated by Ci. However, when the *in vivo* experimental evidence for a response of tmACs to Ci was taken into account it was clear that a small degree of doubt into the validity of the new *in vitro* Ci assay methodology was present.

In order to address this slight doubt, a control protein known categorically to be responsive to Ci was required to be tested to demonstrate the ability of this new *in vitro* Ci assay methodology to show a Ci response. The enzyme chosen was human sAC_t (see Section 6.3), and this control assay was run at the same time as the $7C_1 \bullet 2C_2$ assay shown below (Figure 6.2).

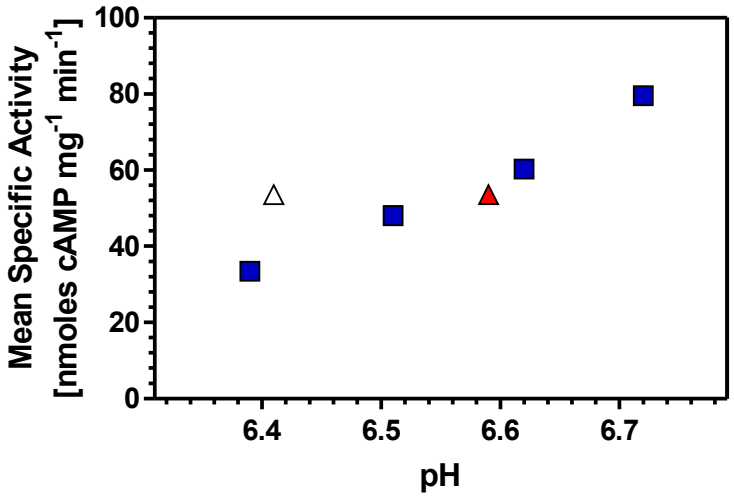

Figure 6.1: $7C_1 \bullet 2C_2$ was not activated by Ci using the new *in vitro* Ci assay methodology.

Assays were performed for 30 minutes at 37°C in a volume of 100 µL containing 100 mM Mes-NaOH, 10 mM $MgCl_2$, 1 mM ATP, 100 µM forskolin, 1.4 µM $7C_1$, 770 nM $2C_2$ and 20 mM NaCl (blue squares) or $NaHCO_3$ (triangles; starting pH - clear, final pH red). (n = 3)

6.3 Mammalian sAC

To provide confirmation that the new *in vitro* Ci assay was capable of identifying a Ci responsive protein, the response of human sAC_t to Ci was tested using this methodology. Recombinant human sAC_t was obtained (kind gift from Professor Lonny Levin), and was tested at pH 6.5 using the new *in vitro* Ci assay methodology. Results showed a greater than 2 fold stimulation of sAC_t in the presence of Ci, confirming that sAC_t was responsive to Ci, and more importantly demonstrating that the new *in vitro* Ci assay methodology was capable of identifying a Ci response, when one was present (Figure 6.2).

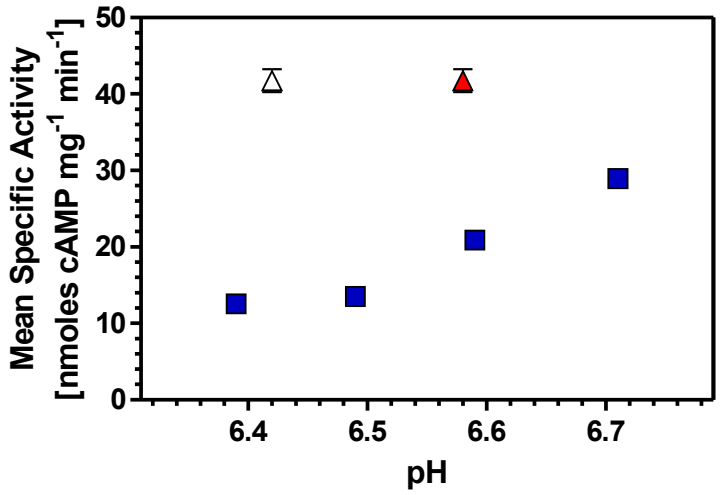

Figure 6.2: sAC_t was activated by Ci using the new *in vitro* Ci assay methodology.

Assays were performed for 40 minutes at 37°C in a volume of 100 µL containing 100 mM Mes-NaOH, 10 mM $MgCl_2$, 1 mM ATP, 200 nM sAC_t and 20 mM NaCl (red squares) or $NaHCO_3$ (triangles; starting pH – clear, final pH red). (n = 3)

6.4 CyaB1 from *Anabaena* PCC 7120

Another enzyme reported to be Ci responsive is CyaB1 from *Anabaena* PCC 7120. It was previously assumed that this enzyme was activated by HCO_3^-, but the species of Ci was later shown to be CO_2 (Cann *et al.*, 2003; Hammer *et al.*, 2006). When assays were carried out under conditions of Ci disequilibrium (10 second, 4°C assays where the predominant species of Ci in the assay remains the form in which it was added) this enzyme showed a higher activity when Ci was supplied in the form of CO_2 as opposed to that of HCO_3^- (or Cl^-).

In order to re-test the response of CyaB1 to Ci it was necessary to express $CyaB1_{595-859}$ in *E. coli* as a 30 kDa hexa-histidine tagged recombinant protein, and purify it to homogeneity (Figure 6.3); as done previously (Hammer *et al.*, 2006). It was first necessary to assess whether $CyaB1_{595-859}$ was activated by Ci using the new *in vitro* Ci assay methodology at around pH 6.5. It was observed that when the new *in vitro* Ci assay methodology was used, that $CyaB1_{595-859}$ was not activated by Ci (Figure 6.4).

Although the new *in vitro* Ci assay showed no response of $CyaB1_{595-859}$ to Ci it was still necessary to address the Ci disequilibrium experiments. The disequilibrium assays were repeated under almost identical conditions to that done previously, with the exception that time was increased from 10 to 15 seconds in order to increase the amount of cAMP produced to higher levels. When these 15 second assays were performed the enzyme was consistently shown to produce more cAMP when Ci was supplied in the form of CO_2 as opposed to HCO_3^- or Cl^- (Figure 6.5). Although this response was similar to that seen previously, the magnitude was much diminished (previous experiments showed a greater than 2 fold increase in activity in the presence of CO_2 compared to HCO_3^- or Cl^-), however, the reason for this remains unclear (Hammer *et al.*, 2006). Due to the importance of this experiment it was deemed necessary to also test whether sodium was potentially inhibiting enzyme activity and consequently misleading the results. The control for this was to include a water experiment as well as a $NaHCO_3$, NaCl and CO_2 experiment. With this control included it was seen that the activity of $CyaB1_{595-859}$ was increased in the presence of water and CO_2 saturated water, when compared to NaCl or $NaHCO_3$ (Figure 6.5). This indicated the possibility that under these conditions, Na^+ was causing an inhibition of $CyaB1_{595-859}$ activity and as such was causing

$CyaB1_{595\text{-}859}$ activity to appear to increase in the presence of CO_2.

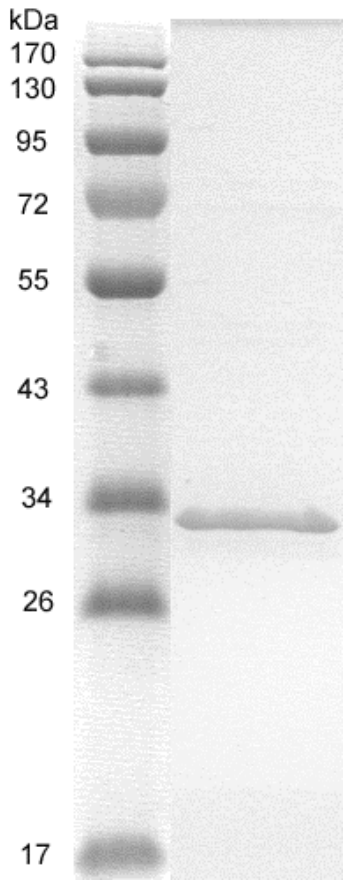

Figure 6.3: Purified recombinant CyaB1$_{595-859}$.

3 µg of purified CyaB1$_{595-859}$ was resolved on a 12 % SDS-PAGE gel. Proteins were stained with Coomassie Brilliant blue dye and protein size was estimated relative to Fermentas PagerRuler™ Prestained Protein ladder.

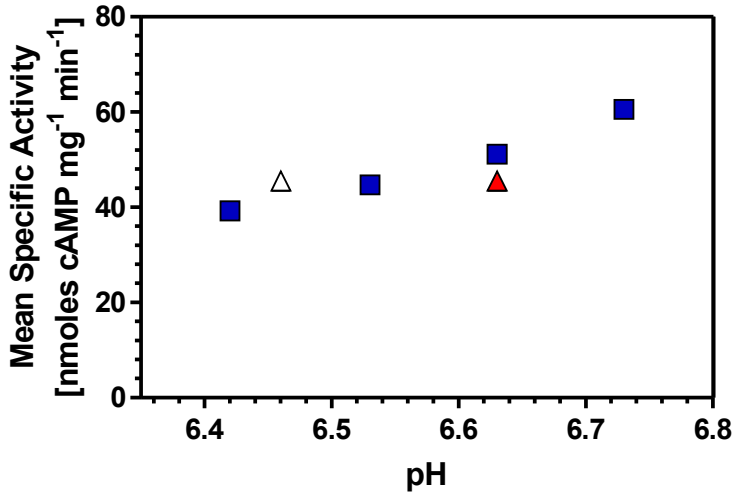

Figure 6.4: CyaB1$_{595-859}$ was not activated by Ci using the new *in vitro* Ci assay methodology.

Assays were performed for 30 minutes at 37°C in a volume of 100 µL containing 100 mM Mes-NaOH, 10 mM $MnCl_2$, 1 mM ATP, 5 µM CyaB1 and 20 mM NaCl (red squares) or $NaHCO_3$ (triangles; starting pH – clear, final pH – red). (n = 5)

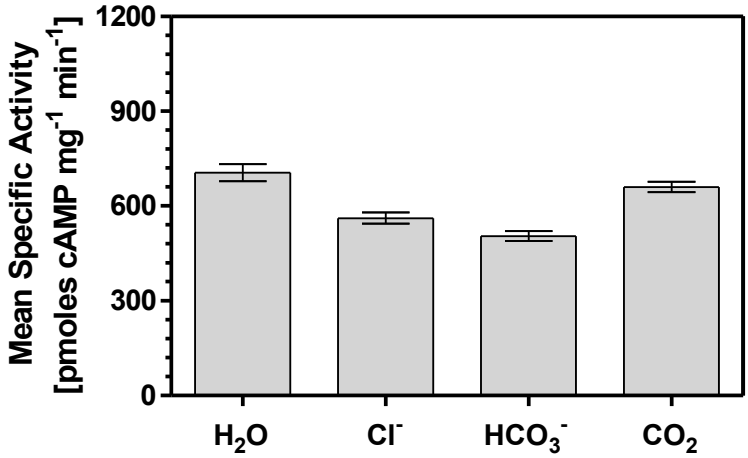

Figure 6.5: Sodium inhibits CyaB1$_{595-859}$ at low temperature.

Assay was performed at 0.4°C for 15 seconds in a total volume of 100 µL in the presence of 100 mM Mes-NaOH pH 6.5, 40 µM CyaB1$_{595-859}$, 1 mM $MnCl_2$, 150 µM ATP and 20 mM NaCl or $NaHCO_3$ or CO_2 or H_2O. (n = 6)

6.5 CyaC from *Spirulina platensis*

Another AC reported to be strongly stimulated by Ci is CyaC from the filamentous cyanobacterium *Spirulina platensis* (Chen *et al.*, 2000; Steegborn *et al.*, 2005b). *In vitro* Ci assays demonstrated a roughly (estimated from graph without numbers) 10 fold stimulation (Ci : H_2O) at pH 7.4; a fold stimulation far greater to that seen with any other enzyme tested by myself (Steegborn *et al.*, 2005b). Due to the magnitude of the stimulation it was unlikely to be due to a pH artefact, however, it was possible that the actual fold stimulation was artificially elevated due to non-specific pH effects caused by Ci increasing the assay pH. Due to this it was decided to re-test CyaC using the new *in vitro* Ci assay methodology to attempt to identify whether this large stimulation was present or whether a small portion was a result of non-specific pH effects.

Recombinant, pure CyaC was obtained (kind gift from Dr. Clemens Steegborn), and was subjected to Ci assays in the presence or absence of Ci using the new *in vitro* Ci assay methodology, at a range of pHs. Before the Ci response could be tested, CyaC was subjected to a pH response assay in the presence or absence of NaCl (Figure 6.6A) to determine how pH effects CyaC activity and whether any effect of sodium was present. It was clearly seen that there was no significant difference in the specific activity of CyaC in the presence or absence of NaCl and the enzyme displayed a response to pH similar to other enzymes tested by myself.

CyaC was subjected to an *in vitro* assay using the new Ci assay methodology at around pH 7.5 in the presence or absence of Ci, using conditions (where appropriate), identical to that of the published work. CyaC was assayed at 37°C for 30 minutes with 10 mM $MgCl_2$ and 5 mM ATP, identical to that done previously, however, the buffer concentration was increased from 50 mM to 100 mM and the salt concentration ($NaHCO_3$ or NaCl) was decreased from 40 mM to 20 mM, to minimise the effects of Ci on assay pH (Figure 6.6B). In contrast to the published work, CyaC, when using these conditions and the new *in vitro* Ci assay methodology, displayed no response to Ci (Chen *et al.*, 2000; Steegborn *et al.*, 2005b).

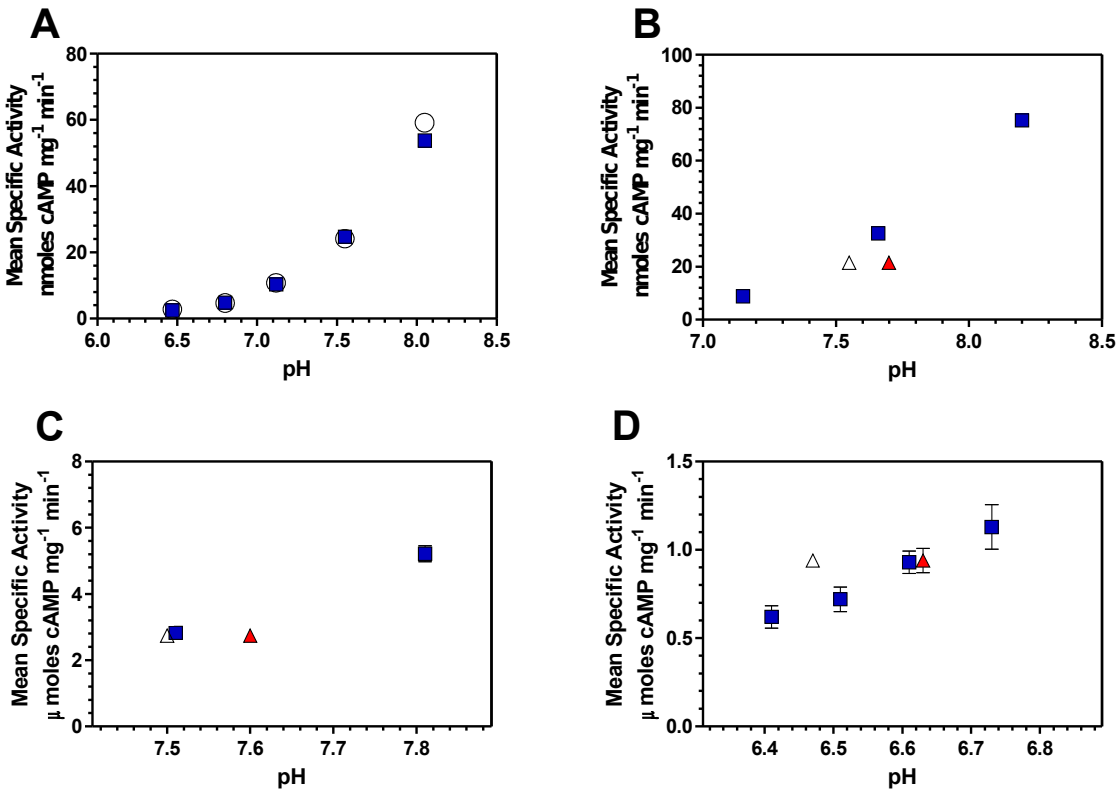

Figure 6.6: CyaC was not activated by Ci using the new *in vitro* Ci assay methodology.

Assays were performed for 30 minutes at 37°C in a volume of 100 µL containing 100 mM buffer (Tris-HCl at pHs ≥ 7.0 and Mes-NaOH at pHs < 7.0) and 20 mM NaCl (blue squares), 20 mM $NaHCO_3$ (triangles; starting pH - clear, final pH - red) or H_2O (clear circles). **(A)** pH response with 10 mM $MgCl_2$, 5 mM ATP and 900 nM CyaC. **(B)** Response to Ci with 10 mM $MgCl_2$, 5 mM ATP and 900 nM CyaC. **(C)** Response to Ci with 2 mM $MnCl_2$, 800 µM ATP and 900 nM CyaC. **(D)** Response to Ci with 2 mM $MnCl_2$, 800 µM ATP and 1.8 µM CyaC. (n > 3)

It was also decided to test the response of this enzyme to Ci in the presence of Mn^{2+} instead of Mg^{2+} at around pH 7.5, and also at pH 6.5 (Figure 6.6C and D). However, despite using these different conditions there was no response to Ci observed.

6.6 Discussion

During pH control experiments carried out whilst investigating T7 RNAP it was discovered that an increase in pH was occurring due to Ci in solution; a pH increase not detected during previous pH control experiments (see Section 4.3). Due to this increase in pH it was necessary to modify the previous *in vitro* Ci assay methodology in order to rule out the possibility that the increase in enzyme activity seen was due to pH and thus prove an effect of Ci. Although the reason why this increase in pH (due to the effects of Ci) was not detected during previous pH control experiments was unknown, this increase in pH was unlikely to be an artefact since it was validated using several different methods. Since all ACs tested by myself showed an increase in activity between pH 6.5 and pH 7.0 (the pH where strong responses to Ci were seen) a re-investigation of their response to Ci was performed due to these pH increases.

The Ci assay performed on $7C_1{\bullet}2C_2$ using the new *in vitro* Ci assay methodology provided evidence in direct contrast to those experiments performed previously (Section 3.4). Previous experimentation demonstrated a 2 fold increase in the activity of $7C_1{\bullet}2C_2$ to Ci at pH 6.5, however, when the new *in vitro* Ci assay methodology was used it was apparent that the response to Ci was likely to be due to non-specific effects of pH. In order to maintain consistency between the earlier and more recent experimentation the assay conditions were kept as consistent as possible, however, the buffer concentration in the recent experiments was increased from 50 to 100 mM in order to more tightly control pH.

At the time of experimentation the question as to whether this new *in vitro* Ci assay methodology was actually capable of detecting a response to Ci was still unanswered. In order to address this problem a control protein known to be responsive to Ci was obtained and tested at the same time as $7C_1{\bullet}2C_2$. The control protein chosen was human sAC_t, and at pH 6.5, under conditions identical to $7C_1{\bullet}2C_2$ it showed a strong response to Ci *in vitro*, whereas there was no response of $7C_1{\bullet}2C_2$. This provided strong evidence to support the notion that the effects of Ci seen previously in $7C_1{\bullet}2C_2$ were in actual fact an artefact of pH. Although this new *in vitro* evidence was compelling, they do not provide any explanation for the Ci response of tmACs seen *in vivo*.

With new evidence showing that $7C_1{\bullet}2C_2$, a class IIIa AC, was not

responsive to Ci it was decided to have a closer look at a class IIIb AC using the new *in vitro* Ci assay methodology. This AC was chosen as CyaB1 from *Anabaena* PCC 7120, due to the ease of obtaining it as a pure recombinant protein. When this was subjected to an *in vitro* Ci response assay under the new methodology the results indicated that at pH 6.5, where a response had previously been seen, there was no response to Ci. Assay conditions were, where appropriate, consistent with previous experiments. Although this *in vitro* assay indicated that this enzyme was not responsive to Ci it did not explain the selective response of this enzyme to CO_2 as opposed to HCO_3^- and Cl^- during low temperature and short time Ci disequilibrium assays. In order to address the response of this enzyme seen during Ci disequilibrium assays it was necessary to repeat this series of experiments. Since these experiments were conducted for 15 seconds only, the effect of Ci on pH was much less of a problem due to the relatively slow speed with which CO_2 degasses from solution. When these Ci disequilibrium assays were repeated with the addition of a control for sodium, the results indicated that the response originally attributed to an effect by CO_2 was possibly due to an inhibition by Na^+. Since the stimulation by CO_2 seen in these experiments was much lower than that seen previously, this experiment must be treated with slight caution and as such does not give full proof that a Ci response was not present (Hammer *et al.*, 2006). However, this experiment does strongly suggest a more lengthy and comprehensive re-evaluation of the responses of such ACs should be undertaken.

The idea that the response of many class IIIb ACs to Ci should be re-tested is further supported by Ci response assays performed on CyaC from *Spirulina platensis*. When the new *in vitro* Ci assay methodology was used to re-test the response of CyaC to Ci, no response was seen. This failure to detect a response to Ci under conditions when a response had previously been seen was surprising (Chen *et al.*, 2000; Steegborn *et al.*, 2005b). Although the response of sAC_t to Ci seen using the new *in vitro* Ci assay methodology gave strong support to the ability of this methodology to actually detect a Ci response, the vast conflict with the result for CyaC with the literature demands caution. Although these experiments using the new *in vitro* Ci assay methodology gave strong support to the notion that some enzymes previously reported to be Ci responsive are in fact non-responsive, the wealth of literature opposing this idea means that absolute proof was still not present. As such, this work indicates that

a fuller re-investigation into the effects of Ci on many ACs is necessary.

7

Final discussion

8.1 Discussion

Evidence suggesting that tmACs are Ci sensitive was obtained from *in vivo* and *in vitro* experiments conducted in Chapter 3. When the endogenous tmACs in HEK 293T cells were stimulated through the β-adrenergic signalling pathway, or with a non-specific tmAC activator (forskolin), the accumulation of cAMP within the cell was affected by the level of CO_2 in the media. It was observed that the levels of accumulated cAMP in HEK 293T cells decreased when the concentration of CO_2 in the media was dropped from normocapnic (5 %) to hypocapnic (0.03 %). However, it was consistently observed that when the CO_2 concentration in the media was increased from normocapnic to hypercapnic (10 %) there was no further increase in the levels of cAMP accumulated within the cell. The effects of CO_2 on a protein downstream of tmACs in the β-adrenergic signalling pathway was also studied; by monitoring phosphorylation status of CREB. It was demonstrated that a decrease in CREB phosphorylation occurred when the media conditions were changed from normocapnic to hypocapnia, however, intriguingly a drop in CREB phosphorylation was also seen when changing from normocapnic to hypercapnic media, although the reason remains unclear. Through the use of a microspectrofluorometric system, and a pH sensitive dye, the effect of CO_2 on pHi were quantified and these shown to be unlikely to have an effect on tmAC activity.

The effects seen between normocapnic and hypocapnic media were consistent with CO_2 stimulating tmAC activity, however, the effects seen between hypercapnic and normocapnic media were not. It might have been expected that the levels of cAMP would increase in the presence of hypercapnic media when compared to normocapnic media. Although the reason for the differences between normocapnic and hypercapnic media is still not clear it is possible to speculate on a few possible reasons. Firstly, it is possible that at 5 % CO_2 in the extracellular medium, the predominant tmAC isoforms in HEK 293T cells reach a maximal stimulation and that a further increase in CO_2 has no effect. Secondly, it is possible that despite pH_i measurements demonstrating that as a whole, the cell stabilises its pH_i following a change in the levels of CO_2, that the tmACs are exposed to a localised change in pH_i at the membrane. If a pH_i change were occurring at the membrane in the presence of 10 % CO_2 it would manifest as an acidification, which would subsequently lower the activity

of tmACs, and as such could mask any possible direct effect of CO_2 on the tmACs. Work by Willoughby *et al.* argues that tmACs are largely protected from pH changes at the membrane, so this possibility is not supported in the literature (Willoughby *et al.*, 2005).

Experiments in Section 3.4, performed *in vitro* on a recombinant 'soluble' tmAC, $7C_1{\bullet}2C_2$, seemed to provide an explanation for the *in vivo* experiments; that Ci was specifically increasing the enzymatic activity of tmAC. The *in vitro* Ci assays indicated that the effects of Ci on $7C_1{\bullet}2C_2$ were mediated through an increase in k_{cat}, brought about through an increased affinity for Mg^{2+}, with no change in E_a or K_m(ATP) observed. Although previous biochemical studies showed an increase in k_{cat}, one study on human sAC showed no alteration in K_m(ATP) (Litvin *et al.*, 2003), whereas the other studies on CyaB1 (*Anabaena* PCC 7120) and Slr1991 (*Synechocystis* PCC 6803) actually showed an increase in K_m(ATP) in the presence of Ci (Cann *et al.*, 2003; Hammer *et al.*, 2006). Although none of these previous biochemical studies addressed the issue of metal affinity, a recent crystallographic study demonstrated that Ci facilitated active site closure and metal recruitment, an observation in support of the kinetic parameters derived in Section 3.4 (Steegborn *et al.*, 2005b). However, all these previous studies were performed on different ACs, and of course it is possible that Ci interacts with different ACs in different ways. What is clear is that the effects of Ci are brought about through increased k_{cat}, which is unlikely to be an effect of reduced substrate affinity.

Although Chapter 3 provided evidence to suggest that tmACs are stimulated by Ci *in vitro*, experiments performed in Sections 4.3 and 6.2 suggested that this stimulation by Ci may be due to a previously undetected pH change. Although *in vitro* pH control experiments carried out prior to the initiation of the *in vitro* biochemical Ci assays on $7C_1{\bullet}2C_2$ suggested that pH was stable, pH control experiments performed in Section 4.3, using slightly different methods, indicated that a previously undetected pH change was occurring during the assay. Although the reason for the discrepancy between the results of the pH control assays in Sections 3.4/4.2 and Section 4.3 is still unclear, the results from Chapter 4 were compelling enough to warrant the design of a new *in vitro* Ci assay methodology. When this new *in vitro* Ci assay methodology, which allows effects of pH to be quantified and ruled out from any possible effect of Ci, was used to re-test the effect of Ci on $7C_1{\bullet}2C_2$, the results

indicated that it was not stimulated by Ci. This finding is consistent with work performed previously on a similar 'soluble' tmAC (Chen *et al.*, 2000), however, it is in contrast to the large stimulation by Ci observed on type III AC (Xie *et al.*, 2006). Although these new *in vitro* assays indicate that $7C_1{\bullet}2C_2$ is not stimulated by Ci, they do not provide an explanation for the effects of Ci seen *in vivo* in HEK 293T cells. The *in vivo* pH control experiments, coupled with the observations of Willoughby *et al.*, indicate that the changes in cAMP accumulation seen between different CO_2 media cannot be explained by pH (Willoughby *et al.*, 2005).

Although the results in Section 6.2 indicate strongly that $7C_1{\bullet}2C_2$ is not regulated by Ci *in vitro*, it is important to stress that this recombinant protein, although it displays very similar biochemical properties to a native tmAC, is not a native tmAC. It is possible that the explanation for the *in vivo* experiments performed in HEK 293T cells is partially correct, in that certain tmACs may be stimulated by Ci. It is entirely possible that Ci binds a site on tmACs that is absent in $7C_1{\bullet}2C_2$, such as the region on the native enzyme which links the C_1 and C_2 domain. Recent experiments investigating the effects of Ci on mammalian receptor GCs have demonstrated that GC-D is regulated by Ci, with the remaining GC isoforms remaining unaffected (Guo *et al.*, 2009; Sun *et al.*, 2009). It is possible that only one (or more) tmAC is regulated by Ci, and as such the change in cAMP levels in response to altered CO_2 in HEK 293T cells was due to specific effects of Ci on a tmAC. However, due to the complexity of cAMP signalling pathways in mammalian cells, several other factors could be contributing to the change in cAMP levels in response to Ci. Although at this stage any explanation would be purely speculative, it is possible that Ci is indirectly influencing tmAC activity by modulating certain ion channels. For example, it is possible that Ci is influencing the levels of intracellular Ca^{2+}, which could be altering tmAC activity through calmodulin. Published experiments have already demonstrated that an increase in Ci is able to cause an increase in intracellular Ca^{2+} in carotid body glomus cells, although the mechanism through which that occurred was not identified (Summers *et al.*, 2002).

Experiments performed in Chapter 4 sought to address the question as to whether proteins containing a palm domain structure were universally regulated by Ci. Following the observation that crystal structures of ACs contained a tertiary structure resembling that found in DNA polymerases, a 'palm' domain, it

was important to test the possible conservation of Ci sensing through the palm domain (Artymiuk *et al.*, 1997). The idea of coupling Ci sensing to the palm domain was compelling, since it would represent an elegant mechanism through which cells could couple the utilisation of nucleotide triphosphates to metabolism; to increase the rate of nucleotide incorporation by polymerases when metabolic rate is high (i.e. a high rate of metabolic CO_2 production being used as a marker for high NTP production). Initial *in vitro* experiments performed on T7 RNA polymerase provided promising evidence to support the notion of the existence of Ci sensitive polymerases. However, due to the magnitude of this initial finding, and the fact that the assay composition was different to the *in vitro* Ci assay conducted in Section 3.4, it was necessary to repeat the *in vitro* pH control experiments to be able to confidently rule out effects of pH on the apparent Ci response. When these pH control assays were repeated, a small pH increase was detected at pH 6.5 during the period of the assay, indicating that there may be a previously undetected pH increase. Due to this pH increase, the methodology of the pH control assay was slightly modified in several ways, and the pH controls were repeated. These pH controls all demonstrated that there was a pH increase of about 0.15 pH units during a 30 minute assay; a pH increase that could account for the apparent stimulation of T7 RNAP by Ci. The reason why this pH change was not detected in pH control experiments in Sections 3.4 and 4.2 is still not clear, but since the pH controls in Section 4.3 were carried out using several different methods, the results from pH controls in Section 4.3 are likely to be correct.

With new *in vitro* pH control experiments indicating that there was a pH increase during the period of *in vitro* Ci assays, efforts were made to prevent this pH increase, however, this was not possible. Due to this pH increase, the original *in vitro* Ci assay was modified to allow this pH increase to be quantified and as such a response to Ci to be tested without potential bias from pH increases. When this new *in vitro* Ci assay methodology was used to re-test the response of T7 RNAP, the results demonstrated that T7 RNAP was unlikely to be regulated by Ci. However, why a small stimulation by Ci was seen at pH 7.0 and 7.5 is unclear, with hindsight it would be wise to test the response of T7 RNAP to Ci at a range of different pHs. Since a response to Ci may not be a conserved feature of all palm domain containing proteins, a second Pol I polymerase was tested; DNA polymerase I from *E. coli*. *In vitro* Ci assays using

this new Ci assay methodology were performed on the Klenow fragment of *E. coli* DNA polymerase I and demonstrated no response to Ci. The response to Ci of DNA polymerase β, a member of the Pol β DNA polymerase family, was also tested using the new in vitro Ci assay methodology and shown not to be responsive to Ci. *In vitro* assays performed on these 3 different polymerases indicate that a response to Ci is unlikely to be a conserved feature of 'palm' domain containing proteins.

In Sections 5.2 and 5.3 the response of mammalian GCs to Ci was tested *in vitro* using the new Ci assay methodology. Mammalian GC-A and GC-E were over-expressed in mammalian cells, however, attempts to over-express other GC isoforms were not successful, and due to the time constraints on the program it was not possible to rectify this. When GC-A and GC-E were subjected to the new *in vitro* Ci assay they were shown to be non-responsive to Ci. Mammalian sGC was also tested using the new *in vitro* Ci assay, and shown to not be regulated by Ci. Work by Sun *et al.* and Guo *et al.*, conducted shortly after experimentation for Sections 5.2 and 5.3 was concluded, provided evidence indicating that while all other mammalian GCs were non-responsive to Ci, GC-D activity was stimulated by Ci (Guo *et al.*, 2009; Sun *et al.*, 2009). This work built upon previous knowledge that rodents are able to sense CO_2 through olfactory receptors in the nose, a sensory response shown to be dependent upon specific GC-D expressing neurons (Hu *et al.*, 2007; Youngentob *et al.*, 1991). It is likely that direct stimulation of GC-D by Ci causes an increase in cGMP levels and initiation of a signalling pathway that culminates in firing of these neurons and as such sensing of Ci.

Although the importance of GCs in the physiology of mammals is indisputable, the presence of GCs in prokaryotes is debatable (Baker and Kelly, 2004). Although cGMP has been detected in cyanobacteria, and genetic of disruption of the *cya2* gene in *Synechocystis* PCC 6803 caused impaired production of cGMP, no prokaryotic enzyme had been proven to be a GC (Herdman and Elmorjani, 1988; Ochoa De Alda *et al.*, 2000). Recently, Rauch *et al.* provided strong crystallographic and *in vitro* biochemical evidence to support the idea that Sll0646 (encoded by *cya2*) from *Synechocystis* PCC 6803 was a GC (Rauch *et al.*, 2008). In Section 5.4 the response of Sll0646 to Ci was tested and it was shown to be non-responsive to Ci, however, the initial *in vitro* biochemical assays on Sll0646 demonstrated a higher AC activity than GC

activity. The initial *in vitro* biochemical assays performed in Section 5.4, carried out on a truncated recombinant protein corresponding to amino acids 424-756 of Sll0646 ($Sll0646_{424-756}$), were in contrast to the published experiments performed on a truncated recombinant protein corresponding to amino acids 434-659 ($Sll0646_{434-659}$) (Rauch *et al.*, 2008). To address this conflict in substrate specificity, a series of *in vitro* biochemical assays were performed on both $Sll0646_{424-756}$ and $Sll0646_{434-659}$. The results from these experiments provided evidence suggesting that Sll0646 was an AC and not a GC, with $Sll0646_{424-756}$ displaying a strong AC activity, whilst the AC activity of $Sll0646_{434-659}$ was lost. It is possible that removal of part of the C-terminus of Sll0646 resulted in the loss of AC activity, however, at this stage this is purely speculative.

Following the identification of a previously undetected pH increase during *in vitro* Ci assays, and subsequent design of a new *in vitro* Ci assay methodology, it was decided to re-test certain Class IIIb ACs. A response to Ci was previously proposed to be a feature conserved in Class IIIb ACs, however, since many of these ACs display a pH profile that make them susceptible to the effects of an assay pH increase biasing a potential Ci response, it was necessary to confirm their Ci responsiveness using the new *in vitro* Ci assay methodology (Cann *et al.*, 2003). Three Class IIIb ACs were re-tested using this new *in vitro* Ci assay methodology, and the results indicated that it was possible that two of these ACs were not Ci responsive. The first AC, sAC_t from *Homo sapiens*, was confirmed to be Ci sensitive at pH 6.5. The second AC, CyaB1 from *Anabaena* PCC 7120, was also tested at pH 6.5, however, in this case was shown to be non-responsive to Ci. Interestingly, even when the effects of pH on the assay were ignored, CyaB1 did not appear to be Ci responsive. The final AC tested was CyaC from *Spirulina platensis*, which was tested *in vitro* at pH 6.5 and pH 7.5, and shown to be non-responsive to Ci.

Although the *in vitro* Ci assays performed on two Class IIIb ACs in Chapter 6 provide evidence to support the idea that certain Class IIIb ACs are not Ci responsive, these experiments are by no means conclusive. The result obtained for CyaC was particularly surprising given that previous studies had shown a fold stimulation (Ci : basal) ranging from 2 to 25 fold (numbers estimated from published figures) (Chen *et al.*, 2000; Steegborn *et al.*, 2005b). The difference in the size of stimulation by Ci observed in experiments performed by Chen *et al.* and Steegborn *et al.* could be explained by differences

in assay composition, since Chen *et al.* included 100 µM ATP and 5 mM Mn^{2+}, whereas Steegborn *et al.* included 5 mM ATP and 10 mM Mg^{2+} (Chen *et al.*, 2000; Steegborn *et al.*, 2005b). Experiments performed by Chen *et al.* demonstrated a roughly 2 fold stimulation of CyaC activity by Ci, at pH 7.5 in the presence of 40 mM total Ci, whereas an assay performed under similar conditions in section 6.5 showed no response (Chen *et al.*, 2000). More recent experiments conducted by Steegborn *et al.* demonstrated a roughly 25 fold stimulation of CyaC activity by Ci, at pH 7.5 in the presence of 40 mM total Ci, whereas an assay performed under similar conditions in Section 6.5 showed no stimulation by Ci (Steegborn *et al.*, 2005b). Experiments performed in section 6.5 used either 5 mM ATP and 10 mM Mg^{2+} or 800 µM ATP and 5 mM Mn^{2+}, however, they used a lower concentration of 20 mM total Ci. Although the possibility exists that this reduced concentration of Ci was responsible for the lack of stimulation seen, work performed by Chen *et al.* would argue against it, since their Ci dose response assay demonstrated a roughly 1.7 fold stimulation of CyaC by 20 mM total Ci (Chen *et al.*, 2000).

When the effects of Ci on assay pH identified in Chapter 4 are taken into account, it is possible to provide an explanation for the stimulation of CyaC by Ci observed by Chen *et al.*, however, an increase in assay pH can in no way account for the stimulation of CyaC by Ci observed by Steegborn *et al.* Although the results obtained in Chapter 6 are compelling, due to the fact that non-specific pH effects cannot explain the stimulation observed by Steegborn *et al.*, they only really emphasise the need for a more thorough re-investigation of the response of Class IIIb ACs to Ci.

7.2 Future work

Due to time constraints on the program there are several outstanding follow-up experiments that need to be conducted.

1. The effect of Ci on the production of cAMP by the endogenous tmACs in HEK 293T cells, seen in Chapter 3, should be addressed. Experiments performed in Chapter 6 indicate that $7C_1 \bullet 2C_2$ might not be regulated by Ci, and as such, tmACs in general might not be regulated by Ci. If the direct actions of Ci on tmAC are not the cause of the changes in cAMP production seen then how is Ci regulating the production of cAMP in HEK 293T cells?

- Although $7C_1 \bullet 2C_2$ might not be regulated by Ci, it is possible that one or more individual mammalian tmACs are, and future investigation should test this first. This could be achieved through over-expressing each individual tmAC in mammalian cells, and subjecting membrane preparations derived from these cells to an *in vitro* Ci assay.

- If no tmAC isoform is found to be Ci responsive it would be necessary to investigate the possible effects of Ci on signalling pathways that are capable of modulating tmAC activity. Since many diverse signalling pathways involve tmACs, this would be a lengthy investigation, however, since previous work has implicated Ca^{2+} as being involved in Ci sensing, investigating the effect of Ci on Ca^{2+} channels first would be logical.
    - It would be necessary to identify any possible changes in intracellular Ca^{2+} concentrations in response to variable Ci. This could be achieved using a method similar to that used to quantify intracellular pH, whereby a cell monolayer would be perfused with various CO_2 solutions and a fluorescent Ca^{2+} indicator used to quantify intracellular Ca^{2+} concentration.
    - If a change in intracellular Ca^{2+} was detected, it would be necessary to identify the Ca^{2+} channel responsible for this change. This would be achieved by repeating cAMP accumulation assays on HEK 293T cells in the presence of inhibitors specific for certain individual ion

channels.

- If changes in intracellular ion concentrations were not shown to be responsible for the effect of Ci on the production of cAMP, then other signalling pathways would need to be investigated. This would be performed by repeating cAMP accumulation assays with the addition of inhibitors specific for individual signalling enzymes.

2. Although experiments conducted in Chapter 5 indicate that Sll0646 may be an AC and not a GC, the results are not definitive, and further experimentation is required. Is Sll0646 an AC or GC?

- In order to conclusively address this question, the AC and GC activity of the full-length native protein would be tested. Since expression of the full-length protein in *E. coli* and HEK 293T cells failed, it would be necessary to attempt expression in a baculovirus system, and also to re-attempt expression in *E. coli* and HEK 293T cells using different expression constructs. Once active full-length Sll0646 was obtained, it would be subjected to *in vitro* biochemical assays where the AC and GC activity would be analysed.

3. Although experiments in Chapter 6 provide strong evidence that indicates that certain class IIIb ACs, which are currently thought to be Ci regulated, are not regulated by Ci, this issue is far from settled. Is the assumption that Class IIIb ACs are universally regulated by Ci correct?

- The response of many Ci responsive Class IIIb ACs to Ci needs to be re-tested using methodologies that allow the effects of pH to be confidently removed from a Ci response. This could be done using the newly devised *in vitro* Ci assay developed within this report, or alternatively using a more complex method. Ideally, the response of ACs to Ci would be tested using a system whereby the levels of Ci in the assay and assay pH could be kept constant, and this could be achieved in 2 ways.
  - Firstly, the assays could be conducted in a sealed box. The concentration of CO_2 in this box would be maintained at a certain concentration designed to prevent the loss of CO_2 from the assay mix,

and as such the enzyme tested would be exposed to a constant Ci concentration, and pH during the period of the assay.

- Secondly, and more ideally, a more elaborate method (Figure 7.1) could be employed to test the response of an enzyme to Ci in real time. A sealed chamber containing a CO_2 electrode would be filled with an assay mix containing enzyme, buffer, cofactor, and a pH sensitive fluorescent dye (e.g. BCECF). Into this cell would be introduced a Ci solution, and the assay would be initiated by the addition of a fluorescent substrate-conjugate (e.g. BODIPY-ATP). The concentration of Ci within the assay would be quantified by the CO_2 electrode, the pH of the solution would be quantified by a fluorometric system quantifying the emission of the pH sensitive dye, and enzyme velocity would be quantified by the emission from the fluorescent product-conjugate (e.g. BODIPY-cAMP).

- If many Ci responsive Class IIIb ACs are shown to be non-responsive to Ci, then attention would be turned towards those Class IIIb ACs that are shown to be Ci responsive. These definitively Ci regulated Class IIIb ACs would be subjected to a full crystallographic, mutational, and biochemical analysis in order to identify the mechanism through which Ci acts on these ACs.
  - The response of an AC to Ci would be tested biochemically to determine what effects (if any) Ci had upon K_m(ATP), K_m(metal), k_{cat}, V_{max} and E_a.
  - It would also be necessary to crystallise a Ci responsive AC in the presence of Ci, in order to identify the amino acids involved in co-ordinating Ci. This would be performed by either exposing AC crystals to HCO_3^- or by exposing frozen AC crystals to CO_2. If amino acids involved in Ci binding were identified then these amino acids would be mutated, and mutant enzymes tested for a response to Ci to confirm a role for these amino acids in Ci binding.

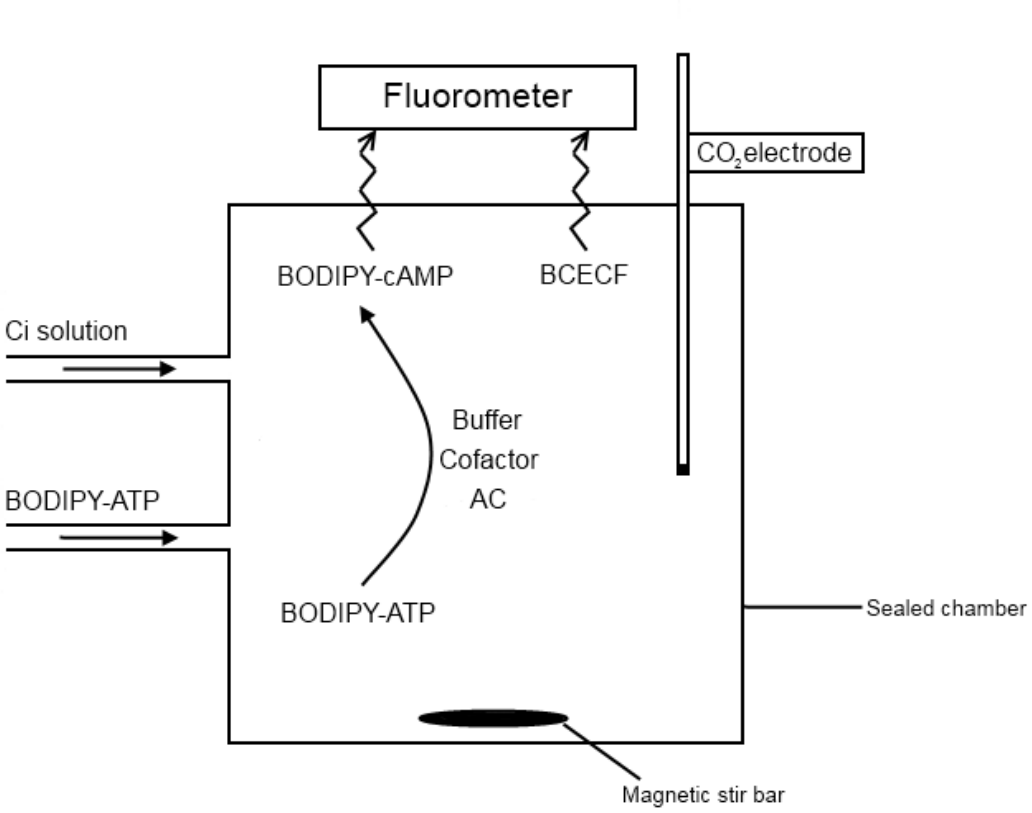

Figure 7.1: Improved *in vitro* Ci assay.

8

Bibliography

8.1 Publications arising from this thesis.

Stimulation of Mammalian G-protein-responsive Adenylyl Cyclases by Carbon Dioxide

Philip D. Townsend, Phillip M. Holliday, Stepan Fenyk, Kenneth C. Hess, Michael A. Gray, David R. W. Hodgson, and Martin J. Cann

J Biol Chem. 2009 January 9; 284(2): 784–791.

Carbon dioxide is fundamental to the physiology of all organisms. There is considerable interest in the precise molecular mechanisms that organisms use to directly sense CO_2. Here we demonstrate that a mammalian recombinant G-protein-activated adenylyl cyclase and the related Rv1625c adenylyl cyclase of *Mycobacterium tuberculosis* are specifically stimulated by CO_2. Stimulation occurred at physiological concentrations of CO_2 through increased k_{cat}. CO_2 increased the affinity of enzyme for metal co-factor, but contact with metal was not necessary as CO_2 interacted directly with apoenzyme. CO_2 stimulated the activity of both G-protein-regulated adenylyl cyclases and Rv1625c *in vivo*. Activation of G-protein regulated adenylyl cyclases by CO_2 gave a corresponding increase in cAMP-response element-binding protein (CREB) phosphorylation. Comparison of the responses of the G-protein regulated adenylyl cyclases and the molecularly, and biochemically distinct mammalian soluble adenylyl cyclase revealed that whereas G-protein-regulated enzymes are responsive to CO_2, the soluble adenylyl cyclase is responsive to both CO_2 and bicarbonate ion. We have, thus, identified a signalling enzyme by which eukaryotes can directly detect and respond to fluctuating CO_2.

8.2 References

Adrogue, H.E., and Adrogue, H.J. (2001). Acid-base physiology. Respir Care *46*, 328-341.

Artymiuk, P.J., Poirrette, A.R., Rice, D.W., and Willett, P. (1997). A polymerase I palm in adenylyl cyclase? Nature *388*, 33-34.

Badger, M.R., and Price, G.D. (1994). The role of carbonic anhydrase in photosynthesis. Annu Rev Plant Physiol Plant Mol Biol *45*, 369-392.

Badre, N.H., Martin, M.E., and Cooper, R.L. (2005). The physiological and behavioral effects of carbon dioxide on *Drosophila melanogaster* larvae. Comp Biochem Physiol A Mol Integr Physiol *140*, 363-376.

Bahn, Y.S., Cox, G.M., Perfect, J.R., and Heitman, J. (2005). Carbonic anhydrase and CO_2 sensing during *Cryptococcus neoformans* growth, differentiation, and virulence. Curr Biol *15*, 2013-2020.

Bakalyar, H.A., and Reed, R.R. (1990). Identification of a specialized adenylyl cyclase that may mediate odorant detection. Science *250*, 1403-1406.

Baker, D.A., and Kelly, J.M. (2004). Structure, function and evolution of microbial adenylyl and guanylyl cyclases. Mol Microbiol *52*, 1229-1242.

Beerling, D.J., Lomax, B.H., Royer, D.L., Upchurch, G.R., Jr., and Kump, L.R. (2002). An atmospheric pCO_2 reconstruction across the Cretaceous-Tertiary boundary from leaf megafossils. Proc Natl Acad Sci U S A *99*, 7836-7840.

Beese, L.S., Derbyshire, V., and Steitz, T.A. (1993). Structure of DNA polymerase I Klenow fragment bound to duplex DNA. Science *260*, 352-355.

Berndt, T.J., and Knox, F.G. (1985). Nephron site of resistance to phosphaturic effect of PTH during respiratory alkalosis. Am J Physiol *249*, F919-922.

Bernklau, E.a.B., LB (1998). Reinvestigation of Host Location by Western Corn Rootwonn Larvae (Coleoptera: *Chrysomelidae*): CO_2 Is the Only Volatile Attractant. J Econ Entomol *91*, 1331-1340.

Bernklau, E.J., Fromm, E.A., and Bjostad, L.B. (2004). Disruption of host location of western corn rootworm larvae (Coleoptera: *Chrysomelidae*) with carbon dioxide. J Econ Entomol *97*, 330-339.

Bernklau, E.J., Fromm, E.A., Judd, T.M., and Bjostad, L.B. (2005). Attraction of subterranean termites (Isoptera) to carbon dioxide. J Econ Entomol *98*, 476-484.

Boron, W.F. (2004). Regulation of intracellular pH. Adv Physiol Educ *28*, 160-179.

Bowen, M.F. (1991). The sensory physiology of host-seeking behaviour in mosquitoes. Annu Rev Entomol *36*, 139-158.

Braun, T., and Dods, R.F. (1975). Development of a Mn^{2+}-sensitive, "soluble" adenylate cyclase in rat testis. Proc Natl Acad Sci U S A *72*, 1097-1101.

Braun, T., Frank, H., Dods, R., and Sepsenwol, S. (1977). Mn^{2+}-sensitive, soluble adenylate cyclase in rat testis. Differentiation from other testicular nucleotide cyclases. Biochim Biophys Acta *481*, 227-235.

Brazeau, P., and Gilman, A. (1953). Effect of plasma CO_2 tension on renal tubular reabsorption of bicarbonate. Am J Physiol *175*, 33-38.

Breitbart, H., and Naor, Z. (1999). Protein kinases in mammalian sperm capacitation and the acrosome reaction. Rev Reprod *4*, 151-159.

Breton, S., Hammar, K., Smith, P.J., and Brown, D. (1998). Proton secretion in the male

reproductive tract: involvement of Cl^--independent HCO_3^- transport. Am J Physiol *275*, C1134-1142.

Breton, S., Nsumu, N.N., Galli, T., Sabolic, I., Smith, P.J., and Brown, D. (2000). Tetanus toxin-mediated cleavage of cellubrevin inhibits proton secretion in the male reproductive tract. Am J Physiol Renal Physiol *278*, F717-725.

Breton, S., Smith, P.J., Lui, B., and Brown, D. (1996). Acidification of the male reproductive tract by a proton pumping (H^+)-ATPase. Nat Med *2*, 470-472.

Bretscher, A.J., Busch, K.E., and de Bono, M. (2008). A carbon dioxide avoidance behavior is integrated with responses to ambient oxygen and food in *Caenorhabditis elegans*. Proc Natl Acad Sci U S A *105*, 8044-8049.

Briva, A., Vadasz, I., Lecuona, E., Welch, L.C., Chen, J., Dada, L.A., Trejo, H.E., Dumasius, V., Azzam, Z.S., Myrianthefs, P.M.*, et al.* (2007). High CO_2 levels impair alveolar epithelial function independently of pH. PLoS One *2*, e1238.

Brown, D., and Breton, S. (2000). H(+)V-ATPase-dependent luminal acidification in the kidney collecting duct and the epididymis/vas deferens: vesicle recycling and transcytotic pathways. J Exp Biol *203*, 137-145.

Buck, J., Sinclair, M.L., Schapal, L., Cann, M.J., and Levin, L.R. (1999). Cytosolic adenylyl cyclase defines a unique signaling molecule in mammals. Proc Natl Acad Sci U S A *96*, 79-84.

Bundey, R.A., and Insel, P.A. (2004). Discrete intracellular signalling domains of soluble adenylyl cyclase: camps of cAMP? Sci STKE *2004*, pe19.

Burkett, D.A., Lee, W.J., Lee, K.W., Kim, H.C., Lee, H.I., Lee, J.S., Shin, E.H., Wirtz, R.A., Cho, H.W., Claborn, D.M.*, et al.* (2001). Light, carbon dioxide, and octenol-baited mosquito trap and host-seeking activity evaluations for mosquitoes in a malarious area of the Republic of Korea. J Am Mosq Control Assoc *17*, 196-205.

Cali, J.J., Zwaagstra, J.C., Mons, N., Cooper, D.M., and Krupinski, J. (1994). Type VIII adenylyl cyclase. A Ca^{2+}/calmodulin-stimulated enzyme expressed in discrete regions of rat brain. J Biol Chem *269*, 12190-12195.

Campbell, N.A. (1996). Biology, 4th ed. edn (Menlo Park, Calif. ; Wokingham, Benjamin/Cummings).

Cann, M. (2004). Bicarbonate stimulated adenylyl cyclases. IUBMB Life *56*, 529-534.

Cann, M.J., Hammer, A., Zhou, J., and Kanacher, T. (2003). A defined subset of adenylyl cyclases is regulated by bicarbonate ion. J Biol Chem *278*, 35033-35038.

Casson, S.A., and Hetherington, A.M. (2010). Environmental regulation of stomatal development. Curr Opin Plant Biol *13*, 90-95.

Chaloupka, J.A., Bullock, S.A., Iourgenko, V., Levin, L.R., and Buck, J. (2006). Autoinhibitory regulation of soluble adenylyl cyclase. Mol Reprod Dev *73*, 361-368.

Chandrashekar, J., Yarmolinsky, D., von Buchholtz, L., Oka, Y., Sly, W., Ryba, N.J., and Zuker, C.S. (2009). The taste of carbonation. Science *326*, 443-445.

Chen, Y., Cann, M.J., Litvin, T.N., Iourgenko, V., Sinclair, M.L., Levin, L.R., and Buck, J. (2000). Soluble adenylyl cyclase as an evolutionarily conserved bicarbonate sensor. Science *289*, 625-628.

Cooper, D.M. (2003a). Molecular and cellular requirements for the regulation of adenylate cyclases by calcium. Biochem Soc Trans *31*, 912-915.

Cooper, D.M. (2003b). Regulation and organization of adenylyl cyclases and cAMP. Biochem J *375*, 517-529.

Cooperband, M.F., and Carde, R.T. (2006a). Comparison of plume structures of carbon dioxide emitted from different mosquito traps. Med Vet Entomol *20*, 1-10.

Cooperband, M.F., and Carde, R.T. (2006b). Orientation of *Culex* mosquitoes to carbon dioxide-baited traps: flight manoeuvres and trapping efficiency. Med Vet Entomol *20*, 11-26.

Cotelesage, J.J., Puttick, J., Goldie, H., Rajabi, B., Novakovski, B., and Delbaere, L.T. (2007). How does an enzyme recognize CO_2? Int J Biochem Cell Biol *39*, 1204-1210.

Cotta, M.A., Whitehead, T.R., and Wheeler, M.B. (1998). Identification of a novel adenylate cyclase in the ruminal anaerobe, *Prevotella ruminicola* D31d. FEMS Microbiol Lett *164*, 257-260.

Coudart-Cavalli, M.P., Sismeiro, O., and Danchin, A. (1997). Bifunctional structure of two adenylyl cyclases from the myxobacterium *Stigmatella aurantiaca*. Biochimie *79*, 757-767.

Cundari, T.R., Wilson, A.K., Drummond, M.L., Gonzalez, H.E., Jorgensen, K.R., Payne, S., Braunfeld, J., De Jesus, M., and Johnson, V.M. (2009). CO_2-formatics: how do proteins bind carbon dioxide? J Chem Inf Model *49*, 2111-2115.

Danchin, A. (1993). Phylogeny of adenylyl cyclases. Adv Second Messenger Phosphoprotein Res *27*, 109-162.

Daristotle, L., Berssenbrugge, A.D., Engwall, M.J., and Bisgard, G.E. (1990). The effects of carotid body hypocapnia on ventilation in goats. Respir Physiol *79*, 123-135.

de Bruyne, M., Foster, K., and Carlson, J.R. (2001). Odor coding in the Drosophila antenna. Neuron *30*, 537-552.

Defer, N., Best-Belpomme, M., and Hanoune, J. (2000). Tissue specificity and physiological relevance of various isoforms of adenylyl cyclase. Am J Physiol Renal Physiol *279*, F400-416.

Dekker, T., Geier, M., and Carde, R.T. (2005). Carbon dioxide instantly sensitizes female yellow fever mosquitoes to human skin odours. J Exp Biol *208*, 2963-2972.

Dessirier, J.M., Simons, C.T., O'Mahony, M., and Carstens, E. (2001). The oral sensation of carbonated water: cross-desensitization by capsaicin and potentiation by amiloride. Chem Senses *26*, 639-643.

Domsic, J.F., Avvaru, B.S., Kim, C.U., Gruner, S.M., Agbandje-McKenna, M., Silverman, D.N., and McKenna, R. (2008). Entrapment of carbon dioxide in the active site of carbonic anhydrase II. J Biol Chem *283*, 30766-30771.

Dorland, W.A.N. (2003). Dorland's illustrated medical dictionary, 30th ed. edn (Philadelphia, Pa. ; London, Saunders).

Drum, C.L., Yan, S.Z., Bard, J., Shen, Y.Q., Lu, D., Soelaiman, S., Grabarek, Z., Bohm, A., and Tang, W.J. (2002). Structural basis for the activation of anthrax adenylyl cyclase exotoxin by calmodulin. Nature *415*, 396-402.

Drummond, M.L., Wilson, A.K., and Cundari, T.R. (2010). Towards greener carbon capture technologies: A pharmacophore-based approach to predict CO_2 binding sites in proteins. Energy Fuels *24*, 1464-1470.

Dunn, J.J., and Studier, F.W. (1983). Complete nucleotide sequence of bacteriophage T7 DNA and the locations of T7 genetic elements. J Mol Biol *166*, 477-535.

Dusenbery, D.B. (1974). Analysis of chemotaxis in the nematode *Caenorhabditis elegans* by countercurrent separation. J Exp Zool *188*, 41-47.

Epstein, S.K., and Singh, N. (2001). Respiratory acidosis. Respir Care *46*, 366-383.

Esposito, G., Jaiswal, B.S., Xie, F., Krajnc-Franken, M.A., Robben, T.J., Strik, A.M., Kuil, C., Philipsen, R.L., van Duin, M., Conti, M.*, et al.* (2004). Mice deficient for soluble adenylyl cyclase are infertile because of a severe sperm-motility defect. Proc Natl Acad Sci U S A *101*, 2993-2998.

Farrell, J., Ramos, L., Tresguerres, M., Kamenetsky, M., Levin, L.R., and Buck, J. (2008). Somatic 'soluble' adenylyl cyclase isoforms are unaffected in Sacy ^{tm1Lex}/Sacy ^{tm1Lex} 'knockout' mice. PLoS One *3*, e3251.

Faucher, C., Forstreuter, M., Hilker, M., and de Bruyne, M. (2006). Behavioral responses of *Drosophila* to biogenic levels of carbon dioxide depend on life-stage, sex and olfactory context. J Exp Biol *209*, 2739-2748.

Feinstein, P.G., Schrader, K.A., Bakalyar, H.A., Tang, W.J., Krupinski, J., Gilman, A.G., and Reed, R.R. (1991). Molecular cloning and characterization of a Ca^{2+}/calmodulin-insensitive adenylyl cyclase from rat brain. Proc Natl Acad Sci U S A *88*, 10173-10177.

Feng, Q., Zhang, Y., Li, Y., Liu, Z., Zuo, J., and Fang, F. (2006). Two domains are critical for the nuclear localization of soluble adenylyl cyclase. Biochimie *88*, 319-328.

Feng, Q.P., Zuo, J., Meng, Y., and Fang, F.D. (2005). [Nuclear localization region in soluble adenylyl cyclase]. Zhongguo Yi Xue Ke Xue Yuan Xue Bao *27*, 280-284.

Fischler, W., Kong, P., Marella, S., and Scott, K. (2007). The detection of carbonation by the *Drosophila* gustatory system. Nature *448*, 1054-1057.

Foster, G.T., Vaziri, N.D., and Sassoon, C.S. (2001). Respiratory alkalosis. Respir Care *46*, 384-391.

Franko, D., and Wetzel, R. (1981). Dynamics of cellular and extracellular cAMP in *Anabaena flos-aquae* (Cyanophyta): Intrinsic culture variability and correlation with metabolic variables. J Phycol *17*, 129-134.

Franks, P.J., and Beerling, D.J. (2009). Maximum leaf conductance driven by CO_2 effects on stomatal size and density over geologic time. Proc Natl Acad Sci U S A *106*, 10343-10347.

Fulle, H.J., Vassar, R., Foster, D.C., Yang, R.B., Axel, R., and Garbers, D.L. (1995). A receptor guanylyl cyclase expressed specifically in olfactory sensory neurons. Proc Natl Acad Sci U S A *92*, 3571-3575.

Gao, B.N., and Gilman, A.G. (1991). Cloning and expression of a widely distributed (type IV) adenylyl cyclase. Proc Natl Acad Sci U S A *88*, 10178-10182.

Gao, Q., Yuan, B., and Chess, A. (2000). Convergent projections of *Drosophila* olfactory neurons to specific glomeruli in the antennal lobe. Nat Neurosci *3*, 780-785.

Garbers, D.L., Chrisman, T.D., Wiegn, P., Katafuchi, T., Albanesi, J.P., Bielinski, V., Barylko, B., Redfield, M.M., and Burnett, J.C., Jr. (2006). Membrane guanylyl cyclase receptors: an update. Trends Endocrinol Metab *17*, 251-258.

Gillies, M.T. (1980). The role of carbon dioxide in host-finding by mosquitoes (Diptera, *Culicidae*): a review. Bull Entomol Res *70*, 525-532.

Gilman, A., and Brazeau, P. (1953). Role of the kidney in the regulation of acid-base metabolism. Am J Med *15*, 765-770.

Giordano, M., Beardall, J., and Raven, J.A. (2005). CO_2 concentrating mechanisms in algae: mechanisms, environmental modulation, and evolution. Annu Rev Plant Biol *56*, 99-131.

Gloe, A., and Risch, N. (1978). Bacteriochlorophyll *cs*, a new bacteriochlorophyll from *Chloroflexus aurantiacus*. Arch Microbiol *118*, 153-156.

Gluck, S.L., Lee, B.S., Wang, S.P., Underhill, D., Nemoto, J., and Holliday, L.S. (1998). Plasma membrane V-ATPases in proton-transporting cells of the mammalian kidney and osteoclast. Acta Physiol Scand Suppl *643*, 203-212.

Golemi, D., Maveyraud, L., Vakulenko, S., Samama, J.P., and Mobashery, S. (2001). Critical involvement of a carbamylated lysine in catalytic function of class D beta-lactamases. Proc Natl Acad Sci U S A *98*, 14280-14285.

Gonzalez, C., Almaraz, L., Obeso, A., and Rigual, R. (1994). Carotid body chemoreceptors: from natural stimuli to sensory discharges. Physiol Rev *74*, 829-898.

Gonzalez, G.A., and Montminy, M.R. (1989). Cyclic AMP stimulates somatostatin gene transcription by phosphorylation of CREB at serine 133. Cell *59*, 675-680.

Graber, M., and Kelleher, S. (1988). Side effects of acetazolamide: the champagne blues. Am J Med *84*, 979-980.

Granger, D.L., Perfect, J.R., and Durack, D.T. (1985). Virulence of *Cryptococcus neoformans*. Regulation of capsule synthesis by carbon dioxide. J Clin Invest *76*, 508-516.

Gray, J.E., Holroyd, G.H., van der Lee, F.M., Bahrami, A.R., Sijmons, P.C., Woodward, F.I., Schuch, W., and Hetherington, A.M. (2000). The HIC signalling pathway links CO_2 perception to stomatal development. Nature *408*, 713-716.

Guerenstein, P.G., Christensen, T.A., and Hildebrand, J.G. (2004a). Sensory processing of ambient CO_2 information in the brain of the moth Manduca sexta. J Comp Physiol A Neuroethol Sens Neural Behav Physiol *190*, 707-725.

Guerenstein, P.G., E, A.Y., Van Haren, J., Williams, D.G., and Hildebrand, J.G. (2004b). Floral CO(2) emission may indicate food abundance to nectar-feeding moths. Naturwissenschaften *91*, 329-333.

Guo, D., Zhang, J.J., and Huang, X.Y. (2009). Stimulation of guanylyl cyclase-D by bicarbonate. Biochemistry *48*, 4417-4422.

Hallem, E.A., and Sternberg, P.W. (2008). Acute carbon dioxide avoidance in *Caenorhabditis elegans*. Proc Natl Acad Sci U S A *105*, 8038-8043.

Hallows, K.R., Wang, H., Edinger, R.S., Butterworth, M.B., Oyster, N.M., Li, H., Buck, J., Levin, L.R., Johnson, J.P., and Pastor-Soler, N.M. (2009). Regulation of epithelial Na^+ transport by soluble adenylyl cyclase in kidney collecting duct cells. J Biol Chem *284*, 5774-5783.

Hammer, A., Hodgson, D.R., and Cann, M.J. (2006). Regulation of prokaryotic adenylyl cyclases by CO_2. Biochem J *396*, 215-218.

Hardman, J.G., and Sutherland, E.W. (1969). Guanyl cyclase, an enzyme catalyzing the formation of guanosine 3',5'-monophosphate from guanosine trihosphate. J Biol Chem *244*, 6363-6370.

Hartzell, H.C. (1988). Regulation of cardiac ion channels by catecholamines, acetylcholine and second messenger systems. Prog Biophys Mol Biol *52*, 165-247.

Hashimoto, M., Negi, J., Young, J., Israelsson, M., Schroeder, J.I., and Iba, K. (2006). *Arabidopsis* HT1 kinase controls stomatal movements in response to CO_2. Nat Cell Biol *8*, 391-397.

Hatley, M.E., Gilman, A.G., and Sunahara, R.K. (2002). Expression, purification, and assay of cytosolic (catalytic) domains of membrane-bound mammalian adenylyl cyclases. Methods Enzymol *345*, 127-140.

He, B., Rong, M., Lyakhov, D., Gartenstein, H., Diaz, G., Castagna, R., McAllister, W.T., and Durbin, R.K. (1997). Rapid mutagenesis and purification of phage RNA polymerases. Protein Expr Purif *9*, 142-151.

Healy, T.P., and Copland, M.J. (1995). Activation of *Anopheles gambiae* mosquitoes by carbon dioxide and human breath. Med Vet Entomol *9*, 331-336.

Hegyi, P., Rakonczay, Z., Jr., Gray, M.A., and Argent, B.E. (2004). Measurement of intracellular pH in pancreatic duct cells: a new method for calibrating the fluorescence data. Pancreas *28*, 427-434.

Helenius, I.T., Krupinski, T., Turnbull, D.W., Gruenbaum, Y., Silverman, N., Johnson, E.A., Sporn, P.H., Sznajder, J.I., and Beitel, G.J. (2009). Elevated CO_2 suppresses

specific *Drosophila* innate immune responses and resistance to bacterial infection. Proc Natl Acad Sci U S A *106*, 18710-18715.

Herdman, M., and Elmorjani, K. (1988). Cyclic nucleotides. Methods in Enzymology *167*, 584-591.

Hess, K.C., Jones, B.H., Marquez, B., Chen, Y., Ord, T.S., Kamenetsky, M., Miyamoto, C., Zippin, J.H., Kopf, G.S., Suarez, S.S.*, et al.* (2005). The "soluble" adenylyl cyclase in sperm mediates multiple signalling events required for fertilization. Dev Cell *9*, 249-259.

Hetherington, A.M., and Raven, J.A. (2005). The biology of carbon dioxide. Curr Biol *15*, R406-410.

Holm, L., and Sander, C. (1995). DNA polymerase beta belongs to an ancient nucleotidyltransferase superfamily. Trends Biochem Sci *20*, 345-347.

Hoppe, A., Metler, M., Berndt, T.J., Knox, F.G., and Angielski, S. (1982). Effect of respiratory alkalosis on renal phosphate excretion. Am J Physiol *243*, F471-475.

Hoppe, A., Rybczynska, A., Knox, F.G., and Angielski, S. (1988). Beta-receptors in resistance to phosphaturic effect of PTH in respiratory alkalosis. Am J Physiol *255*, R557-562.

Hu, H., Boisson-Dernier, A., Israelsson-Nordstrom, M., Bohmer, M., Xue, S., Ries, A., Godoski, J., Kuhn, J.M., and Schroeder, J.I. (2010). Carbonic anhydrases are upstream regulators of CO_2-controlled stomatal movements in guard cells. Nat Cell Biol *12*, 87-93; sup pp 81-18.

Hu, J., Zhong, C., Ding, C., Chi, Q., Walz, A., Mombaerts, P., Matsunami, H., and Luo, M. (2007). Detection of near-atmospheric concentrations of CO2 by an olfactory subsystem in the mouse. Science *317*, 953-957.

Ishikawa, Y., Katsushika, S., Chen, L., Halnon, N.J., Kawabe, J., and Homcy, C.J. (1992). Isolation and characterization of a novel cardiac adenylyl cyclase cDNA. J Biol Chem *267*, 13553-13557.

Ito, J., and Braithwaite, D.K. (1991). Compilation and alignment of DNA polymerase sequences. Nucleic Acids Res *19*, 4045-4057.

Jaiswal, B.S., and Conti, M. (2001). Identification and functional analysis of splice variants of the germ cell soluble adenylyl cyclase. J Biol Chem *276*, 31698-31708.

Jelamskii, S., Sun, X.C., Herse, P., and Bonanno, J.A. (2000). Basolateral $Na^{(+)}$-$K^{(+)}$-$2Cl^{(-)}$ cotransport in cultured and fresh bovine corneal endothelium. Invest Ophthalmol Vis Sci *41*, 488-495.

Jiang, C., Rojas, A., Wang, R., and Wang, X. (2005). CO_2 central chemosensitivity: why are there so many sensing molecules? Respir Physiol Neurobiol *145*, 115-126.

Jones, W.D., Cayirlioglu, P., Kadow, I.G., and Vosshall, L.B. (2007). Two chemosensory receptors together mediate carbon dioxide detection in *Drosophila*. Nature *445*, 86-90.

Joyce, C.M., and Derbyshire, V. (1995). Purification of *Escherichia coli* DNA polymerase I and Klenow fragment. Methods Enzymol *262*, 3-13.

Joyce, C.M., Kelley, W.S., and Grindley, N.D. (1982). Nucleotide sequence of the *Escherichia coli* polA gene and primary structure of DNA polymerase I. J Biol Chem *257*, 1958-1964.

Kamenetsky, M., Middelhaufe, S., Bank, E.M., Levin, L.R., Buck, J., and Steegborn, C. (2006). Molecular details of cAMP generation in mammalian cells: a tale of two systems. J Mol Biol *362*, 623-639.

Kaplan, A., Helman, Y., Tchernov, D., and Reinhold, L. (2001). Acclimation of photosynthetic microorganisms to changing ambient CO_2 concentration. Proc Natl Acad

Sci U S A *98*, 4817-4818.

Katayama, M., and Ohmori, M. (1997). Isolation and characterization of multiple adenylate cyclase genes from the cyanobacterium *Anabaena* sp. strain PCC 7120. J Bacteriol *179*, 3588-3593.

Katsushika, S., Chen, L., Kawabe, J., Nilakantan, R., Halnon, N.J., Homcy, C.J., and Ishikawa, Y. (1992). Cloning and characterization of a sixth adenylyl cyclase isoform: types V and VI constitute a subgroup within the mammalian adenylyl cyclase family. Proc Natl Acad Sci U S A *89*, 8774-8778.

Kinoshita, T., Doi, M., Suetsugu, N., Kagawa, T., Wada, M., and Shimazaki, K. (2001). Phot1 and Phot2 mediate blue light regulation of stomatal opening. Nature *414*, 656-660.

Klengel, T., Liang, W.J., Chaloupka, J., Ruoff, C., Schroppel, K., Naglik, J.R., Eckert, S.E., Mogensen, E.G., Haynes, K., Tuite, M.F.*, et al.* (2005). Fungal adenylyl cyclase integrates CO_2 sensing with cAMP signaling and virulence. Curr Biol *15*, 2021-2026.

Kobayashi, M., Buck, J., and Levin, L.R. (2004). Conservation of functional domain structure in bicarbonate-regulated "soluble" adenylyl cyclases in bacteria and eukaryotes. Dev Genes Evol *214*, 503-509.

Krupinski, J., Lehman, T.C., Frankenfield, C.D., Zwaagstra, J.C., and Watson, P.A. (1992). Molecular diversity in the adenylyl cyclase family. Evidence for eight forms of the enzyme and cloning of type VI. J Biol Chem *267*, 24858-24862.

Kwon, J.Y., Dahanukar, A., Weiss, L.A., and Carlson, J.R. (2007). The molecular basis of CO_2 reception in Drosophila. Proc Natl Acad Sci U S A *104*, 3574-3578.

Ladant, D., and Ullmann, A. (1999). *Bordatella pertussis* adenylate cyclase: a toxin with multiple talents. Trends Microbiol *7*, 172-176.

Lahiri, S., and DeLaney, R.G. (1975). Relationship between carotid chemoreceptor activity and ventilation in the cat. Respir Physiol *24*, 267-286.

Lahiri, S., and Forster, R.E., 2nd (2003). $CO_2/H^{(+)}$ sensing: peripheral and central chemoreception. Int J Biochem Cell Biol *35*, 1413-1435.

Leblanc, R., and Peterson, E.W. (1989). Role of the cyclic-AMP system in cerebral vasodilation. Stroke *20*, 428.

Leinders-Zufall, T., Cockerham, R.E., Michalakis, S., Biel, M., Garbers, D.L., Reed, R.R., Zufall, F., and Munger, S.D. (2007). Contribution of the receptor guanylyl cyclase GC-D to chemosensory function in the olfactory epithelium. Proc Natl Acad Sci U S A *104*, 14507-14512.

Lemaitre, B., and Hoffmann, J. (2007). The host defense of *Drosophila melanogaster*. Annu Rev Immunol *25*, 697-743.

Levine, N., and Marsh, D.J. (1971). Micropuncture studies of the electrochemical aspects of fluid and electrolyte transport in individual seminiferous tubules, the epididymis and the vas deferens in rats. J Physiol *213*, 557-570.

Liang, J.Y., and Lipscomb, W.N. (1987). Hydration of carbon dioxide by carbonic anhydrase: internal proton transfer of Zn^{2+}-bound HCO_3^-. Biochemistry *26*, 5293-5301.

Linder, J.U. (2010). cGMP production in bacteria. Mol Cell Biochem *334*, 215-219.

Linder, J.U., and Schultz, J.E. (2003). The class III adenylyl cyclases: multi-purpose signalling modules. Cell Signal *15*, 1081-1089.

Litvin, T.N., Kamenetsky, M., Zarifyan, A., Buck, J., and Levin, L.R. (2003). Kinetic properties of "soluble" adenylyl cyclase. Synergism between calcium and bicarbonate. J Biol Chem *278*, 15922-15926.

Lorimer, G.H. (1981). Ribulosebisphosphate carboxylase: amino acid sequence of a

peptide bearing the activator carbon dioxide. Biochemistry *20*, 1236-1240.

Lorimer, G.H., Badger, M.R., and Andrews, T.J. (1976). The activation of ribulose-1,5-bisphosphate carboxylase by carbon dioxide and magnesium ions. Equilibria, kinetics, a suggested mechanism, and physiological implications. Biochemistry *15*, 529-536.

Lorimer, G.H., Badger, M.R., and Heldt, H.W. (1978). The activation of ribulose 1,5-bisphosphate carboxylase/oxygenase. Basic Life Sci *11*, 283-306.

Lorimer, G.H., Chen, Y.R., and Hartman, F.C. (1993). A role for the epsilon-amino group of lysine-334 of ribulose-1,5-bisphosphate carboxylase in the addition of carbon dioxide to the 2,3-enediol(ate) of ribulose 1,5-bisphosphate. Biochemistry *32*, 9018-9024.

Lorimer, G.H., Gutteridge, S., and Reddy, G.S. (1989). The orientation of substrate and reaction intermediates in the active site of ribulose-1,5-bisphosphate carboxylase. J Biol Chem *264*, 9873-9879.

Lorimer, G.H., and Miziorko, H.M. (1980). Carbamate formation on the epsilon-amino group of a lysyl residue as the basis for the activation of ribulosebisphosphate carboxylase by CO_2 and Mg^{2+}. Biochemistry *19*, 5321-5328.

Lowrie, D.B., Aber, V.R., and Jackett, P.S. (1979). Phagosome-lysosome fusion and cyclic adenosine 3':5'-monophosphate in macrophages infected with *Mycobacterium microti*, *Mycobacterium bovis* BCG or *Mycobacterium lepraemurium*. J Gen Microbiol *110*, 431-441.

Lowrie, D.B., Jackett, P.S., and Ratcliffe, N.A. (1975). *Mycobacterium microti* may protect itself from intracellular destruction by releasing cyclic AMP into phagosomes. Nature *254*, 600-602.

Lu, T., Qiu, Y.T., Wang, G., Kwon, J.Y., Rutzler, M., Kwon, H.W., Pitts, R.J., van Loon, J.J., Takken, W., Carlson, J.R.*, et al.* (2007). Odor coding in the maxillary palp of the malaria vector mosquito *Anopheles gambiae*. Curr Biol *17*, 1533-1544.

Luo, M., Sun, L., and Hu, J. (2009). Neural detection of gases--carbon dioxide, oxygen--in vertebrates and invertebrates. Curr Opin Neurobiol *19*, 354-361.

Madigan, M.T., and Brock, T.D. (1975). Photosynthetic sulfide oxidation by *Chloroflexus aurantiacus*, a filamentous, photosynthetic, gliding bacterium. J Bacteriol *122*, 782-784.

Malmstrom, K., and Murer, H. (1986). Parathyroid hormone inhibits phosphate transport in OK cells but not in LLC-PK1 and JTC-12.P3 cells. Am J Physiol *251*, C23-31.

Masuda, S., and Ono, T.A. (2004). Biochemical characterization of the major adenylyl cyclase, Cya1, in the cyanobacterium *Synechocystis* sp. PCC 6803. FEBS Lett *577*, 255-258.

Masuda, S., and Ono, T.A. (2005). Adenylyl cyclase activity of Cya1 from the cyanobacterium *Synechocystis* sp. strain PCC 6803 is inhibited by bicarbonate. J Bacteriol *187*, 5032-5035.

Matthay, M.A., Folkesson, H.G., and Clerici, C. (2002). Lung epithelial fluid transport and the resolution of pulmonary edema. Physiol Rev *82*, 569-600.

Matthew, J.B., Morrow, J.S., Wittebort, R.J., and Gurd, F.R. (1977). Quantitative determination of carbamino adducts of alpha and beta chains in human adult hemoglobin in presence and absence of carbon monoxide and 2,3-diphosphoglycerate. J Biol Chem *252*, 2234-2244.

McEvoy, S. (1998). Sensory evaluation of carbonated beverages utilizing a hyperbaric chamber or what would soda taste like if you could get inside the can? Chemical senses day XIV abstracts Santa Rosa, CA.

Mogensen, E.G., Janbon, G., Chaloupka, J., Steegborn, C., Fu, M.S., Moyrand, F.,

Klengel, T., Pearson, D.S., Geeves, M.A., Buck, J., *et al.* (2006). *Cryptococcus neoformans* senses CO_2 through the carbonic anhydrase Can2 and the adenylyl cyclase Cac1. Eukaryot Cell *5*, 103-111.

Moras, D. (1993). Polymerases. Two sisters and their cousin. Nature *364*, 572-573.

Mou, T.C., Masada, N., Cooper, D.M., and Sprang, S.R. (2009). Structural basis for inhibition of mammalian adenylyl cyclase by calcium. Biochemistry *48*, 3387-3397.

Murer, H., Hernando, N., Forster, I., and Biber, J. (2000). Proximal tubular phosphate reabsorption: molecular mechanisms. Physiol Rev *80*, 1373-1409.

Murer, H., Hernando, N., Forster, I., and Biber, J. (2003). Regulation of Na/Pi transporter in the proximal tubule. Annu Rev Physiol *65*, 531-542.

Myrianthefs, P.M., Briva, A., Lecuona, E., Dumasius, V., Rutschman, D.H., Ridge, K.M., Baltopoulos, G.J., and Sznajder, J.I. (2005). Hypocapnic but not metabolic alkalosis impairs alveolar fluid reabsorption. Am J Respir Crit Care Med *171*, 1267-1271.

Ochoa De Alda, J.A., Ajlani, G., and Houmard, J. (2000). *Synechocystis* strain PCC 6803 cya2, a prokaryotic gene that encodes a guanylyl cyclase. J Bacteriol *182*, 3839-3842.

Ohno, S. (1997). The reason for as well as the consequence of the Cambrian explosion in animal evolution. J Mol Evol *44 Suppl 1*, S23-27.

Omer, S.M.a.G., M.T. (1971). Loss of response to carbon dioxide in palpectomised female mosquitos. Entomology for Experimental Applications *14*, 251-252.

Parfenova, H., and Leffler, C.W. (1996). Effects of hypercapnia on prostanoid and cAMP production by cerebral microvascular cell cultures. Am J Physiol *270*, C1503-1510.

Parkinson, S.J., Jovanovic, A., Jovanovic, S., Wagner, F., Terzic, A., and Waldman, S.A. (1999). Regulation of nitric oxide-responsive recombinant soluble guanylyl cyclase by calcium. Biochemistry *38*, 6441-6448.

Pastor-Soler, N., Beaulieu, V., Litvin, T.N., Da Silva, N., Chen, Y., Brown, D., Buck, J., Levin, L.R., and Breton, S. (2003). Bicarbonate-regulated adenylyl cyclase (sAC) is a sensor that regulates pH-dependent V-ATPase recycling. J Biol Chem *278*, 49523-49529.

Paunescu, T.G., Da Silva, N., Russo, L.M., McKee, M., Lu, H.A., Breton, S., and Brown, D. (2008). Association of soluble adenylyl cyclase with the V-ATPase in renal epithelial cells. Am J Physiol Renal Physiol *294*, F130-138.

Perez-Garcia, M.T., Almaraz, L., and Gonzalez, C. (1990). Effects of different types of stimulation on cyclic AMP content in the rabbit carotid body: functional significance. J Neurochem *55*, 1287-1293.

Pfeuffer, E., Mollner, S., and Pfeuffer, T. (1985). Adenylate cyclase from bovine brain cortex: purification and characterization of the catalytic unit. EMBO J *4*, 3675-3679.

Pierson, B.K., and Castenholz, R.W. (1974). A phototrophic gliding filamentous bacterium of hot springs, *Chloroflexus aurantiacus*, gen. and sp. nov. Arch Microbiol *100*, 5-24.

Poulos, T.L. (2006). Soluble guanylate cyclase. Curr Opin Struct Biol *16*, 736-743.

Premont, R.T., Chen, J., Ma, H.W., Ponnapalli, M., and Iyengar, R. (1992). Two members of a widely expressed subfamily of hormone-stimulated adenylyl cyclases. Proc Natl Acad Sci U S A *89*, 9809-9813.

Premont, R.T., Matsuoka, I., Mattei, M.G., Pouille, Y., Defer, N., and Hanoune, J. (1996). Identification and characterization of a widely expressed form of adenylyl cyclase. J Biol Chem *271*, 13900-13907.

Putnam, R.W., Filosa, J.A., and Ritucci, N.A. (2004). Cellular mechanisms involved in $CO_{(2)}$ and acid signaling in chemosensitive neurons. Am J Physiol Cell Physiol *287*, C1493-1526.

Rasch, C.a.R., H (1994). Carbon dioxide: highly attractive signal for larvae of *Helicoverpa armingera*. Naturwissenschaften *81*, 228-229.

Rauch, A., Leipelt, M., Russwurm, M., and Steegborn, C. (2008). Crystal structure of the guanylyl cyclase Cya2. Proc Natl Acad Sci U S A *105*, 15720-15725.

Raven, J.A. (2003). Inorganic carbon concentrating mechanisms in relation to the biology of algae. Photosynth Res *77*, 155-171.

Raven, J.A., Cockell, C.S., and De La Rocha, C.L. (2008). The evolution of inorganic carbon concentrating mechanisms in photosynthesis. Philos Trans R Soc Lond B Biol Sci *363*, 2641-2650.

Reisen, W.K., Meyer, R.P., Cummings, R.F., and Delgado, O. (2000). Effects of trap design and CO_2 presentation on the measurement of adult mosquito abundance using Centers for Disease Control-style miniature light traps. J Am Mosq Control Assoc *16*, 13-18.

Riley, M.V., Winkler, B.S., Starnes, C.A., and Peters, M.I. (1997). Fluid and ion transport in corneal endothelium: insensitivity to modulators of $Na^{(+)}$-$K^{(+)}$-$2Cl^-$ cotransport. Am J Physiol *273*, C1480-1486.

Robertson, H.M., and Kent, L.B. (2009). Evolution of the gene lineage encoding the carbon dioxide receptor in insects. J Insect Sci *9*, 19.

Rocha, C.R., Schroppel, K., Harcus, D., Marcil, A., Dignard, D., Taylor, B.N., Thomas, D.Y., Whiteway, M., and Leberer, E. (2001). Signaling through adenylyl cyclase is essential for hyphal growth and virulence in the pathogenic fungus *Candida albicans*. Mol Biol Cell *12*, 3631-3643.

Roelofs, J., Meima, M., Schaap, P., and Van Haastert, P.J. (2001). The *Dictyostelium* homologue of mammalian soluble adenylyl cyclase encodes a guanylyl cyclase. EMBO J *20*, 4341-4348.

Rommens, J.M., Dho, S., Bear, C.E., Kartner, N., Kennedy, D., Riordan, J.R., Tsui, L.C., and Foskett, J.K. (1991). cAMP-inducible chloride conductance in mouse fibroblast lines stably expressing the human cystic fibrosis transmembrane conductance regulator. Proc Natl Acad Sci U S A *88*, 7500-7504.

Sawaya, M.R., Pelletier, H., Kumar, A., Wilson, S.H., and Kraut, J. (1994). Crystal structure of rat DNA polymerase beta: evidence for a common polymerase mechanism. Science *264*, 1930-1935.

Sayner, S.L., Alexeyev, M., Dessauer, C.W., and Stevens, T. (2006). Soluble adenylyl cyclase reveals the significance of cAMP compartmentation on pulmonary microvascular endothelial cell barrier. Circ Res *98*, 675-681.

Schlicker, C., Hall, R.A., Vullo, D., Middelhaufe, S., Gertz, M., Supuran, C.T., Muhlschlegel, F.A., and Steegborn, C. (2009). Structure and inhibition of the CO_2-sensing carbonic anhydrase Can2 from the pathogenic fungus *Cryptococcus neoformans*. J Mol Biol *385*, 1207-1220.

Schroeder, J.I., Kwak, J.M., and Allen, G.J. (2001). Guard cell abscisic acid signalling and engineering drought hardiness in plants. Nature *410*, 327-330.

Seamon, K.B., Padgett, W., and Daly, J.W. (1981). Forskolin - Unique Diterpene Activator of Adenylate-Cyclase in Membranes and in Intact-Cells. Proceedings of the National Academy of Sciences of the United States of America-Biological Sciences *78*, 3363-3367.

Seeley, T.D. (1974). Atmospheric carbon dioxide regulation in honey-bee (Apis *mellifera*) colonies. J Insect Physiol *20*, 2301-2305.

Seki, G., Coppola, S., Yoshitomi, K., Burckhardt, B.C., Samarzija, I., Muller-Berger, S., and Fromter, E. (1996). On the mechanism of bicarbonate exit from renal proximal tubular cells. Kidney Int *49*, 1671-1677.

Sharabi, K., Hurwitz, A., Simon, A.J., Beitel, G.J., Morimoto, R.I., Rechavi, G., Sznajder, J.I., and Gruenbaum, Y. (2009a). Elevated CO_2 levels affect development, motility, and fertility and extend life span in *Caenorhabditis elegans*. Proc Natl Acad Sci U S A *106*, 4024-4029.

Sharabi, K., Lecuona, E., Helenius, I.T., Beitel, G.J., Sznajder, J.I., and Gruenbaum, Y. (2009b). Sensing, physiological effects and molecular response to elevated CO_2 levels in eukaryotes. J Cell Mol Med *13*, 4304-4318.

Simons, C.T., Dessirier, J.M., Carstens, M.I., O'Mahony, M., and Carstens, E. (1999). Neurobiological and psychophysical mechanisms underlying the oral sensation produced by carbonated water. J Neurosci *19*, 8134-8144.

Sinclair, M.L., Wang, X.Y., Mattia, M., Conti, M., Buck, J., Wolgemuth, D.J., and Levin, L.R. (2000). Specific expression of soluble adenylyl cyclase in male germ cells. Mol Reprod Dev *56*, 6-11.

Sismeiro, O., Trotot, P., Biville, F., Vivares, C., and Danchin, A. (1998). *Aeromonas hydrophila* adenylyl cyclase 2: a new class of adenylyl cyclases with thermophilic properties and sequence similarities to proteins from hyperthermophilic archaebacteria. J Bacteriol *180*, 3339-3344.

Sly, W.S., and Hu, P.Y. (1995). Human carbonic anhydrases and carbonic anhydrase deficiencies. Annu Rev Biochem *64*, 375-401.

Smith, C.A., Rodman, J.R., Chenuel, B.J., Henderson, K.S., and Dempsey, J.A. (2006). Response time and sensitivity of the ventilatory response to CO_2 in unanesthetized intact dogs: central vs. peripheral chemoreceptors. J Appl Physiol *100*, 13-19.

Smith, K.S., and Ferry, J.G. (2000). Prokaryotic carbonic anhydrases. FEMS Microbiol Rev *24*, 335-366.

Steegborn, C., Litvin, T.N., Hess, K.C., Capper, A.B., Taussig, R., Buck, J., Levin, L.R., and Wu, H. (2005a). A novel mechanism for adenylyl cyclase inhibition from the crystal structure of its complex with catechol estrogen. J Biol Chem *280*, 31754-31759.

Steegborn, C., Litvin, T.N., Levin, L.R., Buck, J., and Wu, H. (2005b). Bicarbonate activation of adenylyl cyclase via promotion of catalytic active site closure and metal recruitment. Nat Struct Mol Biol *12*, 32-37.

Stoven, S., Ando, I., Kadalayil, L., Engstrom, Y., and Hultmark, D. (2000). Activation of the *Drosophila* NF-kappaB factor Relish by rapid endoproteolytic cleavage. EMBO Rep *1*, 347-352.

Suh, G.S., Wong, A.M., Hergarden, A.C., Wang, J.W., Simon, A.F., Benzer, S., Axel, R., and Anderson, D.J. (2004). A single population of olfactory sensory neurons mediates an innate avoidance behaviour in *Drosophila*. Nature *431*, 854-859.

Summers, B.A., Overholt, J.L., and Prabhakar, N.R. (2002). CO_2 and pH independently modulate L-type Ca^{2+} current in rabbit carotid body glomus cells. J Neurophysiol *88*, 604-612.

Summers, W.C., and Siegel, R.B. (1970). Transcription of late phage RNA by T7 RNA polymerase. Nature *228*, 1160-1162.

Sun, L., Wang, H., Hu, J., Han, J., Matsunami, H., and Luo, M. (2009). Guanylyl cyclase-D in the olfactory CO_2 neurons is activated by bicarbonate. Proc Natl Acad Sci U S A *106*, 2041-2046.

Sun, X.C., Bonanno, J.A., Jelamskii, S., and Xie, Q. (2000). Expression and localization of Na^+-HCO_3^- cotransporter in bovine corneal endothelium. Am J Physiol Cell Physiol *279*, C1648-1655.

Sun, X.C., Zhai, C.B., Cui, M., Chen, Y., Levin, L.R., Buck, J., and Bonanno, J.A. (2003). HCO_3^--dependent soluble adenylyl cyclase activates cystic fibrosis transmembrane conductance regulator in corneal endothelium. Am J Physiol Cell Physiol *284*, C1114-1122.

Sunahara, R.K., Beuve, A., Tesmer, J.J., Sprang, S.R., Garbers, D.L., and Gilman, A.G. (1998). Exchange of substrate and inhibitor specificities between adenylyl and guanylyl cyclases. J Biol Chem *273*, 16332-16338.

Sunahara, R.K., and Taussig, R. (2002). Isoforms of mammalian adenylyl cyclase: multiplicities of signaling. Mol Interv *2*, 168-184.

Sutherland, E.W., Rall, T.W., and Menon, T. (1962). Adenyl cylase. I. Distribution, preparation, and properties. J Biol Chem *237*, 1220-1227.

Tabcharani, J.A., Chang, X.B., Riordan, J.R., and Hanrahan, J.W. (1991). Phosphorylation-regulated Cl^- channel in CHO cells stably expressing the cystic fibrosis gene. Nature *352*, 628-631.

Taiz, L., and Zeiger, E. (2006). Plant physiology, 4th ed. edn (New York, W. H. Freeman ; Basingstoke : Palgrave [distributor]).

Takeshita, K., Suzuki, Y., Nishio, K., Aoki, T., Takeuchi, O., Toda, K., Sato, N., Naoki, K., Kudo, H., and Yamaguchi, K. (1999). Hyperoxia and hypercapnic acidosis differentially alter nuclear factor-kappa B activation in human pulmonary artery endothelial cells. Adv Exp Med Biol *471*, 265-270.

Takeshita, K., Suzuki, Y., Nishio, K., Takeuchi, O., Toda, K., Kudo, H., Miyao, N., Ishii, M., Sato, N., Naoki, K.*, et al.* (2003). Hypercapnic acidosis attenuates endotoxin-induced nuclear factor-[kappa]B activation. Am J Respir Cell Mol Biol *29*, 124-132.

Tan, C.M., Kelvin, D.J., Litchfield, D.W., Ferguson, S.S., and Feldman, R.D. (2001). Tyrosine kinase-mediated serine phosphorylation of adenylyl cyclase. Biochemistry *40*, 1702-1709.

Tang, W.J., and Gilman, A.G. (1995). Construction of a soluble adenylyl cyclase activated by Gs alpha and forskolin. Science *268*, 1769-1772.

Tellez-Sosa, J., Soberon, N., Vega-Segura, A., Torres-Marquez, M.E., and Cevallos, M.A. (2002). The *Rhizobium etli* cyaC product: characterization of a novel adenylate cyclase class. J Bacteriol *184*, 3560-3568.

Terauchi, K., and Ohmori, M. (1999). An adenylate cyclase, Cya1, regulates cell motility in the cyanobacterium *Synechocystis* sp. PCC 6803. Plant Cell Physiol *40*, 248-251.

Tesmer, J.J., and Sprang, S.R. (1998). The structure, catalytic mechanism and regulation of adenylyl cyclase. Curr Opin Struct Biol *8*, 713-719.

Tesmer, J.J., Sunahara, R.K., Fancy, D.A., Gilman, A.G., and Sprang, S.R. (2002). Crystallization of complex between soluble domains of adenylyl cyclase and activated Gs alpha. Methods Enzymol *345*, 198-206.

Tesmer, J.J., Sunahara, R.K., Gilman, A.G., and Sprang, S.R. (1997). Crystal structure of the catalytic domains of adenylyl cyclase in a complex with Gsalpha.GTPgammaS. Science *278*, 1907-1916.

Tesmer, J.J., Sunahara, R.K., Johnson, R.A., Gosselin, G., Gilman, A.G., and Sprang, S.R. (1999). Two-metal-Ion catalysis in adenylyl cyclase. Science *285*, 756-760.

Thom, C., Guerenstein, P.G., Mechaber, W.L., and Hildebrand, J.G. (2004). Floral CO_2 reveals flower profitability to moths. J Chem Ecol *30*, 1285-1288.

Townsend, P.D., Holliday, P.M., Fenyk, S., Hess, K.C., Gray, M.A., Hodgson, D.R., and Cann, M.J. (2009). Stimulation of mammalian G-protein-responsive adenylyl cyclases by carbon dioxide. J Biol Chem *284*, 784-791.

Traebert, M., Volkl, H., Biber, J., Murer, H., and Kaissling, B. (2000). Luminal and

contraluminal action of 1-34 and 3-34 PTH peptides on renal type IIa Na-P_i cotransporter. Am J Physiol Renal Physiol *278*, F792-798.

Tripp, B.C., Smith, K., and Ferry, J.G. (2001). Carbonic anhydrase: new insights for an ancient enzyme. J Biol Chem *276*, 48615-48618.

Tucker, R.R., Berndt, T.J., Thotharthri, V., Newcome, J., Joyner, M.J., and Knox, F.G. (1996). Propranolol blocks the hypophosphaturia of acute respiratory alkalosis in human subjects. J Lab Clin Med *128*, 423-428.

Turner, S.L., and Ray, A. (2009). Modification of CO_2 avoidance behaviour in Drosophila by inhibitory odorants. Nature *461*, 277-281.

Vadasz, I., Dada, L.A., Briva, A., Trejo, H.E., Welch, L.C., Chen, J., Toth, P.T., Lecuona, E., Witters, L.A., Schumacker, P.T.*, et al.* (2008). AMP-activated protein kinase regulates CO_2-induced alveolar epithelial dysfunction in rats and human cells by promoting Na,K-ATPase endocytosis. J Clin Invest *118*, 752-762.

Vasquez, G.M., Qualls, F., and White, D. (1985). Morphogenesis of *Stigmatella aurantiaca* fruiting bodies. J Bacteriol *163*, 515-521.

Vavasseur, A., and Raghavendra, A.S. (2005). Guard cell metabolism and CO_2 sensing. New Phytol *165*, 665-682.

Venkatesh, S.a.S., R (1984). Sensilla on the third antennal segment of *Drosophila melanogaster* Meigen. Int J Insect Morphol Embryol *13*, 51-63.

Visconti, P.E., Bailey, J.L., Moore, G.D., Pan, D., Olds-Clarke, P., and Kopf, G.S. (1995a). Capacitation of mouse spermatozoa. I. Correlation between the capacitation state and protein tyrosine phosphorylation. Development *121*, 1129-1137.

Visconti, P.E., Moore, G.D., Bailey, J.L., Leclerc, P., Connors, S.A., Pan, D., Olds-Clarke, P., and Kopf, G.S. (1995b). Capacitation of mouse spermatozoa. II. Protein tyrosine phosphorylation and capacitation are regulated by a cAMP-dependent pathway. Development *121*, 1139-1150.

Visconti, P.E., Stewart-Savage, J., Blasco, A., Battaglia, L., Miranda, P., Kopf, G.S., and Tezon, J.G. (1999). Roles of bicarbonate, cAMP, and protein tyrosine phosphorylation on capacitation and the spontaneous acrosome reaction of hamster sperm. Biol Reprod *61*, 76-84.

Visconti, P.E., Westbrook, V.A., Chertihin, O., Demarco, I., Sleight, S., and Diekman, A.B. (2002). Novel signaling pathways involved in sperm acquisition of fertilizing capacity. J Reprod Immunol *53*, 133-150.

Wang, N., Gates, K.L., Trejo, H., Favoreto, S., Jr., Schleimer, R.P., Sznajder, J.I., Beitel, G.J., and Sporn, P.H. (2010). Elevated CO_2 selectively inhibits interleukin-6 and tumor necrosis factor expression and decreases phagocytosis in the macrophage. FASEB J.

Wang, Q., Bryowsky, J., Minshall, R.D., and Pelligrino, D.A. (1999). Possible obligatory functions of cyclic nucleotides in hypercapnia-induced cerebral vasodilation in adult rats. Am J Physiol *276*, H480-487.

Wang, W., Pizzonia, J.H., and Richerson, G.B. (1998). Chemosensitivity of rat medullary raphe neurones in primary tissue culture. J Physiol *511 (Pt 2)*, 433-450.

Wang, Y., Lam, C.S., Wu, F., Wang, W., Duan, Y., and Huang, P. (2005). Regulation of CFTR channels by HCO_3^--sensitive soluble adenylyl cyclase in human airway epithelial cells. Am J Physiol Cell Physiol *289*, C1145-1151.

Watson, P.A., Krupinski, J., Kempinski, A.M., and Frankenfield, C.D. (1994). Molecular cloning and characterization of the type VII isoform of mammalian adenylyl cyclase expressed widely in mouse tissues and in S49 mouse lymphoma cells. J Biol Chem *269*, 28893-28898.

Wayman, G.A., Wei, J., Wong, S., and Storm, D.R. (1996). Regulation of type I adenylyl cyclase by calmodulin kinase IV *in vivo*. Mol Cell Biol *16*, 6075-6082.

Wei, J., Wayman, G., and Storm, D.R. (1996). Phosphorylation and inhibition of type III adenylyl cyclase by calmodulin-dependent protein kinase II in vivo. J Biol Chem *271*, 24231-24235.

Weinman, E.J., Cunningham, R., Wade, J.B., and Shenolikar, S. (2005). The role of NHERF-1 in the regulation of renal proximal tubule sodium-hydrogen exchanger 3 and sodium-dependent phosphate cotransporter 2a. J Physiol *567*, 27-32.

Willemse, L.P., and Takken, W. (1994). Odor-induced host location in tsetse flies (Diptera: Glossinidae). J Med Entomol *31*, 775-794.

Willoughby, D., Masada, N., Crossthwaite, A.J., Ciruela, A., and Cooper, D.M. (2005). Localized Na^+/H^+ exchanger 1 expression protects Ca^{2+}-regulated adenylyl cyclases from changes in intracellular pH. J Biol Chem *280*, 30864-30872.

Woodward, F. (1987). Stomatal numbers are sensitive to increases in CO_2 from pre-industrial levels. Nature *327*, 617-618.

Xia, Z., Choi, E.J., Wang, F., Blazynski, C., and Storm, D.R. (1993). Type I calmodulin-sensitive adenylyl cyclase is neural specific. J Neurochem *60*, 305-311.

Xia, Z., Choi, E.J., Wang, F., and Storm, D.R. (1992). The type III calcium/calmodulin-sensitive adenylyl cyclase is not specific to olfactory sensory neurons. Neurosci Lett *144*, 169-173.

Xie, F., and Conti, M. (2004). Expression of the soluble adenylyl cyclase during rat spermatogenesis: evidence for cytoplasmic sites of cAMP production in germ cells. Dev Biol *265*, 196-206.

Xie, F., Garcia, M.A., Carlson, A.E., Schuh, S.M., Babcock, D.F., Jaiswal, B.S., Gossen, J.A., Esposito, G., van Duin, M., and Conti, M. (2006). Soluble adenylyl cyclase (sAC) is indispensable for sperm function and fertilization. Dev Biol *296*, 353-362.

Yan, S.Z., and Tang, W.J. (2002). Construction of soluble adenylyl cyclase from human membrane-bound type 7 adenylyl cyclase. Methods Enzymol *345*, 231-241.

Yoshimura, M., and Cooper, D.M. (1992). Cloning and expression of a Ca^{2+}-inhibitable adenylyl cyclase from NCB-20 cells. Proc Natl Acad Sci U S A *89*, 6716-6720.

Youngentob, S.L., Hornung, D.E., and Mozell, M.M. (1991). Determination of carbon dioxide detection thresholds in trained rats. Physiol Behav *49*, 21-26.

Zhang, G., Liu, Y., Qin, J., Vo, B., Tang, W.J., Ruoho, A.E., and Hurley, J.H. (1997a). Characterization and crystallization of a minimal catalytic core domain from mammalian type II adenylyl cyclase. Protein Sci *6*, 903-908.

Zhang, G., Liu, Y., Ruoho, A.E., and Hurley, J.H. (1997b). Structure of the adenylyl cyclase catalytic core. Nature *386*, 247-253.

Zhou, Y., Bouyer, P., and Boron, W.F. (2006). Role of a tyrosine kinase in the CO_2-induced stimulation of HCO_3^- reabsorption by rabbit S2 proximal tubules. Am J Physiol Renal Physiol *291*, F358-367.

Zhou, Y., Zhao, J., Bouyer, P., and Boron, W.F. (2005). Evidence from renal proximal tubules that HCO_3^- and solute reabsorption are acutely regulated not by pH but by basolateral HCO_3^- and CO_2. Proc Natl Acad Sci U S A *102*, 3875-3880.

Zimmermann, G., Zhou, D., and Taussig, R. (1998). Mutations uncover a role for two magnesium ions in the catalytic mechanism of adenylyl cyclase. J Biol Chem *273*, 19650-19655.

Zippin, J.H., Chadwick, P.A., Levin, L.R., Buck, J., and Magro, C.M. (2010). Soluble

Adenylyl Cyclase Defines a Nuclear cAMP Microdomain in Keratinocyte Hyperproliferative Skin Diseases. J Invest Dermatol.

Zippin, J.H., Chen, Y., Nahirney, P., Kamenetsky, M., Wuttke, M.S., Fischman, D.A., Levin, L.R., and Buck, J. (2003). Compartmentalization of bicarbonate-sensitive adenylyl cyclase in distinct signaling microdomains. FASEB J *17*, 82-84.

Zippin, J.H., Farrell, J., Huron, D., Kamenetsky, M., Hess, K.C., Fischman, D.A., Levin, L.R., and Buck, J. (2004). Bicarbonate-responsive "soluble" adenylyl cyclase defines a nuclear cAMP microdomain. J Cell Biol *164*, 527-534.

Zippin, J.H., Levin, L.R., and Buck, J. (2001). CO_2/HCO_3^--responsive soluble adenylyl cyclase as a putative metabolic sensor. Trends Endocrinol Metab *12*, 366-370.